NTNU

Norwegian University of
Science and Technology

Levels of Perfluoroalkyl and Polyfluoroalkyl Substances (PFASs) in Northern Goshawk (*Accipiter gentilis*) nestlings from Norway and Spain and potential effect on innate immune system signalling pathways

Jose Maria Castaño Ortiz

Environmental Toxicology and Chemistry
Submission date: May 2018
Supervisor: Veerle Jaspers, IBI
Co-supervisor: Courtney Waugh, IBI
Nathalie Briels, IBI

Norwegian University of Science and Technology
Department of Biology

Acknowledgements

This thesis was written at the Department of Biology at the Norwegian University of Science and Technology (NTNU). Firstly, I would like to thank my supervisors:

Veerle, thanks for once giving me the opportunity to join the group. That inspiring experience motivated me to come back and spend two wonderful years in Trondheim, which truly changed my life. I will always be very grateful for your guidance and support throughout the process.

Courtney, I thank you for your enormous help in the lab and for introducing me to the exciting world of immunotoxicology. You did your best to help us and make our work easier, and I really appreciate your effort.

Nathalie, thanks for always keeping your office door open to me, for the nice conversations and your critical advice. You always found time to help me when I needed it, no matter how busy you were. I take with me the fantastic memories from the field and the lab, and a true friend!

I would also like to express my gratitude to all collaborators of the NewRaptor project. Many thanks to Trond V. Johnsen (NINA) for his guidance and knowledge on goshawks from Troms, to Dorte Herzke (NILU) for helping with pollutant analyses, and to Igor Eulaers (Aarhus University) for analysing the stable isotopes. Pilar Gómez, José Enrique Martínez, Mario León and Mari Paz Aldeguer, from University of Murcia, you were great hosts and I am looking forward to going back and eat zarangollo again.

Thanks to Alexander Badry for being an excellent lab partner, also outside the facilities, and to my fellow MSc students and friends in Trondheim, who contributed to make these two (or more) years a bit more fun.

Lastly, I would like to thank my family and Laia for their great support in all ways possible and understanding during this period. Gracias por hacerme sentir más cerca que nunca desde tan lejos, familia.

Trondheim, May 2018,

Jose Maria Castaño Ortiz

Abstract

Per- and polyfluoroalkyl substances (PFASs) are environmentally persistent and bioaccumulative chemicals, which reach high levels in apex predators like birds of prey. Immunomodulation is among the most concerning toxic effects linked with PFAS exposure in traditional animal models, and additional studies are needed to determine if and how these apply to birds. Innate immune system signalling pathways provide crucial responses against infection that initiate the clearance of pathogens, and these could be impaired by pollutant exposure. This study aimed to investigate the levels and sources of variation of PFASs in plasma (*n*=38) and feathers (*n*=39) from northern goshawk (*Accipiter gentilis*) nestlings, and evaluate specific immune effects linked with one of the most prominent PFAS using an *in vitro* avian model. The *in vitro* experiment was performed using chicken embryo fibroblasts exposed to perfluorooctane sulfonate (PFOS), and infected with gallid herpesvirus-2 (GaHV-2) or the RNA virus analogue poly(I:C). We investigated the expression of microRNA-155, two pro-inflammatory cytokines (IL-8 and TNF-α), the transcription factor NF-κB, and the anti-inflammatory cytokine IL-4 at four consecutive time points following viral stimulation.

Goshawk nestlings were found to be exposed to a wide range of PFASs, although at relatively low levels, and comparable to those found in previous studies on birds of prey. PFAS profiles differed between the studied regions, with perfluoroalkyl sulfonates (PFSAs) dominating plasma profiles in Troms and Trøndelag (Norway), and perfluoroalkyl carboxylates (PFCAs) being the dominant class in Spanish birds: linear PFOS was at highest levels in Norway (mean: 6.37 ≈ 5.96 > 2.13 ng/mL), while perfluorononanoic acid (PFNA) was the most abundant in Spanish nestlings (2.77 > 1.05 ≈ 0.75 ng/mL). In addition to the likely underlying contribution of local PFSA and PFCA contamination sources, the diet contributed to explain PFAS variation across goshawk nestlings, as individual burdens significantly increased with trophic level. Additionally, this study showed that PFOS exposure could mediate a downregulation of constitutive immune gene expression in bird cells from 36h post-exposure. Overall, these findings indicate that PFOS might deregulate innate signalling pathways and cytokine release in birds, but results should be interpreted with care because the experimental dose of PFOS (22 ppm) is generally not relevant for bird exposure, and the effect of PFOS on virus activated pathways could not be demonstrated here. Further research on the impact of pollutants on host-virus interactions is recommended, as they have been overlooked and might contribute to understand disease outcomes and outbreaks in birds of prey, together with other factors like host genetics or the evolving nature of infectious agents.

Resumen

Los compuestos perfluorados (PFASs) son contaminantes persistentes en el medio ambiente y acumulables en los organismos, que pueden alcanzar niveles elevados en depredadores como las aves rapaces. Las alteraciones del sistema inmune están entre los efectos adversos asociados con la exposición a estas sustancias, aunque las respuestas en aves permanecen mucho menos estudiadas que en modelos animales tradicionales. Las vías de señalización del sistema inmune innato movilizan y facilitan las respuestas efectoras ante las infecciones, y una posible modulación de las mismas podría comprometer la inmunidad del huésped. El objetivo del presente trabajo fue evaluar los niveles de PFASs en plasma (n=38) y plumas (n=39) de pollos de Azor común (*Accipiter gentilis*) e investigar efectos específicos sobre la respuesta inmune de uno de los compuestos perfluorados más prominentes mediante cultivos celulares. Para el experimento *in vitro* se utilizaron fibroblastos de embrión de pollo expuestos a sulfonato de perfluorooctano (PFOS), y estimulados con gallid herpesvirus-2 (GaHV-2) o el análogo viral poly(I:C). Se estudió la expresión de microRNA-155, citoquinas proinflamatorias (IL-8 y TNF-α) y la citoquina antiinflamatoria IL-4 en diferentes momentos después de la infección.

Los resultados indican que los azores están ampliamente expuestos a PFASs, aunque a niveles relativamente bajos y comparables con los encontrados en estudios previos con rapaces. En cuanto a las diferencias entre las regiones estudiadas, los ácidos sulfónicos (PFSAs) predominan en aves noruegas de Troms y Trøndelag, y los ácidos carboxílicos (PFCAs) son preponderantes en azores de Murcia: linPFOS muestra niveles más elevados en las poblaciones noruegas (media: 6.37 ≈5.96>2.13 ng/mL en plasma), mientras que el ácido perfluorononanoico (PFNA) abunda más en aves murcianas (2.77>1.05≈0.75 ng/mL). Además de las posibles diferencias regionales en la contaminación por PFSAs and PFCAs, diferencias en la dieta ayudan a predecir los niveles de PFASs en plasma, ya que estos aumentaron significativamente con la posición trófica (biomagnificación). Los resultados del experimento señalan que PFOS disminuyó la expresión constitutiva de los genes estudiados a partir de 36 horas. Esto sugiere que la exposición a PFOS en aves podría afectar vías de señalización del sistema innato y comprometer la secreción de citoquinas importantes. No obstante, estos hallazgos deben interpretarse con cautela porque la dosis utilizada (22 ppm) es poco relevante ambientalmente, y los efectos no pudieron ser corroborados a nivel de respuesta antiviral. Se necesita más investigación en este sentido para dilucidar las interacciones entre contaminantes ambientales y virus. Estas han sido generalmente pasadas por alto, y podrían ayudar a entender los impactos, prevalencia y brotes de agentes infecciosos en poblaciones de rapaces y otros organismos.

List of abbreviations

AFFFs	Aqueous film forming foams
AHV	Accipitrid herpesvirus
AICc	Akaike Information Criterion corrected for small sample sizes
ANOVA	Analysis of variance
AP-1	Activating protein-1
APC	Antigen-presenting cell
APFN	Ammonium perfluorononanoate
BIC	B-cell integration cluster
cDNA	Complementary DNA
CEFs	Chicken embryo fibroblasts
CF-EA-IRMS	Continuous flow - elemental analysis - isotope ratio mass spectrometry
Cl-PFAES	Chlorinated polyfluorinated ether sulfonate
CoHV	Columbid herpesvirus
Ct	Threshold cycle
DAMP	Damage associated molecular pattern
DC	Dendritic cells
DHV	Duck hepatitis virus
DMSO	Dimethyl sulfoxide
dsDNA	Double-stranded deoxyribonucleic acid
dsRNA	Double-stranded ribonucleic acid
ECF	Electrochemical fluorination
F-53B	Chlorinated polyfluorinated ether sulfonate
FCS	Fetal calf serum
FHV	Falcon herpesvirus
FTS	Fluorotelomer sulfonate
g	Grams
GaHV-2	Gallid herpesvirus-2
HSV	Herpes simplex virus
IFN	Inteferon
IL	Interleukin
iNOS	Nitric oxide synthase
ISTD	Internal standard
I-κB	Inhibitor of kappa B
JNK	c-Jun N-terminal kinase
K_{AW}	Air-water partition coefficient
LOAEL	Lowest observed adverse effect level
LOD	Limit of detection
LOQ	Limit of quantification
LPS	Lipopolysaccharide
LRT	Long-range transport
MCMC	Markov chain monte carlo
MD	Marek's disease
MDV	Marek's disease virus
miRNA	MicroRNA
ml	Milliliters
mM	Millimolar
MOE	Margin of exposure
mRNA	messenger ribonucleic acid
MyD88	Myeloid differentiation primary response 88
NAO	North Atlantic Oscillation
ND10	Nuclear domain 10
NF-kB	Nuclear factor 'kappa-light-chain-enhancer' of activated B-cells
ng	Nanograms
NK	Natural killer cells
NLR	Nucleotide oligomerization domain-like receptor
NO	Nitric oxide
OHCs	Organohalogen contaminants
PAMP	Pathogen associated molecular pattern
PBS	Phosphate-buffered saline
PCA	Principal component analysis
PCBs	Polychlorinated biphenyls
PCR	Polymerase chain reaction
PDUnDA	Perfluoroundecanoic acid
PFAAs	Perfluoroalkyl acids
PFBA	Perfluorobutanoic acid
PFBS	Perfluorobutane sulfonate
PFCAs	Perfluoroalkyl carboxylates
PFDA	Perfluorodecanoic acid
PFDoDA	Perfluorododecanoic acid
PFHpS	Perfluoroheptane sulfonate
PFHxA	Perfluorohexanoic acid
PFHxDA	Perfluorohexadecanoic acid
PFHxS	perfluorohexane sulfonate
PFNA	Perfluorononanoic acid
PFOA	Perfluorooctanoic acid
PFODcA	Perfluorooctadecanoic acid
PFOS	Perfluorooctane sulfonate

List of abbreviations

PFOSA	Perfluorooctane sulfonamide
PFSAs	Perfluoroalkyl sulfonates
PFTeDA	Perfluorotetradecanoic acid
PFTrDA	Perfluorotridecanoic acid
PFU	Plaque forming unit
Poly(I:C)	Polyinosinic-polycytidylic acid
POPs	Persistent organic pollutants
POSF	Perfluorooctanesulfonyl fluoride
PPARα	Peroxisome proliferator-activated receptor α
PRR	Pattern recognition receptor
PVDF	Polyvinylidene fluoride
QF	Quantification frequency
qPCR	Quantitative polymerase chain reaction
RISC	RNA-induced silencing complex
RLR	Retinoic acid-inducible gene I-like receptor
RSTD	Recovery standard
RT	Reverse transcription
SHIP1	SH2 domain-containing inositol 5'-phosphatase 1
SHV	Strigid herpesvirus
SIA	Stable isotope analysis
SMI	Scaled mass index
SOCS1	Suppressor of cytokine signalling 1
ssRNA	Single-stranded ribonucleic acid
TDAR	T-cell dependent antibody response
TEF	Trophic enrichment factor
TFE	Tetrafluoroethylene
TGF	Transforming growth factor
Th1	Helper T cells type 1
Th2	Helper T cells type 2
TLR	Toll-like receptor
TNF	Tumor necrosis factor α
TT4	Total thyroxine
UHPLC-MS/MS	Ultra-high performance liquid chromatography tandem mass spectrometry
µl	microliter
α	Alpha, significance level
$\delta^{13}C$	Ratio of stable carbon isotopes (^{13}C: ^{12}C)
$\delta^{15}N$	Ratio of stable nitrogen isotopes (^{15}N: ^{14}N)
Σ	Sum

Table of contents

1. Introduction

1.1. Per- and polyfluoroalkyl substances (PFASs)

Per- and polyfluoroalkyl substances (PFASs) are highly fluorinated aliphatic compounds that represent a large class of man-made chemicals. They have at least one C atom on which all the H substituents have been replaced by F atoms (Buck et al., 2011). PFASs contain chemically and thermally stable C-F bonds, and exhibit both water and oil repellence (amphiphilicity). These unique properties have prompted their use in a wide variety of industrial and commercial applications since the 1950s, including surfactants, paints, water and stain repellent coatings in textiles and cookware, fire-fighting foams or ski waxes (Kissa, 2001; Lau et al., 2007). The past and ongoing production and use of PFASs has resulted in their widespread distribution in the environment, wildlife and humans (Wang et al., 2017). The perfluoroalkyl moiety is very persistent under natural conditions and biota may only degrade PFASs into highly stable metabolites, such as perfluoroalkyl carboxylates (PFCAs) and perfluoroalkyl sulfonates (PFSAs). These constitute two of the most important classes and are collectively referred to as perfluoroalkyl acids (PFAAs) (Blum et al., 2015; Buck et al., 2011).

PFAAs were initially considered as biologically inactive and nontoxic (Lau et al., 2007). However, the environmental persistence, bioaccumulation potential and toxicity of certain compounds has driven recent regulations. For example, perfluorooctane sulfonate (PFOS) was added to the list of persistent organic pollutants (POPs) in Annex B under the Stockholm Convention, and its use, production, import and export have been restricted (UNEP, 2009). There have also been voluntary initiatives to phase-out the manufacture of certain PFASs, such as perfluorooctanoic acid (PFOA), PFOS and related compounds by the company 3M in 2002 (3M, 2000). In Europe and North America, recent regulations on PFOS, PFOA and long-chain PFCAs have motivated a shift towards shorter-chain alternatives, which are claimed to be less bioaccumulative (Scheringer et al., 2014). However, these alternatives are still as environmentally persistent as long-chain substances, and larger production quantities are expected, in order to compensate for their lower efficiencies. More studies are therefore needed to evaluate the potential environmental impact associated with shorter-chain replacements (Blum et al., 2015; Eriksson et al., 2016). In addition, production and industrial use of legacy compounds in emerging Asian economies continues and represents a major source of global pollution (Wang et al., 2014). PFASs are primarily produced through two major manufacturing processes: electrochemical fluorination (ECF) and telomerisation of tetrafluoroethylene (TFE) units. ECF yields a complex mixture of linear and branched isomers, while telomerisation

results in linear alkyl chains (Alsmeyer et al., 1994). Isomeric profiles of the compounds in the environment can be used to gain insight into emission sources and environmental fate of PFASs as they may relate to the manufacturing process. Nonetheless, patterns in biota can be transformed relative to the emission source, due to e.g. preferential elimination of branched isomers through the food chain (Buck et al., 2011; Butt et al., 2010; Riddell et al., 2009).

PFASs have been globally detected in various abiotic compartments, such as surface waters, snow, sediments, soils and wastewater (Butt et al., 2010; Zareitalabad et al., 2013). Due to their persistence and water solubility, PFAAs may undergo long-range transport through water currents and aerosols. Transport by the water phase constitutes the major pathway for PFCAs into the Arctic. In addition, atmospheric transport and deposition of volatile precursors, such as fluorotelomer alcohols (FTOHs), are indirect alternative sources of PFAAs into remote regions (Prevedouros et al., 2006). 8:2 FTOH is a well-studied example of a precursor that degrades into PFCAs upon atmospheric reactions and contributes to the their global spread (Ellis et al., 2004). The relative importance of atmospheric transport is supported by the prevalence of PFASs in Arctic lakes, which are primarily influenced by atmospheric deposition (Butt et al., 2010). Interannual changes in atmospheric transport (North Atlantic Oscillation, NAO) seem to affect the input of PFASs to local ecosystems (Bustnes et al., 2015). Correlations between the concentrations of PFOS and polychlorinated biphenyls (PCBs) in polar bears may indicate similar long-range transport pathways and source regions for these pollutants (Smithwick et al., 2005). At the local scale, highly populated and industrial areas have been recognized as hotspots of PFAS contamination (Ahrens et al., 2010; D'Hollander et al., 2014).

In organisms, uptake of PFASs occurs mostly through the diet, but respiratory and dermal routes can play a role as well (Stahl et al., 2011). PFASs have a high affinity for proteins and accordingly increase binding in protein rich tissues, such as liver or blood serum. This contrasts with lipophilic pollutants, which predominantly accumulate in fatty tissues (Jones et al., 2003). Pharmacokinetic properties are particularly well studied for PFOS and PFOA. Upon absorption, these primarily bind to serum albumin, as well as β-lipoproteins and fatty acid binding proteins in the liver (Stahl et al., 2011). Metabolism and excretion of PFASs in biota is low, and the elimination rate generally decreases with increasing chain length, with certain variation in elimination patterns across sex and species (Jones et al., 2003; Lau et al., 2007). These processes result in bioaccumulation and widespread occurrence of some PFASs in biota, across terrestrial and marine ecosystems, and through different trophic levels (Butt et al., 2010; D'Hollander et al., 2014; Kannan et al., 2002). Top predators tend to have higher levels of some PFASs (Butt

et al., 2010; Houde et al., 2006), but biomagnification mechanisms are still unclear (Conder et al., 2008; Tomy et al., 2004) and limited data is available for terrestrial birds of prey (Jaspers et al., 2013; Meyer et al., 2009). It seems that PFOS and some long-chain PFCAs have a higher tendency to bioaccumulate and biomagnify. The assessment of biomagnification in PFASs is complicated by the lack of protein-normalized biomagnification factors and species-specific metabolic capabilities (Butt et al., 2010). PFAS biomagnification processes have mostly been investigated in marine food webs (Butt et al., 2010), and terrestrial ecosystems remain understudied (D'Hollander et al., 2014; Müller et al., 2011). The ability of PFASs to accumulate in upper trophic levels is of particular concern because of their potential adverse effects in top predators. These comprise genotoxicity and carcinogenesis, reproductive and developmental toxicity, neurotoxicity, endocrine disruption and immunotoxicity (Lau et al., 2007; Stahl et al., 2011). The activation of peroxisome proliferator-activated receptor α (PPARα) has been suggested as a major mechanism for PFAS toxicity, but this mode of action does not seem to account for all toxicities of all compounds (Wang et al., 2017). The most commonly occurring PFAS in biota is PFOS, followed by long-chain PFCAs such as perfluorononanoic acid (PFNA) or perfluoroundecanoic acid (PFUnDA), and perfluorooctane sulfonamide (PFOSA). The detection of PFOA is less frequent in wildlife, despite its high frequency of detection in air and ocean waters (Butt et al., 2010; Yamashita et al., 2005).

1.2. Biomonitoring of contaminants using raptors

The utility of top predators as powerful sentinels for monitoring environmental contamination has been recognized for over 50 years (García-Fernández et al., 2008; Gómez-Ramírez et al., 2014). Biomonitoring using wildlife ultimately provides a warning system of potential harmful effects on humans and the environment (Pain et al., 2010). Among the features that make raptors appropriate sentinels for biomonitoring are their apex position in food webs, relatively long lifespan, extended home range, and relative ease of monitoring, capture and sampling (Furness, 1993). Nonetheless, the protected conservation status of most birds of prey highlight the importance of using non-destructive sampling techniques in biomonitoring, such as blood, feather and preen oil sampling, or collection of failed eggs, regurgitated pellets, excrements and carcasses (Espín et al., 2016).

Blood is one of the most suitable matrices to monitor recent pollutant exposure (Espín et al., 2016). It provides a snapshot for internal contamination and the possibility to study several associated effect biomarkers (Sonne et al., 2012; Sonne et al., 2010). The blood concentrations of contaminants can be converted into liver-based equivalents by using plasma-to-liver

conversion factors. This allows for comparison across studies when the sampled matrices are different (Smithwick et al., 2005). On the other hand, feathers are widely collected samples across Europe for biomonitoring purposes (Espín et al., 2016). They constitute interesting emerging matrices for pollutant monitoring as they are non-destructive, easy to transport and store, and they can be collected from live and dead individuals (Burger, 1993). Plucking of recently grown nestling feathers provides insight into recent exposure as well, but feathers integrate a longer period of time than plasma. This relates to the fact that feathers remain connected to the bloodstream upon growth and act as a sink for certain pollutants (Burger, 1993; Eulaers et al., 2011b). The contribution of external contamination in nestling feathers is minimized due to their shorter exposure time to air-borne pollutants (Eulaers et al., 2011b). The use of feathers has been evaluated and validated for monitoring various environmental pollutants, particularly for metals at the beginning, but also for organohalogen contaminants (OHCs) more recently (Bustnes et al., 2013a; Dauwe et al., 2003; Eulaers et al., 2013). Significant correlations between feather and internal concentrations of PFASs have been reported by some studies (Eulaers et al., 2011b; Jaspers et al., 2013; Jaspers et al., 2011; Meyer et al., 2009). A recent study on white-tailed eagle nestlings suggests that feathers can be used as a tool to monitor PFASs exposure, as they reflect the concentrations of certain compounds in blood plasma (Gómez-Ramírez et al., 2017). However, the suitability of feathers as a biomonitoring matrix for PFASs is still under investigation, and more research is needed to confirm its reliability.

1.3. Immunomodulatory effects of PFASs

Immunotoxicity is one of the well-known effects associated with PFAS exposure (Lau et al., 2007). Environmental pollutants can increase the susceptibility of organisms to infections by modulating the immune function (Heilmann, 2012). The association between organochlorines and immunosuppression has been widely reported in wildlife (Presley et al., 2010) and immunotoxicity is one of the major toxicological findings associated with PFASs as well (DeWitt et al., 2012). Early reports on PFOS and PFOA immunotoxicity demonstrated that oral exposure caused atrophy of lymphoid organs in rodents, as well as reduction in immune cell numbers and antibody production (Peden-Adams et al., 2008; Yang et al., 2002). Interference with various innate and adaptive responses has later been reported, such as impairment of cytokine signalling, the inflammatory response and lymphocyte proliferation (DeWitt et al., 2012). Laboratory studies have suggested that immunomodulation by PFASs occurs at serum concentrations comparable to those reported in highly exposed humans and wildlife (DeWitt et

al., 2012; Peden-Adams et al., 2008). Environmentally relevant doses of PFOS (145-1607 ng/mL in serum) deregulated both the serum lysozyme activity (innate immunity) and the T-cell dependent antibody response (TDAR) (adaptive immunity) in white leghorn chicken (*Gallus gallus*) (Peden-Adams et al., 2009). Research into the mode of action of PFOS-induced immunosuppression has demonstrated that signalling responses to infection within host cells, such as the nuclear factor 'kappa-light-chain-enhancer' of activated B-cells (NF-κB) response, can be negatively regulated by peroxisome proliferator-activated receptor (PPARα) agonists like PFOS (Cunard et al., 2002). This may lead to the suppression of cytokines like interleukin (IL)-6 in stimulated B-lymphocytes exposed to PFOS (Peden-Adams et al., 2008). To the knowledge of the author, and in addition to Peden-Adams et al. (2009), only two studies have addressed the effects of PFASs on bird immunity. Smits and Nain (2013) found a downregulation of the TDAR to *Escherichia coli* in experimental Japanese quails (*Coturnix japonica*), whereas Sletten et al. (2016) did not find any relationship between PFASs and immunoglobulins in a field study on white-tailed eagle nestlings. The immune effects of PFOS in non-mammalian models is therefore rather understudied, and further investigation has been suggested to understand potential immune effects of PFOS in birds.

1.4. The innate immune system of birds

The immune system constitutes a defence system that protects organisms against diseases. These are often caused by pathogens encountered in the environment, and hosts must be able to recognize the invading agents and trigger an efficient physiological response to neutralize them (Davision, 2008). The avian immune system is structurally and functionally similar to the mammalian, but it has some peculiarities (Davision, 2008). For example, the bursa of Fabricius, whose mammalian equivalent is the bone marrow, is a primary lymphoid organ responsible for antibody production in birds. The spleen is a secondary lymphoid organ that plays an important role in avian lymphopoiesis, but it is not a reservoir of erythrocytes like in mammals. Another difference is that birds do not have true lymph nodes, relying on the spleen and diffuse lymphoid tissues for antigen capture and recognition (Oláh and Vervelde, 2008). The spleen of birds provides a suitable environment for non-lymphoid and lymphoid cell interaction and mediates the rearrangement of B cell progenitors before they colonize the bursa of Fabricius, where they undergo further differentiation (Oláh and Vervelde, 2008). Taken together, the set of protective mechanisms within the avian immune system can be divided into innate and adaptive immunity (Davision, 2008) .

The innate immune system represents the first line of host defence against invading pathogens. It comprises a series of constitutive barriers, such as epithelial surfaces, and rapid biochemical (e.g. complement system) and cellular responses to pathogens. Among the innate cell subsets, natural killer (NK) and dendritic cells (DCs) have remarkable importance, as they target and kill virus-infected cells, or engulf pathogens and facilitate the activation of the adaptive immunity, respectively (Demas and Nelson, 2012; Juul-Madsen et al., 2008). The early activation of innate mechanisms relies on pattern recognition receptors (PRRs) that are encoded in the germline DNA, including Toll-like receptors (TLRs), intracellular nucleotide oligomerization domain-like receptors (NLRs) and retinoic acid-inducible gene I-like receptors (RLRs) (Takeuchi and Akira, 2009). PRRs interact with conserved pathogen associated molecular patterns (PAMPs) or damage associated molecular patterns (DAMPs) and initiate downstream antimicrobial cascades (Juul-Madsen et al., 2008). DAMPs are proteins released upon cell damage during necrotic events, whereas PAMPs typically comprise cell wall components such as bacterial lipopolysaccharides (LPS), or bacterial and viral nucleic acids such as dsRNA (Newton and Dixit, 2012). There are a variety of PRRs with affinities for specific ligands. For example, while viral dsRNA activates the intracellular TLR3, bacterial LPS is recognized by cell surface TLR4 (Akira and Sato, 2003), and RLRs can recognize viral RNA from dsRNA and ssRNA viruses in the host cell cytoplasm (Takeuchi and Akira, 2010) and mediate an inflammatory response in fibroblasts (Kato et al., 2005). The interaction between DAMPs and PAMPs with PRRs generally triggers the activation of inflammatory responses and expression of signalling molecules, such as cytokines (Juul-Madsen et al., 2008), which are essential for the activation, differentiation and regulation of the host immune system (Haq et al., 2013). For example, pro-inflammatory cytokines enhance the maturation of antigen-presenting cells (APCs), which mediate the transition between innate and adaptive immune responses by activating antigen specific T cells in lymphoid organs (Juul-Madsen et al., 2008).

1.5. Disease association with PFASs

The important role that the immune system plays on the defence of organisms against pathogens underlines the importance of keeping it in a healthy status. Because immunomodulation may occur at PFAS concentrations similar to those in highly exposed biota, it is possible that concomitant changes in immune function and disease resistance occur as a consequence of PFAS exposure in birds (DeWitt et al., 2012). It has been suggested that immunotoxicants may increase the prevalence of diseases and compromise the health of wild populations (Heilmann, 2012). Epidemiological studies have connections between exposure to environmental pollutants

and disease emergence (Desforges et al., 2016). For example, glaucous gulls (*Larus hyperboreus*) that were highly exposed to Hg and Se had increased parasite burdens (Sagerup et al., 2009) and the susceptibility of marine mammals to viruses increased in relation to dietary OHC intake. This may contribute to explain mass mortality events during the 1980s, which affected seals from contaminated sites in the Baltic Sea (de Swart et al., 1994; Hall et al., 1992). Studies are more limited for PFASs, but Guruge et al. (2009) demonstrated an increased mortality of mice in response to influenza A infection, which could associate with a PFOS-mediated shift towards activation of helper T cells type 2 (Th2) (Zheng et al., 2011). Kannan et al. (2006) found a link between sea otters that died from infectious diseases and concentrations of PFOS and PFOA in their livers. In humans, an association between pre-natal PFOS and perfluorohexane sulfonate (PFHxS) exposure and increased prevalence of common infectious diseases (e.g. otitis media) has been found (Goudarzi et al., 2017). The margin of exposure (MOE) for PFOS in humans is below 100, especially in occupationally exposed, which is suggestive of potential immunomodulatory risks as well (Fair et al., 2011; Faustman and Omenn, 2001).

Establishing a direct link between exposure and disease prevalence in a population, nonetheless, remains difficult because of the inherent limitations of epidemiological studies (Luster, 2014). In addition to contaminants, other environmental factors (e.g. stress, temperature, nutrition) may contribute to modulate the avian immune system and the overall immunocompetence of wild birds. For example, immune cells possess receptors of endocrine-signalling molecules, such as stress, metabolic and sex hormones. It has been observed that exposure to acute stressful events increases corticosterone levels and enhances the trafficking of leukocytes, while chronic stress promotes a transition to an immunosuppressed state (Koutsos and Klasing, 2008). Therefore, indirect effects of pollutants on immunity through a disruption of the hormonal status could occur as well (Kaminski et al., 2008).

1.6. Herpesviruses: Gallid herpesvirus-2 (GaHV-2) and Marek's disease

Herpesviruses (*Herpesviridae*) are among the highly successful infectious agents that can affect birds and other animals, including humans. Their virions are made up of a core containing nucleic acids, namely dsDNA, within a proteinaceous capsid (Mettenleiter et al., 2008). The capsid is surrounded by a lipidic envelope in which viral glycoproteins are embedded (Mettenleiter et al., 2008). These can interact with host cell surface receptors to initiate the fusion of the viral envelope with the cell membrane and mediate the entry of the virus into a host cell (Spear and Longnecker, 2003). This is crucial because, like any other virus,

herpesviruses are parasites that require a host to reproduce themselves. Inside the cell, the viral genome is released into the nucleus through nuclear pores, where it undergoes transcription to generate mRNA and guarantee viral reproduction (Ojala et al., 2000). The viral dsDNA remains near a crucial nuclear domain (ND10) and disrupts its defensive activity (Maul, 1998). This leads to the replication and transcription of viral DNA within the nucleus via the lytic cycle (Flemington, 2001). In addition to lytic replication, herpesviruses may cause latent infections where the virus is integrated into the host genome and persists in host cells indefinitely (McPherson and Delany, 2016). Herpesviruses in such latent state can become reactivated by switching into the lytic cycle to produce new virions (Schelcher et al., 2005). In fact, one of the typical features linked with herpesviruses is the recurring or reactivating nature of their infections (Spear and Longnecker, 2003).

These pathogens can cause mild and asymptomatic diseases or more serious outcomes, which are sometimes life-threatening (Mettenleiter et al., 2008; Spear and Longnecker, 2003). Among these, gallid herpesvirus-2 (GaHV-2), also referred to as Marek's disease virus (MDV), is of particular importance in domestic fowl. GaHV-2 is an oncogenic α-herpesvirus (*Alphaherpesvirinae*) that causes Marek's disease, which is a contagious lymphoproliferative disease characterized by induction of T-cell lymphomas (Osterrieder et al., 2006). Birds are primarily exposed to GaHV-2 through inhalation of air-borne viral particles. The virus may then infect APCs, such as macrophages, DCs and B cells, either directly or through intermediate cells from the lung epithelium (Baaten et al., 2009). This can trigger the infiltration of macrophages into the infected tissue and upregulation of TLRs and cytokines like IL-8 (Abdul-Careem et al., 2009). Following transportation from the lung tissue to internal organs, the cell-associated virus continues its cytolytic infection in the spleen (lymphocytes), bursa of Fabricius (bursal cells) and thymus (thymocytes) (Osterrieder et al., 2006). B cells are primary target cells during the first phase of a natural *in vivo* infection with GaHV-2 (Baigent et al., 1998). The second phase is less productive in terms of viral replication and a latent infection is established in $CD4^+$ T cells. Reactivation of a subset of latently infected cells leads to increased viral replication in feather follicles and potential horizontal transmission of the virus to other birds (Davison and Nair, 2004). Ultimately, malignant transformation of latently infected cells can occur via modulation of the expression of viral and cellular genes (Gennart et al., 2015; Jarosinski et al., 2006). This gives rise to the onset of GaHV-2 lymphomas in visceral tissues and paralysis after three weeks (Davison and Nair, 2004).

Marek's disease (MD) has had a major and widespread impact on the poultry industry since the 1950s. Although research has contributed to better understand the causative herpesvirus and its disease mechanisms, as well as to provide diagnosis and vaccines, MD remains a risk to poultry health worldwide owing to the emergence of virulent strains (Biggs and Nair, 2012). In addition, GaHV-2 is well known as a model organism in pathogenesis and immune control of virus-induced tumorigenesis in avian hosts (Osterrieder et al., 2006). Even though infection with GaHV-2 is not concerning for birds of prey, other herpesviruses are relatively common in raptors and may impact wild populations (Kaleta, 1990).

Falcon herpesvirus 1 (FHV-1) is the causative agent of inclusion body disease and it is generally regarded as fatal in falcons (Remple, 2000), but latent infections for FHV-1 may occur as well (Zsivanovits et al., 2004). This virus is also referred to as Columbid herpesvirus 1 (CoHV-1) in literature due to its closely related pigeon counterpart (Gailbreath and Oaks, 2008). Similarly, FHV-1 is antigenically related to other β-herpesviruses isolated from eagles (Accipitrid HV 1, AHV-1) and owls (Strigid HV 1, SHV-1) (Kaleta, 1990). Fatal cases of herpesviral infection leading to body inclusion disease have been reported in various species of raptors (Graham et al., 1975; Mare and Graham, 1973; Phalen et al., 2011; Pinkerton et al., 2008). The seroprevalence of these β-herpesviruses ranged from 2.4% to 35.5% in wild raptors from Germany (Zsivanovits et al., 2004). A common feature among herpesviruses is that they have evolved various mechanisms to evade the host immunity and complicate the recognition of virally infected targets. For example, during latency, a very limited subset of viral genes is expressed, minimizing the antigenic immune response by the host to foreign antigens (David-Poynter and Farrell, 1996). Some herpesviruses directly disrupt the host immunity by targeting APCs. In addition certain viral proteins, such as the virion host shutoff (*vhs*) protein, can supress protein synthesis in infected cells via degradation of host mRNA (Taddeo and Roizman, 2006). It has more recently been discovered that viral microRNAs (miRNAs) provide an alternative evasion strategy in herpesviruses, whereas host miRNAs are implicated in the regulation of the immune response and they can enhance inflammatory signalling upon infection (Cullen, 2013).

1.7. The role miRNAs in innate immunity and disease

miRNAs are non-coding and endogenous RNA molecules that modulate gene expression at the post-transcriptional level. Their length is about 22 nucleotides and they generally lie within introns in the genome of multicellular organisms as well as in viruses (Bartel, 2004; Cullen, 2013). By targeting mRNA for cleavage or translational repression, they regulate multiple biological processes, including growth, development and differentiation (Bartel, 2004; Samir

et al., 2016). The first miRNA was discovered in the nematode *Caenorhabditis elegans*, where a non-protein coding transcript was found to be processed into small functional RNAs (miRNAs), which repressed the production of the transcription factor lin-14 (Moss et al., 1997). It has been established that miRNAs can modulate immune signalling pathways through binding of mature miRNAs to the catalytic site of the RNA-induced silencing complex (RISC) (Chendrimada et al., 2005; Mehta and Baltimore, 2016). The role of the RISC-associated miRNA is to antisense a complementary sequence of messenger RNA (mRNA), inducing its cleavage or translational repression (Bartel, 2004). The 'seed region' of the miRNA (from the 5' end, positions 2 to 8) is crucial for the recognition of the mRNA target, regardless of the remainder sequence of the miRNA (Cullen, 2013)

It has recently been demonstrated that miRNAs can play a favourable role for the hosts during the early innate immune response (Lindsay, 2008). The upregulation of certain miRNAs upon infection seems beneficial for the host, as they provide tight regulation of the innate viral detection system. For example, miRNAs expressed by host cells can directly bind to viral mRNA and inhibit viral replication. It seems that infected cells generally retain the capacity to express and use their miRNAs to regulate immune processes, such cytokine production and activation of the cellular response to infection (Lindsay, 2008; Thai et al., 2007). Accordingly, one particular miRNA (miR-155) has received considerable attention owing to its role in the innate host response against viruses (O'Connell et al., 2007). The synthesis of miR-155 by host cells implies the processing of a non-coding RNA transcript from a region known as the B-cell integration cluster (BIC) located on chromosome 21. The homology of the BIC sequence among human, mouse and chicken, together with its high expression in lymphoid organs, suggest an evolutionary conserved function (Lagos-Quintana et al., 2002). The mature miR-155 can target cellular mRNAs by binding to 3' mRNA untranslated regions (UTRs) and either degrade the mRNA or inhibit its translation (Valencia-Sanchez et al., 2006). During viral infections, miR-155 is known to repress viral replication and influence the disease outcomes (Gottwein and Cullen, 2008; Wang et al., 2010). miR-155 expression has also been found to diminish HIV-1 infection by targeting viral factors (Swaminathan et al., 2012), or to limit the replication of Japanese encephalitis virus (JEV) in human microglial cells through modulation of the JEV-mediated innate immune responses (Pareek et al., 2014). The adaptive branch of immunity seems to require miR-155 too, as demonstrated by decreased antibody production in miR-155-deficient mice (Calame, 2007).

The cellular recognition of viruses and early activation of such innate antiviral pathways, including the upregulation of miRNA-155, would be important for the antiviral defence of the host. miR-155 expression was found to be up-regulated via the RIG-I/JNK/NF-κB-dependent pathway in macrophages infected with a RNA virus (Wang et al., 2010). Cells from the innate immune system, such as macrophages, DCs and fibroblasts, recognize pathogens through PRRs and promote the activation of transcription factors such as NF-κB. It was established in macrophages that TLR3 ligands like polyinosinic-polycytidylic acid (poly(I:C)) induce the activation of the NF-κB signalling pathway using the MyD88-independent pathway (Akira and Sato, 2003). This therefore enhances the expression of miR-155, which positively feeds back to the NF-κB response by inhibiting two regulatory proteins, the SH2 domain-containing inositol 5'-phosphatase 1 (SHIP1) and the suppressor of cytokine signalling 1 (SOCS1) (Mehta and Baltimore, 2016; O'Connell et al., 2007). This signalling pathway ultimately drives the production of cytokines, including IL-8, interferon (IFN)-α and tumor necrosis factor (TNF)-α, as well as other mediators of the inflammatory response via the type I IFN-mediated antiviral innate immunity, which stimulates and initiates the clearance of pathogens (Juul-Madsen et al., 2008; Kracht and Saklatvala, 2002; Wang et al., 2010). Type I IFNs have been regarded as an early antiviral defence as most cytokines are triggered later than IFN-β (Smith et al., 2005). In addition, miR-155 was found to be induced in macrophages by innate immune signals such as TNF-α, IFN-β and IFN-γ stimulation (O'Connell et al., 2007; Wang et al., 2010), and some of these cytokines are essential for the early control of viral replication (Heilmann, 2012). An association between miR-155 and the innate immune response was therefore established (Lindsay, 2008), and increased miR-155 expression was demonstrated upon activation of innate signalling pathways by poly(I:C) (O'Connell et al., 2007). On the other hand, anti-inflammatory cytokines have a regulatory role and mediate suppression of pro-inflammatory cytokines. For example, IL-4 may supress the LPS-induced production of TNF-α, and this would prevent excessive inflammation in the infected tissue (Woodward et al., 2010). Host miRNAs with anti-inflammatory roles can be important as well. In line with this, miR-146a is responsive to TLR stimulation and provides negative feedback by targeting cytokine receptors, which prevents an uncontrolled cellular response to infection (Mehta and Baltimore, 2016).

Microbial deregulation of innate miRNA pathways may however account for the link between inflammation and induction of cancer (Karin, 2006; tili 2013). Recent studies have shown that certain miRNAs may play a role as viral determinants in the development of tumours associated with GaHV-2 infection. Chicken infected with GaHV-2 were found to express a distinctive

profile of miRNAs compared to the non-infected ones. The target genes of these miRNAs are associated with lymphomagenesis and may thus contribute to virus-induced oncogenesis (Lian et al., 2012). miR-155 is a known oncogene in the induction of MD lymphomas, as it mediates the transformation of lymphocytes by repressing a set of host genes, including PU.1, Bach1, and Cebpβ genes (O'Connell et al., 2008). It has also been suggested that overexpression of miR-155 leads to cancer by targeting the transcriptional factor SMAD5, thereby impairing the transforming growth factor beta (TGF-β) signals during lymphomagenesis (Rai et al., 2010). Taken together, the disruption of such innate signalling pathways may contribute to explain the association between inflammation and oncogenesis (Tili et al., 2013). In addition, the expression of a viral analogue of miR-155 during infection with GaHV-2, namely miR-M4, mediates the oncogenic transformation of lymphoid cells (Cullen, 2013). GaHV-2 can therefore utilize miR-155 pathways by expressing a miRNA (miR-M4) that mimics and shares a common set of target genes with the host miRNA (miR-155) (Zhao et al., 2009). It has been demonstrated that miR-M4 targets comprise proteins involved in the cleavage and packaging of virion DNA (muylkens 2010). This would constitute one of the mechanisms whereby a viral miRNA functions as a mediator of host immunity evasion (Cullen, 2013).

1.8. PFASs and innate miRNA signalling pathways

It has been established that PFASs can impact an overall indicator of innate immune function in chicken, namely the plasma lysozyme activity (Peden-Adams et al., 2009). It is known from traditional models that innate signalling cascades can be negatively regulated by PFAS-mediated activation of PPARα, which may lead to the attenuation of NF-κB signalling and downregulation of pro-inflammatory genes (DeWitt et al., 2009b). Despite an increasing number of studies have focused on the mechanistic aspects of PFASs immunosuppression (DeWitt et al., 2012), the effect of these compounds on innate miRNA signalling during early immune responses remains unexplored. In fact, only one study to date has looked at the effect of pollutants on miRNA expression in infected in vitro systems (Waugh et al., 2018). This study focused on a mixture of PCBs (Arochlor-1250) and found that chicken embryo fibroblasts (CEFs) were incapable of upregulating miR-155 signalling to poly(I:C) after pollutant exposure. In addition, a limited number of studies have looked at the effect of environmental pollutants on baseline miRNA expression (Baccarelli and Bollati, 2009). For example, PCB concentrations in pregnant women positively related to the expression of miR-191, which targets genes involved in metabolic processes and apoptosis (Guida et al., 2013). Therefore, although the role of miRNA signalling in the cellular response to environmental stimuli is still

under investigation, it is plausible that they contribute to the pro-inflammatory and carcinogenic effects of certain pollutants (Sonkoly and Pivarcsi, 2011). Because of the enormous regulatory potential of miRNAs, also during innate immune responses, modulation of miRNAs activity may constitute a disease risk determinant (Sonkoly and Pivarcsi, 2011; Waugh et al., 2018). Accumulating evidence suggests a link between exposure to environmental pollutants and deregulation of miRNAs, although the mechanisms by which chemicals modulate miRNA expression are not well understood (Guida et al., 2013). In addition, because changes in miRNA profiles may relate to certain diseased states (e.g. cancer) or exposure to pollutants, circulating levels of miRNAs could be used as a novel class of biomarkers (Guida et al., 2013; Sonkoly and Pivarcsi, 2011; Wang et al., 2013). Taken together, the expression of immunologically relevant genes and miRNAs in avian models following combined PFAS exposure and viral infection remains unstudied. Further research has been recommended to better understand the effect of PFOS on innate inflammatory signalling processes and virus-host interactions (DeWitt et al., 2009b). This may ultimately contribute to explain if and how exposure to environmental pollutants can impact disease resistance and increase the severity of viral infections.

1.9. *In vitro* system: chicken embryo fibroblasts

Fibroblasts have been recognized as early mediators of innate immune responses. Besides their known structural role as connective tissue cells that synthesize extracellular matrix proteins, they are capable of recognizing pathogens and inducing the recruitment of inflammatory cells (Jordana et al., 1994). Synthesis of important receptors and inflammatory mediators involved in the early immunity against microorganisms, such as TLRs, pro-inflammatory cytokines, chemokines or antimicrobial peptides has been reported in fibroblasts (Bautista-Hernández et al., 2017; Jordana et al., 1994). For example, although TNF-α is mainly produced by monocytes and macrophages, other cell types like fibroblasts can release it upon inflammation as well (Bradley, 2008). The extracellular matrix (ECM) synthesized by fibroblasts constitutes an adequate environment for the storage of such cytokines, which are implicated in the activation of influxing leukocytes (Vaday and lider 2000). Other signalling proteins, such as IL-8, are chemotactic and facilitate the influx of leukocytes from the blood into the infection site (Smith et al., 1997). Therefore fibroblasts are connective tissue cells, and not strictly immune cells, but they constitute an early barrier against infection with importance for the sensing of microbial invasion (Jordana et al., 1994). These innate responses are very important during the earliest phases of infection, because they are more rapid than and ultimately mediate the interplay with adaptive responses. The innate immune system is the major initiator of inflammatory responses

and can ultimately neutralize or slow down disease development before the adaptive immunity becomes activated (Juul-Madsen et al., 2008). Thus, the adaptive or acquired response takes longer to occur, but it provides a highly specific response and immunological memory through B-lymphocytes (humoral immunity) and T-lymphocytes (cellular immunity) (Demas and Nelson, 2012). Fibroblasts are ubiquitously distributed in different tissues (e.g. lung interstitium) and represent key elements for the initiation of such inflammatory processes and transition between innate and adaptive immunity (Smith et al., 1997). This cell type, namely chicken embryo fibroblasts (CEFs), was used as an *in vitro* system for innate immune toxicity in this study.

Because of the inherent difficulties in experimentally studying multiple stressors *in vivo,* such as in the goshawks, CEFs were selected as useful sentinels to investigate the interaction between viruses, PFOS and immune gene expression in birds. In a broader context, this can provide further insight on how innate immune signalling pathways could be impacted in raptors following pollutant exposure and viral infection. For example, because other viruses from the *Herpesviridae* family are relatively prevalent in birds of prey, the use of GaHV-2 in our *in vitro* system may partially mimic that situation. Previous studies have indicated that CEFs are compatible with GaHV-2, as they show responsiveness during infection and induction of host gene expression (Morgan et al., 2001). The immunocompetence of CEFs has also been demonstrated by their ability to synthesize cytokines (e.g. IL-8) and other antimicrobial components (e.g. iNOS) upon infection (Xing and Schat, 2000). In line with this, it was assumed that CEFs would mount a measurable immune response following infection with the selected herpesvirus. In addition to GaHV-2, poly(I:C), which is a structurally similar synthetic analogue to viral dsRNA (He et al 2012), was selected as alternative viral model to potentially distinguish between the induced host innate signalling pathways upon infection. The involvement of the TLR3 pathway in the activation of epithelial cells has been demonstrated for poly(I:C) and related viruses such as avian influenza virus (ssRNA), which are impactful for wild and domestic birds (Guillot et al., 2005; Ulrich et al., 2018). Although poly(I:C) simulates the action of dsRNA, the genetic material of several viruses, dsRNA can be generated as a replication intermediate in ssRNA viruses as well (Akira et al., 2006). The interactive effect between PFASs and viral infections investigated in this study is of interest because highly exposed populations of raptors might ultimately appear more susceptible to the impact of infections.

1.10. Aims and hypotheses

This study is part of the NewRaptor project co-funded by the Norwegian Research Council and NTNU, which is concerned with environmental exposure to emerging pollutants and biological effects in birds of prey. Within this context, the present work aims to investigate exposure to a wide range of PFASs in Northern Goshawks (*Accipiter gentilis*) and evaluate specific immune effects associated with one of the most prominent PFAS using an *in vitro* avian model. These effects could potentially be relevant for and linked back to the raptors, as they are birds exposed to PFASs and pathogens related to the selected viral models. In line with this, the following aims were addressed in the present study:

1) To investigate the occurrence and levels of PFASs in plasma and feathers of goshawk nestlings in three distinct populations, addressing variation and potential explanatory factors (biological, spatial, ecological). The study populations were situated in northern Norway (Troms), central Norway (Trøndelag) and southern Spain (Murcia), representing a latitudinal gradient and areas with minimal human development, relative urbanization, and agricultural activity, respectively.
   - Hypothesis 1.1. Accumulation during the nestling period will occur, with increased PFAS burdens in older/bigger nestlings. This would result from dietary intake of pollutants by feeding chicks overcompensating the growth dilution effect, based on the bioaccumulative properties of PFASs and suggested by Bustnes et al. (2013b) in raptors.
   - Hypothesis 1.2. Significant differences across populations were expected in relation to distinct dietary sources and/or local sources of PFAS contamination.

2) To characterize the potential effect of perfluorooctane sulfonate (PFOS) on the antiviral response to infection using an *in vitro* model, namely primary chicken embryo fibroblasts (CEFs) stimulated with either gallid herpesvirus-2 (GaHV-2) or the RNA viral analogue poly(I:C). More specifically, this study aimed to evaluate whether PFOS can modulate viral replication (first experiment) and innate immune signalling pathways (second experiment).
   - Hypothesis 2.1. Because PFOS may modulate the innate host defence, it was hypothesized that viral replication and plaque formation will increase in host cells exposed *in vitro* to PFOS and GaHV-2 in combination (experiment 1).
   - Hypothesis 2.2. The expression of innate immune signalling pathways components (miR-155, IL-4, IL-8, NF-κB, TNF-α), studied at four different time points, will be altered by combined exposure to PFOS and viral stimulation (experiment 2).

3) To address how an *in vitro* modulation of the investigated innate immune signalling pathways might be relevant *in vivo* to the raptors, integrating current environmental exposure to PFASs in birds of prey and potential PFOS-mediated effects on the antiviral immunity.

2. Materials and methods

The materials and methods used to address different objectives of the study are covered in different sections. The first part corresponds to the field data and analysis of PFASs in goshawk samples, or *in vivo* study (section 2.1), whereas other sections concern the first (section 2.2) and second (section 2.3) *in vitro* experiments.

2.1. *In vivo* study

2.1.1. Study species

The northern goshawk (*Accipiter gentilis*), hereafter referred to as goshawk, is a large terrestrial raptor that is widely distributed throughout the northern hemisphere (Kenward, 2010). It feeds on a variety of prey items including medium-sized birds and mammals, such as pigeons, corvids, thrushes, grouse, squirrels and rabbits (Widén, 1997). It is considered an opportunistic predator, as it can adjust its feeding ecology to the availability of prey in their particular environment (Mañosa, 1994; Rutz et al., 2006). Accordingly, the diet of the goshawk varies across populations. In Norway, they generally prey on woodland grouse (*Tetraonidae* spp.), redwing (*Turdus iliacus*), fieldfare (*Turdus pilaris*), carrion crow (*Corvus cornix*), and small mammals such as red squirrel (*Sciurus vulgaris*) and mountain hare (*Lepus timidus*) (Grønnesby and Nygard, 2000). This contrasts with their diet in Spain, where other medium-sized birds such as the red-legged partridges (*Alectoris rufa*) or pigeons (*Columba sp*), and mammals like the rabbit (*Oryctolagus cuniculus*) constitute the basis of their diet (Zuberogoitia and Martínez, 2015). The goshawk is a strongly size-dimorphic species, with small males and large females. Additionally, in accordance with Bergmann's rule, goshawk size increases with latitude: birds from southern Europe are smaller than in northern Europe (Kenward, 2010). Adult females lay on average 3.3 eggs (2-4), which are incubated for around 38 days by both adults, and chick fledging occurs at about 6 weeks of age. Although goshawks are adapted to hunt in mature forests, they may use open areas as well (Widén, 1997). Similarly, despite being typically associated with woodland habitats, goshawks have recently colonized urban environments across Europe (Rutz, 2006). In fact, some of the highest breeding densities in Norway are now found in farmland and urban areas with dispersed woods (Grønlien, 2004). Most goshawks are resident in Europe, including Norwegian and Spanish study populations, with overlapping wintering and breeding grounds (del Moral et al., 2012; Grønlien, 2004). The estimated population size was 1500-2000 breeding pairs in Norway (Grønlien, 2004), and between 3500 and 6500 in Spain (Martí et al., 2003). In Trøndelag, the production of chicks is subject to annual fluctuations and the population seems to have stabilized at low levels (Jacobsson and

Sandvik, 2014). Norwegian populations have been declining since the 1950s and, in 1984, goshawks were included on the Norwegian red list of threatened species (Kålås et al., 2010; Widén, 1997). The same applies to populations in southern Spain, which have been recorded as declining since the 1990s, particularly in agricultural areas (Martinez-Lopez et al., 2007). The breeding density of goshawks in Murcia (southern Spain) was estimated as 15-20 pairs (1 pair/238 km^2), remarkably lower than in some populations from NW Spain (1 pair/30 km^2) (Martí et al., 2003; Zuberogoitia and Martínez, 2015) and Norway, where goshawk breeding densities ranged between 0.6 and 4.3 pairs per 100 km^2 (Selås et al., 2008).

Regarding pollutant exposure in goshawks, several studies have detected OHCs, metals and other contaminants in their blood, feathers, internal organs and eggs (Dolan et al., 2017; Eulaers et al., 2013; Gómez-Ramírez et al., 2017; Herzke et al., 2005; Kenntner et al., 2003; Mañosa et al., 2003; Martinez-Lopez et al., 2007; Sonne et al., 2010). This, together with their widespread distribution and well-known feeding ecology, highlights the potential of goshawks as sentinels for monitoring environmental pollutants. The use of goshawks in pollutant biomonitoring has been less common than for other diurnal raptors, such as the common buzzard (*Buteo buteo*) and the kestrel (*Falco tinnunculus*). However, it is important that monitoring programs cover the existing diversity of raptors and account for species with different diets, habitats or migration behaviours (Gómez-Ramírez et al., 2014). Although the levels of OHCs and other pollutants seem too low to cause population-level effects in goshawks (Martinez-Lopez et al., 2007; Rutz et al., 2006), contamination and other anthropogenic factors have been related with past changes in its population trends (Bijlsma, 1991; Widén, 1997). Forestry and forest management affect the availability of suitable nesting and hunting habitats, as well as prey populations (e.g. forest grouse) (Selås et al., 2008). Persecution by humans, especially hunters aiming to protect small game or provide captive birds for falconry, used to be a threat but has diminished following legal protection of the species (Widén, 1997). In Spain, goshawks seem particularly vulnerable to electrocution on power lines (Mañosa, 2001). In addition to human activities, ecological factors can affect goshawk populations too, such as nestling predation by expanding eagle owl (*Bubo bubo*) populations in certain areas of Spain (Tella and Mañosa, 1993) or depleting grouse abundance by the red fox (*Vulpes vulpes*) in Norway (Selås, 1998). In combination with these other factors, contamination could play an important role in the health of goshawk populations.

2.1.2. Study area

The sampling of goshawk nestlings was conducted in June 2016 at three different study regions: northern Norway (Troms), central Norway (Trøndelag) and southeastern Spain (Murcia) (Figure 2.1). A total number of 107 nestlings were used in this study. 33 birds were sampled in Troms (12 nests) during seven days (22/06-28/06), 53 birds were sampled in Trøndelag (20 nests) during ten days (18/06-28/06), and 21 birds were sampled in Murcia (7 nests) during four days (01/06-14/06). Further details about the geographic location of the nesting sites are given in Appendix A (Figures A1-3). In Murcia, these were mostly situated near agricultural areas, while Norwegian nests were located in more urbanized areas (Trøndelag) or areas with minimal human development (Troms). Although the degree of human and agricultural encroachment was fairly similar in all three study populations, Murcia is the leading Spanish producer and exporter of fruits and vegetables. Troms is the least urbanized region, with around 15 hectares of roads and buildings per 5 km nest radii, whereas Trøndelag nests were the most urbanized ones (Dolan et al., 2017). In Murcia, nests were placed on coniferous trees, such as the Aleppo pine (*Pinus halepensis*), while Norwegian nests were either built on coniferous trees, such as the Norway spruce (*Picea abies*), or deciduous stands such as the birch (*Betula* spp.). The latter especially applies to breeding sites in northern Norway (Grønlien, 2004).

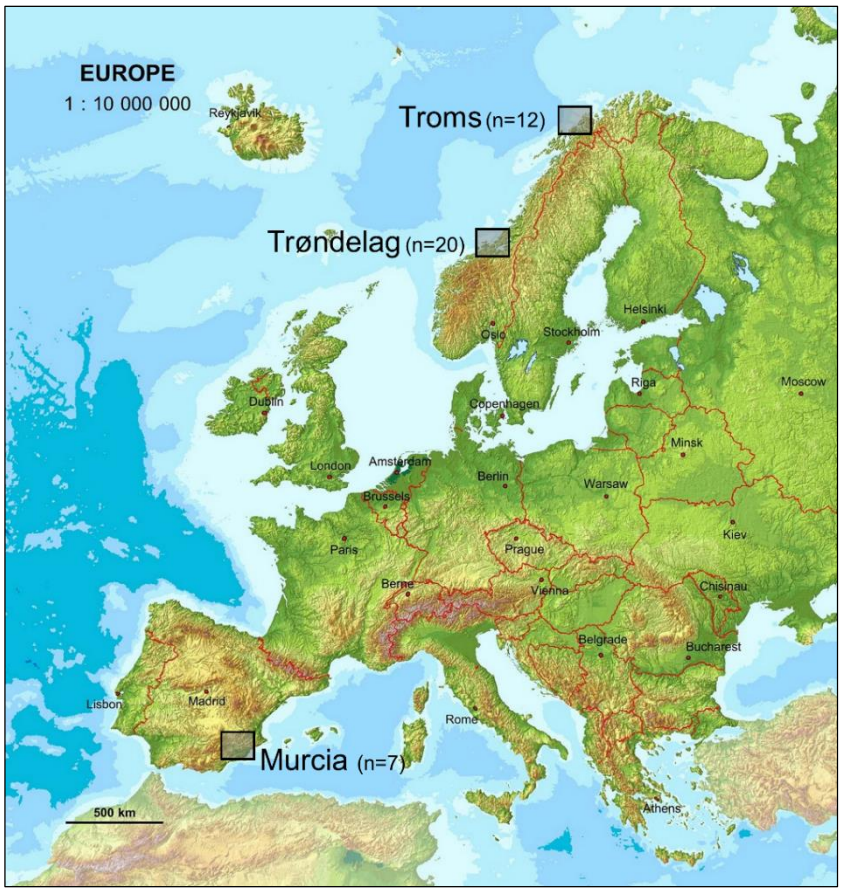

Figure 2.1. Location of the three sampling regions in Norway (Troms and Trøndelag) and Spain (Murcia). The number of nests (*n*) visited in each region is shown in the map. Modified from www.roundtripticket.me

2.1.3. Field sampling

The activity of breeding pairs was observed from the onset of courtship to the nestling period. The fledging date was estimated in order to carry out the sampling prior to this date. Nestlings were 3 to 5 weeks old when the sampling was conducted. At each nest we collected feathers and blood from the nestlings. The chicks were lowered down from the nest in nylon bags, and they were handled on the ground. Feathers were collected from all nestlings, while blood was taken only from the oldest bird. The blood sample (2-5 mL) was taken from the brachial and/or jugular vein using a heparinized needle, and body feathers (10-15) were pulled from the back. Feathers were stored per individual in sealed plastic bags and later pooled per nest for analysis. Blood could not be obtained from one of the nests in Troms owing to poor venous access in the nestlings. A total of 38 blood and 39 feather samples were thus included in later analysis (Table A1, Appendix). Morphometric measurements were additionally recorded following sampling, including body weight, wing length, tarsus width, depth and length, bill length and height, and tail feather length (Table A2, Appendix). The fieldwork was conducted with permission from Mattilsynet in Norway and the General Directorate of Natural Heritage and Biodiversity from the Autonomous Community of Murcia in Spain. An ice cooler was used to store samples during fieldwork. Blood was centrifuged in the laboratory upon arrival at 6000 rpm (10 min) to separate plasma (used in this study) and cells (not used in this study). Plasma and feather samples were then aliquoted for various analyses and frozen at -20ºC. Cold storage was applied to nestling feathers too, as they may contain blood traces when pulled. A plasma volume of at least 200-300 µL was reserved for PFASs analysis.

2.1.4. Determination of sex, age and body condition

Sex was determined based on tarsus width and body mass. These morphometric parameters are correlated and distinctively larger in females (Kenward, 2010). Principal component analysis (PCA) was used to distinguish males and females based on field morphometric data. PC1 clearly separated most individuals into males (negative scores) and females (positive scores) in the three regions. In addition, molecular sexing was applied to a few individuals with intermediate characteristics and whose gender could not be reliably determined using field data (section 2.1.5). Nestling age was estimated in a sex-dependent manner based on wing length (mm) measurements, as recommended in Kenward (2010) (Equations 2.1 & 2.2).

Age_{male} (days) = 0.125 x wing length (mm) + 3.60 (Equation 2.1)

Age_{female} (days) = 0.111 x wing length (mm) + 4.94 (Equation 2.2)

Nestling body condition was estimated by calculating the scaled mass index (SMI). This approach represents a standardized method to control for variation in size across individuals from a population and remove its effect on body condition estimates (Peig and Green, 2009, 2010). It has been suggested that SMI is a more accurate measure of body condition than traditional methods, such as directly using residuals from a regression of body mass on a linear measure of body size. The following equation was applied to calculate individual SMIs:

$$SMI_{ind} = M_i \times \left(\frac{B0}{Bi}\right)^{B_{SMA}} \quad \text{(Equation 2.3)}$$

Where M_i and B_i correspond to individual body mass and bill length measurements, respectively, and B_0 is the arithmetic mean of bill length in a given population. B_{SMA} is the scaling exponent that describes the relationship between body mass and body size. This constant was previously calculated by plotting ln(mass) against ln(size), and dividing the corresponding slope by the Pearson's correlation coefficient (r) (Figure A4, Appendix). In this study, bill length was selected as the measure of body size because it shows the strongest correlations with body mass. The constant parameters (B_0 and B_{SMA}) were independently calculated for each of the study regions. Because SMI was consistently higher in females, and in Norwegian nestlings regardless of the sex, the following equation was applied to obtain a corrected sex- and population-independent measure of body condition:

$$SMI_C = SMI_{ind} \times \left(\frac{\mu\ pop}{\mu\ sex}\right) \times \left(\frac{\mu\ total}{\mu\ pop}\right) \quad \text{(Equation 2.4)}$$

2.1.5. Molecular sexing

The sex of certain goshawk nestlings was molecularly determined at NTNU based on Griffiths et al. (1998). Female birds are heterogametic (ZW) and carry both the CDH-1-Z and the CHD-1-W genes, whereas male birds are homogametic (ZZ) and only carry the CDH-1-Z gene. Using amplification through polymerase chain reaction (PCR), these genes can be targeted and then separated via gel electrophoresis to reliably determine the sex of individual birds. Small bits of frozen blood were transferred into 96% ethanol. The extraction of DNA was carried out using a modified version of the Chelex extraction method described by Walsh et al. (1991). A solution of 5% Chelex 100 resin was used to extract the DNA fraction required in PCR for amplification of the target genes. The PCR reaction mix (10 µl) comprised the following reagents from Taq

PCR Core Kit (Qiagen®, West Sussex, UK): Taq DNA polymerase (0.05 µl), PCR buffer 10x CL (1 µl), Q-solution (2 µl), dNTPs (0.4 µl 10 mM), MgCl (0.6 µl), the primers 2718 (1 µl 10 µM) and 2550 (1 µl 10 µM) and 2 µl of the extracted DNA template. PCR was then performed at GeneAMP® PCR System 9700 thermal cycler (PE Applied Biosystems, Life Technologies, USA). The following program was run: initial denaturation step at 94˚C followed by 35 cycles of 94˚C (30 s), 46˚C (45 s) and 70˚C (45 s). The program ends with 70˚C (10 min) and then the temperature drops to 4˚C. The procedure for gel electrophoresis started by preparing a 1% agarose gel and stain it with 6 µL GelRed when all agarose was dissolved. The liquid was then poured into a gel cast. When the gel was completely set, it was put in a running chamber and 700 mL running buffer (686 mL water and 14 mL 50x TAE buffer) were added. The samples were then loaded into the wells and PCR products were finally separated by electrophoresis at 70 V (45 min) (Figure A5, Appendix).

2.1.6. PFASs analysis

The analysis of PFASs consisted of two major steps: extraction of compounds from target matrices and analytical quantification via UHPLC-MS/MS. The extraction of feathers was performed at the Bird Ecotoxicology lab (NTNU) in March 2017, while plasma extraction and quantification of PFASs in the extracts were conducted at the Norwegian Institute for Air Research (NILU) in Tromsø. This study targeted a wide range of PFASs for analysis (*n*=24), namely perfluorinated carboxylates with a chain length varying between four and fourteen carbon atoms in addition to perfluorohexadecanoic acid (PFHxDA), perfluorooctadecanoic acid (PFODcA), as well as perflorinated sulfonates with a chain length varying between four and ten carbon atoms in addition to perfluorooctane sulfonamide (PFOSA), 4:2 fluorotelomer sulfonate (4:2 FTS), 6:2 fluorotelomer sulfonate (6:2 FTS), 8:2 fluorotelomer sulfonate (8:2 FTS) and chlorinated polyfluorinated ether sulfonate (6:2 Cl-PFAES also called F-53B).

Feather extraction

The extraction of PFASs from feathers was carried out using a modification of Powley et al. (2005) as implemented by Jaspers et al. (2013). This procedure incorporates a washing step before feather extraction. Feathers were pooled per nest to obtain sufficient amount for analysis and overcome analytical constraints regarding the limit of quantification (LOQ). After pooling, feathers were washed in Petri dishes with distilled water, covered with paper tissue and dried overnight at room temperature. The use of water in feather washing targeted for PFAS analyses, instead of organic solvents, has been previously recommended to remove dust without removing PFASs (Jaspers et al., 2013; Jaspers et al., 2011). Tweezers were used to remove the

calamus and soft tissues, and to separate the barbs during the washing step. The equipment was rinsed with methanol before and between samples. Dried feathers were cut into small pieces (<5 mm), weighted inside polypropylene (PP) tubes and further washed with 20 mL of hexane for the removal of lipids from preen oil in an ultrasonic bath for 10 min. Following removal of the hexane using glass Pasteur pipets, the feather homogenate was left to dry overnight in the fume hood.

The next day, 70-340 mg (per nest) of dry sample was spiked with 20 µL of internal standard (ISTD: ^{13}C PFAS mix 100 ng/mL, Appendix B). Two mL of 200 mM NaOH in MeOH was used to denature the feathers, by vortexing and soaking the homogenate for 60 min. MeOH (10 mL) was added and samples were extracted three times by sonicating for 10 min and vortexing in between. Feathers were left soaking in the extraction medium overnight. Two hundred µL of 2M HCl in MeOH were added the next day to adjust the pH of each sample, followed by another vortex-ultrasonic bath cycle and centrifugation at 2000 rpm for 5 min. The sedimentation of the feather content allowed for collection and transfer of the extracts into 15 mL centrifuge tubes. The supernatant was then concentrated to 2 mL under a N_2 stream (RapidVap) on a heated (40ºC) and swirling plate. Approximately 1 mL of the concentrated extract was transferred to an Eppendorf tube containing 25 mg ENVI-carb absorbent and 50 µl of glacial acetic acid, and it was cleaned-up by vortexing and centrifugation at 10000 rpm for 10 min. Finally, exactly 0.5 mL of the supernatant was transferred to a glass autoinjector vial, and a recovery standard (RSTD: 3,7-diMe-PFOA 100 ng/mL) was added before vortexing and storage in the fridge until analysis via UHPLC-MS/MS.

Plasma extraction

The extraction of PFASs from plasma samples resembles feather extraction, but without the preliminary washing step. A modified version of the Powley method (Powley et al., 2005) was implemented as described by Herzke et al. (2009). Plasma samples were processed as follows: A volume of 200 µL was spiked with 20 µL of ISTD (Table B1, Appendix) and mixed with 1 mL of MeOH for extraction in an ultrasonic bath three times for 10 min and with intermittent vortexing. The samples were then centrifuged at 2000 rpm for 5 min, and the supernatant was transferred for purification to Eppendorf tubes containing 25 mg ENVI-Carb absorbent and 50 µL of glacial acetic acid. Following vortexing and centrifugation of the extract at 10000 rpm for 10 min, the supernatant was transferred to autoinjector vials. Finally, a RSTD solution was added, the capped vials were vortexed and stored in a fridge until analysis.

Quantification and quality assurance

The analysis of PFASs was performed at NILU using ultra-high performance liquid chromatography triple quadrupole mass spectrometry (UHPLC-MS/MS). The internal standard method, which takes into consideration the added ^{13}C-labeled ISTD (Table B1), was used for quantification with linear regression of a seven point calibration point. One blank was run for every ten samples (one batch) for quality control, and the three times factor of the corresponding mean value was used as a method detection limit in the occasion of detects in the blanks within the same batch. Similarly, standard reference material (SRM) with a known concentration of PFAS was used every tenth sample to further validate the analysis of PFASs in plasma. In this study, human serum provided by the National Institute of Standards and Technology (NIST) was used as SRM. Unfortunately, no SRM is currently available for feathers, so none was applied in the analysis of this matrix. The recoveries for the ISTD averaged (±standard deviation, SD) 116 % (±15) and 79 % (±14) in feathers and plasma, respectively (Table B2). The limit of detection (LOD) was set to three times the signal to noise ratio for the analysed matrix when no blank concentration was detected. LOQ was defined as three times the LOD.

2.1.7. Stable isotope analysis (SIA)

This approach to feeding ecology can be of interest in exposure assessment studies, because it provides a tool to elucidate the link between diet and contaminant levels in avian tissues (Haukås et al., 2007; Jardine et al., 2006). In this study, differences in diet between locations may influence contaminant loads, as dietary accumulation is expected to be a relevant PFAS exposure pathway in the nestlings. Using carbon and nitrogen stable isotopes (SIs), we investigated the carbon sources in the diet and the trophic position in the food chain, respectively. The ratio of stable carbon isotopes (δ^{13}C) can be used to discriminate between ^{13}C-depleted terrestrial and ^{13}C-enriched marine ecosystems, or between terrestrial diets derived from C_3 and C_4 plants (Kelly et al., 2008). The ratio of stable nitrogen isotopes (δ^{15}N) is typically used to estimate trophic level because the heavier ^{15}N isotope increases throughout the food chain (Hobson and Welch, 1992). The difference in isotopic composition between a consumer's tissue and its diet is known as trophic enrichment and, in the case of δ^{15}N, it is due to preferential use of light amine groups during deamination and transamination processes (Macko et al., 1986). Altogether, the application of SIs as dietary tracers can provide a useful ecological approach in ecotoxicological studies (Jardine et al., 2006).

In this study, body feathers (from several individuals pooled per nest) were analysed for SIs, providing quantitative proxies for trophic ecology over the majority of the nestling stage. Since

blood circulation is connected to growing feathers during this period, feathers archive the changing blood biogeochemistry and hence the assumed dietary sources of PFAS exposure (Eulaers et al., 2013; Jardine et al., 2006). The analysis of stable carbon ($\delta^{13}C$) and nitrogen ($\delta^{15}N$) isotopes was carried out at the Laboratory of Oceanology at the University of Liège (Belgium) using continuous flow - elemental analysis - isotope ratio mass spectrometry (CF-EA-IRMS). A vario MICRO cube elemental analyser (Elementar Analysensysteme GmBH, Germany) was coupled to an IsoPrime100 mass spectrometer (Isoprime, United Kingdom). Isotopic ratios were expressed using the international δ notation (Coplen, 2011). Sucrose (IAEA-C6, $\delta^{13}C = -10.8 \pm 0.5$ ‰, mean ± SD) and ammonium sulphate (IAEA-N2, $\delta^{15}N = +20.3 \pm 0.2$ ‰, mean ± SD) were used as certified reference materials. Both of these reference materials are calibrated against the international isotopic references, i.e. Vienna Pee Dee Belemnite (VPBD) for carbon and Atmospheric Air for nitrogen. Standard deviations on multi-batch replicate measurements of lab standards (fish tissues) analysed interspersed among the samples (2 lab standards for 15 samples) were 0.1 and 0.3 ‰ for $\delta^{13}C$ and $\delta^{15}N$, respectively. Glycine (Merck) was used as elemental standard, and elemental contents were expressed as percentage of dry mass.

The trophic level of goshawk nestlings (per nest) was estimated based on $\delta^{15}N$ in the analysed feathers. To our knowledge, a specific enrichment factor has not been determined for the food chain of the studied species. A trophic enrichment factor (TEF) of $\Delta^{15}N = +3.4$‰ was therefore assumed, as recommended by Jardine et al. (2006) when TEF is unknown in a given food chain. In addition, primary consumers are often employed as baseline trophic level to minimize the effect of temporal and spatial variation at the food web baseline (Borgå et al., 2012). In this study, the Willow Grouse (*Lagopus lagopus*, terrestrial food chain in northern Norway (Halley et al., 2004), with average $\delta^{15}N_{primary\ consumer} = +0.98$‰ was used for Norwegian nestlings, whereas the Wood Pigeon (*Columba palumbus*, terrestrial food chain in SE Spain (Resano-Mayor et al., 2014), with average $\delta^{15}N_{primary\ consumer} = +5.52$‰ was employed for Spanish nestlings. The trophic level of a given predatory nestling was determined as described in Eulaers et al. (2013):

$$TL_{nestling} = \frac{\delta^{15}N_{nest} - (0.98\text{‰} + 3.4\text{‰})}{3.4\text{‰}} + 3 \text{ for Norwegian (Troms, Trøndelag) nestlings}$$

$$TL_{nestling} = \frac{\delta^{15}N_{nest} - (5.52\text{‰} + 3.4\text{‰})}{3.4\text{‰}} + 3 \text{ for Spanish (Murcia) nestlings} \quad \text{(Equations 2.5 \& 2.6)}$$

2.2. *In vitro* experiment 1: Plaque Assay

A plaque assay was carried out to evaluate the influence of PFOS on the severity of gallid herpesvirus-2 (GaHV-2) infection. This was relevant as it seems that environmental pollution increases the susceptibility and mortality of various species upon viral infections as revealed in a meta-analysis by Waugh and Jaspers (2018). The experimental part of this study was fully conducted at NTNU laboratory facilities. The experiments, involving cell culture and use of viruses, were carried out in a cell laboratory that complies with the regulations on the use of our virus model (biosafety level 2). To date, the zoonotic potential of GaHV-2 is very limited and potential infection of humans with this avian herpesvirus is very unlikely (Osterrieder et al., 2006). Two major components of the present *in vitro* experiments were chicken embryo fibroblasts (CEFs) (model system) and GaHV-2. Stocks of these were prepared before the start of the experiments as explained in Appendix C, and the plaque assay was performed as described in Appendix D.

However, the final step of the plaque assay (plaque counting) could not be carried out due to external contamination of the incubator and widespread lysis of CEFs. We noticed the presence of contaminating fungi in the facility, both into the incubator and the water bath after 7 days of infection. After washing off the crystal violet solution, which was used to stain the cell monolayers, we observed no living cells in most experimental wells. Although CEFs in our negative controls were alive after the staining, all the other cell treatments had died as indicated by the lack of stain in the wells after washing it off. It therefore seems that combined exposure to virus and/or pollutant with fungal contamination was too challenging for CEFs. Unfortunately, we did not have the time and resources to repeat this experiment. More studies are warranted to elucidate whether exposure to PFOS increases host cell susceptibility to various pathogens (DeWitt et al., 2012), and to determine the specific viral titer required to induce infection by GaHV-2 in CEF monolayers. Without results for the plaque assay we could not determine the viral titer to optimize infection during the second experiment. Accordingly, we decided to use the lowest possible dilution of the viral stock (10^{-1}).

2.3. *In vitro* experiment 2: PFOS-mediated modulation of gene expression

The second experiment was set to address the modulatory effects of PFOS on the expression of various genes associated with the early antiviral response. CEFs were chosen as a model system to study the combined effects of PFOS exposure and virus (GaHV-2) infection or stimulation with a synthetic RNA virus intermediate, namely poly (I:C). The following treatment groups

(1-8) were selected to carry out this experiment on PFOS-mediated modulation of immune gene expression:

1) Negative control
2) Exposure to PFOS (22.2 ppm)
3) Infection with GaHV-2 (without solvent)
4) Combination of both exposure to PFOS (22.2 ppm) and infection with GaHV-2
5) Infection with poly(I:C) (without solvent)
6) Combination of both exposure to PFOS (22.2 ppm) and infection with poly(I:C)

Two types of controls were included to account for potential pollutant solvent effects. These would provide the response of cells to GaHV-2 and poly(I:C) in the presence of the solvent:

7) Infection with GaHV-2 (with solvent)
8) Stimulation with poly(I:C) (with solvent)

The treatment effects were studied at different time points (or harvests) (Figure 2.2). CEFs were initially seeded in 96-well plates at a density of 5.24 x 10^4 cells/mL (100 µL/well). Eight biological replicates were arranged per treatment and time point (A-H, Figure 2.3). Cells were allowed to rest for 48h at 39ºC with 5% CO_2 before exposure to the corresponding solution (48h post-seed) by adding 80 µL to each well (Table D2: exposure, Appendix). The PFOS-exposed cells, because the stock solution was 50 ppm PFOS, were ultimately exposed to a dose of 22.2 ppm. The plates were then incubated for a 24-hour period before the infection or stimulatory stage (72h post-seed). At this point, we used previously prepared stock solutions of either GaHV-2 dilutions (10^{-1}) (Appendix D) or poly(I:C) (2 µg/mL) to stimulate the cells, with PBS (1% FCS) as negative control. The wells containing exposure solutions from the previous step were emptied, and then 80 µL of the corresponding stock solution was added per well (Table D2: stimulation, Appendix).

The culture CEFs and culture supernatants were harvested at 96h post-seed, every 6 hours for a 24-hour period (Figure 2.2). Firstly, supernatants were removed from cell culture plates using a multichannel pipette, and transferred to new 96-well plates. These were sealed and stored at -80ºC for protein analysis (not here). On the other hand, cell fractions (used here) were harvested via trypsinization. This consisted in first washing the CEF monolayer twice with PBS (100 µL) upon supernatant removal, adding trypsin (50 µL), and incubating at 39ºC for 5 minutes to resuspend the cells. Finally, 50 µL of media were added to stop the trypsinization reaction, and 100 µL of lysis reagent (QIAzol®) were added to break down resuspended cells.

The 96-well plates were covered with parafilm before storage at -80ºC until further use (section 2.3.1).

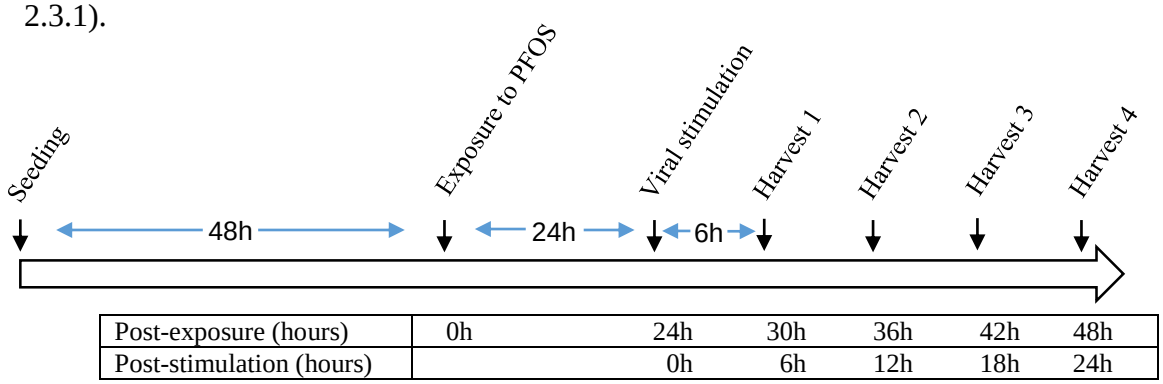

Post-exposure (hours)	0h	24h	30h	36h	42h	48h
Post-stimulation (hours)		0h	6h	12h	18h	24h

Figure 2.2. Timeline of pollutant exposure (PFOS) and viral stimulation (GaHV-2 or poly(I:C)) in this experiment. Harvesting timepoints are given as duration of the exposure period (hours post-exposure) or duration of the viral treatment (hours post-stimulation).

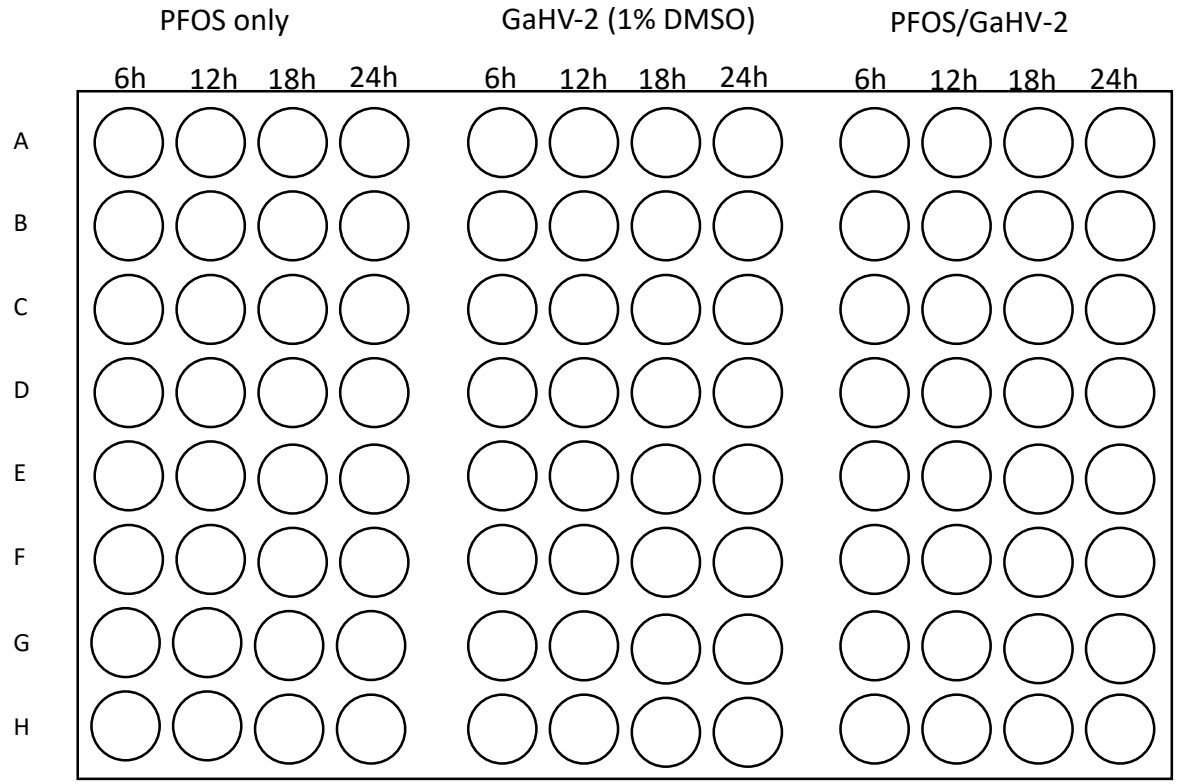

Figure 2.3. Example of 96-well experimental plates with three of the treatments, namely PFOS only, GaHV-2 (1% DMSO) and PFOS/GaHV-2. Each treatment consisted of four harvesting time points: 8h, 12h, 18h and 24h after the infection stage.

2.3.1. RNA isolation

The relative levels of target immune gene mRNA (IL-4, IL-8, NF-κB and TNF-α) and miRNA (miR-155) provide a snapshot of gene expression at the moment CEFs were harvested. Modulation of gene expression is the endpoint of this experiment and it was evaluated using cell harvests through the following procedure. First, the total RNA fraction was extracted using the miRNeasy Kit (Cat. No. 217004, Qiagen®) and the standard operating procedure from the manufacturer.

Replicates from the same treatment and time point were pooled into new tubes to obtain sufficient amount of RNA for later analysis, resulting in eight treatments per time point (32 samples in total). Chloroform (140 µL) was initially added to the tubes and these were shaken vigorously for 15 sec. Then the mixtures were incubated at room temperature for 2.5 min and centrifuged for 15 min at 12000 g and 4ºC. The supernatants (upper aqueous phase), containing the RNA fraction of interest, were transferred to new collection tubes. Ethanol 100% was next added (1.5x volumes) and mixed thoroughly by pipetting. RNeasy® Mini columns were loaded with the mixture and centrifuged at 8000 g for 30 sec to discard the flow-through. Then, we pipetted Buffer RWT (700 µl) onto the RNeasy Mini column, centrifuged and discarded the flow-through again. We repeated the previous step twice using Buffer RPE (500 µl), but with the second centrifugation step lasting 2 min. The extracted RNA fraction, including small RNAs, remains in the porous membrane of the Mini columns until final elution with 30 µL of RNase-free water. The tubes containing the eluted RNA extract were stored at -20ºC overnight.

2.3.2. cDNA synthesis

The RNA extracts were converted into cDNA through reverse transcription (RT) for later quantitative polymerase chain reaction (qPCR) analysis. Prior to this, the template RNA was thawed on ice and the RNA concentration was estimated using a NanoDrop® ND-2000cUV-visible Spectrophotometer (NanoDrop Technologies, Wilmington, DE, USA). This spectrophotometric approach to RNA quantity and quality relies on molecular properties that influence light absorption at different wavelengths (Desjardins and Conklin, 2010). One µL of template RNA was pipetted onto the end of the fiber optic cable of the instrument to obtain its concentration in the samples. RNA concentrations ranged from 14.0 ng/µL to 96.3 ng/µL in the present study. Estimation of total RNA concentration is an important step before cDNA synthesis as we aim to convert a fixed amount of RNA (50 ng/µL) from each sample into cDNA.

RT was then carried out using the miScript® II RT Kit (Cat. No. 218161, Qiagen®) and the standard operating procedure described by the manufacturer. A RT master mix was prepared based on the reagents and relationships presented in Table E.1 (Appendix). The volume of RNase-free water was adjusted based on the concentration of each template RNA. Then the corresponding volume of template RNA was added to each Eppendorf tube containing the reaction mix. Tubes were incubated at 37ºC for 60 min, and then at 95ºC for 5 min to inactivate the miScript RT mix. Finally, tubes were placed on ice and the resulting cDNA was diluted (1000 pg/µL) by adding 80 µL of RNease-free water. cDNA was aliquoted into 4 new tubes (4 x 25 µL) and stored at -20ºC until use in qPCR analysis.

2.3.3. Quantitative polymerase chain reaction (qPCR)

The expression of our target genes was evaluated through qPCR. This technique allows for amplification and real-time monitoring of fluorescently labelled template cDNA. Threshold cycle (Ct) values represent the number of amplification cycles needed to reach a fluorescent signal that is significantly above the background noise. These values relate inversely to the abundance of target genes in cDNA and can be used for relative quantification of gene expression (Gibson et al., 1996). In this study, the registered Ct values were used in statistical analysis (see 2.4.4). A SYBR® Green assay was conducted for this purpose, as recommended by the manufacturer of LightCycler® 96 instrument (Roche Diagnostics, Manheim, Germany). Firstly, cDNA templates were thawed and a reaction mix for amplification of target cDNA products was made. For the mRNA assays (IL-4, IL-8, NF-κB and TNF-α), the mix contained SYBR green and specific forward (10 µM) and reverse (10 µM) primers (Sigma-Aldrich®). For the miRNA assay (miR-155), we used the miScript SYBR green PCR kit, containing SYBR green, miScript Universal primer and specific miScript Primer assay (Qiagen®). Further details about the preparation of these reaction mixes are given in Table E.2 (Appendix). In addition to target genes, two housekeeping genes were incorporated in the qPCR analysis as potential control genes for the immune gene mRNA (28srRNA) and miR-155 (SNORD96A). These have been determined as stable control genes across treatments in a previous study (Waugh et al., 2018). Target and housekeeping gene cDNA was amplified using the primers shown in Table E.3 (Appendix). The analysis of different genes was conducted in separate qPCR runs. For a given gene, 14 µL of the reaction mix was added per well into a 96-well plate. Then, 6 µl of the corresponding template cDNA was transferred to each well. Two technical replicates were included per sample. The plate was covered and centrifuged at 1500 rpm for 1 min to spin down the mixture. Finally, amplification and collection of fluorescence data were carried out on a

LightCycler® 96 instrument, and the running conditions were adjusted for each gene (Table E.4, Appendix). Fluorescence was collected at the extension step. A melt curve analysis was carried out to rule out the possibility of non-specific amplification of the target genes.

2.4. Statistical analysis

Microsoft Excel was used for preliminary data handling and simple calculations. The Excel package *Solver Add-in* was used for imputation of missing concentration data (see 2.4.1). Concentration data plots were made through IBM SPSS Statistics 25 and R version 3.3.2 (R Core Team, 2015). The assumption of normal distribution was tested using quantile-quantile (Q-Q) plots and the Shapiro-Wilcoxon test ($p<0.05$) before further statistical analyses. Most PFASs concentrations were not normally distributed, except for PFUnDA in plasma and PFTrDA in plasma and feathers. Simple correlations between non-normally distributed variables were tested with the Spearman's rank correlation coefficient (rho) setting statistical significance at $p=0.05$. Correlograms were then plotted using the *corrplot* function in R (Taiyun and Viliam, 2017). Log-transformation was applied before one-way ANOVA, in order to meet the normality requirements of parametric statistical tests. Regarding gene expression results, raw Ct data were obtained through the LightCycler® 96 software, running a relative quantification analysis of the fluorescence data. Then, data analysis was performed in R using Markov Chain Monte Carlo simulations in the package *MCMC.qpcr* (Matz et al., 2013) (see 2.4.4) and the obtained estimates were plotted using SigmaPlot 13.0.

2.4.1. Handling concentration data below the LOQ

Only compounds detected above the LOQ in more than 50 % of the samples were included in statistical analyses. There are various methods to deal with samples below the LOQ, such as assigning random values between 0 and LOQ, or replacing by LOQ x QF, where QF corresponds to the quantification frequency (Voorspoels et al., 2002). In this study, a data imputation approach was implemented to obtain missing concentration data. This method requires the use of the package Solver add-in from Microsoft Excel. Briefly, concentrations below the LOQ were imputed by ln-transforming the measured data and fitting these to a cumulative normal distribution. The Solver add-in package uses the Generalized Reduced Gradient algorithm (John, 1998). This approach has been used in other studies as it seems to offer a better estimate of non-detectable concentrations relative to replacement methods (Croghan and Egeghy, 2003; Gyllenhammar et al., 2018). Details regarding LODs, LOQs, and QFs for all target compounds are shown in Appendix F. Pollutant concentrations are expressed in ng/mL (plasma) and ng/g ww (feathers) throughout the study.

2.4.2. Principal Component Analysis (PCA)

Principal component analysis (PCA) was performed using SPSS Statistics 25 to explore the dataset and investigate the preliminary relationships between a wide range of variables, including PFAS compounds and biological, spatial, and ecological variables. PCA was made with data from 37 individual nests. Two were not included due to missing stable isotope and plasma pollutant data. Specifically, the contributing quantitative variables were standardized and comprised all selected PFAS compounds in plasma and feathers, age, body condition, trophic level and $\delta^{13}C$. The corresponding loading and score plots are shown in the results section, whereas further details (eigenvalues, scores) are given in Appendix G. Varimax rotation method was implemented to maximize component's independence. The Kaiser-Meyer-Olkin (KMO) test and Bartlett's test of sphericity were used to confirm sample adequacy and suitability of data for reduction purposes, respectively. Component scores greater than three times the SD of the mean were considered outliers and removed from analysis.

2.4.3. Linear regression analysis

Linear regression from SPSS Statistics 25 was conducted to further address the effect of potential explanatory factors (biological, ecological, spatial) on the variation of PFAS concentrations among goshawk nestlings. All the selected individual compounds were used as dependent variables in separate models, to address the influence of certain predictor variables on their burdens in the nestlings. More specifically, we assessed the contribution of age, trophic level and dietary carbon source to the variation of pollutant concentrations in plasma of the Norwegian subset of nestlings (n=30). Predictor variables were entered/removed from the model in a backward stepwise manner at p=0.05. The AICc (Akaike Information Criterion corrected for small sample sizes) was used for entry/removal of independent variables. The most parsimonious model is presented along with alternative candidate models if $\Delta AIC \leq 2$. Provided R^2 values indicate how much variance a given model explains. Data was explored for influential outliers, normality and homoscedasticity of residuals.

2.4.4. Analysis of qPCR results

Data analysis was performed in R using the package *MCMC.qpcr* (Matz et al., 2013). Briefly, this involves analysis of the complete set of qPCR measurements by fitting a Bayesian linear mixed model with a Poisson distribution using a Markov Chain Monte Carlo (MCMC) chain. A MCMC chain was run for 13000 iterations, and the first 3000 were discarded, to estimate the change in target gene mRNA (or miRNA) in response to the fixed effects of treatment and time point. Control genes were not implemented in this analysis. This package allows for

simultaneous analysis of multiple genes. Firstly, raw Ct values were converted to molecule counts using the following equation:

$$\text{Count} = E^{(Ct1 - Ct)} \qquad \text{(Equation 2.7)}$$

Where E corresponds to the efficiency of amplification and was set to 2 for all the genes; Ct_1 (constant) represents the number of cycles required to detect a single target molecule and was set to 37 as recommended by Matz et al. (2013); and Ct (response) is the experimental value obtained after amplification of target genes (Matz et al., 2013). In this study, mRNA and miRNA transcript levels were modelled in the following way. A two-way design model was fitted using "treatment" and "timepoint" as fixed factors. The response variable of the model is the natural logarithm of transcript counting rate. As various genes are included in the model, "gene" accounts for different levels of expression between genes and constitutes the most basic explanatory variable. Additional terms are added to the model to describe gene-specific effects of experimental treatments ("gene:treatment") and time ("gene:timepoint"), plus their interaction "gene:timepoint:treatment". The random effect of the technical replicate ("sample") is also introduced in the model (Equation 2.8).

$$\ln(\text{rate}) \sim \text{gene} + \text{gene:treatment} + \text{gene:timepoint} + \text{gene:timepoint:treatment} + \text{sample} \qquad \text{(Equation 2.8)}$$

The results may slightly vary for each model fitting run due to the randomness in the MCMC process. The function HPDsummary() is recommended to extract and plot results in a design like this, with two fully crossed multilevel factors (Matz et al., 2013). This provided a summary plot of inferred transcript $\log_2$abundances (model estimates), which were finally arranged by gene using the function trellisByGene. Data for each gene were therefore shown on the same panel, where the x-axis corresponds to the levels of one factor ("time point"), and the levels of the second factor ("treatment") are presented in different lines. These plots were modified using SygmaPlot 13.0 to facilitate comparison between the different treatments of interest. Results were eventually plotted as $\log_2$(abundance) with ± SD of the estimate. Differences in expression across treatments were depicted via Tukey-style *post-hoc* pairwise testing (p=0.05).

All target genes and treatments were incorporated into statistical analysis of gene expression. Ct values and corresponding molecular counts were inspected prior to model fitting. miR-155 Ct values were unexpectedly high across treatments (35-43) and accordingly yielded very small molecular counts (0-3). In addition, high variation between technical replicates was detected

for miR-155 Ct values (Table E5, Appendix). The analysis of this particular target was repeated using a new cDNA template but it led to similar results. The amplification curve, besides indicating high Ct values for all treatments, did not show a sharp rise in the fluorescent signal (Figure E1, Appendix). This contrasts with the qPCR analysis of the other target genes. Altogether, this seems to indicate that the amplification was unsatisfactory, maybe owing to levels of mR-155 in our samples being too low for quantification, and this gene could not be included in the results.

3. Results

3.1. *In vivo* study

3.1.1. Levels of PFASs in plasma

Mean concentrations and ranges of PFASs in plasma of goshawk nestlings from Troms, Trøndelag and Murcia are presented in wet weight ng/mL in Table 3.1. Individual concentrations and additional information can be found in Appendix F. In this study, a total of nine compounds were found above the LOQ in more than 50 % of the samples, namely total perfluorooctane sulfonate (PFOS) (*n*=38/38), linPFOS (*n*=38/38), perfluorononanoic acid (PFNA) (*n*=38/38), perfluoroundecanoic acid (PFUnDA) (*n*=38/38), perfluorodecanoic acid (PFDA) (*n*=37/38), perfluorooctanoic acid (PFOA) (*n*=34/38), perfluorododecanoic acid (PFDoDA) (*n*=32/38), perfluorotridecanoic acid (PFTrDA) (*n*=32/38) and perfluorohexane sulfonate (PFHxS) (*n*=30/38). Of these, linPFOS, PFNA and PFUnDA were the most frequent overall as they were quantified in all individuals, whereas the remaining compounds were present in 79-97 % of the samples (Table F1, Appendix). linPFOS had the highest mean concentrations in Norwegian nestlings (6.4 ng/mL in Troms, 6.0 ng/mL in Trøndelag) followed by PFUnDA (1.0 ng/mL in Troms, 1.1 ng/mL in Trøndelag). PFUnDA therefore had the highest levels among the PFCAs in Norway. On the other hand, PFNA had the highest concentrations in Spanish nestlings (2.8 ng/mL) followed by linPFOS (1.7 ng/mL) and PFUnDA (1.5 ng/mL) (Figure 3.1). PFHxS was the least frequent among the studied compounds overall: it was not detected above the LOQ in any of the plasma samples from Murcia, although it was quantified in all except one sample from Norway (*n*=30/31). A significant difference between populations was found in the concentrations of PFHxS (Murcia<Trøndelag=Troms); $F_{2,35}$=14.1, p<0.001), linPFOS (Murcia<Trøndelag=Troms); $F_{2,35}$=5.5, p=0.008), PFNA (Murcia>Trøndelag=Troms; $F_{2,35}$=13.1, p<0.001) and PFDA (Trøndelag=Troms<Murcia); $F_{2,35}$=10.4, p<0.001) (Table 3.1). This suggested a different pattern of exposure between these populations, which was further investigated. Within each population, no differences between males and females were depicted (p>0.05).

The composition profile of PFASs in plasma (Figure 3.1) differed between Norwegian and Spanish populations, with remarkably lower contribution of ∑PFSAs to the overall burden in Murcia (20.6%) relative to Troms (63.2%) and Trøndelag (53.9%), and higher percentage of ∑PFCAs (79.4%, 36.8% and 46.1%, respectively). The profile of the two Norwegian populations is nearly identical, as suggested by the fairly similar contribution of each colour band to the total burden of PFASs (Figure 3.1). linPFOS was the most prominent PFAS in

plasma samples from Troms (51.7%) and Trøndelag (44.3%), whereas PFNA predominated in samples from Murcia (25.8%). The mean contribution of other PFCAs, such as PFOA, PFUnDA, PFDA and PFDoDA, was also higher in nestlings from Murcia.

Table 3.1. PFAS compounds in goshawk plasma samples from Troms, Trøndelag and Murcia. Arithmetic mean, median and range of plasma concentrations (ng/mL) are shown. Significant differences in the mean concentrations between locations (one-way ANOVA) are marked with different letters[a,b].

	Troms (*n*=11)			**Trøndelag** (*n*=20)			**Murcia** (*n*=7)		
	Mean	Median	Range	Mean	Median	Range	Mean	Median	Range
PFHxS[1]	0.44[a]	0.47	<0.15-0.94	0.47[a]	0.24	0.17-2.13	0.09[b]	0.09	<0.15
linPFOS[1]	6.37[a]	4.14	1.57-12.88	5.96[a]	4.29	0.64-21.65	1.71[b]	2.02	0.45-3.02
brPFOS[1]	0.96	0.57	<0.30-2.56	0.80	0.47	<0.30-3.14	0.33	0.25	<0.30-0.81
∑PFSAs	**7.76[a]**	**4.92**	**1.87-16.38**	**7.23[a]**	**5.11**	**0.93-25.64**	**2.13[b]**	**2.36**	**0.58-3.88**
PFOA[2]	0.44	0.29	<0.15-1.05	0.48	0.42	<0.15-1.62	0.93	0.81	0.34-1.92
PFNA[2]	0.75[a]	0.66	0.33-1.26	1.05[a]	0.98	0.38-2.27	2.77[b]	2.28	0.94-6.49
PFDA[2]	0.46[a]	0.35	0.16-0.89	0.56[a]	0.51	0.17-1.28	1.33[b]	1.09	0.58-2.17
PFUnDA[2]	1.00	0.73	0.39-1.89	1.10	1.09	0.46-1.75	1.46	1.37	0.62-2.78
PFDoDA[2]	0.50	0.48	<0.23-1.95	0.76	0.72	<0.23-1.99	0.93	0.84	0.41-1.36
PFTrDA[2]	0.75	0.63	<0.30-1.24	0.82	0.79	0.41-1.39	0.78	0.87	0.35-1.31
∑PFCAs	**3.91[a]**	**2.78**	**1.66-6.57**	**4.77[a]**	**4.80**	**1.80-9.87**	**8.20[b]**	**7.17**	**3.62-16.01**
∑PFASs	**11.67**	**7.70**	**3.53-22.95**	**12.00**	**10.57**	**2.73-31.36**	**10.32**	**9.08**	**4.38-19.89**

[1]PFSA, [2]PFCA

Despite the differing exposure pattern between Norwegian and Spanish nestlings, no significant differences in mean ΣPFASs were found between Troms (11.7 ng/mL), Trøndelag (12.0 ng/mL) and Murcia (10.3 ng/mL). The highest concentration of ΣPFASs (nine compounds) was measured in a male nestling from Trøndelag (31.4 ng/mL), while the lowest burden was found in another male from the same region (2.7 ng/mL). Among the PFCAs, odd-numbered chain length compounds (PFNA, PFUnDA and PFTrDA) were detected at almost 2-fold higher concentrations than even-numbered PFCAs (PFOA, PFDA, PFDoDA) ($F=19.5$, $p<0.001$). This can be depicted from Figure 3.1 as well, with odd-numbered PFCAs such as PFUnDA generally yielding wider bands relative to even-numbered PFCAs like PFDA, especially in Norwegian nestlings.

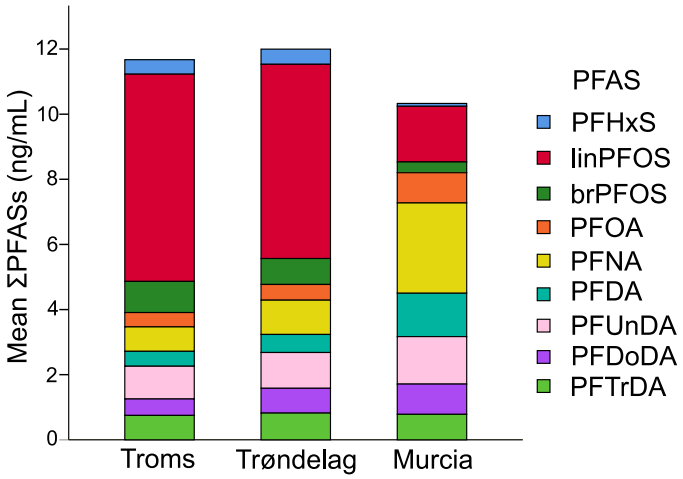

Figure 3.1. Concentration profiles in plasma (ng/mL ww) of selected PFASs in northern goshawk (*Accipiter gentilis*) nestlings from northern Norway (Troms) (*n*=11), central Norway (Trøndelag) (*n*=20) and southern Spain (Murcia) (*n*=7).

3.1.2. Levels of PFASs in feathers

The occurrence, mean concentrations and ranges of studied PFASs in goshawk feathers are presented in wet weight ng/g in Appendix F. Individual concentrations (pooled per nest) are shown too (Table F4, Appendix). A total of 13 compounds were detected in at least one feather sample above the LOQ, including PFTrDA (*n*=33/39), linPFOS (*n*=31/39), PFUnDA (*n*=27/39), PFDoDA (*n*=19/39), PFTeDA (*n*=17/39), PFHxS (*n*=17/39), PFNA (*n*=9/39), PFHpS (*n*=4/39), PFDA (*n*=3/39), PFOA (*n*=2/39), PFHxDA (*n*=2/39), PFOSA (*n*=2/39) and 8:2 FTS (*n*=2/39). Thus, only three of these compounds (PFTrDA, linPFOS, PFUnDA) were quantified in more than 50% of the samples and included into further statistical analysis (Table 3.2), with the long-chain PFTrDA as the most frequent overall, and in Trøndelag (*n*=21/21) and Murcia (*n*=8/8) compared to Troms (*n*=6/11). The prevalence of PFAS compounds in feathers is therefore much lower than in plasma. linPFOS had the highest mean concentration (2.9 ng/g ww) and highest individual nest concentration (9.4 ng/g ww) of all investigated PFASs in feathers. Among the least prevalent compounds, PFOSA, PFHpS and PFOA only occurred above LOQ in Norwegian birds, whereas PFDA could only be quantified in Spanish nestlings.

The occurence of PFOS isomers in feathers was more limited than in plasma and brPFOS was not detected in any sample. In turn, certain compounds were quantified in feathers but not in plasma, such as the long-chain PFHxDA and the intermediates PFOSA and 8:2 FTS. Although less frequent, linPFOS had the highest mean concentrations in feathers from Troms (2.0 ng/g) and Trøndelag (2.9 ng/g) as well, relative to PFUnDA (0.9 and 0.8 ng/g, respectively) and

Table 3.2. PFAS compounds in feather samples from Troms (*n*=12), Trøndelag (*n*=20) and Murcia (*n*=7). Arithmetic mean, median and range of feather concentrations (ng/g ww) are shown. Significant differences in the mean concentrations between locations (one-way ANOVA) are marked with different letters[a,b].

	Troms (*n*=12)			**Trøndelag** (*n*=20)			**Murcia** (*n*=7)		
	Mean	Median	Range	Mean	Median	Range	Mean	Median	Range
linPFOS	2.00	1.21	<0.15-6.7	2.92	2.14	<0.15-9.38	1.19	0.99	<0.15-2.1
PFUnDA	0.87	0.59	<0.54-1.82	0.79	0.84	<0.54-1.48	1.25	1.08	0.57-2.48
PFTrDA	0.78[a]	0.68	<0.56-1.42	2.48[b]	2.36	1.71-4.04	1.11	1.21[a]	0.59-1.64
∑PFASs	**3.81[a]**	**3.18**	**1.25-9.60**	**6.19[b]**	**5.82**	**2.68-12.50**	**3.54[ab]**	**3.23**	**1.83-5.62**

PFTrDA (0.8 and 2.4 ng/g, respectively). This pattern was not observed in Murcia, where the carboxylates PFUnDA (1.2 ng/g) and PFTrDA (1.1 ng/g) had similar contributions compared to linPFOS (1.2 ng/g). The highest burden of ΣPFASs in feathers was observed in a female chick from Trøndelag (12.5 ng/g), while the lowest concentration was detected in a male from the same region (2.7 ng/g). When comparing locations, significant differences were depicted for PFTrDA (Murcia=Troms<Trøndelag); $F_{2,36}$=52.8, p<0.001) and ΣPFASs (Murcia=Troms<Trøndelag; $F_{2,36}$=6.9, p=0.003) (Table 3.2). Therefore, goshawk nestlings from Trøndelag had higher levels of ΣPFASs (3 compounds) in feathers, and this associated with higher mean burdens of linPFOS and PFTrDA in this region, as shown in Figure 3.2. The relationships between individual PFASs in plasma and feathers are fully described and illustrated in Appendix H.

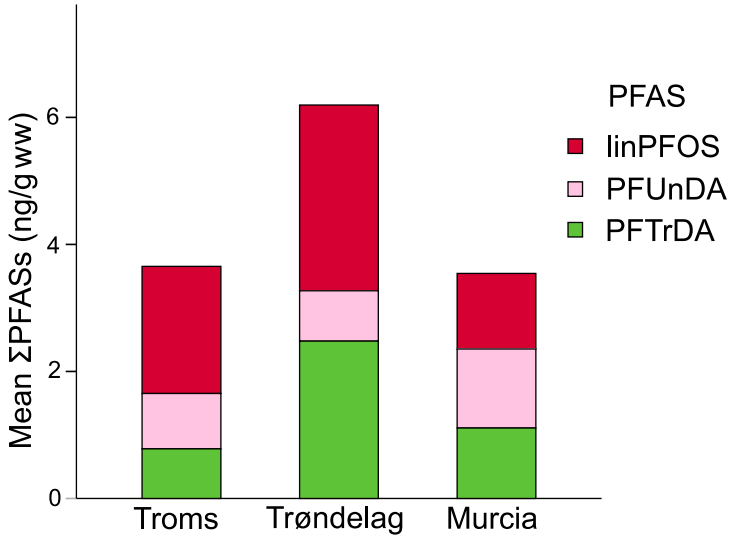

Figure 3.2. Concentration profiles in body feathers (ng/g ww) of selected PFASs in northern goshawk (*Accipiter gentilis*) nestlings from northern Norway (Troms) (*n*=12), central Norway (Trøndelag) (*n*=20) and southern Spain (Murcia) (*n*=7).

3.1.3. Relationships with biological variables

Mean nestling age differed between regions (Murcia< Troms=Trøndelag) ($F_{2,35}$=5.8, p=0.006) (Figure A6, Appendix), and relationships with PFAS levels in plasma were thus addressed on a region-dependent basis. Although positive associations with age were found when considering all samples together (n=38), namely for PFHxS (rho=0.32, p=0.049) and brPFOS (rho=0.31, p=0.054), they disappeared when using the Norwegian subset of nestlings only (p>0.05). Similarly, the relationships with mass were explored on a sex- and region-dependent basis, owing to sexual dimorphism and latitudinal differences in size. Significant positive associations were only found between mass and plasma PFNA for Norwegian females (rho=0.70, p=0.024). In addition, trends were observed for PFHxS (rho=0.55, p=0.10) and PFDoDA (rho=0.58, p=0.079). A positive trend was established for mass and PFNA in Norwegian males (rho=0.37, p=0.098). In the case of Spanish birds, low sample size of females (n=2) and males (n=5) rendered it difficult to address meaningful associations between age or mass with individual PFASs, and these could therefore not be assessed. Finally, correlative analyses showed no significant relationships between body condition and individual plasma PFASs (p>0.05), although the signs of the relationship were always positive.

3.1.4. Relationships with diet (SIA)

The mean isotopic values (‰ ± SD) per nest (pooled feathers) were -20.8 (± 0.59) (Murcia), -23.2 (± 0.48) (Trøndelag) and -23.2 ‰ (± 0.65) (Troms) for $\delta^{13}C$, and 7.67 (± 1.18) (Murcia), 7.34 (± 1.41) (Trøndelag) and 6.04 ‰ (± 2.02) (Troms) for $\delta^{15}N$ (Figure 3.3). No overall significant relationship was established between $\delta^{13}C$ and $\delta^{15}N$ (p=0.36), but a positive association was depicted in Troms (rho=0.69, p=0.019). Raw isotopic data are presented in Appendix I. The dietary carbon source of Norwegian nestlings differed from that of Spanish, where $\delta^{13}C_{TRD}=\delta^{13}C_{TRO}<\delta^{13}C_{MUR}$ (Kruskal-Wallis H_2=16.1, p=0.001) (Table I1, Appendix). No significant relationships were established between $\delta^{13}C$ and individual PFAS levels in Norwegian nestlings. However, within Troms, $\delta^{13}C$ was positively correlated with linPFOS (rho=0.92, p<0.001), PFDA (rho=0.84, p=0.002), PFUnDA (rho=0.84, p=0.003), PFNA (rho=0.82, p=0.004), PFDoDA (rho=0.81, p=0.005), PFOA (rho=0.81, p=0.005) and brPFOS (rho=0.78, p=0.008) in plasma. For $\delta^{15}N$, significant differences between populations were depicted as well, with $\delta^{15}N_{TRO}<\delta^{15}N_{MUR}=\delta^{15}N_{TRD}>$ (H=6.9, p=0.032) (Table I1, Appendix). Nonetheless, raw $\delta^{15}N$ data have limited utility in this study and, to check for variation in trophic level across the three regions, $\delta^{15}N$ data were baseline-corrected (as described in section

2.1.6). Differences in mean trophic level were observed between locations (H_2=19.3, p<0.001), with Norwegian populations feeding at relative higher positions than Spanish nestlings ($\mu_{TL\text{-}TRD}$=3.9, $\mu_{TL\text{-}TRO}$=3.5, $\mu_{TL\text{-}MUR}$=2.6) (Figure I1, Appendix).

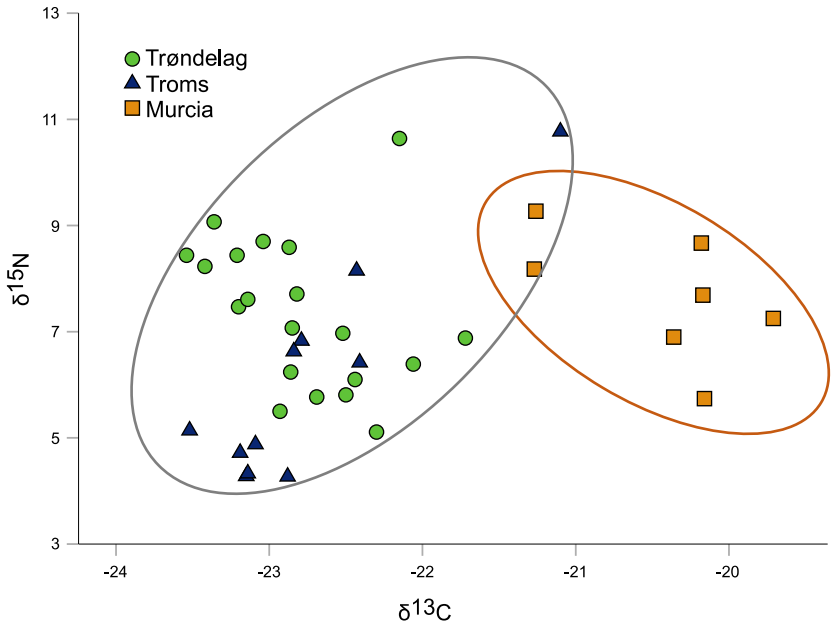

Figure 3.3. Raw $\delta^{13}C$ and $\delta^{15}N$ (‰) in body feathers (pooled per nest) of goshawk nestlings from northern Norway (Troms) (n=11), central Norway (Trøndelag) (n=20) and southern Spain (Murcia) (n=7). The circles represent the segregation of Norwegian (grey) and Spanish (orange) nests by their carbon source ($\delta^{13}C$).

Positive relationships between trophic level and individual PFAS concentrations were established, especially for PFSAs and the long-chain carboxylate PFTrDA in both plasma and feathers. Only positive associations with trophic level were found, with the following compounds showing significant relationships: linPFOS (rho=0.74, p<0.001) (Figure 3.4), PFHxS (rho=0.72, p<0.001), brPFOS (rho=0.69, p<0.001) and PFTrDA (rho=0.43, p=0.008) in plasma, and linPFOS (rho=0.48, p=0.002) and PFTrDA (rho=0.52, p=0.001) in feathers (Figure I2 A-D, Appendix). The ΣPFASs in plasma and feathers were positively correlated to trophic level as well (rho=0.52, p=0.001, rho=0.51, p=0.001, respectively). In addition, all the individual compounds, including PFCAs and PFSAs, were also positively correlated with trophic position when considering the Norwegian subset of birds only, as well as ΣPFASs in plasma and feathers (0.41<rho>0.78, p<0.05).

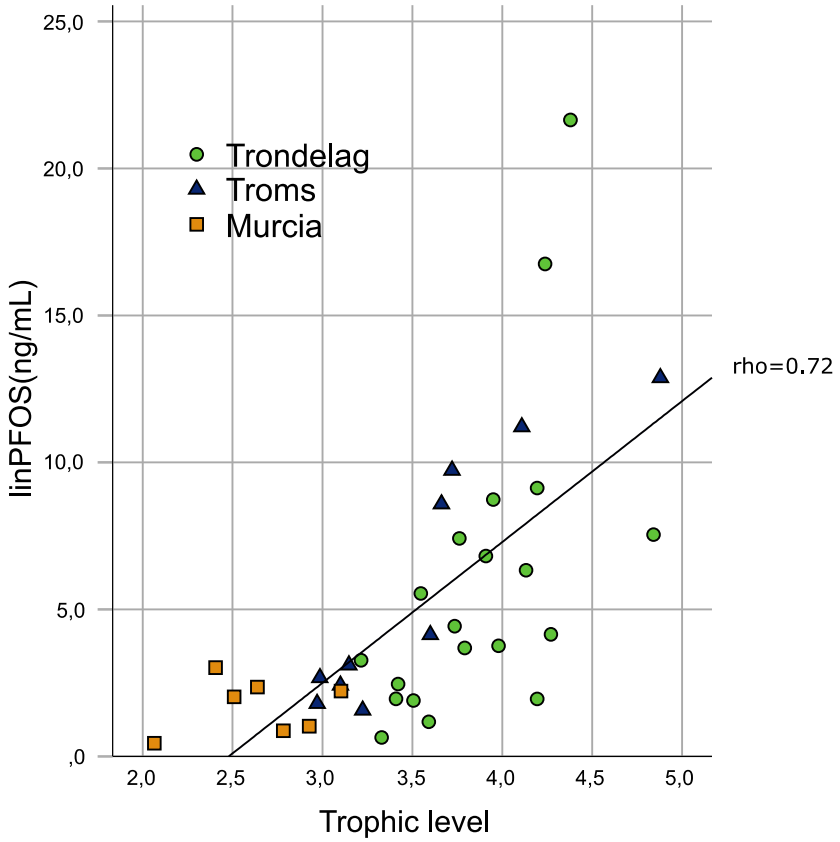

Figure 3.4. Relationship between trophic level and concentration of linPFOS in plasma goshawk nestlings from northern Norway (Troms) (*n*=12), central Norway (Trøndelag) (*n*=20) and southern Spain (Murcia) (*n*=7). A positive correlation was established based on Spearman's rank correlation (rho=0.72).

3.1.5. Evaluating the contribution of biological, spatial and ecological variation

Principal component analysis (PCA)

Principal component analysis (PCA) was used as a preliminary step prior to further statistical analysis, to visualize patterns between PFASs, biological, spatial, and ecological variables. A two-component solution was retained based on eigenvalues from the scree plot (Table G2, Appendix). Thus, two components (PC1 and PC2) were extracted and used to address the relationships between PFASs (plasma and feathers) and potential explanatory factors (age, body condition, $\delta^{13}C$, trophic level). PC1 and PC2 explained 66% of the total variation (PC1: 39%, PC2: 27%). The loading plot shows the relationships between the selected variables (Figure 3.5). The first component (PC1) included a clear grouping of most individual PFCAs (0.63<loading score<0.97), except PFTrDA in feathers. On the other hand, individual PFSAs were grouped into the second component (PC2) (0.71<loading score<0.91) (Table G3, Appendix). Among the potential explanatory variables, $\delta^{13}C$ and trophic level were relatively

well projected in the first (0.63) and second (0.83) dimensions, respectively. Body condition and age were however less well projected in any of the selected dimensions (loading score<0.6), and not significantly associated with each other.

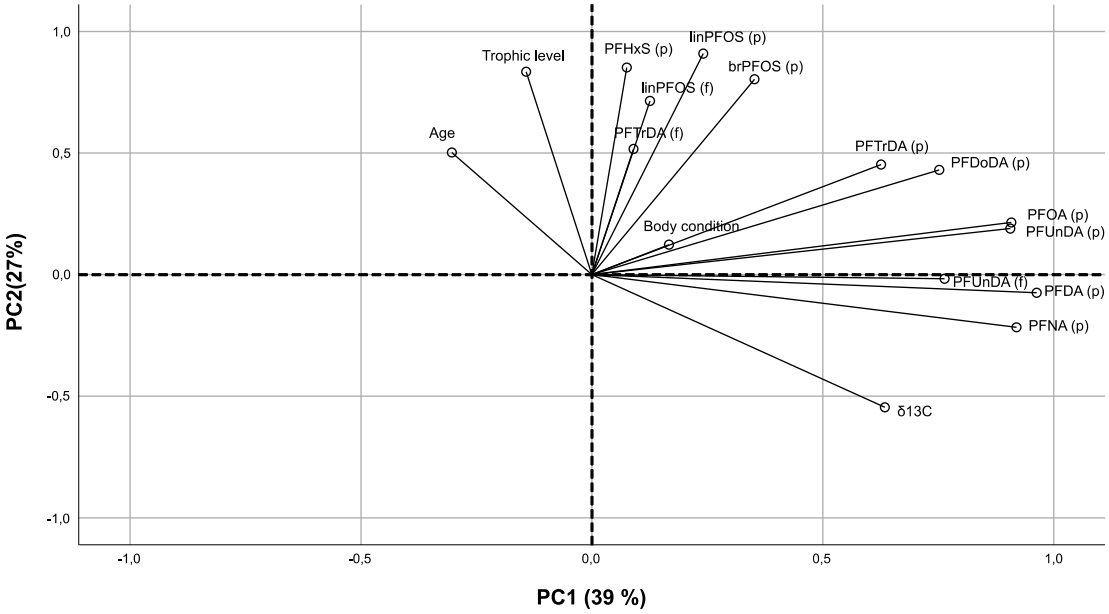

Figure 3.5. Loading plot corresponding to the Principal Component Analysis (PCA) of contaminants and selected biological, ecological and spatial variables. Dimension 1 (PC1) explained 39% of the total variation, whereas Dimension 2 (PC2) accounted for 27%.

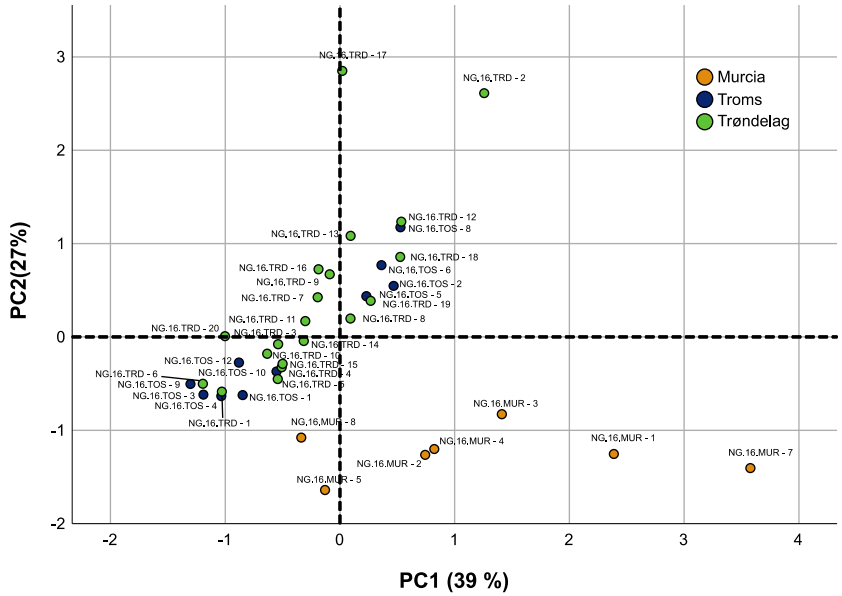

Figure 3.6. Score plot corresponding to the Principal Component Analysis (PCA) of contaminants and selected biological, ecological and spatial variables. Individuals (nests) are scattered in a two-dimensional space (PC1, PC2) and coloured after population.

The score plot (Figure 3.6) was used to represent all individuals, coloured after population, in a two-dimensional space according to their loadings. Spanish birds have on average higher PC1 scores (to the right) relative to Norwegian nestlings (to the left) (H=9.1, p=0.011). On the other hand, Norwegian birds have higher PC2 scores (higher up) (H=18.0, p<0.001). Furthermore, a broader range of PC2 scores was observed among Norwegian nestlings.

The relationships between individual PFASs, which can be inferred from the loading plot, were further explored using the nine congeners in plasma, and only positive correlations were established (Figure 3.7). Several significant associations were found, with pairwise correlations for brPFOS, PFOA, PFNA, PFDA, PFUnDA, PFDoDA, and PFTrDA with rho between 0.33 and 0.91. The strongest correlations were observed for the following pairs: PFOA-PFDA (p<0.001), linPFOS-brPFOS (p<0.001), PFDA-PFDoDA (p<0.001), PFOA-PFDoDA (p<0.001), PFNA-PFDA (p<0.001) and PFDA-PFUnDA (p<0.001). The associations between PFSAs and PFCAs were weak or absent. PFHxS was only correlated to linPFOS and brPFOS. These results are in line with the PCA loading plot and further suggest the need to account for the different PFASs in further statistical analyses.

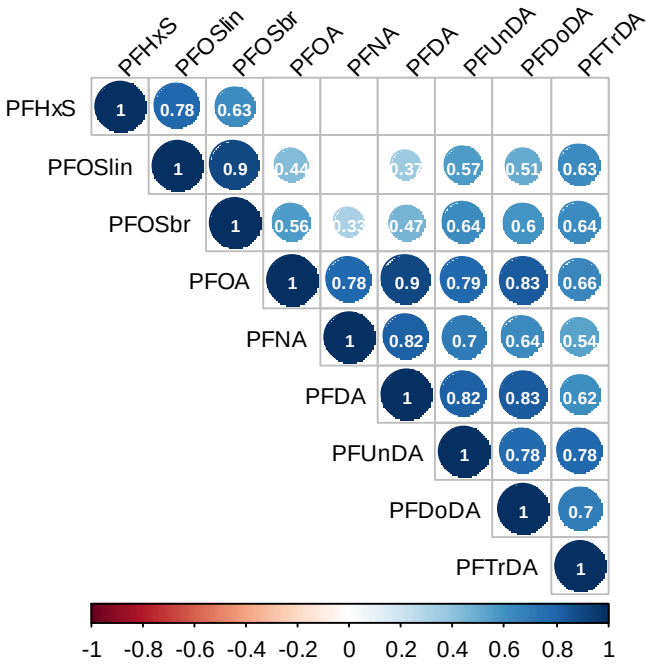

Figure 3.7. Non-parametric Spearman rank correlations between individual PFAS compounds in plasma (n=38) (*corrplo*t package in R). The correlation matrix was combined with the p-values from a significance test. Positive correlations are shown in blue circles, with colour intensity and circle size being proportional to the Spearman's rank correlation coefficients (rho). Correlations with p>0.05 are considered as insignificant and left blank in the plot.

Linear regression analysis

PCA was used as a preliminary step before linear regression analysis. More specifically, it helped to confirm variables of interest. Based on this, and in order to account for the apparently different sources of PFSAs and PFCAs, all selected individual compounds were taken as dependent variables in separate models. In addition, age, trophic level and dietary carbon source were selected as potential predictor variables, as we suspected based on their loadings that differences in age and diet could contribute to explain the variation in PFAS levels across nestlings in a given population. Therefore, the contribution of selected predictor variables to the variation of PFAS levels in plasma was further assessed in this section. Only Norwegian birds were included and pooled together for this analysis (n=30). A multiple linear regression was calculated to predict plasma PFAS concentrations based on the age, trophic level and $\delta^{13}C$ of goshawk nestlings.

Trophic level was the sole predictor for PFAS variation in all most parsimonious models (Table 3.3). The estimates of this predictor variable exclusively exhibited positive slopes ($0.23 < \beta < 0.51$, $p<0.05$). Regarding plausible alternative candidate models ($\Delta AIC \leq 2$), only three individual PFAS compounds, namely PFOA, PFTrDA and brPFOS, included age as a non-significant predictor in addition to trophic level (Table G5, Appendix). The contribution of age was positive for PFOA (p=0.24) and brPFOS (p=0.41), and negative for PFTrDA (p=0.29) levels in plasma. $\delta^{13}C$ was not included as a predictor of variation in any of the most parsimonious or alternative candidate models. Significant regression models were obtained for all individual PFAS compounds. PFHxS results did however not meet the assumptions of linear models and this compound was excluded from the table, in contrast to all other investigated PFASs (log-transformed). The strongest influence of trophic level was reported for PFOA and the two PFOS isomers, with regression coefficients ranging between 0.43 ($p<0.001$) and 0.51 ($p<0.001$), and the lowest for PFTrDA (β=0.23, $p<0.001$) (Table 3.3). The best fit models, with only trophic level as predictor, explained between 34% and 57% of the total variance in the levels of individual PFASs ($0.34 < R^2 < 0.57$).

Table 3.3. Model selection including the best fit models that predict variation in plasma concentrations of individual PFAS compounds (ng/mL) in relation to age (days), trophic level (TL) and dietary carbon source ($\delta^{13}C$) in Norwegian goshawk nestlings (*n*=30). Model selection was performed according to AICc.

log(PFOA)	β	SE	t	*p*-val
intercept	-2.00	0.37	-5.41	0.001
TL	0.43	0.10	4.19	0.003
F(1,28)=29.02 (p<0.001) R^2=0.51 AICc= -2.64				

log(PFNA)	β	SE	t	*p*-val
intercept	-1.00	0.25	-4.01	<0.001
TL	0.25	0.07	3.76	0.001
F(1,28)=14.12 (*p*=0.001) R^2=0.34 AICc= -13.74				

log(PFDA)	β	SE	t	*p*-val
intercept	-1.70	0.22	-7.64	<0.001
TL	0.36	0.06	6.14	<0.001
F(1,28)=37.72 (p<0.001) R^2=0.57 AICc= -20.67				

log(PFUnDA)	β	SE	t	*p*-val
intercept	-0.99	0.22	-4.48	<0.001
TL	0.26	0.06	4.43	<0.001
F(1,28)=19.62 (p<0.001) R^2=0.41 AICc=-20.86				

log(PFDoDA)	β	SE	t	*p*-val
intercept	-1.69	0.31	-5.39	<0.001
TL	0.38	0.083	4.59	<0.001
F(1,28)=21.02 (p<0.001) R^2=0.43 AICc= -0.15				

log(PFTrDA)	β	SE	t	*p*-val
intercept	-1.00	0.21	-4.87	<0.001
TL	0.23	0.05	4.22	<0.001
F(1,28)=17.84 (p<0.001) R^2=0.39 AICc=-25.5				

log(linPFOS)	β	SE	t	*p*-val
intercept	-1.16	0.39	-3.02	0.005
TL	0.48	0.10	4.71	<0.001
F(1,28)=22.16 (p<0.001) R^2=0.44 AICc=12.25				

log(brPFOS)	β	SE	t	*p*-val
intercept	-2.17	0.49	-4.48	<0.001
TL	0.51	0.13	3.97	<0.001
F(1,28)=15.78 (p<0.001) R^2=0.36 AICc=26.10				

3.2. *In vitro* experiment: PFOS-mediated modulation of gene expression

The results presented are referred to as changes in the relative mRNA expression (transcript log_2abundance) of four immune genes, namely NF-κB, TNF-α, IL-8 and IL-4, representing a relevant transcription factor in immune signalling, a classical cytokine marker of inflammation, a major pro-inflammatory chemokine and an anti-inflammatory cytokine, respectively. miR-155 expression was not included in the results due to analytical limitations for quantification (see 2.4.4). The indicated harvests (or time points) correspond to either the duration of the exposure to the pollutant (30, 36, 42, 48 hours post-exposure) or the duration of the poly(I:C) treatment and infection with GaHV-2 (6, 12, 18 and 24h post-stimulation) (see Figure 2.2). Different genes are presented in different plots (line colours), where treatments of interest (symbol colours) are compared.

3.2.1. PFOS-mediated effect on baseline immune gene expression

The potential effect of PFOS on the baseline expression of these genes (without viral stimulation) was firstly adressed. This was studied through pairwise comparisons of the negative control and PFOS-exposed cells at the different post-exposure time points. Following exposure to PFOS, the baseline expression of the cytokines IL-4 and IL-8 and the transcription factor NF-κB in general showed a decrease (Figure E2, Appendix). Such differences in relative

gene expression were particularly remarkable at 42h and 48h post-exposure. Specifically, the expression of IL-4 in PFOS-exposed CEFs was significantly lower relative to the control at 48h (p=0.004), with a trend at the previous time point as well (p=0.086) (Figure 3.8A). In a similar manner, baseline expression of IL-8 was lower in PFOS- exposed cells than in control cells, with lower mean values from 36h and a significant difference at 48h (p=0.021) (Figure 3.8B). Lastly, this pattern also applied to the transcription factor NF-κB, with lower baseline expression in PFOS-exposed cells over time (36h: p<0.001, 42h: p=0.007, 48h: p<0.001) relative to the control (Figure 3.8C).

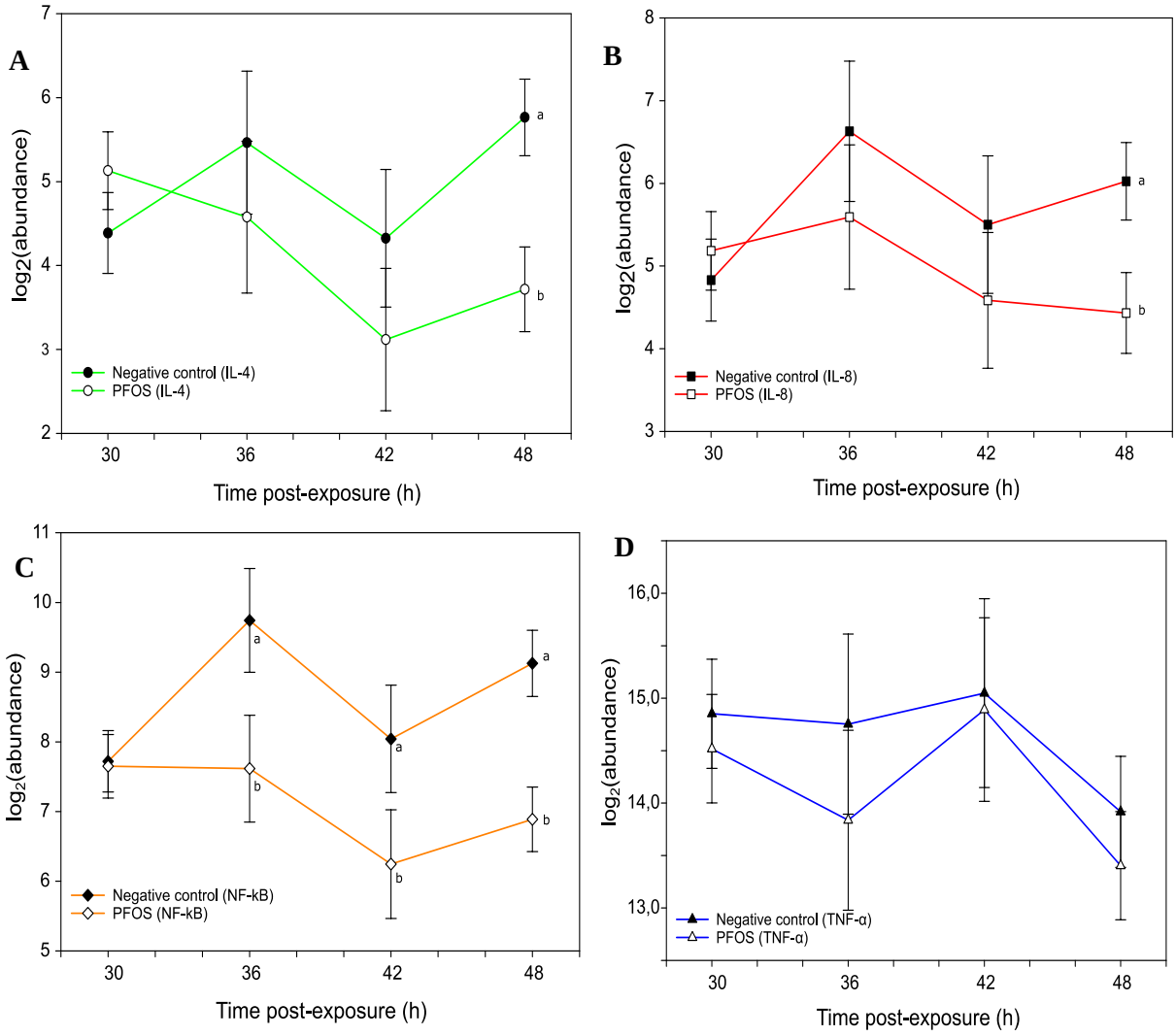

Figure 3.8. log_2(abundance) of gene transcripts (mRNA expression) in chicken embryo fibroblasts (CEFs) treated with PFOS (white symbol) versus the negative control (black symbol). The x-axis denotes duration of the post-exposure period and the y-axis the model estimate for IL-4 (A), IL-8 (B), NF-κB (C) and TNF-α (D). Model estimates are presented along with the SD in whiskers. Different letters denote a significant pairwise difference between the illustrated treatments. Reactions were performed in two technical replicates.

For TNF-α, mean expression in PFOS-exposed CEFs was similar or lower than in control cells, but no significant deregulation could be inferred in this case (Figure 3.8D). Overall, these findings indicate that PFOS deregulates the baseline expression of target immune genes, including two of the cytokines (IL-8 and IL-4) and the transcription factor NF-κB. This pattern is strongest for NF-κB at 48h, where PFOS induces a 5-fold decrease in gene expression relative to the control.

3.2.2. Gallid herpesvirus 2 (GaHV-2)

Response to viral stimulation

Potential changes in immune gene expression in response to GaHV-2 infection (without PFOS) were addressed in this section. This was investigated by comparing relative expression in control versus virally stimulated cells (Figures 3.9 A-D). Target gene expression following infection with GaHV-2 did not differ from the negative control for any of the investigated genes and time points (p>0.05). In the figures, this can be depicted from the proximity of the treatment estimates and overlapping error bars, which would indicate no differences between the treatments at 6, 12, 18 or 24h post-infection with GaHV-2. Solvent effects were ruled out by comparing gene expression in GaHV-2 against GaHV-2 (1% DMSO) –infected cells (Figure E3, Appendix).

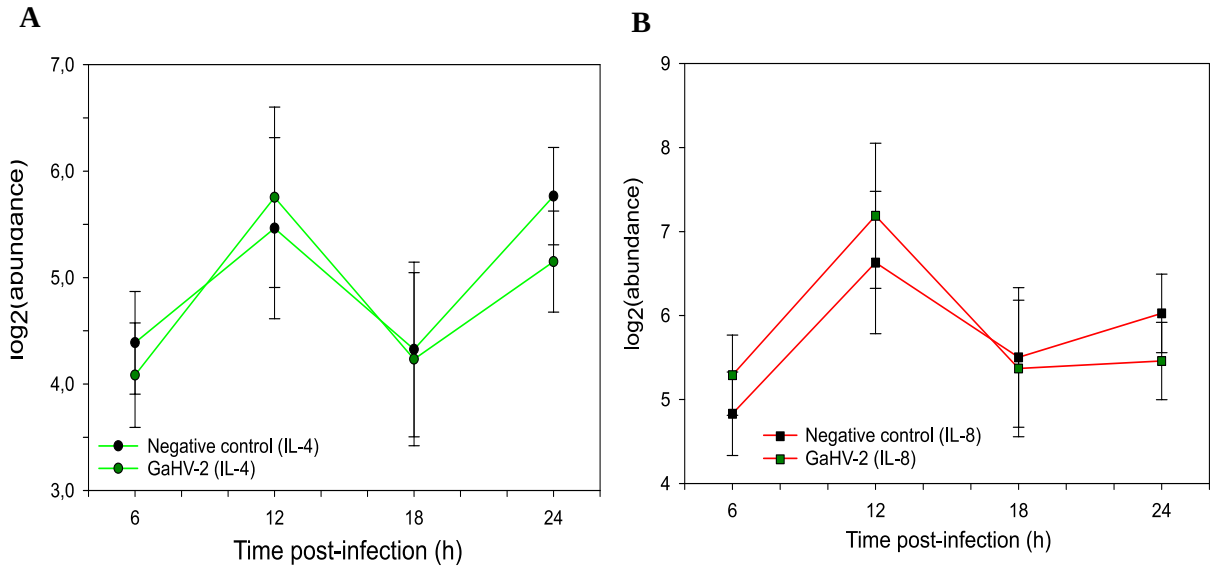

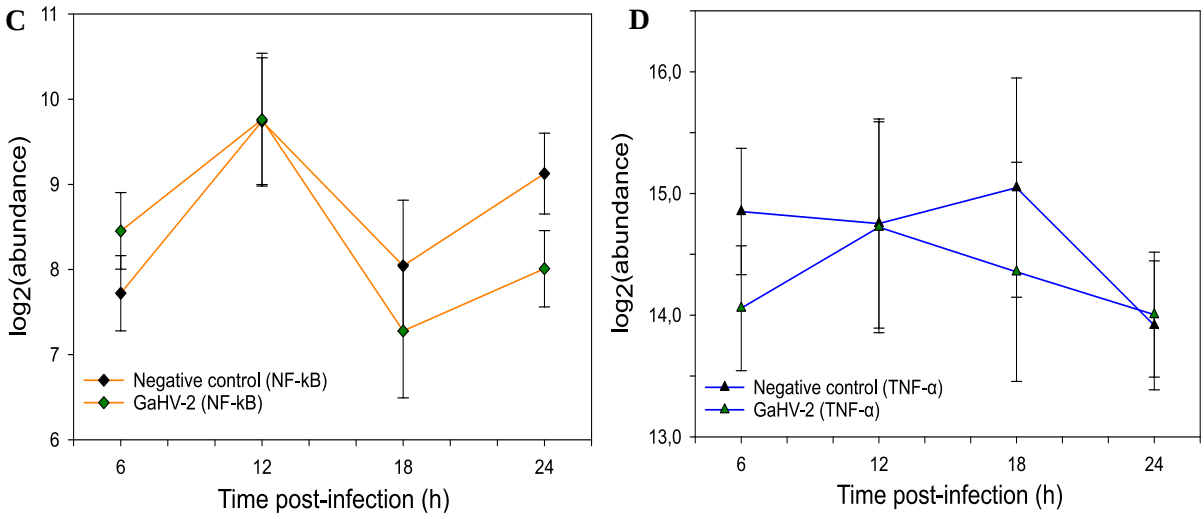

Figure 3.9. $\log_2$(abundance) of gene transcripts (mRNA expression) in chicken embryo fibroblasts (CEFs) infected with gallid herpesvirus-2 (GaHV-2) (green symbol) versus the negative control (black symbol).The x-axis denotes duration of the post-infection period and the y-axis the model estimate for IL-4 (A), IL-8 (B), NF-κB (C) and TNF-α (D). Model estimates are presented along with the SD in whiskers. Different letters denote a significant pairwise difference between the illustrated treatments. Reactions were performed in two technical replicates.

Response to PFOS exposure and viral stimulation

The expression in response to combined exposure and infection (PFOS/GaHV-2) was assessed in relation to the negative control and PFOS-exposed cells. No significant differences relative to the control were found for any of the investigated genes and time points ($p>0.05$). This can be depicted by looking at the latest post-infection time point (24h), which suggests a significant increase in expression relative to that in cells solely exposed to PFOS, for IL-4 ($p<0.001$), IL-8 ($p=0.013$) and NF-κB ($p=0.002$) (Figure 3.10 A-D). At 18h post-infection, there was a trend towards a higher expression of IL-8 in PFOS/GaHV-2 cells than in PFOS-exposed cells ($p=0.077$). For NF-κB, where expression decreased in response to PFOS only, mean expression was also higher but no trends could be established. For TNF-α, expression levels after 12h were higher in PFOS/GaHV-2 relative to PFOS-exposed cells ($p=0.031$). The expression of NF-κB after 6h was however higher in the PFOS/GaHV-2 group relative to control ($p=0.042$) and PFOS-exposed cells ($p=0.036$). In addition, both GaHV-2 only and PFOS/GaHV-2 yielded similar immune gene expression levels compared to the negative control (Figure E5, Appendix).

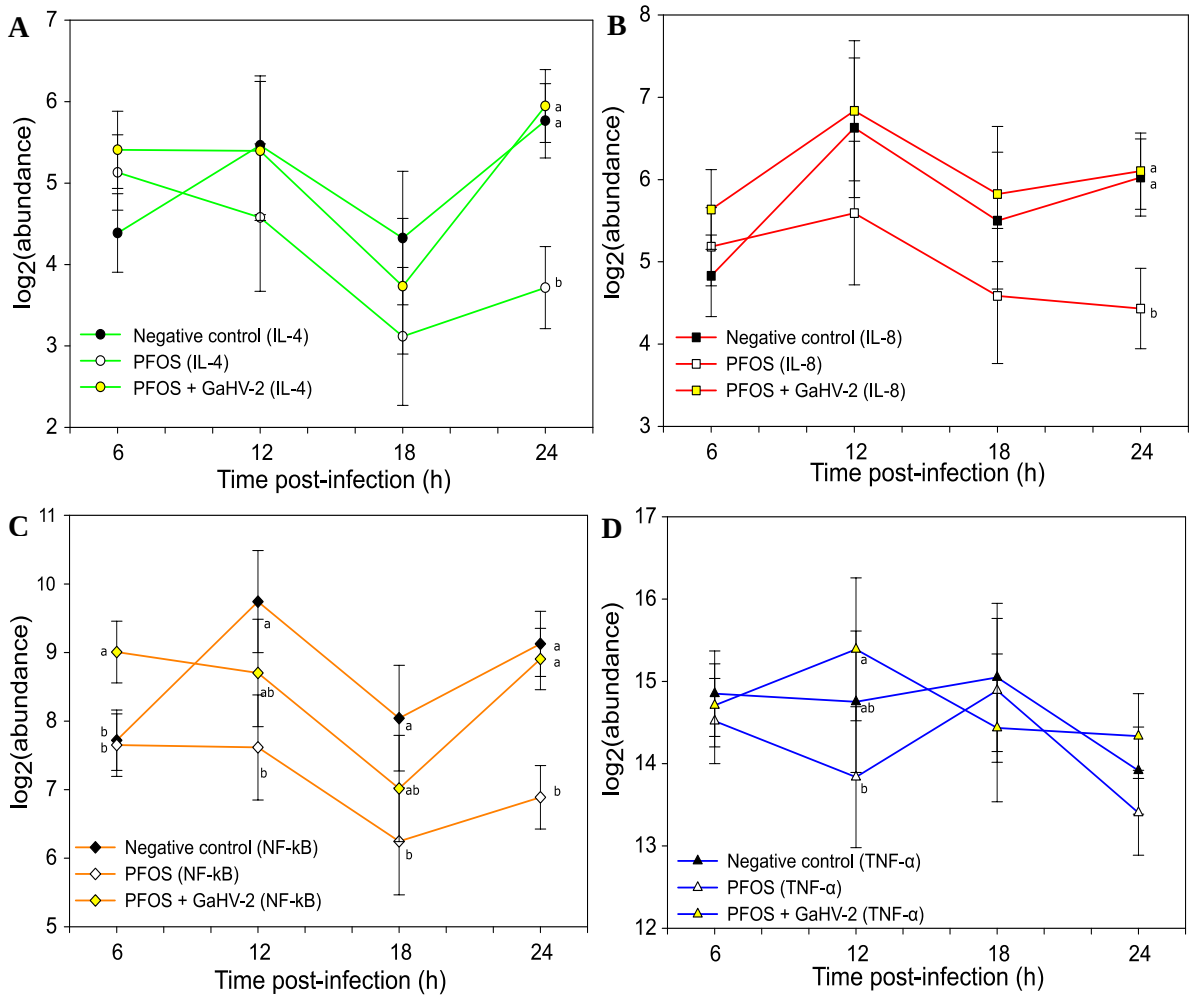

Figure 3.10. $\log_2$(abundance) of gene transcripts (mRNA expression) in chicken embryo fibroblasts (CEFs) treated with PFOS (white symbol), treated with PFOS and infected with gallid herpesvirus-2 (GaHV-2) (yellow symbol) versus the negative control (black symbol).The x-axis denotes duration of the post-stimulation period and the y-axis the model estimate for IL-4 (A), IL-8 (B), NF-κB (C) and TNF-α (D). Model estimates are presented along with the SD in whiskers. Different letters denote a significant pairwise difference between the illustrated treatments. Reactions were performed in two technical replicates.

3.2.3. RNA virus analogue poly(I:C)

Response to viral stimulation

Potential gene expression changes in response to poly(I:C) stimulation (without PFOS) were addressed in this section. IL-8 expression upon poly(I:C) stimulation decreased after 18h (p<0.001) and 24h (p<0.001) relative to the control (Figure 3.11B). Similarly, NF-κB expression was down-regulated at 18h (p<0.001) and 24h (p<0.001) post-stimulation (Figure

3.11C). The mean expression levels of TNF-α were nonetheless lower from the beginning, with significant differe1ces at 6h (p<0.001), 12h (p=0.002), 18h (p<0.001) and 24h (p<0.001) (Figure 3.11D). IL-4 expression after 24h was significantly decreased relative to the control as well (p=0.017) (Figure 3.11A). The strongest down-regulation of gene expression occurred after 24h and for the pro-inflammatory genes IL-8 (13-fold), NF-κB (5-fold) TNF-α (33-fold). Solvent effects were studied and ruled out as well by comparing gene expression in poly(I:C) against poly (I:C) (1% DMSO) –stimulated cells (Figure E4, Appendix).

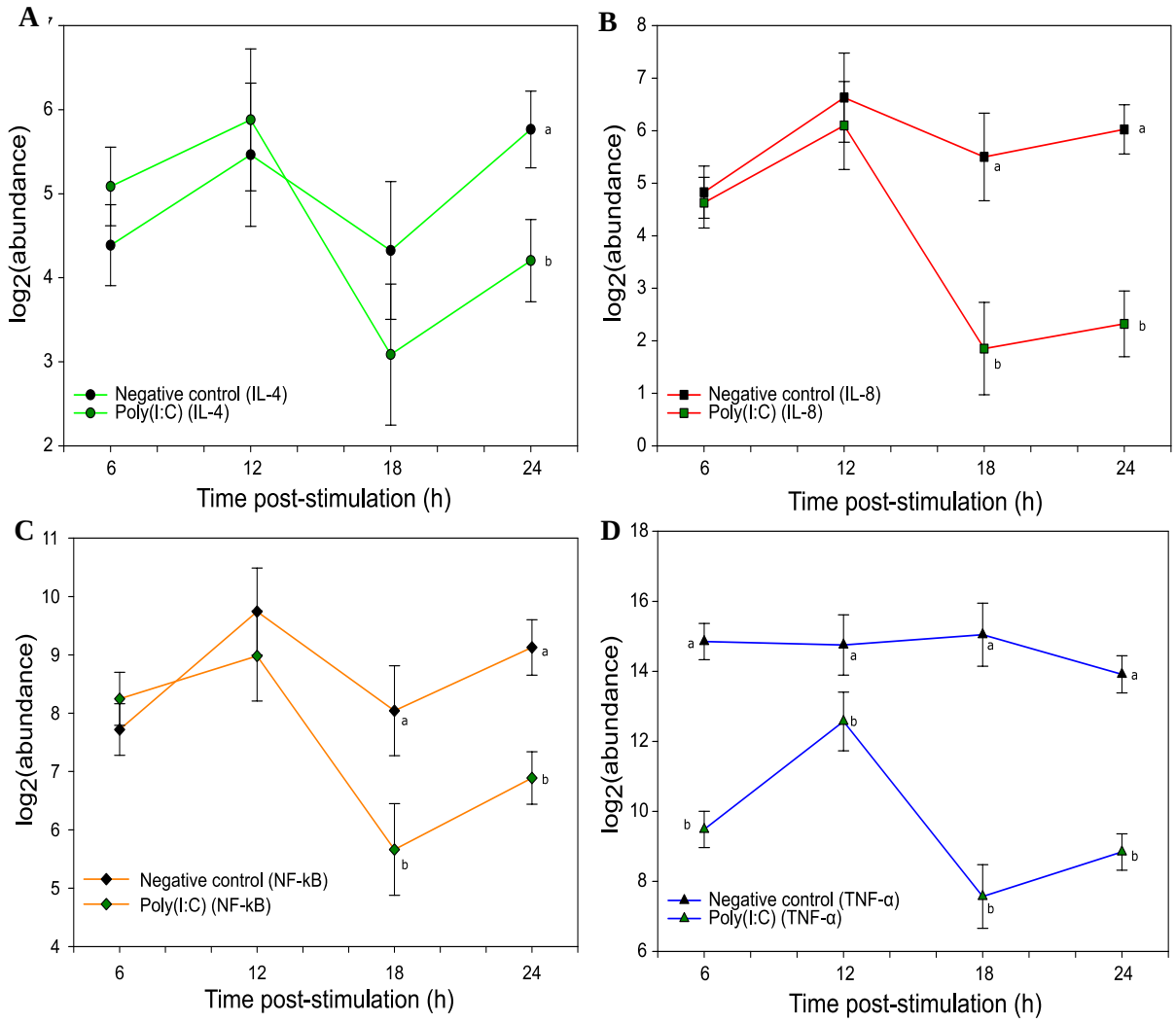

Figure 3.11. $\log_2$(abundance) of gene transcripts (mRNA expression) in chicken embryo fibroblasts (CEFs) stimulated with the synthetic RNA virus poly(I:C) (green symbol) versus the negative control (black symbol).The x-axis denotes duration of the post-stimulation period and the y-axis the model estimate for IL-4 (A), IL-8 (B), NF-κB (C) and TNF-α (D). Model estimates are presented along with the SD in whiskers. Different letters denote a significant pairwise difference between the illustrated treatments. Reactions were performed in two technical replicates.

Response to PFOS exposure and viral stimulation

Gene expression in response to combined exposure and viral stimulation (PFOS/poly(I:C)) WAS assessed in relation to that in control and PFOS-exposed cells. It was found that upon combined exposure to PFOS and poly(I:C), gene expression was similar (IL-4, NF-κB) or lower (IL-8, TNF-α) to that following single PFOS exposure (Figure 12 A-D). More specifically, the expression of IL-4 was lower than in the negative control at 24h (p=0.019), but it remains at similar levels relative to PFOS-exposed cells (Figure 3.12A). A similar pattern applies to NF-κB, with lower expression relative to the negative control at 18h (p=0.017) and 24h (p<0.001) (Figure 3.12C).

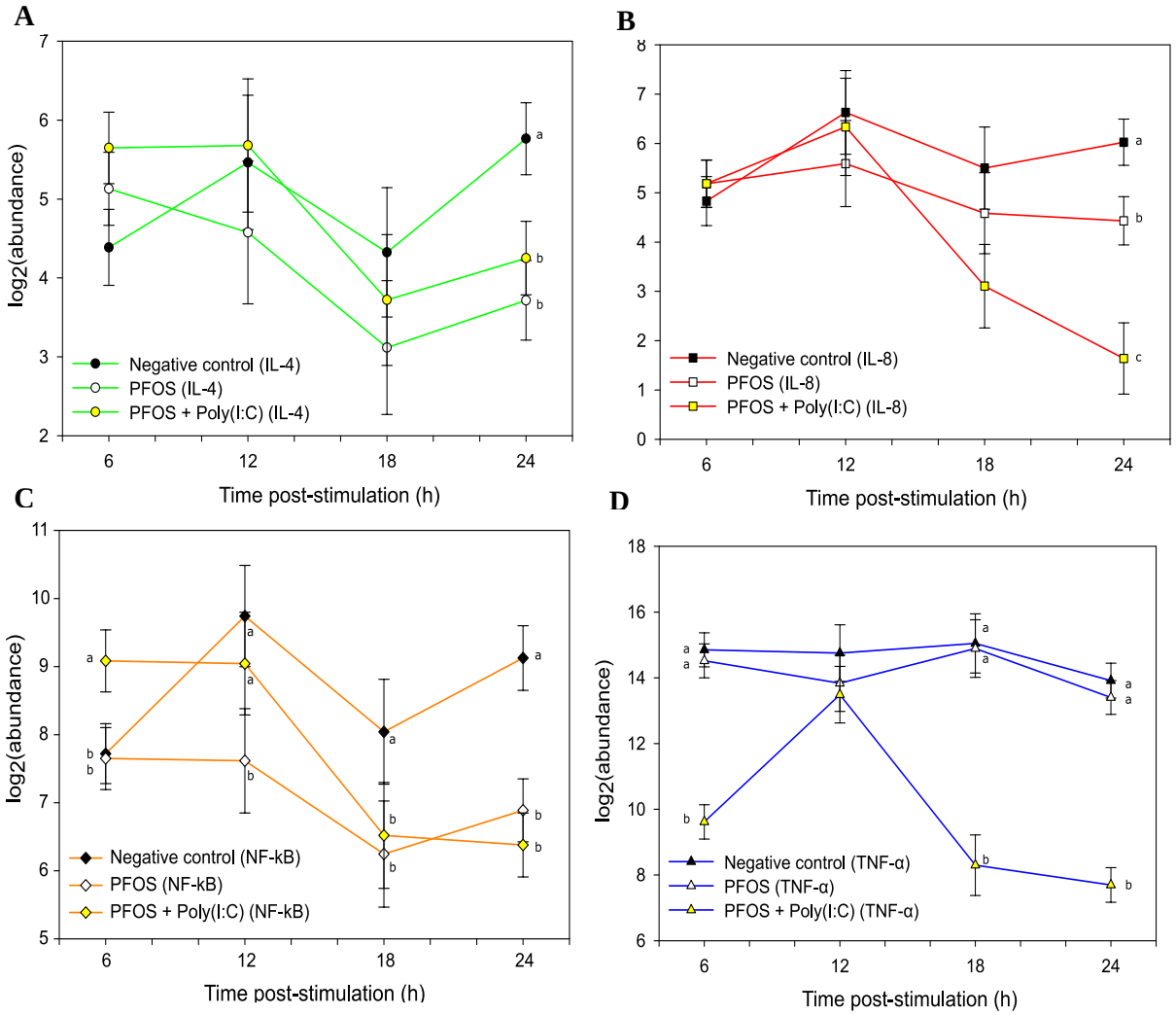

Figure 3.12. log_2(abundance) of gene transcripts (mRNA expression) in chicken embryo fibroblasts (CEFs) treated with PFOS (white symbol), treated with PFOS and stimulated with the synthetic RNA virus poly(I:C) (yellow symbol) versus the negative control (black symbol).The x-axis denotes duration of the post-stimulation period and the y-axis the model estimate for IL-4 (A), IL-8 (B), NF-κB (C) and TNF-α (D). Model estimates are presented along with the SD in whiskers. Different letters denote a significant pairwise difference between the illustrated treatments. Reactions were performed in two technical replicates.

For IL-8 and TNF-α, transcript levels at 24h were significantly lower in PFOS/poly(I:C) – treated cells than in the other two treatments (p<0.001) (Figure 3.12B & 3.12D). However, poly(I:C) only and PFOS/poly(I:C) treatments similarly yielded similar expression levels, and lower compared to the negative control (Figure E6, Appendix).

4. Discussion

This study aimed to investigate the levels of PFASs in wild goshawk nestlings and to evaluate the combined effects of one of the most prominent PFAS and virus infection, in a time-dependent manner, on innate immune signalling pathways. The results of the *in vivo* study are discussed before the results of *in vitro* expression of immunologically relevant genes. In the last section, the possible relevance of these findings to raptors is further discussed.

4.1. In vivo study

4.1.1. Levels of PFASs in goshawk plasma

Reports of PFASs in the terrestrial environment have been more limited than in the marine ecosystem (Butt et al., 2010), but there has been increasing interest over recent years. The plasma concentrations of total and individual PFASs reported in the study populations (Figure 3.1) were slightly lower than in goshawks from Troms area in 2008 (21 ng/mL – 10 compounds), much lower than in 2009 (151 ng/mL – 10 compounds), and slightly lower than in 2010 (25 ng/mL – 10 compounds) (Sonne et al., 2012) and 2015 (19 ng/mL – 8 compounds) (Gómez-Ramírez et al., 2017). The PFAS plasma profile in Norwegian populations of the current study was however comparable to Gómez-Ramírez et al. (2017), with linPFOS as the dominant compound (10.9 ± 8.1 ng/mL) followed by PFUnDA (1.7 ± 0.7 ng/mL) and PFNA (1.5 ± 1.4 ng/mL), although our nestlings had 1.7 (Troms) – 5.9 (Murcia) times lower PFOS levels. It was suggested that the relatively low levels of PFASs in Norwegian raptors result from combined long-range transport and bioaccumulation in local food webs, and high environmental persistence (Gómez-Ramírez et al., 2017)

Higher concentrations of total PFASs were detected in white-tailed eagles from northern Norway (45.4 ± 14.8 ng/mL) compared to goshawks, and this variation was attributed to differences in dietary habits between the two species (Gómez-Ramírez et al., 2017). In a similar study, PFOS clearly dominated the plasma profile of PFASs in white-tailed eagles from Steigen (23.1 ng/mL ww) and Smøla (17.8 ng/mL ww). This compound was followed by PFUnDA (3.7 and 3.4 ng/mL ww) > PFNA > PFDA > PFOA > PFHpS (Flo et al., 2016). The lower prevalence of PFOA among the PFCAs in wildlife, like in this study, is in agreement with its predominance in abiotic environmental matrices (Butt et al., 2010). Regarding PFOS isomers, linPFOS was much more abundant than brPFOS in this study. This is in agreement with preferential elimination of branched isomers through the food chain, with subsequent enrichment of the linear isomer in predators (Butt et al., 2010). Powley et al. (2008) reported levels of brPFOS

comprising 50% of the total PFOS burden in Arctic cod (*Arctogadus glacialis*) but only 5% in seals from the same food web in the Canadian Arctic (Powley et al., 2008). Therefore, the utility of PFAS isomers in source identification may be confounded by isomer discrimination during trophic transfer.

Among PFCAs, the higher proportion of longer and odd-numbered compounds has been related to the increased rate of elimination with decreasing carbon chain length, and higher bioaccumulation factors with increasing chain length up to PFTeDA (Lau et al., 2007; Martin et al., 2003). The tissue-specific accumulation of PFCAs and PFSAs appears to be associated with protein factors that are chain length dependent (Gebbink and Letcher, 2012). In addition, the depuration half-life of PFOA in white leghorn chicken is relatively short (5 days) compared to PFOS (125 days), which have the same chain length (Yoo et al., 2009). This may explain the higher prevalence of long-chain PFCAs and PFOS, and the non-detection (e.g. PFBS or PFBA) or lower concentrations (e.g. PFOA) of shorter-chain compounds in the current study. It could also be that the levels of certain compounds (4C-7C) in the environment are still low compared to longer-chain counterparts. Similarly, the emerging PFOS alternative F-53B was not detected in any goshawk sample. However, other studies have already reported increasing levels of the shorter-chain homologues (PFBA) in water and air, likely associated with conversion from longer chain perfluoroalkyl products (Möller et al., 2010; Pignotti et al., 2017; Weinberg et al., 2011), as well as bioaccumulation of F-53B in Chinese crucian carp (*Carassius carassius*) (Shi et al., 2015)

Altogether, it seems that plasma concentrations of PFASs in goshawks are similar or lower than previously reported in terrestrial and marine raptors. The composition profile does not differ much, with PFOS being the dominant compound overall followed by long-chain carboxylates (particularly odd-numbered). The current levels of PFASs in raptors rarely exceed toxicity reference values, which is estimated as 1.7 µg/mL for PFOS based on dietary intake in fish-eating raptors (Newsted et al., 2005), but bald eagle (*Haliaeetus leucocephalus*) nestlings have recently been found to be exposed to concentrations above that threshold (Route et al., 2014). In this study, none of the individuals approached the reference value, since highest levels of PFOS were 23.5 and 19.9 ng/mL in two nestlings from Trøndelag. These were also below the experimental lowest observed effect level (LOAEL) for any immune parameter in mice (91.5 ng/mL) (Peden-Adams et al., 2008) and chickens (154 ng/g serum) (Peden-Adams et al., 2009). Our findings would indicate that the investigated nestlings are not exposed to toxic levels of PFASs. However, slightly higher levels of ∑PFASs in kittiwake plasma (19.2 ± 5.25 ng/g ww)

associated positively with total thyroxin (TT4) and may relate to disruption of thyroid homeostasis (Nøst et al., 2012). In addition, the potential cocktail long-term effect of complex mixtures of PFASs and other pollutants in wild birds should not be overlooked. Toxicity is only well understood for a limited selection of PFASs (DeWitt, 2016), and the great number of compounds that coexist in animal tissues complicates risk assessment (Gómez-Ramírez et al., 2017).

4.1.2. Levels of PFASs in goshawk feathers

To our knowledge, this is the first study to report PFASs in both plasma and feathers of goshawks, and only a few others have looked at these compounds in feathers of birds of prey. The prevalence and concentrations of PFASs in adult feathers of eagle owls were remarkably higher than in the present study, with median levels of ΣPFAS (16 compounds) ranging from 17.5 ng/g ww in northern Norway to 41.6 ng/g ww in southern Norway (Dahlberg et al., 2017). Although at higher concentrations, the dominant compounds in feathers coincided with the ones in this study, namely linPFOS, PFTrDA and PFUnDA. The higher burdens in adult raptor feathers may underline the influence of external contamination on the feathers, which is probably higher in adults, since it is affected by moult strategy and preening behaviour (Espín et al., 2016). Nestling body feathers are minimally exposed to external contamination, whereas adult feathers of large raptors moult over 2 or more years and external contamination through atmospheric deposition and preen oil can occur over a more extended period (Eulaers et al., 2011b). In line with this, lower levels of PFASs than in adult terrestrial raptors were to be expected in our nestlings.

The overall predominance of linPFOS in feather samples as well, in terms of frequency of quantification and mean concentrations, is in agreement with its high prevalence and levels in biota and other tissues (Butt et al., 2010). Jaspers et al. (2013) investigated the levels of PFASs in tail feathers and soft tissues of barn owls (*Tyto alba*) near a point source of PFASs. PFOS was the most prevalent and abundant compound, with median concentrations ranging from 15.8 ng/g ww in feathers to 431 ng/g ww in adipose tissue. The median concentration of PFOS in feathers was therefore 7 (Trøndelag) to 16 (Murcia) times lower in this study. Eurasian sparrowhawks (*Accipiter nisus*) from the Antwerp region (Belgium), highly impacted by background levels of PFAS contamination, had even higher mean levels of PFASs in feathers (PFOS: 100 ng/g ww) (Meyer et al., 2009). Similarly, PFOS was the predominant compound in Accipiter sp. feathers from the Tibetan Plateau (4.67 ng/g ww) followed by the short-chain compounds PFBS (1.91 ng/g) and PFBA (1.39 ng/g). while the long-chain PFCAs were rarely

detected (Li et al., 2017b). This switch in the PFAS profile towards shorter-chain compounds has not been observed in the current study. In white-tailed eagles from Norway, linPFOS had the highest concentrations in feathers (5.2 ± 2.6 ng/g ww), while PFUnDA (1.01 ± 0.36) and PFTrDA (1.1 ± 0.4) dominated the PFCA profiles (Gómez-Ramírez et al., 2017). This resembles the pattern of Norwegian goshawk nestlings in this study, as these were the most frequent compounds in feathers, although at generally lower mean concentrations (Figure 3.2). The only exception was PFTrDA in goshawk feathers from Trøndelag, with a mean concentration more than two times higher (2.48 ng/g ww) compared to the white-tailed eagles. Nonetheless, the levels of ∑PFASs were 2-4 times lower than those found in white-tailed eagle nestlings (12.3 ng/g ww) (Gómez-Ramírez et al., 2017) and adults (12.5 ng/g ww) (Herzke et al., 2011) from Norway and Greenland.

In this study, the PFAAs precursors PFOSA and 8:2 FTS could be quantified in two feather samples from Trøndelag. Interestingly, the two nests with PFOSA burdens were located in the same area (Stjørdal) near the airport. In addition, one of these nests had the highest concentrations of linPFOS in plasma (21.6 ng/mL) and feathers (9.4 ng/g ww). This may indicate a local past or current source of PFAS contamination. The major source of PFAS contamination around airports is their historical use in aqueous film forming foams (AFFFs) during fire-fighting trainings and accidents (Awad et al., 2011). PFOS-containing AFFFs have a long shelf life (>20 years) and may still be used in accidental fires around the world (Posner, 2013). In contrast to feathers, PFOSA was not detected in any plasma sample. Løseth et al, submitted, Herzke et al. (2011) and Gómez-Ramírez et al. (2017) also detected PFOSA in feathers but not in plasma, although at higher frequencies (46-100 %) than this study. Higher frequency and concentrations of PFOSA in feathers than in plasma are suggestive that feathers may act as a passive air- and dust sampler, reflecting external contamination rather than internal burdens. An alternative explanation is that feathers constitute routes of excretion of PFOSA (Herzke et al., 2011), or that it is not detected in plasma owing to its stronger affinity to whole blood (Kärrman et al., 2006). This could apply to PFHpS as well, which was quantified in four feather samples from Norway but not in plasma. A different washing method may contribute to elucidate the origin of compounds detected in feathers but not in plasma (Gómez-Ramírez et al., 2017) and also to explain the overall higher levels of PFASs in feathers from Trøndelag. The influence of external contamination in this region might be higher due to proximity to urbanization and relatively older nestlings, which would result in longer exposure time to higher levels of air-borne pollutants. Regarding PFOA in feathers, Jaspers et al. (2013) suggested that

high levels may reflect external contamination from the air in the surroundings of point sources, but in this study, its prevalence and concentrations were much lower in feathers than in plasma. However, we cannot rule out the utility of feathers as passive air samplers of PFOA in the vicinity of point sources.

The significant associations between the investigated PFAS compounds in plasma and feathers (Figure H1, Appendix)) indicate that goshawk nestling feathers likely reflect internal concentrations. This is essential to use feathers as a biomonitoring matrix (Eulaers et al., 2011a). Previous studies addressing the utility of feathers in PFAS biomonitoring have mostly focused on the associations between concentrations in feathers and protein-rich internal organs like liver and muscle (Jaspers et al., 2013; Meyer et al., 2009). The relationships reported here are not as strong as in Eulaers et al. (2011a) for legacy POPs in plasma and feathers from white-tailed eagles ($p < 0.05$; $0.78 < r < 0.99$). This may indicate a limited suitability of feathers as non-invasive biomarker of PFAS exposure. Also, only three compounds could be investigated for relationships between feathers and blood (Figure H2), owing to the lower prevalence of PFASs in feathers ($n=3$) compared to plasma ($n=9$). This could be a downside for the use of feathers in PFAS monitoring, as they may not reflect all compounds detected in internal compartments. However, the fact that we used pooled (per nest) instead of individual feathers might have weakened the actual associations between the two matrices. Further investigation is required before feathers can be used in the monitoring of these compounds as a replacement to more invasive techniques (Gómez-Ramírez et al., 2017), and to better understand the stability and binding affinities of PFASs in feathers (García-Fernández et al., 2013). It has recently been suggested that feathers might not be a reliable PFAS biomonitoring matrix and that plasma should be prioritized (Løseth et al, submitted).

4.1.3. Comparison of goshawk populations

The prevalence and concentrations of PFASs in plasma of goshawk nestlings differed significantly between the populations of study. The composition profile was remarkably different between Spanish and Norwegian nestlings, in contrast to the highly comparable pattern between birds from Trøndelag and Troms. The fact that Spanish nestlings were significantly different to Norwegian in terms of age and trophic level (Figures A6 and I1, Appendix) complicated the assessment of predictors of PFAS variation. This could already be depicted from the PCA (Figures 3.5 & 3.6), where Spanish goshawks were consistently younger and feeding lower in the food chain. The possible influence of such biological and ecological variables is discussed in the next section (see 4.1.4). Generally, the levels of PFSAs in plasma

were higher in Norwegian birds while PFCAs predominated in Spanish nestlings. In line with this, PFOS represented a minor fraction of the total burden in Murcia, and so was true for PFNA in Trøndelag and Troms (Figure 3.1). We hypothesize that such differences in concentrations and profiles are partially explained by the contribution of differing sources of PFAS contamination. This is supported by a study on Audouin's gulls (*Larus audouinii*) from NE Spain, where PFNA in egg yolk (<LOD – 7.8 ng/g ww) was also the dominant PFCA (Vicente et al., 2015), like in plasma of Spanish goshawks from this study. However, PFOS was the most prominent compound overall in that study and in shearwaters (*Calonectris* spp.) from Murcia (Escoruela et al., 2018), which might indicate that PFCA contamination outweighs PFSAs in terrestrial but not in marine environments.

PFCAs have been primarily used as fluoropolymer processing aids and in numerous industrial and consumer applications (Kissa, 2001). In this study, PFNA concentrations were 3- to 4-fold higher in Spanish than in Norwegian goshawks. This compound has typically been used, in its ammonium salt form (APFN), for producing fluoropolymer dispersions like polyvinylidene fluoride (PVDF) (Prevedouros et al., 2006). PFNA is not an intended component of PVDF and derived uses, where this compound is only present at trace levels (Prevedouros et al., 2006). Nonetheless, it was estimated that 60% of the PFNA utilized in the manufacture of PVDF was emitted to the environment, making up a worldwide total of 400 to 1400 tonnes between 1974 and 2004. A commercial APFN was found to contain significant proportions of longer PFCA homologues like PFUnDA and PFTrDA as well (Prevedouros et al., 2006). To the knowledge of the author, fluoropolymer manufacturing sites have never been established in Scandinavia, whereas there are active production sites in Western European countries such as France or Italy (Ring et al., 2002). Major global producers committed to reduce and work towards the elimination of PFOA, higher homologues and precursors under the PFOA Stewardship Program (USEPA, 2006). These companies have recently met the USEPA program goals (USEPA, 2015), but past and current emissions by these and other manufacturers may account for the higher levels of PFCAs in the Spanish environment (Kannan, 2011). The use of ski waxes in Norway, which is connected to FTOH and related PFCA contamination (Chropeňová et al., 2016; Nilsson et al., 2010), does not seem to constitute an important local source of PFCA contamination into the Norwegian food webs of study.

Higher levels of long-chain and odd numbered PFCAs (e.g. PFTrDA) relative to their adjacent even chain counterparts (e.g. PFDoDA) indicate a contribution of atmospheric inputs via precursors (Braune and Letcher, 2012; Verreault et al., 2007). In line with this, we found a more

pronounced difference between odd and even numbered compounds (odd>even) in Norwegian nestlings. In addition, the contribution of atmospheric transport to overall long-range transport (LRT) is higher in PFCAs with longer-chain length, due to increasing air-water partition coefficients (K_{AW}) with chain length (Armitage et al., 2009). Accordingly, the higher ratios between longer- and shorter-chain compounds (e.g. PFTrDA/PFNA) found in Norwegian compared to Spanish nestlings could indicate LRT from direct sources of PFCAs as well. Altogether this can indicate that Norwegian populations are exposed to lower levels of PFCAs via atmospheric LRT of precursors and metabolites, in contrast with less distant sources of PFCA contamination in Spain.

The levels of PFSAs in plasma, on the other hand, are 3 to 4-fold higher in the two Norwegian populations. Although this might be more connected to ecological predictors like the diet (see 4.1.4), differing contribution of local sources could partially explain the observed differences between Norway and Spain as well. Estimates indicate that POSF-derived consumer products account for the historical release of 450-2700 tonnes PFOS into the environment (Paul et al., 2009). Among these, waterproof clothing, stain repellent treated carpets or AFFFs greatly contribute to the indirect emission of POSF derivatives into to the environment (Paul et al., 2009). The extent to which differences between consumer products in Norway and Spain can impact our findings is difficult to evaluate. However, it is likely that there is a differential use of consumer products between the countries, including outdoor clothing, which could contain and release PFSAs to the local environment. The estimated historical (1970 – 2002) global release of PFOS from textiles to the environment ranged from 120 to 600 tonnes (Paul et al., 2009), while the use of fluorinated substances as impregnating agents in general was between 13 and 34 tonnes in Denmark (Poulsen et al., 2005).

Although PFOS and related substances have been banned in Norway since 2007 (Seow, 2013), releases from existing stocks and high environmental persistence associated with past emissions could still impact the local environment. In addition, PFHxS, which shares common exposure sources with PFOS, was found at low levels but in all Norwegian nestlings and in none of the Spanish in this study. Increasing levels of PFHxS have been attributed to its use as surfactant substitute for PFOS and in textile protective coatings, for example (Zhang et al., 2017). The contribution of the metal plating industry, which uses PFSAs as mist suppressants, seems negligible in the Nordic countries, with less than 90 kg used every year (Posner, 2013). Altogether, the higher levels of PFSAs in plasma of Norwegian goshawks should be discussed in relation to biological/ecological factors and are not easily linkable with local pollution

sources, but they may relate to a differential historical use of POSF-derived consumer products in Norway (Posner, 2013). Despite the difficulties of PFAS source identification, which is beyond the scope of this study, these findings further underline the potential of predatory nestlings as sentinels for biomonitoring regional pollution as well.

4.1.4. Influence of the ecological and biological variables

The comparison between the populations should be discussed in relation to other potential predictors of variation which may actually contribute to explain the observed differences in plasma levels of PFASs among goshawk nestlings. The potential importance of age, trophic level and dietary carbon source is discussed here.

The importance of age

Age was one of the variables of interest in this study, as we hypothesized that dietary intake of PFASs would overcome the growth dilution of maternally transferred loads over time. The PCA suggested that age was more positively related to PFSAs and inversely related to PFCAs, although the loading of age into the extracted PCs was rather limited (Figure 3.5). The former was further supported by positive associations between age, PFHxS and brPFOS. Altogether, this could indicate a higher influence of dietary intake for PFSAs and maternally transferred loads (growth dilution) for PFCAs. The PFCA profile in blood of herring gulls (*Larus argentatus*) resembled the yolk pattern, indicating the potential of PFCAs for maternal transfer (Gebbink and Letcher, 2012). However, the highest concentrations of both PFSAs and PFCAs among the analysed matrices were in yolk (258 ng/g ww and 88 ng/g ww), which would highlight the potential for *in ovo* transfer of a wide range of PFAAs, including both PFCAs and PFSAs.

Nonetheless, according to our preliminary PCA and correlation results, we could not rule out the possibility that in the studied chicks 1) bioaccumulation of PFOS over time compensates the growth dilution of maternally transferred loads, and 2) the *in ovo* transfer of PFCAs has a higher influence than dietary intake. Interestingly, the former was suggested by Bustnes et al. (2013b) in predatory bird nestlings, where PFOS concentrations increased from 1 to 3 weeks after hatching and were notably higher (2.5-fold) than predicted from growth dilution. Similarly, the dietary uptake of PFOS outweighed elimination rates and explained its bioaccumulation over time , in yellow-legged gulls (*Larus michahellis*) and Audouin's gulls (*Larus audouinii*) (Bertolero et al., 2015).

In this study, however, the overall trend for positive relationships between age and PFSAs and negative between age and PFCAs might arise from a confounding effect of age: because Spanish nestlings were consistently younger than Norwegian, and they had lower burdens of PFSAs and higher levels of PFCAs, the overall relationships might not reflect the actual effect of age. The same would apply to the relationships between trophic level and individual PFASs, since lower trophic positions were reported in Spanish birds (Figure 3.4). This is why we decided to address the impact of age and trophic level only across Norwegian nestlings in linear regression analysis, to better understand if these were actually relevant intraspecific predictors of variation. Age was not selected as a predictor in any of the most parsimonious models. A combination of trophic level and age was only included in three alternative candidate models, and suggested a possible influence of age on PFAS burdens. In line with the previously discussed overall effect, age was positively related to the levels of brPFOS, and negatively associated with PFTrDA, indicating that dietary intake may predominate over growth dilution in PFSAs relative to PFCAs. The levels of PFOA in plasma, nevertheless, positively related to age. The influence of maternal transfer on PFOA levels seems lower than that on longer-chain PFCAs like PFTrDA (Holmström and Berger, 2008). PFOA was only detected in one out of ten clutches of Audouin's gulls (Vicente et al., 2015) and exhibited the lowest detection frequencies and concentrations among the PFCAs osprey and common kestrel eggs (Eriksson et al., 2016). This would result in low levels of PFOA from maternal transfer and PFOA being mostly incorporated through dietary intake. It is therefore possible that the levels of these compounds are influenced by a combination of trophic level and nestling age, but only trophic level was a significant predictor of PFASs overall.

The lack of a clear and significant trend regarding PFAS variation over time may reflect that dietary intake by feeding chicks compensates growth dilution, resulting in fairly stable levels of PFASs over time. Alternatively, we cannot rule out that the relatively narrow range of age in the studied Norwegian nestlings (27-35 days) may have weakened the associations. Sampling the same bird twice at the early and late nestling period, like in Bustnes et al. (2013b), is recommended to specifically address the influence of growth dilution and dietary intake on PFAS levels in nestlings.

The importance of trophic level

The influence of trophic level was addressed using food web $\delta^{15}N$ baseline correction. This approach employed available isotopic data from relevant primary consumers in the Spanish and Norwegian goshawk food chains (Halley et al., 2004; Resano-Mayor et al., 2014) to estimate their relative position in the food web. Ideally, a study of prey items would have been included to obtain our own baseline values. Therefore, the reported trophic levels only represent an approximation to trophic ecology, but underline the importance of baseline correction when aiming to compare different food webs. This approach resulted in Spanish nestlings feeding at significantly lower trophic levels (Figure I1, Appendix). The diet of goshawks from Murcia comprises mostly pigeons, as implemented in the baseline correction, and to a lower extent other medium-size birds like Eurasian jay (*Garrulus glandarius*), blackbird (*Turdus merula*) or song thrush (*Turdus philomelos*), mammals like rabbit (*Oryctolagus cuniculus*) and red squirrel (*Sciurus vulgaris*), and reptiles like ocellated lizard (*Timon lepidus*) (pers. comm. J.E. Martínez). A switch in the diet from rabbits to small birds resulted in increased accumulation of organochlorines in Spanish goshawks (Mañosa et al., 2003). Rabbits can represent a prominent low-trophic-level prey item for goshawks in Spain (15-23% of total) (Mañosa, 1994; Padial et al., 1998; Pelufo et al., 1990; Verdejo, 1994). This may partially account for a lower exposure to certain PFASs, with known biomagnification potential (Butt et al., 2010), in goshawk nestlings from Murcia (e.g. PFOS). It has also been suggested that a higher contribution of small birds in the diet enhances the accumulation of POPs in birds of prey (Jaspers et al., 2006), and this could apply to certain PFASs as well (Jaspers et al., 2013). Annual variation in PFAS exposure in goshawks has been reported (Sonne et al., 2012), which might be explained by such dietary shifts.

In this study, trophic level was the main predictor of individual PFAS exposure within the Norwegian populations. It significantly contributed to explain the variation of all selected compounds, including both PFSAs and PFCAs. The log-transformed concentrations of the individual compounds (e.g. logPFOA) increased between 0.24 and 0.51 per trophic level (Table 3.3). For example, the predicted PFOA burden in Norwegian nestlings (log-transformed) was equal to -2.00 + 0.43 (trophic level). This indicates that not only PFSAs, but also PFCAs can biomagnify across the goshawk food chain. The fact that overall relationships (including Spanish nestlings) between trophic level and individual PFCAs were generally not significant further suggests that differences in baseline PFCA contamination between these regions might blur biomagnification processes. In fact, positive overall relationships were only found for the

PFSAs, except for a weak association with PFTrDA (Figure I2, Appendix). Higher baseline levels of PFCA contamination in Murcia may have obscured the positive relationship between individual PFCAs and trophic level. This is also suggested by significant and positive associations when only considering the Norwegian subset of birds. It is therefore likely that PFCAs, especially the long-chain, also have the ability to biomagnify across the studied food chains (Butt et al., 2010).

The reported intraspecific increase in PFAS levels with trophic level contrasts with Bustnes et al. (2013b) who did not find any relationship between trophic position and PFOS concentrations in goshawks and white-tailed eagles. Similarly, no correlations were found between egg PFOS concentration and trophic levels in black guillemot and glaucous gulls (Haukås et al., 2007). The associations between $\delta^{15}N$ and PFASs in feathers of white-tailed eagles were positive but non-significant (Gómez-Ramírez et al., 2017). This may relate to broader ranges of trophic level in the current study, which would be necessary to reflect biomagnification processes within a given species. The positive relationships between trophic level (based on feather analysis) and levels of PFASs in plasma also underline the utility of feathers as dietary tracers in ecotoxicology (Jardine et al., 2006). While stable isotopes in blood provides recent information about the diet, growing feathers integrate dietary information over a longer period of time (Pearson et al., 2003). In this sense, recent ingestion of highly polluted prey items could weaken the associations between feather-based trophic level and PFASs in plasma, but this does not seem to be the case in this study.

The importance of the dietary carbon source ($\delta^{13}C$)

The dietary carbon source ($\delta^{13}C$) was not included in any of the most parsimonious models as well, neither in alternative candidate models. In Eulaers et al. (2013), similarly, $\delta^{13}C$ did not contribute to explain the levels of POPs in goshawk nestlings from Troms. However, in that study, regional nest location influenced the burden of certain pollutants, such as PCB-153, which was at higher levels in coastal relative to inland nests. Interestingly, in this study, the positive association between $\delta^{13}C$ and individual PFASs in Troms may suggest that within this population there is an effect of the carbon source. Positive relationships between contaminants and $\delta^{13}C$ indicate marine sources, whereas negative ones are linked with freshwater or terrestrial intake (Boutton, 1991). This might therefore indicate an influence of marine-derived diets on PFAS exposure in goshawks from Troms in this study. The higher levels of PFASs found in a marine predator, namely the white-tailed eagle relative to the goshawk in Troms, associated

with higher $\delta^{13}C$ values as well (Gómez-Ramírez et al., 2017). Fish-eating animals generally accumulate higher burdens of PFASs (Lau et al., 2007), and lower concentrations have been found in terrestrial relative to aquatic species (Borg and Håkansson, 2012). Because goshawks can feed on marine prey like waders and gulls (Cramp and Simmons, 1980), particularly in Troms (pers. comm. K.O Jacobsen), the positive association between $\delta^{13}C$ and $\delta^{15}N$ in that region could be attributed to a higher frequency of such higher trophic level and marine prey in the goshawk diet (Tornberg et al., 2009). The breeding range of the goshawk in Troms is mostly dominated by coastal and fjord habitats (Figure A2), and the broadest trophic ($\delta^{15}N$) and habitat ($\delta^{13}C$) ranges were found in there. Altogether, this would have resulted in a higher exposure of goshawks partially feeding on marine-derived diets and could explain the positive association between $\delta^{13}C$ and PFASs in this region. This contrasts with similar studies where intraspecific variation of PFOS (Bustnes et al., 2013b) and POPs (Eulaers et al., 2013) in goshawks from the study region was not explained by the dietary carbon origin.

Lastly, Spanish and Norwegian nests were clearly distinguished by their $\delta^{13}C$ in goshawk feathers (higher in Murcia). This could be easily depicted from the PCA (Figures 3.5 & 3.6), where nestlings from Murcia were placed on the right bottom side of the plot owing to their higher $\delta^{13}C$ values, as well as younger age, higher levels of PFCAs and lower trophic position. Regarding $\delta^{13}C$, it is well established that different sites yield different stable carbon isotopic profiles if their food webs are driven by primary productivity with different signatures (Szép et al., 2009). Terrestrial diets derived from C4 plants are comparatively enriched in ^{13}C (Kelly et al., 2008), ultimately yielding higher $\delta^{13}C$ values in food web predators like the goshawk. The abundance of C4 plants in Europe increases with mean daily temperature and there are more species in SW Europe (39-115) than in NW Europe (0-18) (Pyankov et al., 2010). Therefore, a difference in the isotopic baseline of primary producers likely explains the observed difference in $\delta^{13}C$ between Spanish and Norwegian nestlings. The $\delta^{13}C$ values in Norwegian nestlings are in the range previously established for this species in Troms area (–24.7‰ to –22.7‰) (Gómez-Ramírez et al., 2017), while values in Spanish birds were comparatively enriched.

Taken together, differences in trophic level accounted for the most part of PFAS variation within a goshawk population. This further underlines the biomagnifying potential of PFASs, including PFOS and all studied PFCAs. The contribution of differing baseline PFAS contamination between Norway and Spain probably plays a role as well, since it is unlikely that ecological (diet) and biological (age) predictors account for the generally remarkably higher

levels of most PFCAs in Murcia. We can however not rule out that the lower burden of PFOS in goshawks from Murcia is more connected to their lower position in the food web.

4.2. *In vitro* study

To investigate the importance of the most dominant PFAS in the Norwegian goshawks, i.e. PFOS, in affecting the immune response, we performed *in vitro* studies using bird cell lines as a model system, as practically no information is currently available on immunomodulatory properties of PFASs in birds (Peden-Adams et al., 2009; Sletten et al., 2016; Smits and Nain, 2013)

4.2.1. PFOS downregulates baseline immune gene expression

In this study we report a PFOS-mediated decrease in the expression of three immune genes in chicken embryo fibroblasts (CEFs), namely the cytokines IL-4, IL-8 and the transcription factor NF-κB. Therefore, it seems that the constitutive expression of NF-κB, IL-8 and IL-4 was negatively modulated following exposure to PFOS, in the absence of viral stimulation. Expression changes range between 3.0- (IL-8) and 4.7-fold (NF-κB) decreases at 48h post-exposure (Figure 3.8). Fold change differences higher than two-fold were considered as biologically relevant in a study on the innate immune response to GaHV-2 (Katneni, 2015). PFOS also attenuated the immune status of exposed mice, with a downregulation of constitutive hepatic levels of various cytokines, such as TNF-α, IL-4 and IFN-γ. There is scarce information about PFOS-mediated effects on innate immune signalling, and current knowledge is mostly based on traditional laboratory mammalian models (DeWitt et al., 2012).

It has been suggested that the biological effects of PFASs are often mediated by the nuclear receptor PPARα, which can be activated by PFASs like PFOS and PFOA. For example, negative regulation of NF-κB upon PPARα activation by various ligands modulates the expression of cytokines that are relevant in antibody production in B cells (DeWitt et al., 2009b). This is further supported by studies showing that natural PPARα ligands, such as dietary fatty acids and endogenous prostaglandins, tend to decrease the circulating levels of pro-inflammatory cytokines (e.g. TNF-α) (Jiang et al., 1998). It is typically conceived that PPARα activators downregulate NF-κB and subsequent activation of inflammatory cytokines (DeWitt et al., 2009b). In line with this, it has been suggested that PPARα ligands are anti-inflammatory and PFAS exposure modulates the balance between pro-inflammatory and anti-inflammatory capacities in macrophages (DeWitt et al., 2009b). In addition, the effect of PFOS on pro-inflammatory cytokine release was demonstrated to be pre-transcriptional (mRNA

expression) in monocytes (Corsini et al., 2011). Differential expression of hepatic genes upon PFOA and PFOS exposures has been reported in chicken, which underlines the importance of separately evaluating the toxicities of PFOS and PFOA (Yeung et al., 2007). PFOA is a more potent activator of PPARα in murine models (Takacs and Abbott, 2006), and it has been suggested that the immunotoxicity of PFOS is only partially dependent on PPARα activation (Qazi et al., 2010). PFOS can downregulate gene expression through other pathways, including inhibition of I-κB degradation (upstream effect) and inhibition of p65 phosphorylation (downstream effect), which are necessary for optimal NF-κB dependent gene transcription (Corsini et al., 2014). It is therefore likely that, in this study, PFOS can interfere with target gene expression in chicken fibroblasts via binding the nuclear receptor PPARα or these other mechanisms.

In line with this, the expression of the pro-inflammatory mediators NF-κB and IL-8 was lower in PFOS-exposed cells in this study, while TNF-α expression was lower across all the investigated time points but non-significant (Figure 3.8). Because macrophages are the largest producers of TNF-α (Beutler and Cerami, 1989), PFASs may affect the basal production of this cytokine by these cells (Qazi et al., 2010) to a larger extent than in fibroblasts as observed in this study. Regarding IL-4, a Th2 anti-inflammatory cytokine, previous studies have reported increased expression following exposure to PFOS. For example, the *ex vivo* production of IL-4 by splenocytes increased in a dose-dependent manner after PFOS exposure in mice (Dong et al., 2011). Interestingly, it has also been observed that serum IL-4 and PFAAs levels were higher in asthmatic male humans (Zhu et al., 2016). It therefore seems that PFOS exposure may modulate the balance between type I (Th1) and type II cytokines, and this switch in cytokine balance towards humoral immunity (Th2-like state) could constitute a risk factor for disease development (Zhu et al., 2016). The suppression of the cellular response in favour of the humoral response may diminish the antiviral activity of the innate immune system (Biron, 1999). It is unclear why we detected a decrease in IL-4 expression upon PFOS exposure as well, but a previous study on murine hepatic macrophages also found an attenuation in the levels of IL-4 upon PFOS exposure (Qazi et al., 2010), and the production of this anti-inflammatory cytokine was attenuated in human leukocytes exposed to PFOA and PFOS (Corsini et al., 2011).

Although PFAS immunotoxicity, at least in laboratory rodents, is associated with ligand activation of PPARα (Peraza et al., 2005), interspecific differences in receptor specificity, activity and related ligand binding may account for different susceptibilities to PFAS toxicity (Corsini et al., 2011). This highlights the need to continue to investigate PFOS-mediated

immune effects in birds, as previous research is mostly based on mammalian models. Altogether, the apparently anti-inflammatory role of PFASs would contrast with the effect of other pollutants like phthalates, which can increase pro-inflammatory gene expression, such as TNF-α and IL-8 in macrophages (Nishioka et al., 2012). However, further studies have been recommended to fully understand the role of PPARα ligands like PFOS on inflammatory responses (DeWitt et al., 2009b).

In this study, the transcription factor NF-κB and the cytokines IL-8 and IL-4 were downregulated following exposure of CEFs to PFOS, which is in agreement with the general ability of PFASs to attenuate cytokine production in mammalian immune cells (Corsini et al., 2011; Corsini et al., 2012). To the knowledge of the author, few studies have looked at PFOS-mediated effects on gene expression using avian models (Yeung et al., 2007), and this is the first to assess changes in immune gene expression. These findings would indicate that PFOS could affect cytokine release in birds similarly to mammals. The potential adverse effects of PFOS to the cells (or host) linked with the observed effects remain unclear. It has previously been suggested that attenuated immune gene expression (TNF-α, IFN-γ and IL-4) in macrophages and NK cells following PFOS exposure likely exerts a negative influence on the functionality of these cells (Qazi et al., 2010). Because PPARα ligands may reprogram macrophages into the anti-inflammatory M2-phenotype in rodents, this may ultimately impair the generation of cytotoxic T cells and cause to immunosuppression to certain diseases (DeWitt et al., 2009b). In addition, as PPARs are implicated in the regulation of other physiological processes besides inflammation, the same ligand-activated pathways may deregulate lipid homeostasis, adipogenesis or reproduction as well (Peraza et al., 2005). A study of cell viability, alongside with the exposure experiment, is recommended for further experiments to rule out the possibility that differences in the amount of living cells between treatments account for changes in expression levels, although this is unlikely as concentrations below cytotoxic thresholds (100 ppm in human HepG2 cells) (Florentin et al., 2011) were used.

4.2.2. Immune gene expression upon viral stimulation

GaHV-2 infection

In this section, the response of CEFs at the gene expression level to GaHV-2 infection was addressed. The production of cytokines and their roles during infection with GaHV-2 have been relatively well established in the chicken (Abdul-Careem et al., 2007). However, in the current study, stimulation of CEFs with GaHV-2 did not yield detectable changes in immune gene

expression between 6h and 24h post-infection for any of the investigated genes (Figure 3.9). This was unexpected based on previous research using CEFs as a suitable model to study responses to GaHV-2 infection. It is known that herpesviruses trigger immune signalling cascades when binding to PRRs, including TLRs, retinoic acid-inducible gene I (RIG-I) like receptors, and cytosolic DNA sensors (Ma and He, 2014). These initiate a complex program that leads to the activation of transcription factors like NF-κB (Ma and He, 2014). The evoked innate immune response typically involves the secretion of type I IFNs and pro-inflammatory cytokines, as well as the activation of innate immune cells such as macrophages and NK cells (Ma and He, 2014; Parvizi et al., 2010).

The expression of various cytokines increased after *in vivo* infection of chicken with GaHV-2, including IFN-γ, IL-1, IL-2, IL-8 and IL-18 genes (Jarosinski et al., 2006; Xing and Schat, 2000). In chicken embryos vaccinated with GaHV-2, IFN-γ was similarly up-regulated in the spleen at 24h post-infection, whereas there were no differences to the control at 48h and 72h (Katneni, 2015). In addition, it has been reported that genes implicated in GaHV-2 induced inflammatory responses are consistently upregulated at 24h post-infection in CEFs (Morgan et al., 2001), and that the antiviral effects in infected CEFs are linked to the early synthesis of inflammatory cytokines (Zou et al., 2017). This would underline that the cytokine response to GaHV-2 in fibroblasts may take place soon after infection, and this was one of the reasons to account for relatively early post-infection time points in this study.

In relation to this, a possible explanation for the lack of differences between GaHV-2 infected and control cells is that changes in inflammatory gene expression in response to experimental infection are peaking later than measured in this study. This would be in line with other studies on CEFs that reported responses to GaHV-2 after 24h post-infection. This is the case of a microarray study on CEFs where gene expression differed between GaHV-2 infected and non-infected cells at 56h, with several inflammatory genes up-regulated by 8-fold (Li et al., 2017a). In addition, Morgan et al. (2001) found that genes related to inflammation, cell growth and differentiation, and antigen presentation were induced at two and four days after infection of CEFs with GaHV-2 (Morgan et al., 2001). Therefore, a mismatch between the harvesting time points and the peak response may partially account for the lack of detectable differences between control and GaHV-2 infected cells in this study.

An efficient response by cell types implicated in the early recognition of GaHV-2 seems crucial to fight off infection (Zou et al., 2017). The production of pro-inflammatory cytokines in

response to GaHV-2 has been linked with increased synthesis of NO by iNOS, a critical innate response in macrophages that inhibits viral replication (Xing and Schat, 2000). IL-8 is one of the pro-inflammatory factors whose production up-regulates the expression of iNOS, (Sunyer et al., 1996), and it is produced by several cell types, including fibroblasts like in this study, macrophages or T cells (Sun et al., 2005). In fact, increased expression of this pro-inflammatory cytokine has been observed in chicken lung tissue upon infection with GaHV-2 using aerosols, suggesting an association between TLR3 signalling and IL-8 induction with host resistance (Abdul-Careem et al., 2009; Li et al., 2017a). It has been hypothesized that IL-18, via TNF-α production, mediates the up-regulation of IL-8 in human mononuclear cells and fibroblasts (Puren et al., 1998; Sun et al., 2005). Altogether, the pro-inflammatory response to GaHV-2 has been associated with upregulation of cytokines at an early post-infection stage (cytolytic phase) and increased host resistance (Li et al., 2017a).

Regarding the lack of differences for IL-4, previous studies suggest that the cytokine balance in response to GaHV-2 in splenic T cells is inclined towards a Th1 cytokine response (Parvizi et al., 2010). Accordingly, it was observed by Thai et al. (2007) that miR-155 knockout cells produced more IL-4 and were more prone to differentiate into Th2 cells. The expression of this cytokine may therefore be negatively regulated by upregulation of miR-155 during early GaHV-2 infection under normal conditions. This has been demonstrated by Rodriguez et al. (2007) since it was found that the transcription factor c-MAF, which is a potent activator of the IL-4 promoter, constitutes a target for miR-155. In line with this, we expected to report a downregulation of IL-4 concomitant with an increase in miR-155 expression after infection. The fact that miR-155 might not be upregulated to a significant extent in this experiment could therefore account for the lack of IL-4 downregulation. Furthermore, Ghiasi et al. (1999) suggested that the IL-4 (Th2)-related responses to herpes simplex virus (HSV-1) are detrimental because they suppress cytotoxic T-lymphocytes (Th1 response) (Ghiasi et al., 1999). This might be relevant in this study, since the PFOS-mediated downregulation of IL-4 could modulate the adaptive immunity of birds due to the described role of IL-4 in the differentiation of T cells. This effect could however not be corroborated in infected cells as the present study did not find a significant regulation of IL-4 compared to the control.

Poly(I:C) stimulation

As for GaHV-2, in this study it was expected that pro-inflammatory genes would be upregulated upon poly(I:C) binding to TLR3 and initiation of innate immune signalling pathways. It has previously been reported in mice macrophages that NF-κB was activated upon poly(I:C) stimulation and the production of associated pro-inflammatory cytokines (e.g. TNF-α) increased in a dose-dependent manner (Alexopoulou et al., 2001). Despite most studies are based on traditional models, poly(I:C) stimulation in chickens induces a rapid up-regulation of pro-inflammatory cytokines (e.g. IFN-β) through TLR3 similar to that observed in mammals (Karpala et al., 2008). The involvement of TLR3 in antiviral responses has been demonstrated for poly(I:C) (Alexopoulou et al., 2001) and suggested for GaHV-2 as well (Parvizi et al., 2010; Zou et al., 2017). It was established in macrophages that poly(I:C) induces the activation of NF-κB through TLR3 signalling using the MyD88-independent pathway (Akira and Sato, 2003).

In this study, an inflammatory response was not detected in CEFs treated with poly(I:C), as none of the target genes were upregulated at the investigated time points (Figure 3.11). This contrasts with Haunshi and Cheng (2014), where IL-8 was significantly induced after 8h in CEFs treated with poly(I:C), and the same applied to TNF-α after 6h in murine macrophages treated with poly(I:C) (O'Connell et al., 2007). It has been suggested that another inflammatory transcription factor besides NF-κB, namely AP-1, plays a major role in the antiviral response mediated by miR-155. In fact, the action of TLR3 (virus-activated) has been shown to be mediated via AP-1 (JNK pathway) in macrophages (Lindsay, 2008; O'Connell et al., 2007), and it was suggested that the induction of miR-155 in response to poly(I:C) relies on this pathway (O'Connell et al., 2007; Wang et al., 2010). It is therefore possible that both NF-κB and the JNK pathways are involved in the upregulation of miR-155 (O'Connell et al., 2007). In any case, the inducible miR-155 seems to positively feedback the activation of NF-κB and coordinate the rapid up-regulation of several cytokines (Wang et al., 2010; Waugh et al., 2018). This should either way result in the upregulation of the studied inflammatory genes upon stimulation with poly(I:C) in this study, especially at the early post-infection stages (6h and 12h). It remains unclear why we did not observe that. A possible explanation would be that the inflammatory response to poly(I:C) peaked before 6h instead, and by then the regulation of inflammatory genes was already comparable to the control. In a study that used the same concentration of poly(I:C) (2 µg/ml) in murine macrophages, miR-155 was the only upregulated miRNA and became detectable already 2h after infection, although it remained elevated to 8h (O'Connell et al., 2007). It is therefore suspected that there might have been an earlier induction of miR-155

and related inflammatory genes in this experiment, but we could not confirm this. This would be important for the immunity of the host, as increased expression of miR-155 in human macrophages was detected after stimulation with poly(I:C) and linked with anti-HIV-1 effects (Swaminathan et al., 2012). It is known that miRNA-155 is involved in a feed-forward loop that positively feedback to its transcription factor NF-κB, amplifying the inflammatory signalling (Mehta and Baltimore, 2016; O'Connell et al., 2007). Therefore for the associated NF-κB, because it is likely that its activation by poly(I:C) triggered signalling occurs at the post-transcriptional level (Alexopoulou et al., 2001), no remarkable differences in its expression would necessarily be expected. In this study NF-κB expression in poly(I:C) stimulated CEFs did not differ from the control at 6h and 12h, but it lowered down after 18h and 24h, and the same applied to the associated pro-inflammatory chemokine IL-8. It is known that the inflammatory response driven by NF-κB and associated cytokines like TNF-α can be amplified and extended as TNF-α itself can activate NF-κB (Wallach et al., 1999).

Because a prolonged activation of NF-κB may lead to the detrimental effects of inflammation, various feedback mechanisms provide a negative regulatory loop to balance the activity of NF-κB (Liu et al., 2012). This could further suggest that CEFs react to poly(I:C) in this study, but the inflammatory response was triggered earlier than we started to measure, and by 18h the expression machinery was adaptively shut down. This would result in the lower expression levels detected for NF-κB, IL-8 and TNF-α at 18h and 24h post-stimulation (Figure 3.11). The downregulation is therefore especially consistent across pro-inflammatory genes and at late post-stimulation harvests. TNF-α expression was lower than the control from 6h in this study, although it reached the lowest levels at 18h and 24h post-stimulation as well. These results further underline the importance of evaluating changes in gene expression in a time dependent manner, as the inflammatory response seems to differ from early (i.e. 6h) to later (i.e. 24h) post-infection stages. Lastly, in this study the expression of the anti-inflammatory cytokine IL-4 was negatively regulated after 18h and 24h as well. A study using chicken macrophages demonstrated a downregulation of this Th2 cytokine within 24h after infection with influenza A virus H9N2 (Xing et al., 2008). The interference of poly(I:C) with the expression of IL-4 in CEFs after 18h in this study could have a negative impact on the adaptive responses of the host, as concluded by Xing et al. (2008) given the role of IL-4 in the activation of humoral immunity. This suggests that manipulation of IL-4 expression by viruses, and potentially by pollutants, could impact immunity and disease outcomes.

Taken together, results concerning the response of CEFs to viral stimulation were unexpected for both GaHV-2 and poly(I:C). It had been hypothesized that the (early) expression of pro-inflammatory genes would increase upon infection with GaHV-2 or stimulation with poly(I:C), and this could not be confirmed in the present study. In accordance to the results discussed in the next section, it is possible that the initially triggered immune response to GaHV-2 was below our detection methods, not that it did not occur. Alternative explanations could be infection with a too low viral titer of GaHV-2, or changes in immune gene expression occurring (or peaking) before (poly(I:C)) or after (GaHV-2) the selected harvesting time points. The former was unfortunately not optimized prior to the start of this experiment due to the problem with the plaque assay. Overall, the fact that the selected viral models did not yield detectable increases in immune gene expression complicated the study of immunomodulation by PFOS. In short, if GaHV-infection did not trigger a detectable upregulation of target genes at first instance (i.e. normal response), then it remains difficult to address how PFOS alters it (i.e. immunomodulatory effects) (see 4.2.4).

4.2.3. GaHV-2 infection compensates the effect of PFOS

Interestingly, in this study there was not a difference in expression between control and PFOS/GaHV-2 treated cells for any of the investigated time points. This contrasts with the above mentioned downregulation of IL-8, NF-κB and IL-4 in PFOS exposed cells (see 4.2.1). It therefore seems that overall the combination of PFOS and GaHV-2 paradoxically upregulated expression back to the baseline condition (Figure 3.10). The induction of these genes when GaHV-2 and PFOS are together, relative to PFOS only, would suggest that the virus is actually triggering a response that we could not detect in Figure 3.9. In other words, it is likely that GaHV-2 started to activate cells through pathogen recognition receptors, but the response to only viral stimulation was below our detection methods at the investigated time points.

It remains unclear why combined exposure and infection compensated the toxic effect exerted by PFOS alone on immune gene expression, namely for IL-8, NF-κB and IL-4 after 24h post-infection (Figure 3.10). A protective effect of viruses on pollutant toxicity has previously been recorded in birds by Friend and Trainer (1972). In that study, mortality in mallard ducklings infected with duck hepatitis virus (DHV) and exposed to pesticides, namely DDT and dieldrin, was lower than in birds exposed to the pesticides only. It was hypothesized that this compensatory effect could relate to viral stimulation of pollutant metabolism into less toxic or more readily excreted metabolites, as pesticide residues were 3-4 times greater in the pesticide alone group. This finding is not easily extrapolated to this study, where host susceptibility is

not the endpoint and different viruses and pollutants are used. Therefore, although we cannot refer to a "protective" effect in this study, the compensatory effect of GaHV-2 infection is of interest for discussion. Kato et al. (1963) was the first study to report an increased microsomal metabolism of hexobarbital 12h post-infection of mice with murine hepatitis virus. The viral influence on xenobiotic metabolism becomes most apparent in subclinical infections where viral replication is dissociated from cell necrosis (Buynitzky et al., 1978). In line with this, it could be speculated that infection with GaHV-2 affects the metabolism of foreign compounds like PFOS. However, although fibroblasts can participate in the biotransformation of certain environmental pollutants like benzo(a)pyrene (Don et al., 1989), it is unlikely that they can metabolize PFOS due to its well-known stability and bioaccumulation potential (Olsen et al., 2007; Stahl et al., 2011). Furthermore, chicken vaccination against MDV resulted in decreased hepatic activities of CYP450-dependent microsomal enzymes, which are often implicated in the metabolism of xenobiotics (Sakar et al., 2004). It is thefefore unlikely that the lack of significant regulation compared to the control for PFOS/GaHV-2 in this study derives from a virus-mediated decrease in the concentration of PFOS in the system.

An alternative explanation could be that PFOS exposure increases CEF susceptibility and the subsequent amount of infected cells in the experimental well. It has been suggested that the presence of environmental toxicants in the body can increase the number of infected cells in the system (Dubey et al., 2011). PFOS is known to alter cell membrane properties and increase its permeability (Hu et al., 2003), and this could increase the amount of infected cells in the treatment. Therefore, an alternative hypothesis would be that in the presence of PFOS there are more infected cells, which induce gene expression above our detection methods and back to baseline expression levels. In addition, the upregulation of IL-4 in PFOS/GaHV-2 (Figure 3.10 A) could be explained by the synergistic production of damage associated molecular patterns in response to PFOS and GaHV-2. PFOS is known to exert cell damage at sublethal concentrations and, in combination with infectious signals, this could induce IL-4 as survival factor owing to its antiapoptotic properties (Conticello et al., 2004). Badry et al. (2018) suggested a similar mechanism for TNF-α in CEFs exposed to poly(I:C) and PCBs, where non-specific cell damage signals likely triggered an upregulation of TNF-α. To the knowledge of the author, no previous study has reported a protective effect of viruses on PFAS-mediated effects, but this is the first to study combined PFOS/viral effects in birds. Considering that the above reported "protective" role of DHV on pesticide effects was also seen in birds (Friend and Trainer, 1970), the interaction between PFOS and infectious agents warrants further

investigation, as it remains unclear why GaHV-2 infection compensated the effect of PFOS on immune gene expression.

4.2.4. Immunomodulation of the viral response by PFOS

Generally, no modulatory effects by PFOS on the response to GaHV-2 could be depicted in this study, as both treatments (GaHV-2 only and PFOS/GaHV-2) yielded similar immune gene expression levels compared to the negative control (Figure E5, Appendix). On the other hand, the downregulation of target genes after PFOS/poly(I:C) treatment relative to the control (Figure 3.12) needs to be discussed in relation to the normal response to poly(I:C) only (Figure E6, Appendix): this indicates that the response to PFOS/poly(I:C) was very similar to poly(I:C) only. It therefore seems that the immune response of CEFs to poly(I:C) was similarly not modulated by PFOS exposure. PFOS and other PFASs have been reported to alter inflammatory responses in experimental models, including production of cytokines and other regulatory proteins (DeWitt et al., 2009b). For example, PFOS can inhibit LPS-induced cytokine production in human leukocytes (Corsini et al., 2011). Specifically, pollutant exposure decreased the release of IL-4 and TNF-α in activated human monocytes and T lymphocytes, respectively, while IL-8 release was unaffected. This mechanism seems to occur independently of PPARα activation, by inhibiting the degradation of I-κB degradation, a regulatory protein that complexes with and inhibits NF-κB in the cytoplasm (Corsini et al., 2011). Similarly, PFOS down-regulated the TNF-α levels in isolated splenocytes of orally exposed mice following stimulation with LPS (Mollenhauer et al., 2011), while *ex vivo* exposure of mice macrophages to PFOS enhanced the inflammatory response (e.g. TNF-α) to LPS (Qazi et al., 2010). On the other hand, there is mounting experimental animal data demonstrating PPARα dependence of certain immune effects (DeWitt et al., 2009a). For example it has been reported that phosphorylation of p65, which is necessary for optimal gene transcription linked with NF-κB (Schmitz et al., 2001), is a relevant target for PFOA-induced PPARα activation and may account for defective cytokine production (Corsini et al., 2011). Overall, these studies suggest that PFASs affect NF-κB activation and generally suppress cytokine secretion by immune cells, and that PFOA and PFOS may have different mechanisms of action (Corsini et al., 2012). An unaltered expression of pro-inflammatory cytokines is essential for the antiviral defence, such as IFN-α to enhance activity of crucial innate immune cells like NK cells upon GaHV-2 infection (Ding and Lam, 1986), which are the main effectors of the first line of defence against GaHV-2, targeting virus-infected cells for apoptosis (Haq et al., 2013)

However, as described above, in this study the expression of target genes following combined exposure to PFOS and either GaHV-2 or poly(I:C) remained similar to that observed after sole viral stimulation. The only exception was the expression of NF-κB in PFOS/GaHV-2 at 6h post-infection, which was upregulated compared to the negative control and only poly(I:C). This could indicate that danger signals generated at a sublethal PFOS concentration by the damaged tissue increase NF-κB expression after 6h. Therefore, sensing GaHV-2 via PRRs (Parvizi et al., 2010) might not be sufficient to upregulate NF-κB signalling in fibroblasts under our experimental conditions. In the case of poly(I:C), the late downregulation of immune gene expression was similarly observed in CEFs exposed to poly(I:C) and PFOS in combination, indicating that the presence of PFOS did not alter the response to poly(I:C) (Figure E6, Appendix). This contrasts with Waugh et al. (2018), where NF-κB expression after 24h was downregulated in CEFs treated with PCBs/poly(I:C) relative to the individual treatments.

Therefore, with these results it cannot be confirmed that increased susceptibility to viral infection in organisms exposed to PFOS link to deregulation of activated innate signalling pathways. This can however not be ruled out either due to the limitations of our study and the observed deregulation of constitutive levels of certain pro-inflammatory mediators (e.g. IL-8) in PFOS-exposed CEFs (see 4.1.1). The ability of this and other environmental factors to interfere with miRNA immune signalling is just beginning to be studied (Guida et al., 2013; Waugh et al., 2018) and , to the knowledge of the author, no study has yet focused on PFOS-driven alteration of miR-155 expression upon viral infection. This could be an important mechanism for immunomodulation and requires further investigation (Sonkoly and Pivarcsi, 2011), to better understand how PFOS may interfere with innate immune system signalling pathways.

4.3. Linking the *in* vitro and the *in* vivo: the relevance of our effects to raptors

Innate immune signalling pathways are tightly regulated and any disruption may lead to chronic inflammation, increased host susceptibility and cancer. PFASs are associated with a range of adverse immune effects in traditional animal models, including impairment of the innate immune system and antiviral activities (DeWitt et al., 2012). The possible existence of different mechanisms of action in complex PFAS mixtures (Corsini et al., 2011) further complicates the assessment of PFAS immunotoxicity. Nonetheless, as specifically reported in our *in vivo* study, PFOS generally occurs at the highest concentration among PFASs in wildlife and it is often chosen as a model in exposure experiments (DeWitt et al., 2012). It is however unclear how most pollutants interfere with cellular processes that ultimately affect the outcome of viral

infections (Desforges et al., 2018). There is a very limited knowledge on PFOS-mediated immune effects in birds, and this is the first study to address changes in immune gene expression in response to PFOS using a bird cell line. The reported results on attenuated gene expression following PFOS exposure are consistent with previous studies that found altered cytokine release in *in vivo* mammalian models exposed to PFOS (Corsini et al., 2014).

Contaminants have been overlooked as potential causative factors in infectious disease outcomes and severity (Presley et al., 2010), and it is important to keep in mind that effects on immune gene expression can potentially scale-up to the organismal and population levels (Heilmann, 2012). CEFs are suitable models for GaHV-2 infections (Haunshi and Cheng, 2014), and this system could partially mimic responses to other dsDNA herpesviruses in wild birds. FHV-1, SHV-1 and AHV-1 are known infectious agents in raptors that can cause respiratory distress, histologic lesions and acute death (Jones, 2006). Consumption of infected pigeons constitute a major route of virus transmission and increased the risk of fatal herpesviral infection in birds of prey (Aini et al., 1993; Pinkerton et al., 2008). In addition, stimulation of cells with the synthetic virus model poly(I:C) may simulate infection with RNA viruses in birds of prey. For example, the West Nile virus (WNV) is one of the major infectious diseases in raptors (Pello and Olsen, 2013) and the emergence of this RNA virus in birds of prey from Austria showed a 66% seroprevalence (Wodak et al., 2011).

However, our results should be interpreted with caution and the relevancy of these findings to birds of prey should be discussed in relation to various aspects. Firstly, the PFOS concentration used in this exposure experiment (22.2 ppm) is one order of magnitude higher than reported in liver and plasma of highly polluted birds of prey (1740 ng/g and 2220 ng/mL in bald eagle) (Kannan et al., 2005) and three orders of magnitude higher than found in goshawk plasma in this study. However, levels of liver PFOS of up to 11359 ng/g have been measured in insectivorous birds from a PFOS-contaminated hotspot, and it was suspected that raptors from that area may reach even higher levels (Meyer et al., 2009). Therefore, the experimental exposure might be environmentally relevant only for highly polluted sites. A more realistic exposome could have provided insight into effects on immune processes at the molecular level under more environmentally relevant profiles and doses (Desforges et al., 2017). In this study, it was initially aimed to carry out an additional experiment using PFAS extracts from the goshawks, but this did not happen due to time constraints. Secondly, because there might be interspecific differences in the susceptibility to toxicants, as suggested for the chicken, which appears more sensitive than other wild bird species to organochlorines (Brunstrom, 1988). Also,

because immune effects *in vivo* do not always translate into *in vivo* impairments (Lankveld et al., 2010), and effects on immune parameters do not necessarily link to increased host susceptibility (Koutsos and Klasing, 2008; Smits and Nain, 2013)

Taken together, this study indicates that PFOS could potentially interfere with innate immune signalling pathways in birds (Figure E2, Appendix). However, further investigation on virus-activated signalling is warranted, at the *in vitro* and *in vivo* levels, before any conclusions can be drawn about PFOS-mediated modulation of immune responses and disease outcomes in birds of prey. To study effects of pollutants on immunity and disease resistance in organisms, it has previously been recommended to focus on innate functions (e.g. inflammatory processes), like in this study, since they can impact resistance and are most likely to be traded off with other relevant physiological processes (Martin et al., 2010).

5. Conclusions

This study indicates that goshawk nestlings from southern Spain, central and northern Norway are exposed to a wide range of PFASs, but at relatively low concentration in plasma and feathers. Differences between locations were established, with PFSAs dominating PFAS profiles in plasma from Norwegian nestlings, and PFCAs being the dominant class in Spanish birds. This could indicate the influence of PFCA contamination sources near Murcia, where PFNA was the most prominent PFAS compound and its levels were remarkably higher than in Norway. In addition, differences in trophic level accounted for the most part of PFAS variation within a population. This further underlines the biomagnifying potential of PFASs, including PFOS and all studied PFCAs. Bioaccumulation through dietary uptake could not be confirmed, as nestling age was not a significant predictor in best fit models, but trends might indicate the need of broader age ranges to address the dietary intake and/or growth dilution of PFASs over the nestling period.

The immune effects of PFOS, the most prominent PFAS in goshawk nestlings from this study and wildlife in general, were studied using an avian *in vitro* model. Exposure to PFOS deregulated the baseline expression of four immune genes, namely NF-κB, IL-8, TNF-α and IL-4 from 36 hours post-exposure, and this effect was ameliorated by additional infection of CEFs with GaHV-2. Although we have not investigated immune gene expression in the goshawks, these results suggest that PFOS might be capable of deregulating innate immune system signalling pathways in birds as well. This is of interest because disruption of these pathways may link with immunosuppression and enhanced susceptibility of wild bird populations, which could ultimately contribute to the expansion, emergence and or resurgence of viral diseases. However, these results need to be interpreted with care because the experimental dose of PFOS is generally not relevant for bird exposure, and the effect of PFOS on virus activated pathways could not be demonstrated here.

6. References

3M (2000). Phase-Out Plan for POSF-based Products. USEPA Administrative Record AR226-0600. Available from: http://www.regulations.gov, as document EPA-HQ-OPPT-2002-0051-0006.

Abdul-Careem, M.F., Haq, K., Shanmuganathan, S., Read, L.R., Schat, K.A., Heidari, M., and Sharif, S. (2009). Induction of innate host responses in the lungs of chickens following infection with a very virulent strain of Marek's disease virus. Virology *393*, 250-257.

Abdul-Careem, M.F., Hunter, B.D., Parvizi, P., Haghighi, H.R., Thanthrige-Don, N., and Sharif, S. (2007). Cytokine gene expression patterns associated with immunization against Marek's disease in chickens. Vaccine *25*, 424-432.

Ahrens, L., Gerwinski, W., Theobald, N., and Ebinghaus, R. (2010). Sources of polyfluoroalkyl compounds in the North Sea, Baltic Sea and Norwegian Sea: Evidence from their spatial distribution in surface water. Marine Pollution Bulletin *60*, 255-260.

Aini, I., Shih, L., Castro, A., and Zee, Y. (1993). Comparison of herpesvirus isolates from falcons, pigeons and psittacines by restriction endonuclease analysis. Journal of wildlife diseases *29*, 196-202.

Akira, S., and Sato, S. (2003). Toll-like receptors and their signaling mechanisms. Scandinavian journal of infectious diseases *35*, 555-562.

Akira, S., Uematsu, S., and Takeuchi, O. (2006). Pathogen recognition and innate immunity. Cell *124*, 783-801.

Alexopoulou, L., Holt, A.C., Medzhitov, R., and Flavell, R.A. (2001). Recognition of double-stranded RNA and activation of NF-κB by Toll-like receptor 3. Nature *413*, 732.

Alsmeyer, Y., WV, C., RM, F., and GGI, M. (1994). Organofluorine chemistry: Principles and commercial applications. (New York (NY): Plenum).

Annamalai, T., and Selvaraj, R.K. (2012). Interleukin 4 increases CCR9 expression and homing of lymphocytes to gut-associated lymphoid tissue in chickens. Veterinary Immunology and Immunopathology *145*, 257-263.

Armitage, J.M., MacLeod, M., and Cousins, I.T. (2009). Comparative assessment of the global fate and transport pathways of long-chain perfluorocarboxylic acids (PFCAs) and perfluorocarboxylates (PFCs) emitted from direct sources. Environmental science & technology *43*, 5830-5836.

Awad, E., Zhang, X., Bhavsar, S.P., Petro, S., Crozier, P.W., Reiner, E.J., Fletcher, R., Tittlemier, S.A., and Braekevelt, E. (2011). Long-Term Environmental Fate of Perfluorinated Compounds after Accidental Release at Toronto Airport. Environmental Science & Technology *45*, 8081-8089.

Baaten, B., Staines, K., Smith, L., Skinner, H., Davison, T., and Butter, C. (2009). Early replication in pulmonary B cells after infection with Marek's disease herpesvirus by the respiratory route. Viral immunology *22*, 431-444.

Baccarelli, A., and Bollati, V. (2009). Epigenetics and environmental chemicals. Current opinion in pediatrics *21*, 243.

Badry, A.M. (2018). Effect of environmental pollutants on virus activated innate immune system signalling pathways. Master Thesis. In University of Duisburg-Essen in cooperation with Norwegian University of Science and Technology.

Baigent, S.J., Ross, L., and Davison, T. (1998). Differential susceptibility to Marek's disease is associated with differences in number, but not phenotype or location, of pp38+ lymphocytes. Journal of general virology *79*, 2795-2802.

Bartel, D.P. (2004). MicroRNAs: Genomics, Biogenesis, Mechanism, and Function. Cell *116*, 281-297.

Bautista-Hernández, L.A., Gómez-Olivares, J.L., Buentello-Volante, B., and Bautista-de Lucio, V.M. (2017). Fibroblasts: the unknown sentinels eliciting immune responses against microorganisms. European Journal of Microbiology and Immunology *7*, 151-157.

Bertolero, A., Vicente, J., Meyer, J., and Lacorte, S. (2015). Accumulation and maternal transfer of perfluorooctane sulphonic acid in yellow-legged (Larus michahellis) and Audouin's gull (Larus audouinii) from the Ebro Delta Natural Park. Environmental research *137*, 208-214.

Beutler, B., and Cerami, A. (1989). The biology of cachectin/TNF--a primary mediator of the host response. Annual review of immunology *7*, 625-655.

Biggs, P.M., and Nair, V. (2012). The long view: 40 years of Marek's disease research and Avian Pathology. Avian pathology *41*, 3-9.

Bijlsma, R. (1991). Trends in European Goshawks Accipiter gentilis: an overview. Bird Census News *4*, 3.

Biron, C.A. (1999). Initial and innate responses to viral infections—pattern setting in immunity or disease. Current opinion in microbiology *2*, 374-381.

Blum, A., Balan, S.A., Scheringer, M., Trier, X., Goldenman, G., Cousins, I.T., Diamond, M., Fletcher, T., Higgins, C., and Lindeman, A.E. (2015). The Madrid statement on poly-and perfluoroalkyl substances (PFASs). Environmental health perspectives *123*, A107.

Borg, D., and Håkansson, H. (2012). Environmental and health risk assessment of perfluoroalkylated and polyfluoroalkylated substances (PFASs) in Sweden.

Borgå, K., Kidd, K.A., Muir, D.C., Berglund, O., Conder, J.M., Gobas, F.A., Kucklick, J., Malm, O., and Powell, D.E. (2012). Trophic magnification factors: Considerations of ecology, ecosystems, and study design. Integrated Environmental Assessment and Management *8*, 64-84.

Boutton, T.W. (1991). Stable carbon isotope ratios of natural materials: II. Atmospheric, terrestrial, marine, and freshwater environments. Carbon isotope techniques *1*, 173.

Bradley, J. (2008). TNF-mediated inflammatory disease. The Journal of pathology *214*, 149-160.

Braune, B.M., and Letcher, R.J. (2012). Perfluorinated sulfonate and carboxylate compounds in eggs of seabirds breeding in the Canadian Arctic: temporal trends (1975–2011) and interspecies comparison. Environmental science & technology *47*, 616-624.

Brunstrom, B. (1988). Sensitivity of embryos from duck, goose, herring gull, and various chicken breeds to 3, 3′, 4, 4′-tetrachlorobiphenyl. Poultry science *67*, 52-57.

Buck, R.C., Franklin, J., Berger, U., Conder, J.M., Cousins, I.T., De Voogt, P., Jensen, A.A., Kannan, K., Mabury, S.A., and van Leeuwen, S.P. (2011). Perfluoroalkyl and polyfluoroalkyl substances in the environment: terminology, classification, and origins. Integrated environmental assessment and management *7*, 513-541.

Burger, J. (1993). Metals in avian feathers: bioindicators of environmental pollution. Rev environ toxicol *5*, 203-311.

Burns, G., Brooks, K., Wildung, M., Navakanitworakul, R., Christenson, L.K., and Spencer, T.E. (2014). Extracellular vesicles in luminal fluid of the ovine uterus. PloS one *9*, e90913.

Bustnes, J.O., Bangjord, G., Ahrens, L., Herzke, D., and Yoccoz, N.G. (2015). Perfluoroalkyl substance concentrations in a terrestrial raptor: Relationships to environmental conditions and individual traits. Environmental toxicology and chemistry *34*, 184-191.

Bustnes, J.O., Bårdsen, B.-J., Bangjord, G., Lierhagen, S., and Yoccoz, N.G. (2013a). Temporal trends (1986–2005) of essential and non-essential elements in a terrestrial raptor in northern Europe. Science of the Total Environment *458*, 101-106.

Bustnes, J.O., Bårdsen, B.J., Herzke, D., Johnsen, T.V., Eulaers, I., Ballesteros, M., Hanssen, S.A., Covaci, A., Jaspers, V.L., and Eens, M. (2013b). Plasma concentrations of organohalogenated pollutants in predatory bird nestlings: associations to growth rate and dietary tracers. Environmental toxicology and chemistry *32*, 2520-2527.

Butt, C.M., Berger, U., Bossi, R., and Tomy, G.T. (2010). Levels and trends of poly-and perfluorinated compounds in the arctic environment. Science of the total environment *408*, 2936-2965.

Buynitzky, S., Ware, G., and Ragland, W. (1978). Effect of viral infection on drug metabolism and pesticide disposition in ducks. Toxicology and applied pharmacology *46*, 267-278.

Calame, K. (2007). MicroRNA-155 Function in B Cells. Immunity *27*, 825-827.

Chendrimada, T.P., Gregory, R.I., Kumaraswamy, E., Norman, J., Cooch, N., Nishikura, K., and Shiekhattar, R. (2005). TRBP recruits the Dicer complex to Ago2 for microRNA processing and gene silencing. Nature *436*, 740.

Chropeňová, M., Karásková, P., Kallenborn, R., Gregušková, E.K., and Čupr, P. (2016). Pine Needles for the Screening of Perfluorinated Alkylated Substances (PFASs) along Ski Tracks. Environmental Science & Technology *50*, 9487-9496.

Conder, J.M., Hoke, R.A., Wolf, W.d., Russell, M.H., and Buck, R.C. (2008). Are PFCAs Bioaccumulative? A Critical Review and Comparison with Regulatory Criteria and Persistent Lipophilic Compounds. Environmental Science & Technology *42*, 995-1003.

Conticello, C., Pedini, F., Zeuner, A., Patti, M., Zerilli, M., Stassi, G., Messina, A., Peschle, C., and De Maria, R. (2004). IL-4 protects tumor cells from anti-CD95 and chemotherapeutic agents via up-regulation of antiapoptotic proteins. The Journal of Immunology *172*, 5467-5477.

Cooper, P. (1962). The plaque assay of animal viruses. In Advances in virus research (Elsevier), pp. 319-378.

Coplen, T.B. (2011). Guidelines and recommended terms for expression of stable-isotope-ratio and gas-ratio measurement results. Rapid communications in mass spectrometry *25*, 2538-2560.

Corsini, E., Avogadro, A., Galbiati, V., dell'Agli, M., Marinovich, M., Galli, C.L., and Germolec, D.R. (2011). In vitro evaluation of the immunotoxic potential of perfluorinated compounds (PFCs). Toxicology and Applied Pharmacology *250*, 108-116.

Corsini, E., Luebke, R.W., Germolec, D.R., and DeWitt, J.C. (2014). Perfluorinated compounds: Emerging POPs with potential immunotoxicity. Toxicology Letters *230*, 263-270.

Corsini, E., Sangiovanni, E., Avogadro, A., Galbiati, V., Viviani, B., Marinovich, M., Galli, C.L., Dell'Agli, M., and Germolec, D.R. (2012). In vitro characterization of the immunotoxic potential of several perfluorinated compounds (PFCs). Toxicology and applied pharmacology *258*, 248-255.

Cramp, S., and Simmons, K. (1980). 1983. Handbook of the birds of Europe, the Middle East and North Africa. The birds of Western Paleartic 3–Waders to Gulls.

Croghan, C., and Egeghy, P. (2003). Methods of dealing with values below the limit of detection using SAS. Southern SAS User Group, 22-24.

Cullen, B.R. (2013). MicroRNAs as mediators of viral evasion of the immune system. Nature immunology *14*, 205-210.

Cunard, R., Ricote, M., DiCampli, D., Archer, D.C., Kahn, D.A., Glass, C.K., and Kelly, C.J. (2002). Regulation of cytokine expression by ligands of peroxisome proliferator activated receptors. The Journal of Immunology *168*, 2795-2802.

D'Hollander, W., De Bruyn, L., Hagenaars, A., de Voogt, P., and Bervoets, L. (2014). Characterisation of perfluorooctane sulfonate (PFOS) in a terrestrial ecosystem near a fluorochemical plant in Flanders, Belgium. Environmental Science and Pollution Research *21*, 11856-11866.

Dahlberg, M. (2017). Levels of Perfluoroalkyl and Polyfluoroalkyl Substances (PFASs) in Feathers of Eurasian Eagle-Owls (Bubo bubo) in Norway. Master Thesis. In Norwegian University of Science and Technology.

Dauwe, T., Bervoets, L., Pinxten, R., Blust, R., and Eens, M. (2003). Variation of heavy metals within and among feathers of birds of prey: effects of molt and external contamination. Environmental Pollution *124*, 429-436.

David-Poynter, N.J., and Farrell, H.E. (1996). Masters of deception: a review of herpesvirus immune evasion strategies. Immunology & Cell Biology *74*, 513-522.

Davision, F. (2008). The importance of the avian immune system and its unique features. Avian immunology *1*, 1-11.

Davison, F., and Nair, V. (2004). Marek's disease: an evolving problem (Academic Press).

de Swart, R.L., Ross, P.S., Vedder, L.J., and Timmerman, H.H. (1994). Impairment of immune function in harbour seals (Phoca vitulina) feeding on fish from polluted waters. Impaired immunity in seals exposed to bioaccumulated environmental contaminants, 35.

del Moral, J.C., Molina, M.V., Bermejo, A.B., and Palomino, P.N. (2012). Atlas de las aves en invierno en España, 2007-2010 (Organismo Autónomo Parques Nacionales).

Demas, G., and Nelson, R. (2012). Ecoimmunology (Oxford University Press).

Desforges, J.-P., Bandoro, C., Shehata, L., Sonne, C., Dietz, R., Puryear, W.B., and Runstadler, J.A. (2018). Environmental contaminant mixtures modulate in vitro influenza infection. Science of The Total Environment *634*, 20-28.

Desforges, J.-P., Levin, M., Jasperse, L., De Guise, S., Eulaers, I., Letcher, R.J., Acquarone, M., Nordøy, E., Folkow, L.P., Hammer Jensen, T.*, et al.* (2017). Effects of Polar Bear and Killer Whale Derived

Contaminant Cocktails on Marine Mammal Immunity. Environmental Science & Technology *51*, 11431-11439.

Desforges, J.-P.W., Sonne, C., Levin, M., Siebert, U., De Guise, S., and Dietz, R. (2016). Immunotoxic effects of environmental pollutants in marine mammals. Environment international *86*, 126-139.

Desjardins, P., and Conklin, D. (2010). NanoDrop microvolume quantitation of nucleic acids. Journal of visualized experiments: JoVE.

DeWitt, J.C. (2016). Toxicological effects of perfluoroalkyl and polyfluoroalkyl substances (Springer).

DeWitt, J.C., Copeland, C.B., and Luebke, R.W. (2009a). Suppression of humoral immunity by perfluorooctanoic acid is independent of elevated serum corticosterone concentration in mice. Toxicological sciences *109*, 106-112.

DeWitt, J.C., Peden-Adams, M.M., Keller, J.M., and Germolec, D.R. (2012). Immunotoxicity of perfluorinated compounds: recent developments. Toxicologic pathology *40*, 300-311.

DeWitt, J.C., Shnyra, A., Badr, M.Z., Loveless, S.E., Hoban, D., Frame, S.R., Cunard, R., Anderson, S.E., Meade, B.J., Peden-Adams, M.M.*, et al.* (2009b). Immunotoxicity of Perfluorooctanoic Acid and Perfluorooctane Sulfonate and the Role of Peroxisome Proliferator-Activated Receptor Alpha. Critical Reviews in Toxicology *39*, 76-94.

Ding, A.H., and Lam, K. (1986). Enhancement by interferon of chicken splenocyte natural killer cell activity against Marek's disease tumor cells. Veterinary immunology and immunopathology *11*, 65-72.

Dolan, K.J., Ciesielski, T.M., Lierhagen, S., Eulaers, I., Nygård, T., Johnsen, T.V., Gómez-Ramírez, P., García-Fernández, A.J., Bustnes, J.O., Ortiz-Santaliestra, M.E., and Jaspers, V.L.B. (2017). Trace element concentrations in feathers and blood of Northern goshawk (Accipiter gentilis) nestlings from Norway and Spain. Ecotoxicology and Environmental Safety *144*, 564-571.

Don, P., Mukhtar, H., Das, M., Berger, N., and Bickers, D. (1989). Benzo (a) pyrene metabolism, DNA-binding and UV-induced repair of DNA damage in cultured skin fibroblasts from a patient with unilateral multiple basal cell carcinoma. British journal of Dermatology *120*, 161-171.

Dong, G.-H., Liu, M.-M., Wang, D., Zheng, L., Liang, Z.-F., and Jin, Y.-H. (2011). Sub-chronic effect of perfluorooctanesulfonate (PFOS) on the balance of type 1 and type 2 cytokine in adult C57BL6 mice. Archives of toxicology *85*, 1235-1244.

Dubey, B., Dubey, U.S., and Hussain, J. (2011). Modeling effects of toxicant on uninfected cells, infected cells and immune response in the presence of virus. Journal of Biological Systems *19*, 479-503.

Dulbecco, R., and Vogt, M. (1954). Plaque formation and isolation of pure lines with poliomyelitis viruses. Journal of Experimental Medicine *99*, 167-182.

Ellis, D.A., Martin, J.W., De Silva, A.O., Mabury, S.A., Hurley, M.D., Sulbaek Andersen, M.P., and Wallington, T.J. (2004). Degradation of fluorotelomer alcohols: a likely atmospheric source of perfluorinated carboxylic acids. Environmental science & technology *38*, 3316-3321.

Eriksson, U., Roos, A., Lind, Y., Hope, K., Ekblad, A., and Kärrman, A. (2016). Comparison of PFASs contamination in the freshwater and terrestrial environments by analysis of eggs from osprey (Pandion haliaetus), tawny owl (Strix aluco), and common kestrel (Falco tinnunculus). Environmental Research *149*, 40-47.

Escoruela, J., Garreta, E., Ramos, R., González-Solís, J., and Lacorte, S. (2018). Occurrence of Per-and Polyfluoroalkyl substances in Calonectris shearwaters breeding along the Mediterranean and Atlantic colonies. Marine Pollution Bulletin *131*, 335-340.

Espín, S., García-Fernández, A.J., Herzke, D., Shore, R.F., van Hattum, B., Martínez-López, E., Coeurdassier, M., Eulaers, I., Fritsch, C., and Gómez-Ramírez, P. (2016). Tracking pan-continental trends in environmental contamination using sentinel raptors—what types of samples should we use? Ecotoxicology *25*, 777-801.

Eulaers, I., Covaci, A., Herzke, D., Eens, M., Sonne, C., Moum, T., Schnug, L., Hanssen, S.A., Johnsen, T.V., Bustnes, J.O., and Jaspers, V.L.B. (2011a). A first evaluation of the usefulness of feathers of nestling predatory birds for non-destructive biomonitoring of persistent organic pollutants. Environment International *37*, 622-630.

Eulaers, I., Covaci, A., Hofman, J., Nygård, T., Halley, D.J., Pinxten, R., Eens, M., and Jaspers, V.L.B. (2011b). A comparison of non-destructive sampling strategies to assess the exposure of white-tailed eagle nestlings (Haliaeetus albicilla) to persistent organic pollutants. Science of The Total Environment *410-411*, 258-265.

Eulaers, I., Jaspers, V.L.B., Bustnes, J.O., Covaci, A., Johnsen, T.V., Halley, D.J., Moum, T., Ims, R.A., Hanssen, S.A., Erikstad, K.E.*, et al.* (2013). Ecological and spatial factors drive intra- and interspecific variation in exposure of subarctic predatory bird nestlings to persistent organic pollutants. Environment International *57-58*, 25-33.

Fair, P.A., Driscoll, E., Mollenhauer, M.A.M., Bradshaw, S.G., Yun, S.H., Kannan, K., Bossart, G.D., Keil, D.E., and Peden-Adams, M.M. (2011). Effects of environmentally-relevant levels of perfluorooctane sulfonate on clinical parameters and immunological functions in B6C3F1 mice. Journal of Immunotoxicology *8*, 17-29.

Faustman, E.M., and Omenn, G.S. (2001). Risk assessment. Cassarett and Doull's Toxicology (Klaassen C, ed). 6th ed. San Francisco, CA: McGraw-Hill, 83-104.

Flemington, E.K. (2001). Herpesvirus lytic replication and the cell cycle: arresting new developments. Journal of virology *75*, 4475-4481.

Florentin, A., Deblonde, T., Diguio, N., Hautemaniere, A., and Hartemann, P. (2011). Impacts of two perfluorinated compounds (PFOS and PFOA) on human hepatoma cells: Cytotoxicity but no genotoxicity? International Journal of Hygiene and Environmental Health *214*, 493-499.

Friend, M., and Trainer, D.O. (1970). Polychlorinated biphenyl: interaction with duck hepatitis virus. Science *170*, 1314-1316.

Furness, R. (1993). Birds as monitors of pollutants. In Birds as monitors of environmental change (Springer), pp. 86-143.

Gailbreath, K.L., and Oaks, J.L. (2008). Herpesviral inclusion body disease in owls and falcons is caused by the pigeon herpesvirus (columbid herpesvirus 1). Journal of wildlife diseases *44*, 427-433.

García-Fernández, A.J., Calvo, J.F., Martínez-López, E., María-Mojica, P., and Martínez, J.E. (2008). Raptor Ecotoxicology in Spain: A Review on Persistent Environmental Contaminants. AMBIO: A Journal of the Human Environment *37*, 432-439.

García-Fernández, A.J., Espín, S., and Martínez-López, E. (2013). Feathers as a Biomonitoring Tool of Polyhalogenated Compounds: A Review. Environmental Science & Technology *47*, 3028-3043.

Gebbink, W.A., and Letcher, R.J. (2012). Comparative tissue and body compartment accumulation and maternal transfer to eggs of perfluoroalkyl sulfonates and carboxylates in Great Lakes herring gulls. Environmental pollution *162*, 40-47.

Gennart, I., Coupeau, D., Pejaković, S., Laurent, S., Rasschaert, D., and Muylkens, B. (2015). Marek's disease: Genetic regulation of gallid herpesvirus 2 infection and latency. The Veterinary Journal *205*, 339-348.

Ghareeb, K., Awad, W.A., Soodoi, C., Sasgary, S., Strasser, A., and Böhm, J. (2013). Effects of feed contaminant deoxynivalenol on plasma cytokines and mRNA expression of immune genes in the intestine of broiler chickens. PloS one *8*, e71492.

Ghiasi, H., Cai, S., Slanina, S.M., Perng, G.-C., Nesburn, A.B., and Wechsler, S.L. (1999). The role of interleukin (IL)-2 and IL-4 in herpes simplex virus type 1 ocular replication and eye disease. The Journal of infectious diseases *179*, 1086-1093.

Gibson, U., Heid, C.A., and Williams, P.M. (1996). A novel method for real time quantitative RT-PCR. Genome research *6*, 995-1001.

Gómez-Ramírez, P., Bustnes, J.O., Eulaers, I., Herzke, D., Johnsen, T.V., Lepoint, G., Pérez-García, J.M., García-Fernández, A.J., and Jaspers, V.L.B. (2017). Per- and polyfluoroalkyl substances in plasma and feathers of nestling birds of prey from northern Norway. Environmental Research *158*, 277-285.

Gómez-Ramírez, P., Shore, R., Van den Brink, N., Van Hattum, B., Bustnes, J., Duke, G., Fritsch, C., García-Fernández, A., Helander, B., and Jaspers, V. (2014). An overview of existing raptor contaminant monitoring activities in Europe. Environment international *67*, 12-21.

Gottwein, E., and Cullen, B.R. (2008). Viral and Cellular MicroRNAs as Determinants of Viral Pathogenesis and Immunity. Cell Host & Microbe *3*, 375-387.

Goudarzi, H., Miyashita, C., Okada, E., Kashino, I., Chen, C.-J., Ito, S., Araki, A., Kobayashi, S., Matsuura, H., and Kishi, R. (2017). Prenatal exposure to perfluoroalkyl acids and prevalence of infectious diseases up to 4years of age. Environment International *104*, 132-138.

Graham, D., Mare, C., Ward, F., and Peckham, M. (1975). Inclusion body disease (herpesvirus infection) of falcons (IBDF). Journal of wildlife diseases *11*, 83-91.

Griffiths, R., Double, M.C., Orr, K., and Dawson, R.J. (1998). A DNA test to sex most birds. Molecular ecology *7*, 1071-1075.

Grønlien, H. (2004). Hønsehauken i Norge. Bestandens status og utvikling siste 150 år. NOF Rapportserie, 40.

Grønnesby, S., and Nygard, T. (2000). Using time-lapse video monitoring to study prey selection by breeding goshawks Accipiter gentilis in central Norway. Ornis Fennica *77*, 117-129.

Guida, M., Marra, M., Zullo, F., Guida, M., Trifuoggi, M., Biffali, E., Borra, M., De Mieri, G., D'Alessandro, R., and De Felice, B. (2013). Association between exposure to dioxin-like polychlorinated biphenyls and miR-191 expression in human peripheral blood mononuclear cells. Mutation Research/Genetic Toxicology and Environmental Mutagenesis *753*, 36-41.

Guillot, L., Le Goffic, R., Bloch, S., Escriou, N., Akira, S., Chignard, M., and Si-Tahar, M. (2005). Involvement of toll-like receptor 3 in the immune response of lung epithelial cells to double-stranded RNA and influenza A virus. Journal of Biological Chemistry *280*, 5571-5580.

Guruge, K.S., Hikono, H., Shimada, N., Murakami, K., Hasegawa, J., Yeung, L.W., Yamanaka, N., and Yamashita, N. (2009). Effect of perfluorooctane sulfonate (PFOS) on influenza A virus-induced mortality in female B6C3F1 mice. The Journal of toxicological sciences *34*, 687-691.

Gyllenhammar, I., Diderholm, B., Gustafsson, J., Berger, U., Ridefelt, P., Benskin, J.P., Lignell, S., Lampa, E., and Glynn, A. (2018). Perfluoroalkyl acid levels in first-time mothers in relation to offspring weight gain and growth. Environment international *111*, 191-199.

Hall, A., Law, R., Wells, D., Harwood, J., Ross, H., Kennedy, S., Allchin, C., Campbell, L., and Pomeroy, P. (1992). Organochlorine levels in common seals (Phoca vitulina) which were victims and survivors of the 1988 phocine distemper epizootic. Science of the total environment *115*, 145-162.

Halley, D., Nygård, T., Minagawa, M., Systad, G., Jacobsen, K., and Johnsen, T. (2004). Rein som næring hos kongeørn i hekketida i et område i Finnmark undersøkt ved hjelp av stabil isotopteknikk. (Prosjektrapport).

Haq, K., Schat, K.A., and Sharif, S. (2013). Immunity to Marek's disease: Where are we now? Developmental & Comparative Immunology *41*, 439-446.

Haukås, M., Berger, U., Hop, H., Gulliksen, B., and Gabrielsen, G.W. (2007). Bioaccumulation of per- and polyfluorinated alkyl substances (PFAS) in selected species from the Barents Sea food web. Environmental Pollution *148*, 360-371.

Haunshi, S., and Cheng, H.H. (2014). Differential expression of Toll-like receptor pathway genes in chicken embryo fibroblasts from chickens resistant and susceptible to Marek's disease. Poultry science *93*, 550-555.

Heilmann, C. (2012). Environmental toxicants and susceptibility to infection. In Immunotoxicity, Immune Dysfunction, and Chronic Disease (Springer), pp. 389-398.

Herzke, D., Berger, U., Kallenborn, R., Nygård, T., and Vetter, W. (2005). Brominated flame retardants and other organobromines in Norwegian predatory bird eggs. Chemosphere *61*, 441-449.

Herzke, D., Jaspers, V., Rodriguez, F., Boertmann, D., Rasmussen, L.M., Sonne, C., Dietz, R., Covaci, A., and Bustnes, J. (2011). PFCs in feathers of white tailed eagles (Haliaeetus albicilla) from Greenland and Norway; usefull for non-destructive sampling? In Dioxin 2011, pp. 1337-1339.

Herzke, D., Nygård, T., Berger, U., Huber, S., and Røv, N. (2009). Perfluorinated and other persistent halogenated organic compounds in European shag (Phalacrocorax aristotelis) and common eider (Somateria mollissima) from Norway: A suburban to remote pollutant gradient. Science of The Total Environment *408*, 340-348.

Hobson, K.A., and Welch, H.E. (1992). Determination of trophic relationships within a high Arctic marine food web using δ 13 C and δ 15 N analysis. Marine Ecology Progress Series, 9-18.

Holmström, K.E., and Berger, U. (2008). Tissue Distribution of Perfluorinated Surfactants in Common Guillemot (Uria aalge) from the Baltic Sea. Environmental Science & Technology *42*, 5879-5884.

Houde, M., Bujas, T.A.D., Small, J., Wells, R.S., Fair, P.A., Bossart, G.D., Solomon, K.R., and Muir, D.C.G. (2006). Biomagnification of Perfluoroalkyl Compounds in the Bottlenose Dolphin (Tursiops truncatus) Food Web. Environmental Science & Technology *40*, 4138-4144.

Hu, W., Jones, P.D., DeCoen, W., King, L., Fraker, P., Newsted, J., and Giesy, J.P. (2003). Alterations in cell membrane properties caused by perfluorinated compounds. Comparative Biochemistry and Physiology Part C: Toxicology & Pharmacology *135*, 77-88.

Hu, X., Zou, H., Qin, A., Qian, K., Shao, H., and Ye, J. (2016). Activation of Toll-like receptor 3 inhibits Marek's disease virus infection in chicken embryo fibroblast cells. Archives of virology *161*, 521-528.

Jacobsson, R., and Sandvik, J. (2014). Hønsehauk i Sør-Trøndelag 1994-2013. NOF-rapport *12*, 20.

Jardine, T.D., Kidd, K.A., and Fisk, A.T. (2006). Applications, considerations, and sources of uncertainty when using stable isotope analysis in ecotoxicology. Environmental Science & Technology *40*, 7501-7511.

Jarosinski, K.W., Tischer, B.K., Trapp, S., and Osterrieder, N. (2006). Marek's disease virus: lytic replication, oncogenesis and control. Expert review of vaccines *5*, 761-772.

Jaspers, V., Covaci, A., Voorspoels, S., Dauwe, T., Eens, M., and Schepens, P. (2006). Brominated flame retardants and organochlorine pollutants in aquatic and terrestrial predatory birds of Belgium: levels, patterns, tissue distribution and condition factors. Environmental Pollution *139*, 340-352.

Jaspers, V.L.B., Herzke, D., Eulaers, I., Gillespie, B.W., and Eens, M. (2013). Perfluoroalkyl substances in soft tissues and tail feathers of Belgian barn owls (Tyto alba) using statistical methods for left-censored data to handle non-detects. Environment International *52*, 9-16.

Jaspers, V.L.B., Rodriguez, F.S., Boertmann, D., Sonne, C., Dietz, R., Rasmussen, L.M., Eens, M., and Covaci, A. (2011). Body feathers as a potential new biomonitoring tool in raptors: A study on organohalogenated contaminants in different feather types and preen oil of West Greenland white-tailed eagles (Haliaeetus albicilla). Environment International *37*, 1349-1356.

Jiang, C., Ting, A.T., and Seed, B. (1998). PPAR-γ agonists inhibit production of monocyte inflammatory cytokines. Nature *391*, 82.

John, E. (1998). Simplified curve fitting using spreadsheet add-ins. International Journal of Engineering Education *14*, 375-380.

Jones, M.P. (2006). Selected infectious diseases of birds of prey. Journal of Exotic Pet Medicine *15*, 5-17.

Jones, P.D., Hu, W., De Coen, W., Newsted, J.L., and Giesy, J.P. (2003). Binding of perfluorinated fatty acids to serum proteins. Environmental Toxicology and Chemistry *22*, 2639-2649.

Jordana, M., Sarnstrand, B., Sime, P., and Ramis, I. (1994). Immune-inflammatory functions of fibroblasts. European Respiratory Journal *7*, 2212-2222.

Juul-Madsen, H.R., Viertlboeck, B., Smith, A.L., and Göbel, T.W. (2008). Avian innate immune responses. Avian immunology, 129-158.

Kålås, J.A., Viken, Å., Henriksen, S., and Skjelseth, S. (2010). The 2010 Norwegian red list for species. Norwegian Biodiversity Information Centre, Norway.

Kaleta, E. (1990). Herpesviruses of birds-a review. Avian Pathology *19*, 193-211.

Kaminski, N.E., Kaplan, B.F., and Holsapple, M.P. (2008). Toxic responses of the immune system. Casarett & Doull's Toxicology The Basic Science of Poisons *12*, 485-555.

Kannan, K. (2011). Perfluoroalkyl and polyfluoroalkyl substances: current and future perspectives. Environmental Chemistry *8*, 333-338.

Kannan, K., Corsolini, S., Falandysz, J., Oehme, G., Focardi, S., and Giesy, J.P. (2002). Perfluorooctanesulfonate and related fluorinated hydrocarbons in marine mammals, fishes,

and birds from coasts of the Baltic and the Mediterranean Seas. Environmental Science & Technology *36*, 3210-3216.

Kannan, K., Perrotta, E., and Thomas, N.J. (2006). Association between perfluorinated compounds and pathological conditions in southern sea otters. Environmental science & technology *40*, 4943-4948.

Kannan, K., Tao, L., Sinclair, E., Pastva, S.D., Jude, D.J., and Giesy, J.P. (2005). Perfluorinated Compounds in Aquatic Organisms at Various Trophic Levels in a Great Lakes Food Chain. Archives of Environmental Contamination and Toxicology *48*, 559-566.

Karpala, A.J., Lowenthal, J.W., and Bean, A.G. (2008). Activation of the TLR3 pathway regulates IFNβ production in chickens. Developmental & Comparative Immunology *32*, 435-444.

Kärrman, A., van Bavel, B., Järnberg, U., Hardell, L., and Lindström, G. (2006). Perfluorinated chemicals in relation to other persistent organic pollutants in human blood. Chemosphere *64*, 1582-1591.

Katneni, U.K. (2015). Innate patterning of the immune response to Marek's disease virus (MDV) during pathogenesis and vaccination (University of Delaware).

Kato, H., Sato, S., Yoneyama, M., Yamamoto, M., Uematsu, S., Matsui, K., Tsujimura, T., Takeda, K., Fujita, T., and Takeuchi, O. (2005). Cell type-specific involvement of RIG-I in antiviral response. Immunity *23*, 19-28.

Kato, R., Nakamura, Y., and Chiesara, E. (1963). Enhanced phenobarbital induction of liver microsomal drug-metabolizing enzymes in mice infected with murine hepatitus virus. Biochemical pharmacology *12*, 365-370.

Kelly, E.J., Hadac, E.M., Greiner, S., and Russell, S.J. (2008). Engineering microRNA responsiveness to decrease virus pathogenicity. Nature medicine *14*, 1278-1283.

Kenntner, N., Krone, O., Altenkamp, R., and Tataruch, F. (2003). Environmental contaminants in liver and kidney of free-ranging northern goshawks (Accipiter gentilis) from three regions of Germany. Archives of Environmental Contamination and Toxicology *45*, 0128-0135.

Kenward, R. (2010). The goshawk (Bloomsbury Publishing).

Kissa, E. (2001). Fluorinated surfactants and repellents, Vol 97 (CRC Press).

Koutsos, E.A., and Klasing, K.C. (2008). Factors modulating the avian immune system. Avian Immunology, 323.

Kracht, M., and Saklatvala, J. (2002). Transcriptional and post-transcriptional control of gene expression in inflammation. Cytokine *20*, 91-106.

Lagos-Quintana, M., Rauhut, R., Yalcin, A., Meyer, J., Lendeckel, W., and Tuschl, T. (2002). Identification of tissue-specific microRNAs from mouse. Current biology *12*, 735-739.

Lankveld, D., Van Loveren, H., Baken, K., and Vandebriel, R. (2010). In vitro testing for direct immunotoxicity: state of the art. In Immunotoxicity Testing (Springer), pp. 401-423.

Lau, C., Anitole, K., Hodes, C., Lai, D., Pfahles-Hutchens, A., and Seed, J. (2007). Perfluoroalkyl acids: a review of monitoring and toxicological findings. Toxicological sciences *99*, 366-394.

Li, X., Su, S., Cui, N., Zhou, H., Liu, X., and Cui, Z. (2017a). Transcriptome Analysis of Chicken Embryo Fibroblast Cell Infected with Marek's Disease Virus of GX0101Δ LTR. Revista Brasileira de Ciência Avícola *19*, 179-184.

Li, Y., Gao, K., Duo, B., Zhang, G., Cong, Z., Gao, Y., Fu, J., Zhang, A., and Jiang, G. (2017b). Analysis of a broad range of perfluoroalkyl acids in accipiter feathers: method optimization and their occurrence in Nam Co Basin, Tibetan Plateau. Environmental Geochemistry and Health.

Lian, L., Qu, L., Chen, Y., Lamont, S.J., and Yang, N. (2012). A systematic analysis of miRNA transcriptome in Marek's disease virus-induced lymphoma reveals novel and differentially expressed miRNAs. PLoS One *7*, e51003.

Lindsay, M.A. (2008). microRNAs and the immune response. Trends in Immunology *29*, 343-351.

Liu, Y., Bridges, R., Wortham, A., and Kulesz-Martin, M. (2012). NF-κB repression by PIAS3 mediated RelA SUMOylation. PloS one *7*, e37636.

Løseth, M., Briels, N., Flo, J., Malarvannan, G., Poma, G., Covaci, A., Herzke, D., Nygård, T., Bustnes, J.O., Jenssen, B.M., and Jaspers, V. First extensive evaluation of feathers for monitoring of both legacy and emerging contaminants. Submitted to Science of the Total Environment. .

Luster, M.I. (2014). A historical perspective of immunotoxicology. Journal of immunotoxicology *11*, 197-202.
Ma, Y., and He, B. (2014). Recognition of herpes simplex viruses: toll-like receptors and beyond. Journal of molecular biology *426*, 1133-1147.
Macko, S.A., Estep, M.L.F., Engel, M.H., and Hare, P. (1986). Kinetic fractionation of stable nitrogen isotopes during amino acid transamination. Geochimica et Cosmochimica Acta *50*, 2143-2146.
Mañosa, S. (1994). Goshawk diet in a Mediterranean area of northeastern Spain. J Raptor Res *28*, 84-92.
Mañosa, S. (2001). Strategies to identify dangerous electricity pylons for birds. Biodiversity and Conservation *10*, 1997-2012.
Mañosa, S., Mateo, R., Freixa, C., and Guitart, R. (2003). Persistent organochlorine contaminants in eggs of northern goshawk and Eurasian buzzard from northeastern Spain: temporal trends related to changes in the diet. Environmental Pollution *122*, 351-359.
Mare, C., and Graham, D. (1973). Falcon herpesvirus, the etiologic agent of inclusion body disease of falcons. Infection and immunity *8*, 118-126.
Martí, R., Del Moral, J.C., and de Ornitología, S.E. (2003). Atlas de la aves reproductoras de España (Ministerio de Medio Ambiente, Dirección General de Conservación de la Naturaleza; Sociedad Española de Ornitología (SEO/BirdLife)).
Martin, J.W., Mabury, S.A., Solomon, K.R., and Muir, D.C. (2003). Bioconcentration and tissue distribution of perfluorinated acids in rainbow trout (Oncorhynchus mykiss). Environmental Toxicology and Chemistry *22*, 196-204.
Martin, L.B., Hopkins, W.A., Mydlarz, L.D., and Rohr, J.R. (2010). The effects of anthropogenic global changes on immune functions and disease resistance. Annals of the New York Academy of Sciences *1195*, 129-148.
Martinez-Lopez, E., Maria-Mojica, P., Martinez, J.E., Calvo, J.F., Wright, J., Shore, R.F., Romero, D., and Garcia-Fernandez, A.J. (2007). Organochlorine residues in booted eagle (Hieraaetus pennatus) and goshawk (Accipiter gentilis) eggs from southeastern Spain. Environmental Toxicology and Chemistry *26*, 2373-2378.
Matz, M.V., Wright, R.M., and Scott, J.G. (2013). No control genes required: Bayesian analysis of qRT-PCR data. PloS one *8*, e71448.
Maul, G.G. (1998). Nuclear domain 10, the site of DNA virus transcription and replication. Bioessays *20*, 660-667.
McPherson, M., and Delany, M. (2016). Virus and host genomic, molecular, and cellular interactions during Marek's disease pathogenesis and oncogenesis. Poultry science *95*, 412-429.
Mehta, A., and Baltimore, D. (2016). MicroRNAs as regulatory elements in immune system logic. Nature Reviews Immunology *16*, 279-294.
Mettenleiter, T.C., Keil, G.M., and Fuchs, W. (2008). Molecular biology of animal herpesviruses. Animal viruses: molecular biology *12*, P531.
Meyer, J., Jaspers, V.L.B., Eens, M., and de Coen, W. (2009). The relationship between perfluorinated chemical levels in the feathers and livers of birds from different trophic levels. Science of The Total Environment *407*, 5894-5900.
Mollenhauer, M.A., Bradshaw, S.G., Fair, P.A., McGuinn, W.D., and Peden-Adams, M.M. (2011). Effects of perfluorooctane sulfonate (PFOS) exposure on markers of inflammation in female B6C3F1 mice. Journal of Environmental Science and Health, Part A *46*, 97-108.
Möller, A., Ahrens, L., Surm, R., Westerveld, J., van der Wielen, F., Ebinghaus, R., and de Voogt, P. (2010). Distribution and sources of polyfluoroalkyl substances (PFAS) in the River Rhine watershed. Environmental Pollution *158*, 3243-3250.
Morgan, R.W., Sofer, L., Anderson, A.S., Bernberg, E.L., Cui, J., and Burnside, J. (2001). Induction of host gene expression following infection of chicken embryo fibroblasts with oncogenic Marek's disease virus. Journal of virology *75*, 533-539.
Moss, E.G., Lee, R.C., and Ambros, V. (1997). The cold shock domain protein LIN-28 controls developmental timing in C. elegans and is regulated by the lin-4 RNA. Cell *88*, 637-646.

Müller, C.E., De Silva, A.O., Small, J., Williamson, M., Wang, X., Morris, A., Katz, S., Gamberg, M., and Muir, D.C. (2011). Biomagnification of perfluorinated compounds in a remote terrestrial food chain: lichen–caribou–wolf. Environmental science & technology *45*, 8665-8673.

Neerukonda, S.N., Katneni, U.K., Golovan, S., and Parcells, M.S. (2016). Evaluation and validation of reference gene stability during Marek's disease virus (MDV) infection. Journal of virological methods *236*, 111-116.

Newsted, J.L., Jones, P.D., Coady, K., and Giesy, J.P. (2005). Avian toxicity reference values for perfluorooctane sulfonate. Environmental science & technology *39*, 9357-9362.

Newton, K., and Dixit, V.M. (2012). Signaling in innate immunity and inflammation. Cold Spring Harbor perspectives in biology *4*, a006049.

Nilsson, H., Kärrman, A., Rotander, A., van Bavel, B., Lindström, G., and Westberg, H. (2010). Inhalation exposure to fluorotelomer alcohols yield perfluorocarboxylates in human blood? Environmental science & technology *44*, 7717-7722.

Nishioka, J., Iwahara, C., Kawasaki, M., Yoshizaki, F., Nakayama, H., Takamori, K., Ogawa, H., and Iwabuchi, K. (2012). Di-(2-ethylhexyl) phthalate induces production of inflammatory molecules in human macrophages. Inflammation Research *61*, 69-78.

Nøst, T.H., Helgason, L.B., Harju, M., Heimstad, E.S., Gabrielsen, G.W., and Jenssen, B.M. (2012). Halogenated organic contaminants and their correlations with circulating thyroid hormones in developing Arctic seabirds. Science of The Total Environment *414*, 248-256.

O'Connell, R.M., Rao, D.S., Chaudhuri, A.A., Boldin, M.P., Taganov, K.D., Nicoll, J., Paquette, R.L., and Baltimore, D. (2008). Sustained expression of microRNA-155 in hematopoietic stem cells causes a myeloproliferative disorder. Journal of Experimental Medicine *205*, 585-594.

O'Connell, R.M., Taganov, K.D., Boldin, M.P., Cheng, G., and Baltimore, D. (2007). MicroRNA-155 is induced during the macrophage inflammatory response. Proceedings of the National Academy of Sciences *104*, 1604-1609.

Ojala, P.M., Sodeik, B., Ebersold, M.W., Kutay, U., and Helenius, A. (2000). Herpes simplex virus type 1 entry into host cells: reconstitution of capsid binding and uncoating at the nuclear pore complex in vitro. Molecular and cellular biology *20*, 4922-4931.

Oláh, I., and Vervelde, L. (2008). Structure of the avian lymphoid system (Academic Press, London).

Olsen, G.W., Burris, J.M., Ehresman, D.J., Froehlich, J.W., Seacat, A.M., Butenhoff, J.L., and Zobel, L.R. (2007). Half-life of serum elimination of perfluorooctanesulfonate, perfluorohexanesulfonate, and perfluorooctanoate in retired fluorochemical production workers. Environmental health perspectives *115*, 1298.

Osterrieder, N., Kamil, J.P., Schumacher, D., Tischer, B.K., and Trapp, S. (2006). Marek's disease virus: from miasma to model. Nature Reviews Microbiology *4*, 283.

Padial, J.M., Barea, J.M., Contreras, F.J., Ávila, E., and Pérez, J. (1998). Dieta del azor común (Accipiter gentilis) en las sierras béticas de Granada durante el periodo de reproducción. Ardeola *45*, 55-62.

Pain, D.J., Cromie, R.L., Newth, J., Brown, M.J., Crutcher, E., Hardman, P., Hurst, L., Mateo, R., Meharg, A.A., and Moran, A.C. (2010). Potential hazard to human health from exposure to fragments of lead bullets and shot in the tissues of game animals. PLoS One *5*, e10315.

Pareek, S., Roy, S., Kumari, B., Jain, P., Banerjee, A., and Vrati, S. (2014). miR-155 induction in microglial cells suppresses Japanese encephalitis virus replication and negatively modulates innate immune responses. Journal of Neuroinflammation *11*, 97.

Parvizi, P., Abdul-Careem, M.F., Haq, K., Thanthrige-Don, N., Schat, K.A., and Sharif, S. (2010). Immune responses against Marek's disease virus. Animal health research reviews *11*, 123-134.

Paul, A.G., Jones, K.C., and Sweetman, A.J. (2009). A First Global Production, Emission,

And Environmental Inventory For

Perfluorooctane Sulfonate. Environmental Science & Technology *43*, 386-392.

Pearson, S.F., Levey, D.J., Greenberg, C.H., and Del Rio, C.M. (2003). Effects of elemental composition on the incorporation of dietary nitrogen and carbon isotopic signatures in an omnivorous songbird. Oecologia *135*, 516-523.

Peden-Adams, M.M., Keller, J.M., EuDaly, J.G., Berger, J., Gilkeson, G.S., and Keil, D.E. (2008). Suppression of humoral immunity in mice following exposure to perfluorooctane sulfonate. Toxicological Sciences *104*, 144-154.

Peden-Adams, M.M., Stuckey, J.E., Gaworecki, K.M., Berger-Ritchie, J., Bryant, K., Jodice, P.G., Scott, T.R., Ferrario, J.B., Guan, B., and Vigo, C. (2009). Developmental toxicity in white leghorn chickens following in ovo exposure to perfluorooctane sulfonate (PFOS). Reproductive Toxicology *27*, 307-318.

Peig, J., and Green, A.J. (2009). New perspectives for estimating body condition from mass/length data: the scaled mass index as an alternative method. Oikos *118*, 1883-1891.

Peig, J., and Green, A.J. (2010). The paradigm of body condition: a critical reappraisal of current methods based on mass and length. Functional Ecology *24*, 1323-1332.

Pello, S.J., and Olsen, G.H. (2013). Emerging and reemerging diseases of avian wildlife. Veterinary Clinics: Exotic Animal Practice *16*, 357-381.

Pelufo, R.G., Cano, R.M., and Hernández, A.M. (1990). Introducción al estudio de la biología del Azor ('Accipiter gentilis', L., 1758) en Albacete. Al-Basit: Revista de estudios albacetenses, 123-162.

Peraza, M.A., Burdick, A.D., Marin, H.E., Gonzalez, F.J., and Peters, J.M. (2005). The toxicology of ligands for peroxisome proliferator-activated receptors (PPAR). Toxicological Sciences *90*, 269-295.

Phalen, D., Holz, P., Rasmussen, L., and Bayley, C. (2011). Fatal columbid herpesvirus-1 infections in three species of Australian birds of prey. Australian veterinary journal *89*, 193-196.

Pignotti, E., Casas, G., Llorca, M., Tellbüscher, A., Almeida, D., Dinelli, E., Farré, M., and Barceló, D. (2017). Seasonal variations in the occurrence of perfluoroalkyl substances in water, sediment and fish samples from Ebro Delta (Catalonia, Spain). Science of The Total Environment *607*, 933-943.

Pinkerton, M.E., James F. X. Wellehan, J., Johnson, A.J., Childress, A.J., Fitzgerald, S.D., and Kinsel, M.J. (2008). Columbid herpesvirus-1 in two Cooper's Hawks (Accipiter cooperi) with fatal inclusion body disease. Journal of Wildlife Diseases *44*, 622-628.

Posner, S. (2013). Per and polyfluorinated substances in the Nordic Countries (Nordic Council of Ministers).

Poulsen, P.B., Jensen, A.A., Wallström, E., and Aps, E. (2005). More environmentally friendly alternatives to PFOS-compounds and PFOA. Environmental Project *1013*, 2005.

Powley, C.R., George, S.W., Russell, M.H., Hoke, R.A., and Buck, R.C. (2008). Polyfluorinated chemicals in a spatially and temporally integrated food web in the Western Arctic. Chemosphere *70*, 664-672.

Powley, C.R., George, S.W., Ryan, T.W., and Buck, R.C. (2005). Matrix effect-free analytical methods for determination of perfluorinated carboxylic acids in environmental matrixes. Analytical chemistry *77*, 6353-6358.

Presley, S.M., Austin, G.P., and Dabbert, C.B. (2010). 4 Influence of Pesticides and Environmental Contaminants on Emerging Diseases of Wildlife. Wildlife Toxicology: Emerging Contaminant and Biodiversity Issues, 73.

Prevedouros, K., Cousins, I.T., Buck, R.C., and Korzeniowski, S.H. (2006). Sources, Fate and Transport of Perfluorocarboxylates. Environmental Science & Technology *40*, 32-44.

Puren, A.J., Fantuzzi, G., Gu, Y., Su, M.S.-S., and Dinarello, C.A. (1998). Interleukin-18 (IFNgamma-inducing factor) induces IL-8 and IL-1beta via TNFalpha production from non-CD14+ human blood mononuclear cells. The Journal of clinical investigation *101*, 711-721.

Pyankov, V.I., Ziegler, H., Akhani, H., Deigele, C., and Luettge, U. (2010). European plants with C4 photosynthesis: geographical and taxonomic distribution and relations to climate parameters. Botanical Journal of the Linnean Society *163*, 283-304.

Qazi, M.R., Abedi, M.R., Nelson, B.D., DePierre, J.W., and Abedi-Valugerdi, M. (2010). Dietary exposure to perfluorooctanoate or perfluorooctane sulfonate induces hypertrophy in centrilobular hepatocytes and alters the hepatic immune status in mice. International immunopharmacology *10*, 1420-1427.

R Core Team (2015). R: A language and environment for statistical computing. R Foundation for Statistical Computing. 2014.

Rai, D., Kim, S.-W., McKeller, M.R., Dahia, P.L., and Aguiar, R.C. (2010). Targeting of SMAD5 links microRNA-155 to the TGF-β pathway and lymphomagenesis. Proceedings of the National Academy of Sciences *107*, 3111-3116.

Remple, J. (2000). Considerations on the production of a safe and efficacious falcon herpesvirus vaccine. Lumeij, JT, D. Remple, PT.

Resano-Mayor, J., Hernández-Matías, A., Real, J., Moleón, M., Parés, F., Inger, R., and Bearhop, S. (2014). Multi-scale effects of nestling diet on breeding performance in a terrestrial top predator inferred from stable isotope analysis. PLoS One *9*, e95320.

Riddell, N., Arsenault, G., Benskin, J.P., Chittim, B., Martin, J.W., McAlees, A., and McCrindle, R. (2009). Branched Perfluorooctane Sulfonate Isomer Quantification and Characterization in Blood Serum Samples by HPLC/ESI-MS(/MS). Environmental Science & Technology *43*, 7902-7908.

Ring, K., Kalin, T., and Kishi, A. (2002). Fluoropolymers. (CEH Marketing Research Report. Chemical Economics Handbook—SRI International).

Rodriguez, A., Vigorito, E., Clare, S., Warren, M.V., Couttet, P., Soond, D.R., van Dongen, S., Grocock, R.J., Das, P.P., Miska, E.A*., et al.* (2007). Requirement of bic/microRNA-155 for Normal Immune Function. Science *316*, 608-611.

Route, W.T., Russell, R.E., Lindstrom, A.B., Strynar, M.J., and Key, R.L. (2014). Spatial and temporal patterns in concentrations of perfluorinated compounds in bald eagle nestlings in the upper midwestern United States. Environmental science & technology *48*, 6653-6660.

Rutz, C. (2006). Home range size, habitat use, activity patterns and hunting behaviour of urban-breeding Northern Goshawks Accipiter gentilis. ARDEA-WAGENINGEN- *94*, 185.

Rutz, C., Bijlsma, R., Marquiss, M., and Kenward, R.E. (2006). Population limitation in the Northern Goshawk in Europe: a review with case studies. Studies in Avian Biology *31*, 158.

Sagerup, K., Savinov, V., Savinova, T., Kuklin, V., Muir, D.C., and Gabrielsen, G.W. (2009). Persistent organic pollutants, heavy metals and parasites in the glaucous gull (Larus hyperboreus) on Spitsbergen. Environmental pollution *157*, 2282-2290.

Sakar, D., Prukner-Radovčić, E., Prevendar Crnić, A., Pompe-Gotal, J., Ragland, W., and Mazija, H. (2004). Marek's disease vaccination, with turkey herpesvirus, and enrofloxacin modulate the activities of hepatic microsomal enzymes in broiler chickens. Acta Veterinaria Hungarica *52*, 211-217.

Samir, M., Vaas, L.A.I., and Pessler, F. (2016). MicroRNAs in the Host Response to Viral Infections of Veterinary Importance. Frontiers in Veterinary Science *3*, 86.

Schelcher, C., Valencia, S., Delecluse, H.-J., Hicks, M., and Sinclair, A.J. (2005). Mutation of a single amino acid residue in the basic region of the Epstein-Barr virus (EBV) lytic cycle switch protein Zta (BZLF1) prevents reactivation of EBV from latency. Journal of virology *79*, 13822-13828.

Scheringer, M., Trier, X., Cousins, I.T., de Voogt, P., Fletcher, T., Wang, Z., and Webster, T.F. (2014). Helsingør Statement on poly- and perfluorinated alkyl substances (PFASs). Chemosphere *114*, 337-339.

Schmitz, M.L., Bacher, S., and Kracht, M. (2001). IκB-independent control of NF-κB activity by modulatory phosphorylations. Trends in biochemical sciences *26*, 186-190.

Selås, V. (1998). Does food competition from red fox (Vulpes vulpes) influence the breeding density of goshawk (Accipiter gentilis)? Evidence from a natural experiment. Journal of Zoology *246*, 325-335.

Selås, V., Steen, O.F., and Johnsen, J.T. (2008). Goshawk breeding densities in relation to mature forest in southeastern Norway. Forest Ecology and Management *256*, 446-451.

Seow, J. (2013). Fire Fighting Foams with Perfluorochemicals-Environmental Review. Conservation Western Australia (Hemming Information Services).

Shi, Y., Vestergren, R., Zhou, Z., Song, X., Xu, L., Liang, Y., and Cai, Y. (2015). Tissue distribution and whole body burden of the chlorinated polyfluoroalkyl ether sulfonic acid F-53B in crucian carp (Carassius carassius): Evidence for a highly bioaccumulative contaminant of emerging concern. Environmental science & technology *49*, 14156-14165.

Sletten, S., Bourgeon, S., Bårdsen, B.-J., Herzke, D., Criscuolo, F., Massemin, S., Zahn, S., Johnsen, T.V., and Bustnes, J.O. (2016). Organohalogenated contaminants in white-tailed eagle (Haliaeetus albicilla) nestlings: An assessment of relationships to immunoglobulin levels, telomeres and oxidative stress. Science of the Total Environment *539*, 337-349.

Smith, P.L., Lombardi, G., and Foster, G.R. (2005). Type I interferons and the innate immune response—more than just antiviral cytokines. Molecular immunology *42*, 869-877.

Smith, R.S., Smith, T.J., Blieden, T.M., and Phipps, R.P. (1997). Fibroblasts as sentinel cells. Synthesis of chemokines and regulation of inflammation. The American journal of pathology *151*, 317.

Smithwick, M., Mabury, S.A., Solomon, K.R., Sonne, C., Martin, J.W., Born, E.W., Dietz, R., Derocher, A.E., Letcher, R.J., and Evans, T.J. (2005). Circumpolar study of perfluoroalkyl contaminants in polar bears (Ursus maritimus). Environmental science & technology *39*, 5517-5523.

Smits, J.E., and Nain, S. (2013). Immunomodulation and hormonal disruption without compromised disease resistance in perfluorooctanoic acid (PFOA) exposed Japanese quail. Environmental pollution *179*, 13-18.

Sonkoly, E., and Pivarcsi, A. (2011). MicroRNAs in inflammation and response to injuries induced by environmental pollution. Mutation Research/Fundamental and Molecular Mechanisms of Mutagenesis *717*, 46-53.

Sonne, C., Bustnes, J.O., Herzke, D., Jaspers, V.L., Covaci, A., Eulaers, I., Halley, D.J., Moum, T., Ballesteros, M., and Eens, M. (2012). Blood plasma clinical–chemical parameters as biomarker endpoints for organohalogen contaminant exposure in Norwegian raptor nestlings. Ecotoxicology and environmental safety *80*, 76-83.

Sonne, C., Bustnes, J.O., Herzke, D., Jaspers, V.L.B., Covaci, A., Halley, D.J., Moum, T., Eulaers, I., Eens, M., Ims, R.A*., et al.* (2010). Relationships between organohalogen contaminants and blood plasma clinical–chemical parameters in chicks of three raptor species from Northern Norway. Ecotoxicology and Environmental Safety *73*, 7-17.

Spear, P.G., and Longnecker, R. (2003). Herpesvirus entry: an update. Journal of virology *77*, 10179-10185.

Stahl, T., Mattern, D., and Brunn, H. (2011). Toxicology of perfluorinated compounds. Environmental Sciences Europe *23*, 38.

Sun, A., Wang, J., Chia, J., and Chiang, C. (2005). Serum interleukin-8 level is a more sensitive marker than serum interleukin-6 level in monitoring the disease activity of oral lichen planus. British Journal of Dermatology *152*, 1187-1192.

Sunyer, T., Rothe, L., Jiang, X., Osdoby, P., and Collin-Osdoby, P. (1996). Proinflammatory agents, IL-8 and IL-10, upregulate inducible nitric oxide synthase expression and nitric oxide production in avian osteoclast-like cells. Journal of cellular biochemistry *60*, 469-483.

Swaminathan, G., Rossi, F., Sierra, L.-J., Gupta, A., Navas-Martín, S., and Martín-García, J. (2012). A role for microRNA-155 modulation in the anti-HIV-1 effects of Toll-like receptor 3 stimulation in macrophages. PLoS pathogens *8*, e1002937.

Szép, T., Hobson, K., Vallner, J., Piper, S., Kovács, B., Szabó, D., and Møller, A. (2009). Comparison of trace element and stable isotope approaches to the study of migratory connectivity: an example using two hirundine species breeding in Europe and wintering in Africa. Journal of Ornithology *150*, 621.

Taddeo, B., and Roizman, B. (2006). The virion host shutoff protein (UL41) of herpes simplex virus 1 is an endoribonuclease with a substrate specificity similar to that of RNase A. Journal of virology *80*, 9341-9345.

Taiyun, W., and Viliam, S. (2017). R package "corrplot": Visualization of a Correlation Matrix (Version 0.84). Available from https://github.com/taiyun/corrplot.

Takacs, M.L., and Abbott, B.D. (2006). Activation of mouse and human peroxisome proliferator–activated receptors (α, β/δ, γ) by perfluorooctanoic acid and perfluorooctane sulfonate. Toxicological Sciences *95*, 108-117.

Takeuchi, O., and Akira, S. (2009). Innate immunity to virus infection. Immunological reviews *227*, 75-86.

Takeuchi, O., and Akira, S. (2010). Pattern recognition receptors and inflammation. Cell *140*, 805-820.

Tella, J., and Mañosa, S. (1993). Eagle Owl predation on Egyptian Vulture and Northern Goshawk: possible effect of a decrease in European rabbit availability. J Raptor Res *27*, 111-112.

Thai, T.-H., Calado, D.P., Casola, S., Ansel, K.M., Xiao, C., Xue, Y., Murphy, A., Frendewey, D., Valenzuela, D., and Kutok, J.L. (2007). Regulation of the germinal center response by microRNA-155. Science *316*, 604-608.

Tili, E., Michaille, J.J., and Croce, C.M. (2013). MicroRNAs play a central role in molecular dysfunctions linking inflammation with cancer. Immunological reviews *253*, 167-184.

Tomy, G.T., Budakowski, W., Halldorson, T., Helm, P.A., Stern, G.A., Friesen, K., Pepper, K., Tittlemier, S.A., and Fisk, A.T. (2004). Fluorinated Organic Compounds in an Eastern Arctic Marine Food Web. Environmental Science & Technology *38*, 6475-6481.

Tornberg, R., Mönkkönen, M., and Kivelä, S.M. (2009). Landscape and season effects on the diet of the Goshawk. Ibis *151*, 396-400.

Ulrich, R., Schinköthe, J., Krone, O., and Harder, T. (2018). Lesion Profile in Raptors Monitored During the 2016–2017 H5N8 Outbreak in Northern Germany. Journal of Comparative Pathology *158*, 114.

UNEP (2009). Stockholm Convention on POPs. The 9 new POPs. In: An Introduction to the Nine Chemicals Added to the Stockholm Convention by the Conference of the Parties at its Fourth Meeting. 10. UNEP

USEPA (2006). 010/15 PFOA Stewardship Program. http://www.epa.gov/oppt/pfoa/pubs/pfoastewardship.htm (accessed 30/04/2018). .

USEPA (2015). EPA's Non-CBI Summary Tables for 2015 Company Progress Reports (Final Progress Reports). https://www.epa.gov/sites/production/files/2017-02/documents/2016_pfoa_stewardship_summary_table_0.pdf (accessed 30/04/2018).

Valencia-Sanchez, M.A., Liu, J., Hannon, G.J., and Parker, R. (2006). Control of translation and mRNA degradation by miRNAs and siRNAs. Genes & development *20*, 515-524.

Verdejo, J. (1994). Datos sobre la reproducción y alimentación del azor (Accipiter gentilis) en un área mediterránea. Ardeola *41*, 37-43.

Verreault, J., Berger, U., and Gabrielsen, G.W. (2007). Trends of perfluorinated alkyl substances in herring gull eggs from two coastal colonies in northern Norway: 1983− 2003. Environmental science & technology *41*, 6671-6677.

Vicente, J., Sanpera, C., García-Tarrasón, M., Pérez, A., and Lacorte, S. (2015). Perfluoroalkyl and polyfluoroalkyl substances in entire clutches of Audouin's gulls from the Ebro delta. Chemosphere *119*, S62-S68.

Voorspoels, S., Covaci, A., Maervoet, J., and Schepens, P. (2002). Relationship between age and levels of organochlorine contaminants in human serum of a Belgian population. Bulletin of environmental contamination and toxicology *69*, 22-29.

Wallach, D., Varfolomeev, E., Malinin, N., Goltsev, Y.V., Kovalenko, A., and Boldin, M. (1999). Tumor necrosis factor receptor and Fas signaling mechanisms. Annual review of immunology *17*, 331-367.

Walsh, P.S., Metzger, D.A., and Higuchi, R. (1991). Chelex 100 as a medium for simple extraction of DNA for PCR-based typing from forensic material. Biotechniques *10*, 506-513.

Wang, L., Bammler, T.K., Beyer, R.P., and Gallagher, E.P. (2013). Copper-Induced Deregulation of microRNA Expression in the Zebrafish Olfactory System. Environmental Science & Technology *47*, 7466-7474.

Wang, P., Hou, J., Lin, L., Wang, C., Liu, X., Li, D., Ma, F., Wang, Z., and Cao, X. (2010). Inducible microRNA-155 Feedback Promotes Type I IFN Signaling in Antiviral Innate Immunity by Targeting Suppressor of Cytokine Signaling 1. The Journal of Immunology *185*, 6226-6233.

Wang, Z., Cousins, I.T., Scheringer, M., Buck, R.C., and Hungerbühler, K. (2014). Global emission inventories for C4–C14 perfluoroalkyl carboxylic acid (PFCA) homologues from 1951 to 2030, Part I: production and emissions from quantifiable sources. Environment International *70*, 62-75.

Wang, Z., DeWitt, J.C., Higgins, C.P., and Cousins, I.T. (2017). A Never-Ending Story of Per- and Polyfluoroalkyl Substances (PFASs)? Environmental Science & Technology *51*, 2508-2518.

Waugh, C.A., Arukwe, A., and Jaspers, V.L. (2018). Deregulation of microRNA-155 and its transcription factor NF-kB by polychlorinated biphenyls during viral infections. APMIS.

Waugh, C.A., and Jaspers, V. (2018). Virus infections are augmented by exposure to environmental pollutants in vertebrates. Submitted to Nature Communications.

Weinberg, I., Dreyer, A., and Ebinghaus, R. (2011). Waste water treatment plants as sources of polyfluorinated compounds, polybrominated diphenyl ethers and musk fragrances to ambient air. Environmental Pollution *159*, 125-132.

Widén, P. (1997). HOW, AND WHY, IS THE GOSHAWK (ACCIPITER GENTILIS). J. Raptor Res *31*, 107-113.

Wodak, E., Richter, S., Bagó, Z., Revilla-Fernández, S., Weissenböck, H., Nowotny, N., and Winter, P. (2011). Detection and molecular analysis of West Nile virus infections in birds of prey in the eastern part of Austria in 2008 and 2009. Veterinary microbiology *149*, 358-366.

Woodward, E.A., Prêle, C.M., Nicholson, S.E., Kolesnik, T.B., and Hart, P.H. (2010). The anti-inflammatory effects of interleukin-4 are not mediated by suppressor of cytokine signalling-1 (SOCS1). Immunology *131*, 118-127.

Xing, Z., Cardona, C.J., Li, J., Dao, N., Tran, T., and Andrada, J. (2008). Modulation of the immune responses in chickens by low-pathogenicity avian influenza virus H9N2. Journal of General Virology *89*, 1288-1299.

Xing, Z., and Schat, K.A. (2000). Expression of cytokine genes in Marek's disease virus-infected chickens and chicken embryo fibroblast cultures. Immunology *100*, 70-76.

Yamashita, N., Kannan, K., Taniyasu, S., Horii, Y., Petrick, G., and Gamo, T. (2005). A global survey of perfluorinated acids in oceans. Marine Pollution Bulletin *51*, 658-668.

Yang, Q., Abedi-Valugerdi, M., Xie, Y., Zhao, X.-Y., Möller, G., Nelson, B.D., and DePierre, J.W. (2002). Potent suppression of the adaptive immune response in mice upon dietary exposure to the potent peroxisome proliferator, perfluorooctanoic acid. International immunopharmacology *2*, 389-397.

Yeung, L.W.Y., Guruge, K.S., Yamanaka, N., Miyazaki, S., and Lam, P.K.S. (2007). Differential expression of chicken hepatic genes responsive to PFOA and PFOS. Toxicology *237*, 111-125.

Yoo, H., Guruge, K.S., Yamanaka, N., Sato, C., Mikami, O., Miyazaki, S., Yamashita, N., and Giesy, J.P. (2009). Depuration kinetics and tissue disposition of PFOA and PFOS in white leghorn chickens (Gallus gallus) administered by subcutaneous implantation. Ecotoxicology and environmental safety *72*, 26-36.

Zareitalabad, P., Siemens, J., Hamer, M., and Amelung, W. (2013). Perfluorooctanoic acid (PFOA) and perfluorooctanesulfonic acid (PFOS) in surface waters, sediments, soils and wastewater – A review on concentrations and distribution coefficients. Chemosphere *91*, 725-732.

Zhang, Y.-Z., Zeng, X.-W., Qian, Z., Vaughn, M.G., Geiger, S.D., Hu, L.-W., Lu, L., Fu, C., and Dong, G.-H. (2017). Perfluoroalkyl substances with isomer analysis in umbilical cord serum in China. Environmental Science and Pollution Research *24*, 13626-13637.

Zhao, Y., Yao, Y., Xu, H., Lambeth, L., Smith, L.P., Kgosana, L., Wang, X., and Nair, V. (2009). A functional MicroRNA-155 ortholog encoded by the oncogenic Marek's disease virus. Journal of virology *83*, 489-492.

Zheng, L., Dong, G.-H., Zhang, Y.-H., Liang, Z.-F., Jin, Y.-H., and He, Q.-C. (2011). Type 1 and Type 2 cytokines imbalance in adult male C57BL/6 mice following a 7-day oral exposure to perfluorooctanesulfonate (PFOS). Journal of immunotoxicology *8*, 30-38.

Zhu, Y., Qin, X.-D., Zeng, X.-W., Paul, G., Morawska, L., Su, M.-W., Tsai, C.-H., Wang, S.-Q., Lee, Y.L., and Dong, G.-H. (2016). Associations of serum perfluoroalkyl acid levels with T-helper cell-specific cytokines in children: By gender and asthma status. Science of the Total Environment *559*, 166-173.

Zou, H., Su, R., Ruan, J., Shao, H., Qian, K., Ye, J., and Qin, A. (2017). Toll-like receptor 3 pathway restricts Marek's disease virus infection. Oncotarget *8*, 70847.

Zsivanovits, P., Forbes, N.A., Zvonar, L.T., Williams, M.R., Lierz, M., Prusas, C., and Hafez, M.M. (2004). Investigation into the seroprevalence of falcon herpesvirus antibodies in raptors in the UK using virus neutralization tests and different herpesvirus isolates. Avian pathology *33*, 599-604.

Zuberogoitia, I., and Martínez, J.E. (2015). Azor común–Accipiter gentilis (Linnaeus, 1758).

Appendix A

Figure A1. Goshawk nesting sites in Trøndelag (n=20), central Norway. Nestlings from these nests were sampled between 18/06/2016 and 28/06/2016. Modified from https://www.geoplaner.com.

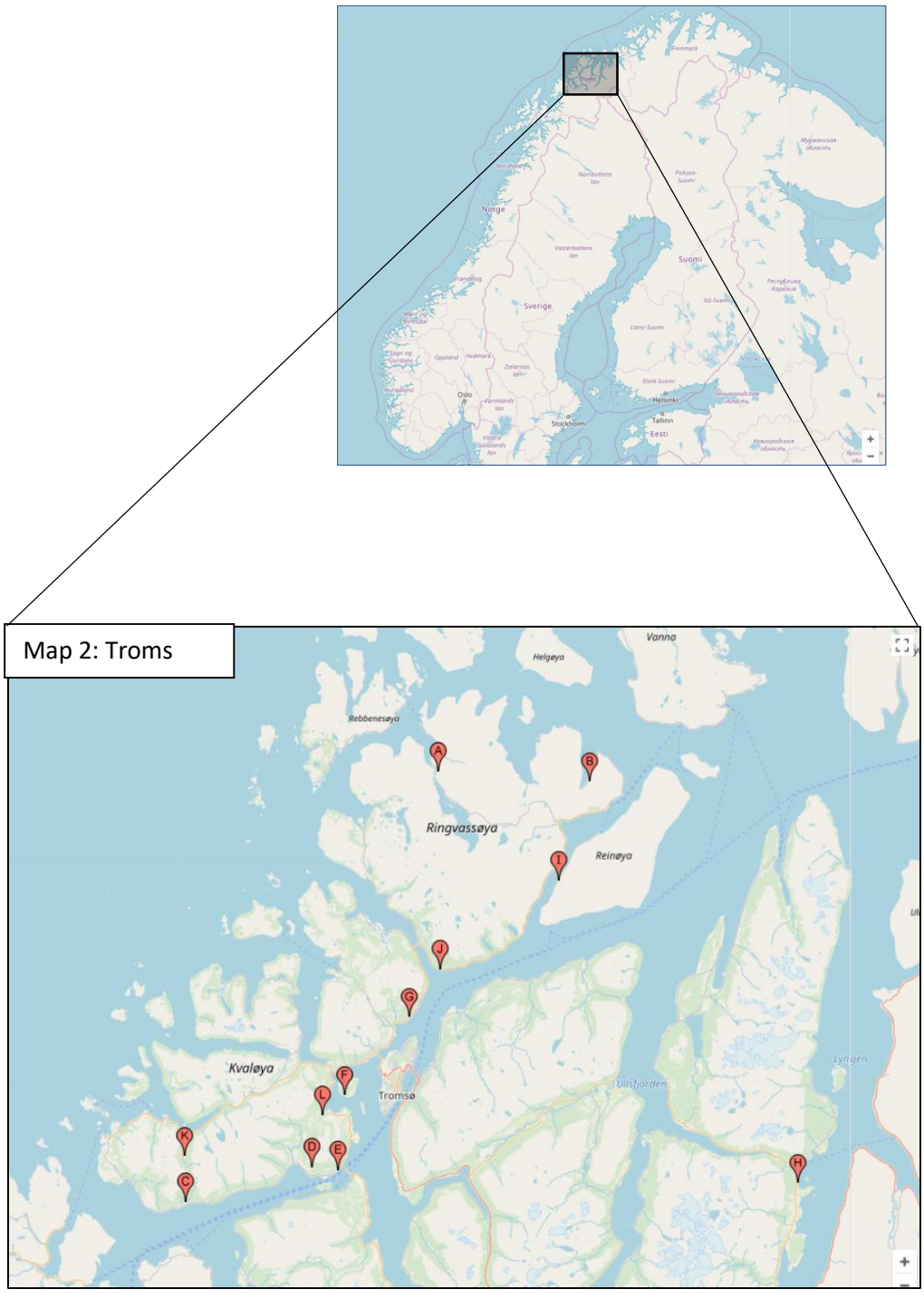

Figure A2. Goshawk nesting sites in Troms (n=12), northern Norway. Nestlings from these nests were sampled between 22/06/2016 and 28/06/2016. Modified from https://www.geoplaner.com.

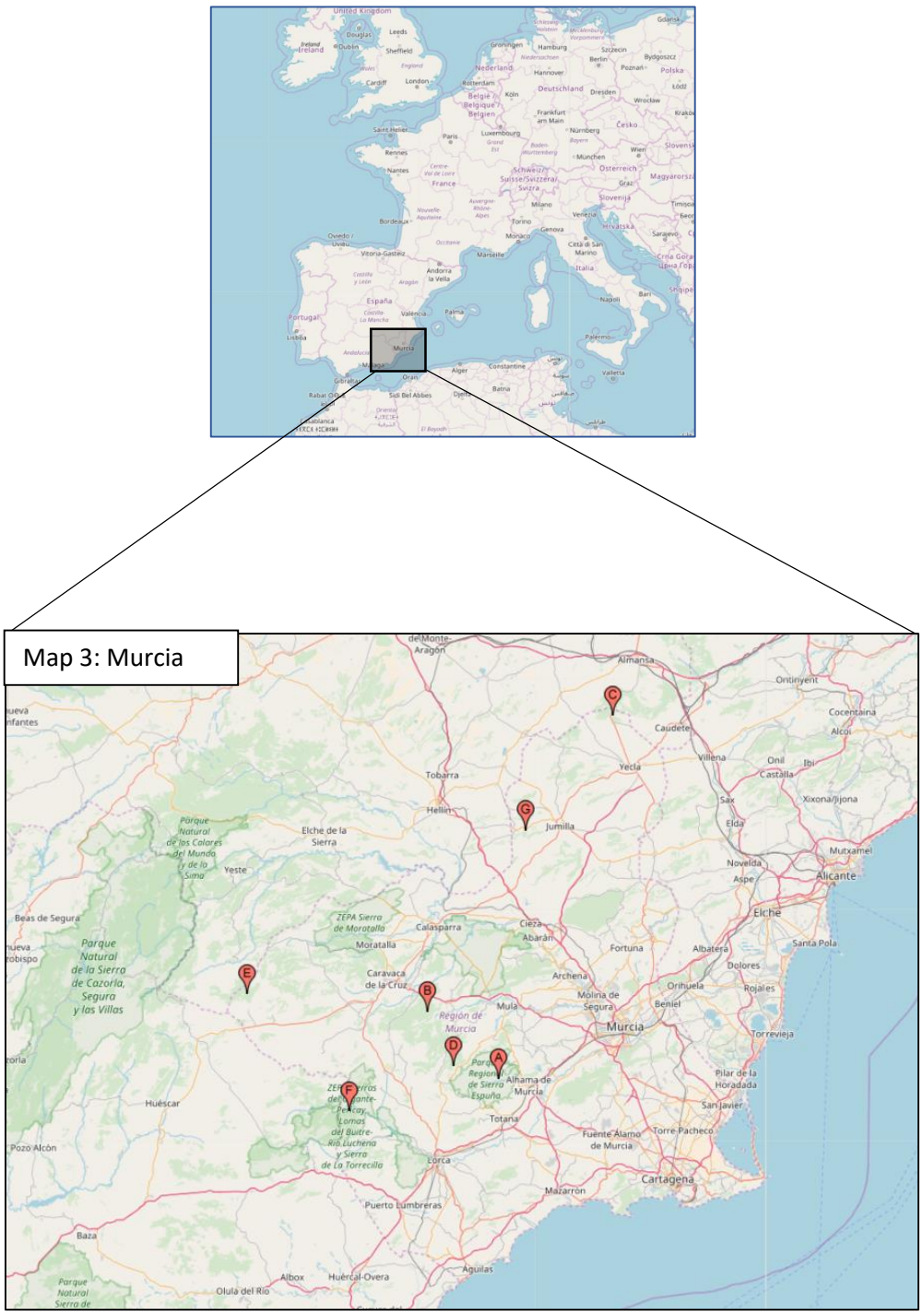

Figure A3. Goshawk nesting sites in Murcia (*n*=**7**), southeastern Spain. Nestlings from these nests were sampled between 01/06/2016 and 14/06/2016. Modified from https://www.geoplaner.com.

Table A1. Overview of the number of blood and feather samples (*N*) per sex and location.

	Troms (*n*=11)			**Trøndelag** (*n*=20)			**Murcia** (*n*=7)		
	N	*N* (males)	*N* (females)	*N*	*N* (males)	*N* (females)	*N*	*N* (males)	*N* (females)
Blood	11	9	2	20	12	8	7	5	2
Feathers	12	-[a]	-[a]	20	-[a]	-[a]	7	-[a]	-[a]

[a]Feathers were pooled per nest and thus do not correspond to a specific sex.

Table A2. Morphometrics, age and sex of goshawk nestlings from Troms, Trøndelag and Murcia. Only relevant measurements for this study were included in the table.

ID	Region	Sex	Age (days)	Mass (g)	Wing length (cm)	Bill length (mm)
NG.16.TOS - 1	Troms	M	27	780	19	19.4
NG.16.TOS - 2	Troms	M	26	740	18	19
NG.16.TOS - 3	Troms	M	29	785	20.7	19.4
NG.16.TOS - 4	Troms	F	30	1050	22.2	22
NG.16.TOS - 5	Troms	M	33	850	23.2	20.8
NG.16.TOS - 6	Troms	M	29	550	20	14
NG.16.TOS - 8	Troms	M	30	810	21.4	20.5
NG.16.TOS - 9	Troms	F	32	1030	24.2	18.8
NG.16.TOS - 10	Troms	M	34	880	24	20.2
NG.16.TOS - 11	Troms	M	33	740	23.5	19.8
NG.16.TOS - 12	Troms	M	34	680	24.5	20.1
NG.16.TRD - 1	Trøndelag	F	29	1050	22	22.3
NG.16.TRD - 2	Trøndelag	M	34	715	24.3	19.5
NG.16.TRD - 3	Trøndelag	M	35	775	25	20.1
NG.16.TRD - 4	Trøndelag	M	27	775	18.5	19.3
NG.16.TRD - 5	Trøndelag	M	30	775	21.1	19.8
NG.16.TRD - 6	Trøndelag	M	31	830	22.1	20.1
NG.16.TRD - 7	Trøndelag	F	30	1175	22.8	23.1
NG.16.TRD - 8	Trøndelag	F	33	1225	25.1	21.5
NG.16.TRD - 9	Trøndelag	F	31	1200	23.1	22.8
NG.16.TRD - 10	Trøndelag	F	27	1060	20.2	21.7
NG.16.TRD - 11	Trøndelag	M	31	850	21.8	20.2
NG.16.TRD - 12	Trøndelag	M	29	815	20.6	20
NG.16.TRD - 13	Trøndelag	M	32	855	22.6	20
NG.16.TRD - 14	Trøndelag	M	34	825	24.3	19.1
NG.16.TRD - 15	Trøndelag	M	28	730	19.7	20.3
NG.16.TRD - 16	Trøndelag	F	33	1175	25.3	23.9
NG.16.TRD - 17	Trøndelag	F	34	1250	26	22.7
NG.16.TRD - 18	Trøndelag	F	27	1100	20.2	22.2
NG.16.TRD - 19	Trøndelag	M	32	890	22.5	20.1
NG.16.TRD - 20	Trøndelag	M	34	785	24.4	20.2
NG.16.MUR - 1	Murcia	F	27	825	20	21
NG.16.MUR - 2	Murcia	F	26	875	18.8	20
NG.16.MUR - 3	Murcia	F	27	850	19.6	20.5
NG.16.MUR - 4	Murcia	F	28	760	21	21
NG.16.MUR - 5	Murcia	F	27	920	20	20
NG.16.MUR - 7	Murcia	F	24	775	17.4	19.4
NG.16.MUR - 8	Murcia	M	29	585	20.1	19

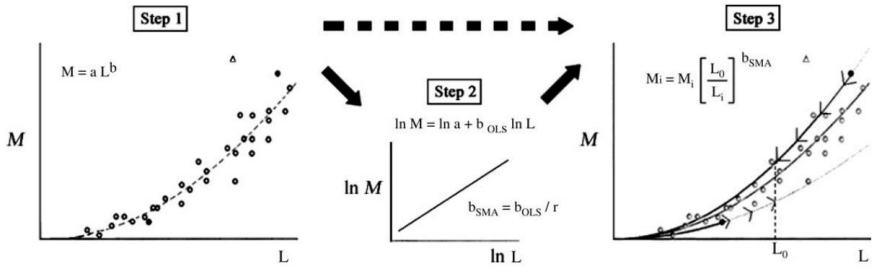

Figure A4. Stepwise method to calculate the scaled mass index (SMI), as explained in Peig and Green (2009) which was used as a body condition index in this study after correction for sex- and region-dependent differences.

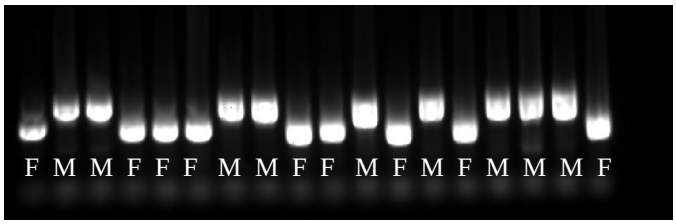

Figure A5. Gel electrophoresis as last step in the molecular sexing of goshawk nestlings that presented intermediate characteristics between males and females and could not be reliably sexed based on morphometric data. CHD-1-Z and CHD-1-W were extracted from blood and amplified prior to electrophoresis. Lower and higher fluorescent bands correspond to females and males, respectively.

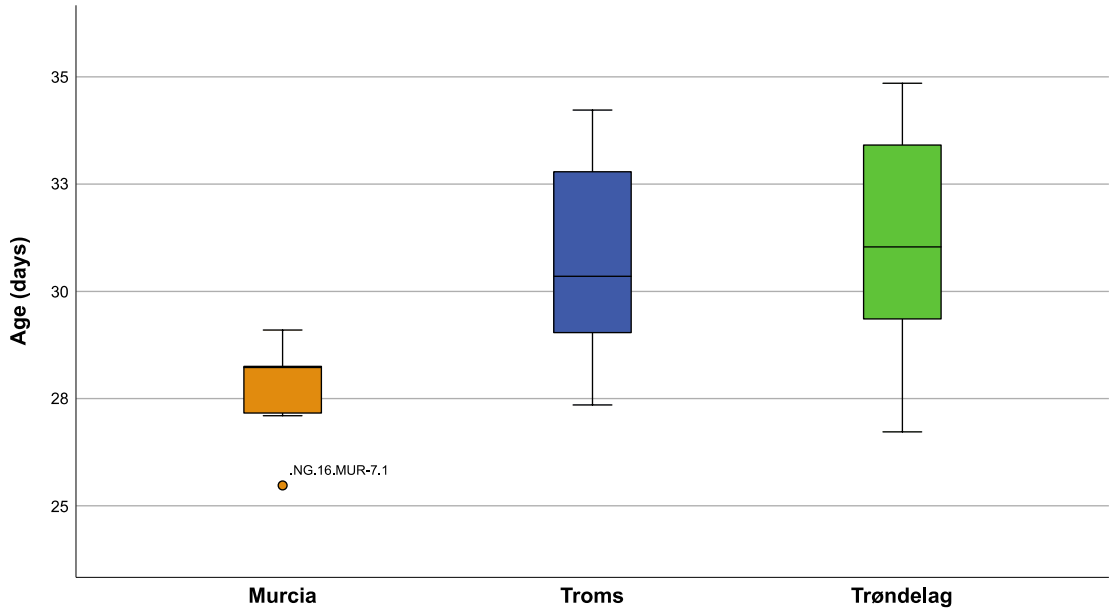

Figure A6. Box and whisker plot of nestling age (days) within Murcia, Troms and Trøndelag. Horizontal lines represent median values. Boxes represent 25th – 75th percentiles, whiskers correspond to 95% confidence intervals and outliers are shown as dots.

Appendix B

Table B1. Internal standard (ISTD) mix (^{13}C PFAS mix) for plasma and feather samples provided by NILU and used during extraction and clean-up prior to target PFAS quantification.

Compound	Abbreviation	Concentration (ng/mL)
Perfluorobutanoic acid	PFBA	100
Perfluoropentanoic acid	PFPA	100
Perfluorohexanoic acid	PFHxA	100
Perfluoroheptanoic acid	PFHpA	100
Perfluorooctanoic acid	PFOA	100
Perfluorononanoic acid	PFNA	100
Perfluorodecanoic acid	PFDA	100
Perfluoroundecanoic acid	PFUnDA	100
Perfluorododecanoic acid	PFDoDA	100
Perfluorotetradecanoic acid	PFTeDA	100
Perfluorobutane sulfonate	PFBS	100
Perfluorohexane sulfonate	PFHxS	100
Perfluorooctane sulfonate	PFOS	100
Perfluorooctane sulfonamide	PFOSA	100
6:2 Fluorotelomer sulfonate	6:2 FTS	100
8:2 Fluorotelomer sulfonate	8:2 FTS	100

Table B2. Mean recoveries (%) of the internal standard from the ISTD mix in plasma and feathers.

	PFBA	PFPA	PFHxA	PFHpA	PFOA	PFNA	PFDA	PFUnDA	PFDoDA
Feather recovery (%)		112	110	135	122		119	123	138
Plasma recovery (%)	75	87	86	93	89	83	85	75	63

	PFTeDA	PFHxS	PFOS	PFOSA	6:2 FTS
Feather recovery (%)		96	97	95	127
Plasma recovery (%)	36	87	84	75	81

Appendix C

C1. Preparation of cell cultures and viral stocks

Chicken embryo fibroblasts (CEFs)

Chicken embryo fibroblasts (ATCC® CRL-12203TM, *Gallus gallus* embryo) were purchased from a commercial supplier (LGC Standards GmbH, Germany). The base growth medium for chicken embryo fibroblasts (CEFs) is ATCC-formulated Dulbecco's Modified Eagle's Medium (Sigma, Cat. No. 30-2002). Complete growth medium (DMEM 10% FCS) was obtained by adding 10% fetal calf serum (FCS), 50 mg/mL Gentamycin, 100 units/mL Penicillin and 100 µg/mL Streptomycin. Preparation of the CEF stock consisted in subculturing cells that had been cryopreserved in liquid nitrogen. Handling of frozen cells was initiated by thawing the original CEF-containing vial through gentle agitation in a 39ºC water bath for 2 min. Following decontamination by spraying the vial with 70% ethanol, the content was transferred to a centrifuge tube containing 9 mL DMEM (10% FCS) and spun at 150 g for 5 min. The supernatant, which contained unwanted freezing medium, was discarded and the cell pellet was resuspended with 2 mL of pre-warmed DMEM (10% FCS). The resuspended cells were placed into a pre-warmed culture flask (T75 flask) with 9 mL of media and incubated at 39ºC with 5% CO_2 (first passage). The growing cells were inspected daily. They progressively attached to the flask surface, changed their shape, and increased in number and confluency.

After four days of incubation, they were 90% confluent and ready to subculture into new T75 flasks for the first time. The subculturing or splitting procedure started with the removal of old media and rinsing of the cell layer with pre-warmed PBS to eliminate any traces of serum. Serum contains natural trypsin inhibitors (e.g. serpins) that may impair the following step and must therefore be removed in advance. 1 mL of TrypsinEDTA was then added to cover the entire cell monolayer with the solution. This leads to the detachment of CEFs upon incubation at 39ºC for 5 min, which was confirmed under an inverted microscope prior to splitting. 8 mL of DMEM (10% FCS) was added to the flask, and cells were aspirated by gentle pipetting. The cell suspension was eventually added in 3 ml aliquots to three pre-warmed T75 flasks and incubated (second passage). This procedure was repeated twice more (fourth passage). CEFs were only split after reaching a minimum confluency of 70%, which generally took them around 48h per passage. CEFs from the fourth passage were later used in the experiments. The passage number should be high enough to provide enough cells for the planned experiments, but excessive passages may introduce unwanted genetic variation and should therefore be avoided (pers. comm. C.A Waugh). Immediately after subculturing, CEFs were cryopreserved until experimental use. For this purpose, we prepared freezing media (containing 5% dimethyl sulfoxide) and kept it cold in the fridge. The cells were then trypsinized and resuspended in DMEM (10% FCS) as previously described. The cell suspension was centrifuged, the supernatant was discarded and the cell pellet was resuspended in 1 mL of cold cryopreservation media. The CEFs were then transferred to 1.5 mL cryovials, which were quickly placed in an isopropanol chamber. The chamber with the cryovials was kept at -80ºC overnight, and the cryovials were eventually stored in liquid nitrogen. Before the experimental use of CEFs, they were resuscitated in order to get them into the dividing state.

Gallid herpesvirus-2 (GaHV-2)

The gallid herpesvirus-2 (GaHV-2) model used in this study (ATCC® VR-2175™) was purchased from a commercial supplier (LGC Standards GmbH, Germany). GaHV-2 is a cell-associated virus and is commercially available in infected CEF seeds. The infected cell seed was stored in liquid nitrogen upon arrival. Viruses were propagated on cultured CEFs. The preparation of the virus stock consisted in inoculating CEFs with the infectious agents to facilitate their replication. For this purpose, we initially seeded and cultured non-infected CEFs in T75 flasks until they reached at least 80% confluency. The culture media was changed once before infection, as it would stay with the infected CEFs for 4-7 additional days following infection. The infected cell seed was thawed and added to 10 mL of pre-warmed DMEM (10% FCS). Two flasks were kept as negative uninfected controls. The flasks were incubated for 7 days at 39ºC with 5% CO_2, and we daily checked for microscopically visible signs of virus replication. Infected cells typically undergo structural alterations, known as cytopathic effect, that result in the formation of lytic plaques. This phenomenon was observed 6 after infection, and we then proceeded to cryopreserve the virus stock the next day. The viruses were harvested via trypsinization and centrifugation of the cell pellet. Cells were then resuspended in 1 mL of fresh DMEM with 10% FCS and 10% DMSO, and transferred to cryovials. The virus-containing cryovials were kept at -80ºC inside the isopropanol chamber overnight, and stored in liquid nitrogen later on.

Appendix D

D1. Plaque assay of GaHV-2 on CEF monolayers

Preparation of stock solutions for exposure and infection

Prior to the exposure stage, a stock PFOS solution was prepared from its potassium salt, also known as heptadecafluorooctanesulfonic acid potassium (Cat. No 7782, Sigma Aldrich, St Louis, USA). PFOS potassium salt contains branched and linear PFOS isomers, and 70% of the total is linear. The salt (50 mg) was initially diluted in a solvent, namely 100% DMSO (10 ml) to reach a concentration of 5000 ppm PFOS in 100% DMSO. The stock PFOS solution (50 ppm of PFOS in 1% DMSO) was then obtained by diluting 0.5 mL of the previous solution into 49.5 mL of DMEM (10% FCS). In addition, a stock solution of 1% DMSO in media (without PFOS) was prepared for use in treatment as solvent control. The handling of the PFOS salt was carried out with protective masks in the fume hood in order to minimize unnecessary exposure to the pollutant.

In addition, serial ten-fold dilutions of the virus inoculum were prepared for infection. 1.8 mL of PBS (1% FBS) were added to a 6-well plate. Then, 0.2 mL of the virus inoculum were transferred to the first well (10^{-1} dilution) and mixed well. After, we transferred 0.2 mL from the first well to the second and mixed again (10^{-2} dilution). This process was repeated through the next wells until the 10^{-5} dilution in the fifth well. An additional well was left with no virus (negative control). Pipette tips were changed between dilutions to avoid contamination. This stock plate was then used to inoculate CEFs with the different viral dilutions in the infection stage.

The experiment

The plaque assay constitutes a widely used approach to quantify the number of infectious particles in a virus preparation. Through this experiment, we wanted to address PFOS-mediated

changes in viral replication on infected CEF monolayers. When individual infected cells undergo cell lysis, in the presence of gel-forming substances such as agar, infectious particles expand to neighbouring cells in a concentric manner and create a zone of visible cell destruction known as plaque. The amount of plaques in the system can be easily counted and positively relates to the quantity of infectious particles (Dulbecco and Vogt, 1954). In this study, we infected CEF monolayers with GaHV-2 under different experimental conditions to assess changes in viral replication. Three major treatment groups were selected:

1) Exposure to PFOS (16.7 ppm)
2) Infection with GaHV-2 (without solvent)
3) Combination of both exposure to PFOS (16.7 ppm) and infection with GaHV-2

In addition, two types of controls were included. The first (4) was to confirm that the solvent itself (1% DMSO) did not interfere with the infection process and formation of plaques. The second (5) was used to make sure that we did not introduce any external factor affecting the CEF monolayer (e.g. viral contamination) (Table D1).

4) Infection with GaHV-2 (with solvent).
5) Negative control.

Table D1. Overview of the different experimental treatments (1-5) and solutions used at both the exposure and infection stages. PFOS (50 ppm) was diluted in the well-containing growth media to the final PFOS dose used in this experiment (16.67 ppm).

	Treatment	**Exposure (48h post-seed)**	**Infection (72h post-seed)**
1)	Exposure to PFOS	PFOS (50 ppm in 1% DMSO)	PBS (1% FCS)
2)	Infection with GaHV-2 (without solvent)	Complete media	GaHV-2 dilutions
3)	Exposure to PFOS / Infection with GaHV-2	PFOS (50 ppm in 1% DMSO)	GaHV-2 dilutions
4)	Infection with GaHV-2 (with solvent)	1% DMSO	GaHV-2 dilutions
5)	Negative control	Complete media	PBS (1% FCS)

CEFs were seeded in 6-well plates at a density of 0.3 x 10^6 cells/mL (2 mL). The counting of cells to attain such density was carried out on a counting chamber (hemocytometer). These cells were allowed to colonize the wells and rest for two days at 39ºC with 5% CO_2 before the exposure stage (48h post-seed) (Table D1: Exposure). The preparation of exposure and infection solutions is described in the previous section. One mL of the exposure solution was added to the corresponding well, which already contained 2 mL of complete media from the seeding stage. Therefore, the final concentration of PFOS available in the system was 16.67 ppm. The cells were exposed for one day, before the infection stage (72h post-seed). This consisted in inoculating CEFs with 0.8 mL of either GaHV-2 serial dilutions or PBS (1% FCS) as the negative control (Table D1: Infection) The purpose of serial dilutions (from 10^{-1} to 10^{-5}) was to reach a countable range of plaques in at least one of the dilutions, as shown in Figure D1 for one of the treatments (GaHV-2 only).

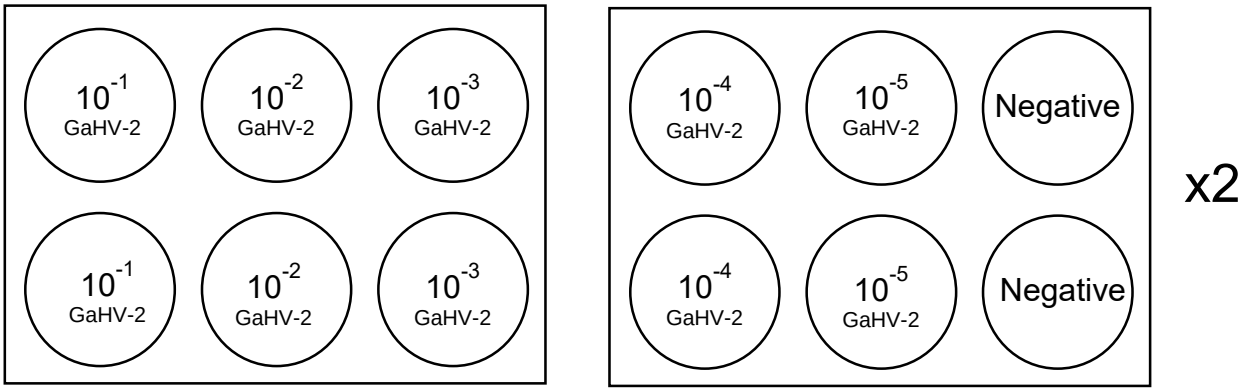

Figure D1. Example of 6-well experimental plates for one of the treatments, namely GaHV-2 only. Each dilution was analysed in duplicates per plate, and each plate was repeated twice (4 wells per treatment and dilution). In addition, four wells contained only media (negative).

The plates were then incubated at 39ºC for 1 hour, and rocked manually every 15 minutes to spread the viral contents over the well surface. A mix of agar and DMEM 10% FCS (1:1) was then used to overlay the wells with the solution (3 mL), which rapidly cools down, hardens and creates an agar overlay within 30 min at room temperature. The plates were swirled to distribute the agar overlay evenly on the wells before solidification. The plates with the virus dilutions (or PBS) and the agar overlay were incubated at 39ºC for 7 days. The final step of the plaque assay is plaque visualization and counting. It involves fixation (formaldehyde) and staining (crystal violet) of the cells prior to counting of plaques under the inverted microscope. Therefore, seven days after infection, we added the formaldehyde solution for 1 h to fixate the cells. The solution and the agar plugs were discarded before staining with crystal violet for 15 min. Plaque counting, which could not be carried out in this study, takes place after washing off the crystal violet stain with water (section 2.2). The best virus dilution factor for counting is that whose wells contain between 100 and 300 plaques (Cooper, 1962). Based on simple plaque counting and corresponding dilution factors, the viral titer in plaque forming units per mL (pfu/mL) can be determined:

$$\text{Virus titer (pfu/ml)} = \frac{\text{Number of plaques}}{\text{D x V}}$$

Where D is the dilution factor ranging from 0.1 (10^{-1}) to 0.00001 (10^{-5}), and V is the volume of diluted virus added (0.8 mL).

D2. PFOS-mediated modulation of gene expression

Table D2. Overview of the experimental treatments (1-8) and the corresponding solutions used at both the exposure and infection stages. PFOS (50 ppm) was diluted in the well-containing growth media to the final PFOS dose used in this experiment (22.2 ppm)

	Treatments	**Exposure to PFOS**	**Viral stimulation**
1)	Negative control	Complete media	PBS (1% FCS)
2)	Exposure to PFOS	PFOS (50 ppm in 1% DMSO)	PBS (1% FCS)
3)	Infection with GaHV-2 (without solvent)	Complete media	GaHV-2 dilution
4)	Exposure to PFOS / Infection with GaHV-2	PFOS (50 ppm in 1% DMSO)	GaHV-2 dilution
5)	Stimulation with poly(I:C) (with solvent)	Complete media	Poly(I:C)
6)	Exposure to PFOS / Stimulation with poly(I:C)	PFOS (50 ppm in 1% DMSO)	Poly(I:C)
7)	Infection with GaHV-2 (with solvent)	1% DMSO	GaHV-2 dilution
8)	Stimulation with poly(I:C) (with solvent)	1% DMSO	Poly(I:C)

Appendix E

Table E.1. Master mix prepared for all samples (reaction tubes) in order to perform the reverse transcription of extracted RNA into cDNA using the Qiagen miScript® II RT Kit.

Component	**Volume**
5x miScript HiSpec Buffer	4 µl
10x miScript Nucleics Mix	2 µl
miScript Reverse Transcriptase Mix	2 µl
RNase-free water	Variable
Template RNA	Variable
Total volume	20 µl

Table E.2. Master mix used for qPCR analysis of mRNA and miRNA expression

mRNA assay		**miRNA assay**	
Component	**Volume**	**Component**	**Volume**
SYBR green	10 µl	SYBR green	10 µl
Forward primer (10 µM)	2 µl	miScript Universal primer	2 µl
Reverse primer (10 µM)	2 µl	miScript Primer assay	2 µl
cDNA sample	6 µl	cDNA sample	6 µl
Total volume	20 µl	Total volume	20 µl

Table E.3. Primers used for qPCR analysis of target and control genes. The specific sequences corresponding to miR-155 and SNORD96A primer assay are not provided by the manufacturer. Primers were obtained from Sigma-Aldrich® (IL-4, IL-8, NF-κB. TNF-α and 28sRNA) and Qiagen® (miR-155 and SNORD96A).

Gene	**Sense (5' -3')**	**Antisense 5'-3')**	**Reference**
IL-4	GAGAGGTTTCCTGCGTCAAG	TGGTGGAAGAAGGTACGTAGG	(Annamalai and Selvaraj, 2012)
IL-8	CTGGCCCTCCTCCTGGTT	GCAGCTCATTCCCCATCTTTAC	(Ghareeb et al., 2013)
NF-κB	GCAACTATGTTGGACCTGCAA A	ACCCACCAAGCTGTGAGCAT	(Ghareeb et al., 2013)
TNF-α	CCCCTACCCTGTCCCACAA	TGAGTACTGCGGAGGGTTCAT	(Ghareeb et al., 2013)
miR-155	Primer assay ID: MSC0003997		(Hu et al., 2016)
28sRNA	GGTATGGGCCCGACGCT	CCGATGCCGACGCTCAT	(Neerukonda et al., 2016)
SNORD96A	Primer assay ID: MS00033733		(Burns et al., 2014)

Table E.4. qPCR running conditions (temperature program) for target and control genes.

	miR-155 – SNORD96	**IL-4 – IL-8 – NF-κB**	**TNF-α – 28srRNA**
Activation step	900 sec at 95ºC	900 sec at 95ºC	900 sec at 95ºC
Denaturation step	15 sec at 94ºC	15 sec at 94ºC	15 sec at 94ºC
Annealing step	30 sec at 55ºC	30 sec at 52ºC	30 sec at 55ºC
Extension step	30 sec at 70ºC	45 sec at 68ºC	45 sec at 68ºC
Cycle number	50	50	50

Table E5. Raw qPCR data presented as threshold cycle (Ct) values for the different treatments and timepoints (harvests), including target and housekeeping genes. Reactions were performed in two technical replicates (consecutive rows).

Treatment	Harvest	IL-4	IL-8	TNF-α	NF-κB	28srRNA	miR-155	SNORD96
PFOS	1	31.71	31.78	22.49	29.70	22.81	38.31	34.11
PFOS	1	31.94	31.78	22.50	29.02	22.64	38.91	33.83
PFOS	2	33.65	32.64	24.29	30.01	24.09	37.27	34.53
PFOS	2	33.14	33.20	24.54	30.55	24.24	38.10	34.67
PFOS	3	33.27	32.15	21.71	29.72	23.68	38.10	33.47
PFOS	3	33.22	31.71	21.98	29.90	23.30	37.43	33.33
PFOS	4	33.51	32.23	23.72	29.76	23.74	38.46	34.10
PFOS	4	32.97	32.82	23.47	30.45	23.69	41.35	34.27
GaHV-2 (DMSO)	1	32.48	30.97	22.59	28.66	21.38	37.39	32.85
GaHV-2 (DMSO)	1	31.85	30.89	22.44	28.06	21.34	35.96	32.19
GaHV-2 (DMSO)	2	33.39	33.02	24.40	29.88	22.53	37.81	33.52
GaHV-2 (DMSO)	2	33.30	31.95	23.54	29.70	22.44	36.61	33.82
GaHV-2 (DMSO)	3	32.03	30.53	22.80	27.40	20.22	35.43	31.77
GaHV-2 (DMSO)	3	31.69	30.48	22.13	28.41	20.28	35.58	31.60
GaHV-2 (DMSO)	4	32.53	30.94	22.17	28.89	20.43	36.36	32.20
GaHV-2 (DMSO)	4	32.29	30.98	23.25	28.87	20.55	36.96	32.54
PFOS/GaHV-2	1	31.74	31.20	22.03	27.89	21.35	36.27	32.61
PFOS/GaHV-2	1	31.41	31.52	22.57	28.05	21.38	35.82	31.86
PFOS/GaHV-2	2	32.37	31.62	22.79	28.86	22.31	38.51	32.62
PFOS/GaHV-2	2	32.75	31.70	22.98	29.58	22.40	38.44	32.59
PFOS/GaHV-2	3	32.59	30.60	22.44	29.47	21.99	37.34	32.51
PFOS/GaHV-2	3	32.73	30.80	22.17	28.59	21.69	36.79	32.36
PFOS/GaHV-2	4	31.04	30.59	22.03	27.86	20.07	36.63	31.69
PFOS/GaHV-2	4	30.99	31.15	23.26	28.36	20.21	35.78	31.74
Negative	1	32.74	31.76	22.25	29.03	22.77	40.30	33.92
Negative	1	32.39	32.58	22.01	29.53	22.75	37.68	33.33
Negative	2	32.41	31.74	23.02	28.48	22.01	38.38	32.41
Negative	2	32.64	31.95	24.03	27.84	22.23	37.10	32.44
Negative	3	32.10	30.85	21.60	28.47	22.14	36.56	32.56
Negative	3	32.09	31.13	21.75	27.54	21.96	37.56	32.50
Negative	4	31.32	31.09	22.11	27.97	20.63	36.78	32.01
Negative	4	31.16	30.88	24.06	27.76	20.66	37.38	32.21
GaHV-2	1	32.95	31.52	22.83	28.81	22.08	36.74	33.10
GaHV-2	1	32.81	31.90	23.01	28.27	21.95	36.70	32.89
GaHV-2	2	32.01	31.42	23.06	27.75	21.30	36.50	32.36
GaHV-2	2	32.39	31.21	24.07	28.57	21.86	37.34	32.47
GaHV-2	3	32.28	31.43	22.72	28.81	21.34	37.60	32.50
GaHV-2	3	32.15	30.91	22.09	28.69	21.46	35.86	32.07
GaHV-2	4	32.55	31.45	23.27	29.18	21.16	38.34	32.49
GaHV-2	4	31.22	31.61	22.74	28.80	21.34	37.03	32.81

Treatment	Harvest	IL-4	IL-8	TNF-α	NF-κB	28srRNA	miR-155	SNORD96
Poly(I:C) (DMSO)	1	33.09	27.11	30.64	28.46	18.38	41.63	34.51
Poly(I:C) (DMSO)	1	32.52	27.16	30.64	28.02	18.13	39.46	34.35
Poly(I:C) (DMSO)	2	32.48	32.33	24.88	29.17	21.38	37.81	34.54
Poly(I:C) (DMSO)	2	33.24	32.79	26.40	29.30	21.56	38.69	35.10
Poly(I:C) (DMSO)	3	32.95	34.30	27.75	29.80	18.65	37.35	36.72
Poly(I:C) (DMSO)	3	32.04	33.77	27.48	29.59	18.59	36.80	36.48
Poly(I:C) (DMSO)	4	33.75	35.86	30.57	30.64	21.42	38.52	37.23
Poly(I:C) (DMSO)	4	33.67	35.47	29.46	31.75	21.69	38.85	40.73
PFOS/poly(I:C)	1	31.55	32.37	27.65	28.20	NA	37.14	34.34
PFOS/poly(I:C)	1	31.18	31.32	27.17	27.62	NA	36.98	34.14
PFOS/poly(I:C)	2	32.33	32.21	24.04	28.70	19.11	36.99	34.86
PFOS/poly(I:C)	2	32.22	NA	25.57	29.04	19.19	36.82	35.27
PFOS/poly(I:C)	3	32.91	33.44	28.64	29.60	NA	38.79	35.34
PFOS/poly(I:C)	3	32.48	33.27	28.24	29.43	NA	38.52	36.52
PFOS/poly(I:C)	4	32.55	36.19	29.30	30.28	20.35	37.77	37.39
PFOS/poly(I:C)	4	32.93	34.64	29.33	30.98	20.54	38.94	37.20
Poly(I:C)	1	32.11	32.68	27.15	29.03	NA	36.95	35.14
Poly(I:C)	1	31.66	32.05	27.90	28.42	NA	36.10	34.72
Poly(I:C)	2	31.87	32.31	25.28	29.17	18.31	36.86	34.55
Poly(I:C)	2	32.32	32.48	26.12	28.73	18.39	36.86	34.51
Poly(I:C)	3	33.33	34.88	29.37	30.77	NA	38.19	35.92
Poly(I:C)	3	33.26	34.17	29.01	29.98	NA	38.05	37.02
Poly(I:C)	4	32.70	33.96	28.14	29.82	19.48	36.39	36.91
Poly(I:C)	4	32.83	35.26	28.20	30.37	19.50	37.80	38.02

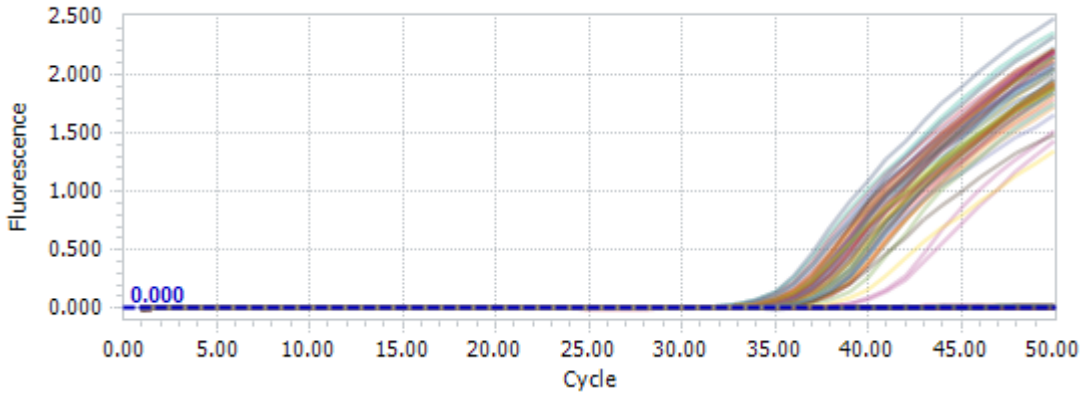

Figure E1. MicroRNA-155 (miR-155) qPCR amplification curve for all treatments included in the experiment, showing very high Ct values (35-43) and a weak rise in the fluorescent signal compared to other target genes.

Table E6. Results of the analysis of qPCR results using Bayesian MCMC methods in MCMC.qPCR R package. The table includes model point estimates (mean) of transcript abundances (log_2abundances), standard deviation from the estimate and confidence interval (CI), used to compare treatments across the investigated time points (harvest). These data correspond to the typical summary plot (trellis plot) of a two-way design.

Treatment	Gene	Harvest	Mean	SD	CI (upper)	CI (lower)
GaHV-2 (DMSO)	IL-4	1	4.83	0.45	4.05	5.55
GaHV-2 (DMSO)	IL-4	2	3.56	0.53	2.67	4.42
GaHV-2 (DMSO)	IL-4	3	5.11	0.47	4.34	5.87
GaHV-2 (DMSO)	IL-4	4	4.55	0.48	3.76	5.35
GaHV	IL-4	1	4.08	0.49	3.27	4.88
GaHV	IL-4	2	5.75	0.85	4.28	7.07
GaHV	IL-4	3	4.23	0.81	2.91	5.56
GaHV	IL-4	4	5.15	0.48	4.35	5.96
Negative	IL-4	1	4.39	0.48	3.57	5.19
Negative	IL-4	2	5.46	0.85	4.02	6.87
Negative	IL-4	3	4.33	0.82	2.98	5.73
Negative	IL-4	4	5.77	0.46	5	6.51
PFOS/GaHV-2	IL-4	1	5.41	0.47	4.62	6.19
PFOS/GaHV-3	IL-4	2	5.4	0.85	3.98	6.81
PFOS/GaHV-4	IL-4	3	3.73	0.83	2.35	5.14
PFOS/GaHV-5	IL-4	4	5.95	0.45	5.18	6.64
PFOS	IL-4	1	5.13	0.46	4.37	5.91
PFOS	IL-4	2	4.58	0.91	3.07	6.11
PFOS	IL-4	3	3.12	0.85	1.77	4.54
PFOS	IL-4	4	3.72	0.5	2.9	4.57
PFOS/poly(I:C)	IL-4	1	5.65	0.45	4.91	6.4
PFOS/poly(I:C)	IL-4	2	5.68	0.84	4.29	7.04
PFOS/poly(I:C)	IL-4	3	3.72	0.83	2.39	5.06
PFOS/poly(I:C)	IL-4	4	4.25	0.47	3.48	5.03
Poly(I:C) (DMSO)	IL-4	1	4.17	0.5	3.32	4.99
Poly(I:C) (DMSO)	IL-4	2	5.16	0.83	3.82	6.58
Poly(I:C) (DMSO)	IL-4	3	3.93	0.82	2.59	5.26
Poly(I:C) (DMSO)	IL-4	4	3.27	0.56	2.35	4.15
Poly(I:C)	IL-4	1	5.09	0.47	4.33	5.87
Poly(I:C)	IL-4	2	5.88	0.84	4.53	7.26
Poly(I:C)	IL-4	3	3.09	0.84	1.67	4.45
Poly(I:C)	IL-4	4	4.2	0.49	3.44	5.02
GaHV-2 (DMSO)	IL-8	1	6.05	0.45	5.3	6.78
GaHV-2 (DMSO)	IL-8	2	4.53	0.5	3.67	5.36
GaHV-2 (DMSO)	IL-8	3	6.51	0.45	5.79	7.27
GaHV-2 (DMSO)	IL-8	4	6.04	0.47	5.27	6.81
GaHV	IL-8	1	5.29	0.48	4.54	6.07
GaHV	IL-8	2	7.19	0.86	5.73	8.62
GaHV	IL-8	3	5.37	0.81	4.05	6.68
GaHV	IL-8	4	5.46	0.46	4.7	6.21
Negative	IL-8	1	4.83	0.5	4.04	5.64
Negative	IL-8	2	6.63	0.85	5.23	8.03
Negative	IL-8	3	5.5	0.83	4.11	6.84
Negative	IL-8	4	6.03	0.47	5.23	6.79
PFOS/GaHV-2	IL-8	1	5.64	0.49	4.84	6.46
PFOS/GaHV-3	IL-8	2	6.84	0.85	5.5	8.24
PFOS/GaHV-4	IL-8	3	5.82	0.82	4.5	7.12
PFOS/GaHV-5	IL-8	4	6.1	0.46	5.32	6.85
PFOS	IL-8	1	5.18	0.48	4.37	5.94
PFOS	IL-8	2	5.59	0.87	4.24	7.02

Treatment	Gene	Harvest	Mean	SD	CI (upper)	CI (lower)
PFOS	IL-8	3	4.59	0.82	3.28	5.97
PFOS	IL-8	4	4.43	0.49	3.67	5.25
PFOS/poly(I:C)	IL-8	1	5.18	0.48	4.38	5.97
PFOS/poly(I:C)	IL-8	2	6.34	0.99	4.7	7.9
PFOS/poly(I:C)	IL-8	3	3.1	0.85	1.67	4.48
PFOS/poly(I:C)	IL-8	4	1.64	0.72	0.41	2.82
Poly(I:C) (DMSO)	IL-8	1	9.87	0.42	9.19	10.56
Poly(I:C) (DMSO)	IL-8	2	5.9	0.86	4.43	7.28
Poly(I:C) (DMSO)	IL-8	3	2.33	0.9	0.82	3.8
Poly(I:C) (DMSO)	IL-8	4	1.08	0.81	-0.37	2.27
Poly(I:C)	IL-8	1	4.63	0.48	3.82	5.4
Poly(I:C)	IL-8	2	6.1	0.84	4.71	7.5
Poly(I:C)	IL-8	3	1.85	0.88	0.38	3.33
Poly(I:C)	IL-8	4	2.32	0.62	1.25	3.37
GaHV-2 (DMSO)	NF-κB	1	8.63	0.45	7.88	9.38
GaHV-2 (DMSO)	NF-κB	2	7.19	0.47	6.42	7.95
GaHV-2 (DMSO)	NF-κB	3	9.07	0.46	8.29	9.84
GaHV-2 (DMSO)	NF-κB	4	8.11	0.44	7.39	8.84
GaHV	NF-κB	1	8.45	0.45	7.75	9.2
GaHV	NF-κB	2	9.76	0.78	8.49	11
GaHV	NF-κB	3	7.28	0.79	6.07	8.6
GaHV	NF-κB	4	8.01	0.45	7.23	8.7
Negative	NF-κB	1	7.72	0.44	7.03	8.44
Negative	NF-κB	2	9.74	0.74	8.5	10.96
Negative	NF-κB	3	8.04	0.77	6.8	9.31
Negative	NF-κB	4	9.13	0.48	8.36	9.92
PFOS/GaHV-2	NF-κB	1	9.01	0.45	8.26	9.76
PFOS/GaHV-3	NF-κB	2	8.7	0.78	7.42	9.99
PFOS/GaHV-4	NF-κB	3	7.02	0.78	5.81	8.31
PFOS/GaHV-5	NF-κB	4	8.91	0.45	8.18	9.64
PFOS	NF-κB	1	7.65	0.46	6.9	8.47
PFOS	NF-κB	2	7.62	0.77	6.37	8.9
PFOS	NF-κB	3	6.25	0.78	4.96	7.55
PFOS	NF-κB	4	6.89	0.46	6.14	7.64
PFOS/poly(I:C)	NF-κB	1	9.09	0.45	8.39	9.85
PFOS/poly(I:C)	NF-κB	2	9.04	0.75	7.89	10.29
PFOS/poly(I:C)	NF-κB	3	6.52	0.78	5.24	7.8
PFOS/poly(I:C)	NF-κB	4	6.38	0.47	5.63	7.16
Poly(I:C) (DMSO)	NF-κB	1	8.78	0.46	8.04	9.5
Poly(I:C) (DMSO)	NF-κB	2	8.69	0.79	7.42	10.03
Poly(I:C) (DMSO)	NF-κB	3	6.35	0.79	5.12	7.7
Poly(I:C) (DMSO)	NF-κB	4	5.79	0.49	4.98	6.63
Poly(I:C)	NF-κB	1	8.25	0.45	7.46	9.02
Poly(I:C)	NF-κB	2	8.98	0.77	7.69	10.24
Poly(I:C)	NF-κB	3	5.66	0.79	4.44	6.98
Poly(I:C)	NF-κB	4	6.89	0.45	6.11	7.59
GaHV-2 (DMSO)	TNF-α	1	14.51	0.51	13.68	15.36
GaHV-2 (DMSO)	TNF-α	2	13.01	0.51	12.16	13.82
GaHV-2 (DMSO)	TNF-α	3	14.55	0.51	13.75	15.39
GaHV-2 (DMSO)	TNF-α	4	14.29	0.51	13.47	15.11
GaHV	TNF-α	1	14.06	0.51	13.23	14.89
GaHV	TNF-α	2	14.72	0.87	13.32	16.16
GaHV	TNF-α	3	14.36	0.9	12.87	15.8
GaHV	TNF-α	4	14	0.51	13.18	14.84
Negative	TNF-α	1	14.85	0.52	14.02	15.72
Negative	TNF-α	2	14.75	0.86	13.31	16.2
Negative	TNF-α	3	15.05	0.9	13.5	16.53

Treatment	Gene	Harvest	Mean	SD	CI (upper)	CI (lower)
Negative	TNF-α	4	13.92	0.53	13.05	14.75
PFOS/GaHV-2	TNF-α	1	14.71	0.51	13.85	15.53
PFOS/GaHV-3	TNF-α	2	15.39	0.87	13.99	16.8
PFOS/GaHV-4	TNF-α	3	14.44	0.9	12.93	15.85
PFOS/GaHV-5	TNF-α	4	14.34	0.52	13.5	15.17
PFOS	TNF-α	1	14.52	0.52	13.7	15.41
PFOS	TNF-α	2	13.84	0.86	12.44	15.19
PFOS	TNF-α	3	14.89	0.88	13.45	16.32
PFOS	TNF-α	4	13.4	0.52	12.57	14.21
PFOS/poly(I:C)	TNF-α	1	9.61	0.52	8.77	10.47
PFOS/poly(I:C)	TNF-α	2	13.49	0.86	11.98	14.99
PFOS/poly(I:C)	TNF-α	3	8.3	0.92	6.8	9.76
PFOS/poly(I:C)	TNF-α	4	7.7	0.53	6.79	8.51
Poly(I:C) (DMSO)	TNF-α	1	6.32	0.53	5.41	7.17
Poly(I:C) (DMSO)	TNF-α	2	12.63	0.87	11.27	14.06
Poly(I:C) (DMSO)	TNF-α	3	9.13	0.9	7.62	10.56
Poly(I:C) (DMSO)	TNF-α	4	6.99	0.53	6.12	7.84
Poly(I:C)	TNF-α	1	9.48	0.52	8.66	10.34
Poly(I:C)	TNF-α	2	12.57	0.84	11.14	13.92
Poly(I:C)	TNF-α	3	7.57	0.91	6.07	9.06
Poly(I:C)	TNF-α	4	8.84	0.52	7.99	9.67

PFOS-mediated effect on baseline immune gene expression

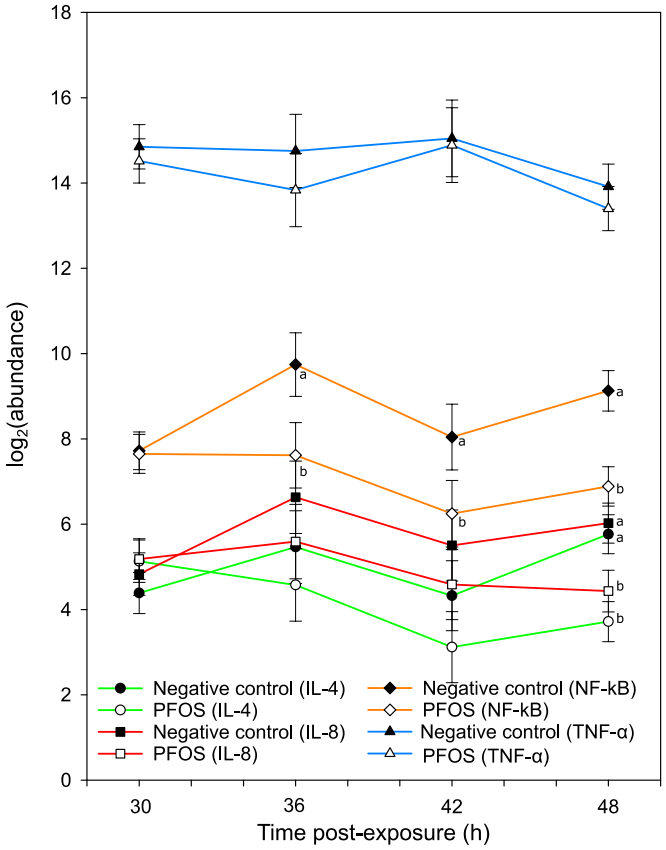

Figure E2. Overview of differences in $\log_2$(abundance) of gene transcripts (mRNA expression) in chicken embryo fibroblasts (CEFs) treated with PFOS (white symbol) versus the negative control (black symbol).The x-axis denotes duration of the post-exposure period and the y-axis the model estimate for IL-4 (green), IL-8 (red), NF-κB (orange) and TNF-α (blue). Model estimates are presented along with its SD in whiskers. Different letters denote a significant pairwise difference between the illustrated treatments. Reactions were performed in two technical replicates.

Solvent effects

GaHV-2 infection

The response to GaHV-2 (without solvent) was compared with the response to GaHV-2 (with solvent). At 12h post-infection, the inferred mean abundances of immune gene transcripts (IL-4, IL-8, NF-κB, TNF-α) were lower in the 1% DMSO- exposed group, although this trend was only significant for IL-8 (p=0.031) and NF-κB (p=0.021). This however seems to constitute an artefact since CEFs exposed to PFOS only did not experience a time-specific decrease in expression at 12h. A solvent effect was therefore not attributed to the DMSO that was used to dissolve the PFOS salt.

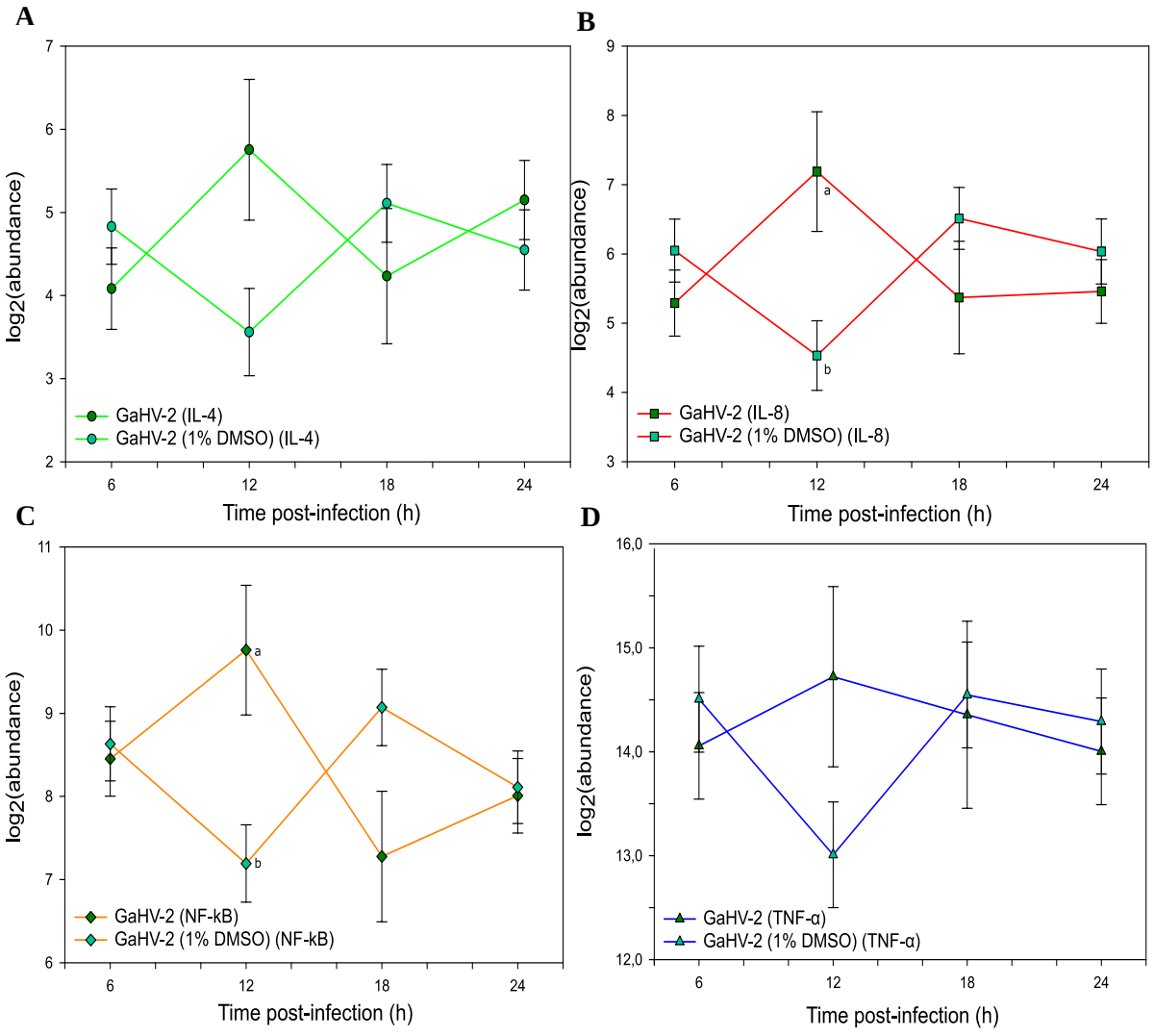

Figure E3. $\log_2$(abundance) of gene transcripts (mRNA expression) in chicken embryo fibroblasts (CEFs) infected with GaHV-2 (green symbol) versus infected with GaHV-2 (1% DMSO) (light green symbol).The x-axis denotes duration of the post-infection period and the y-axis the model estimate for IL-4 (A), IL-8 (B), NF-κB (C) and TNF-α (D). Model estimates are presented along with the SD in whiskers. Different letters denote a significant pairwise difference between the illustrated treatments. Reactions were performed in two technical replicates.

Poly(I:C) stimulation

The lack of a solvent effect was similarly confirmed using the response to poly(I:C) (without solvent) and to poly (I:C) (with solvent). This yielded similar mean expression levels for the two treatments over time ($p<0.05$), with two exceptions at 6h post-stimulation. For IL-8, there was a significant up-regulation of gene expression in response to 1% DMSO ($p<0.001$). The transcript levels of this gene after exposure to poly(I:C) (without solvent) were however similar to poly(I:C) (with PFOS), indicating that the unexpectedly higher expression in response to poly (I:C) (with solvent) may just be an artefact. For TNF-α, there was a significant down-regulation of gene expression in response to 1% DMSO ($p<0.001$). This difference disappeared when comparing poly(I:C) (without solvent) to poly (I:C) (with PFOS), as in the previous case, and this was therefore not considered a relevant solvent effect either.

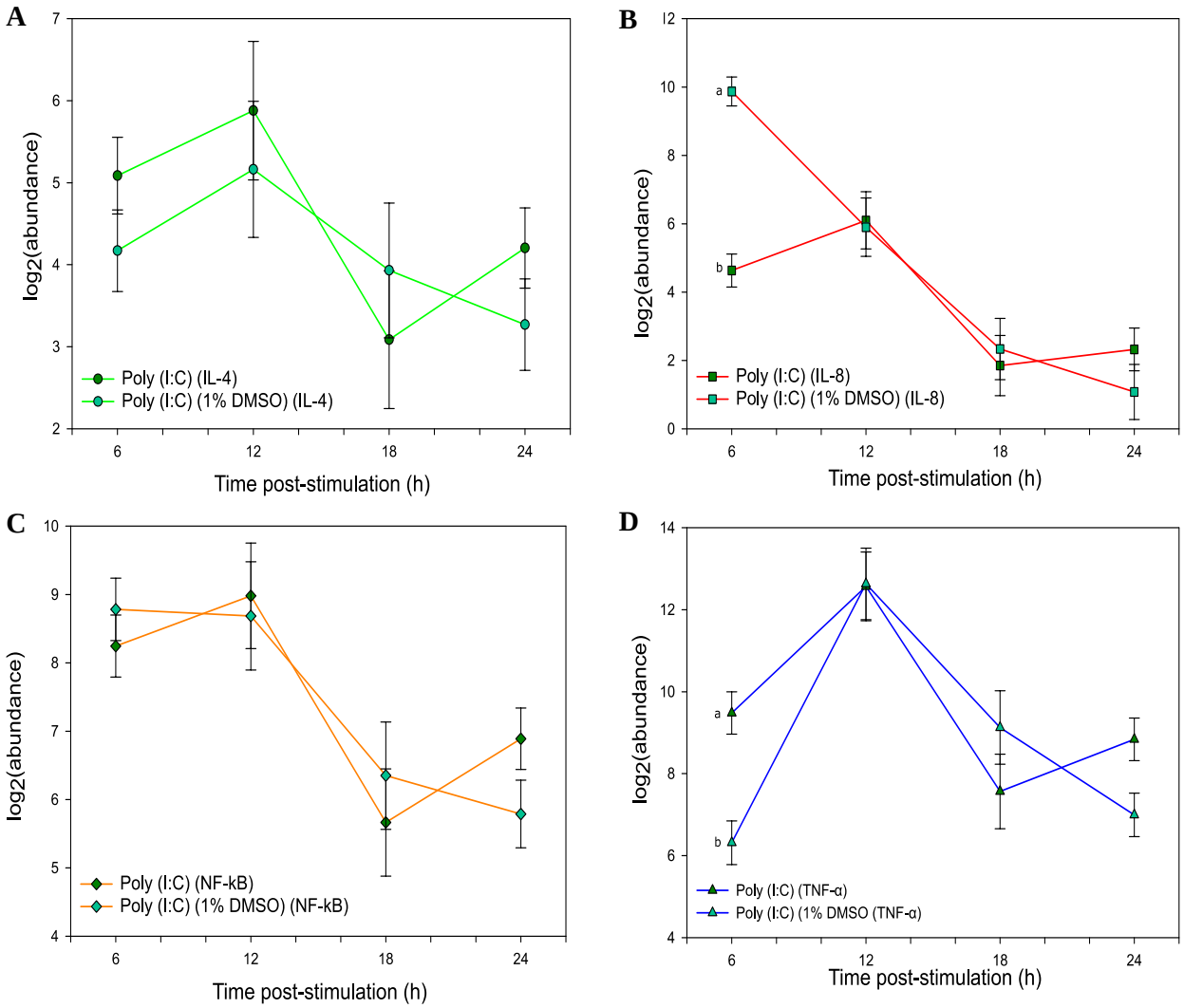

Figure E4. log_2(abundance) of gene transcripts (mRNA expression) in chicken embryo fibroblasts (CEFs) infected with the synthetic RNA virus poly(I:C) (green symbol) versus infected with poly(I:C) (1% DMSO) (light green symbol).The x-axis denotes duration of the post-stimulation period and the y-axis the model estimate for IL-4 (A), IL-8 (B), NF-κB (C) and TNF-α (D). Model estimates are presented along with the SD in whiskers. Different letters denote a significant pairwise difference between the illustrated treatments. Reactions were performed in two technical replicates.

Immunomodulatory effects by PFOS

GaHV-2 infection

Although there was not a significant change in immune gene expression associated with GaHV-2 infection for the studied genes (Figure 3.9), the potential modulation of this response by PFOS was addressed (Figure E5 A-D). No significant differences in target gene expression were found between cells exposed to GaHV-2 and cells exposed to a combination of PFOS and GaHV-2. In other words, gene expression did not change following infection neither after combined exposure to PFOS and the infectious agent. The only exception is the higher expression of NF-κB in PFOS/GaHV-2 exposed relative to control cells at 6h post-infection (p=0.042). Thus, overall no immunomodulatory effects of PFOS on GaHV-2 response could be established for the investigated genes and time points.

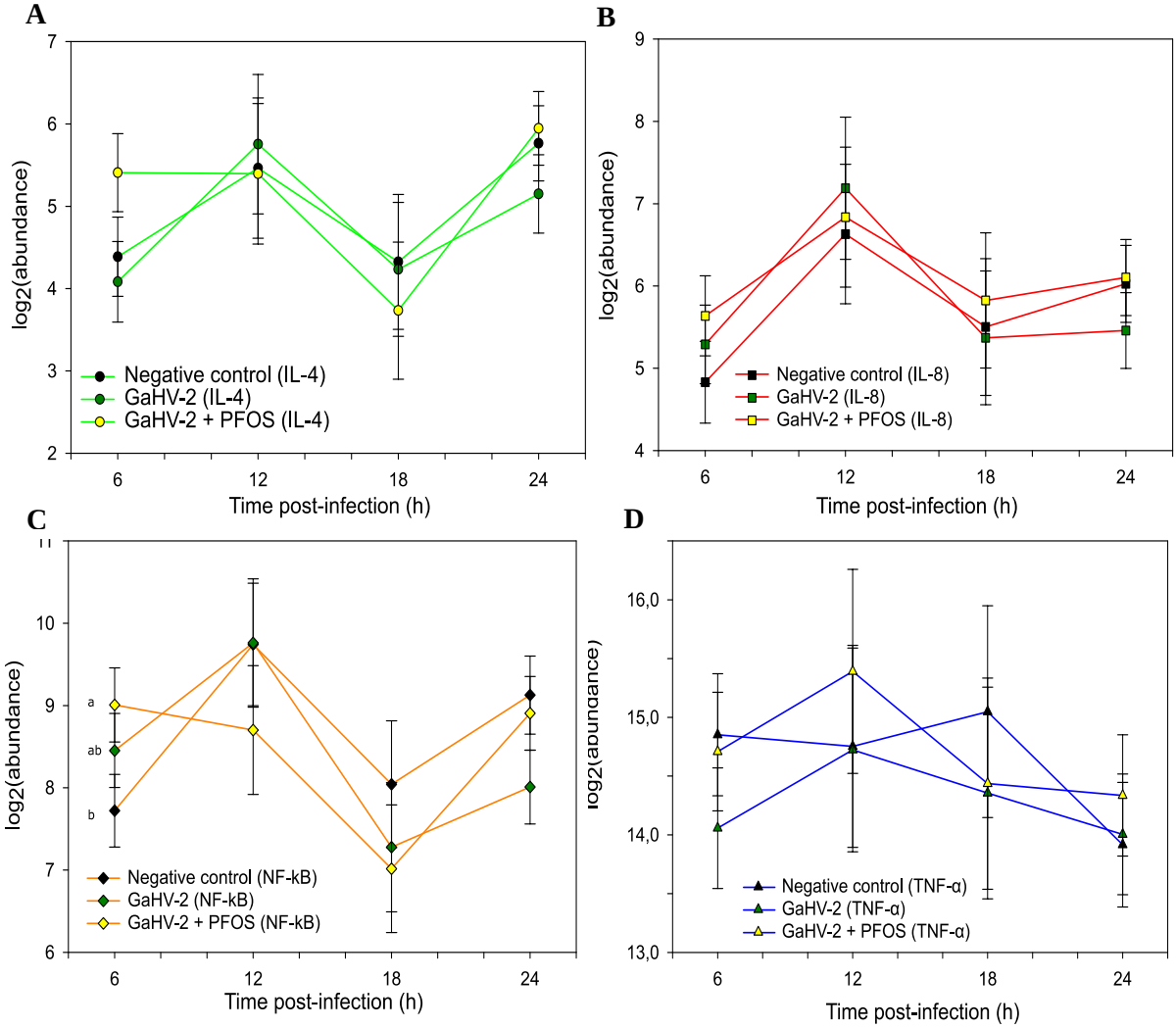

Figure E5. $\log_2$(abundance) of gene transcripts (mRNA expression) in chicken embryo fibroblasts (CEFs) infected with gallid herpesvirus-2 (GaHV-2) (green symbol), treated with PFOS and infected GaHV-2 (yellow symbol) versus the negative control (black symbol).The x-axis denotes duration of the post-infection period and the y-axis the model estimate for IL-4 (A), IL-8 (B), NF-κB (C) and TNF-α (D). Model estimates are presented along with the SD in whiskers. Different letters denote a significant pairwise difference between the illustrated treatments. Reactions were performed in two technical replicates.

Poly(I:C) stimulation

The observed response to poly (I:C) was not modulated by previous exposure to PFOS. In line with this, no significant differences between expression of immune genes in cells exposed to poly (I:C) and PFOS/poly (I:C) (Figure E6 A-D). In broad terms, gene expression did not change following combined exposure to PFOS and the viral analogue, with transcript levels remaining similar to those seen after stimulation with poly (I:C) alone.

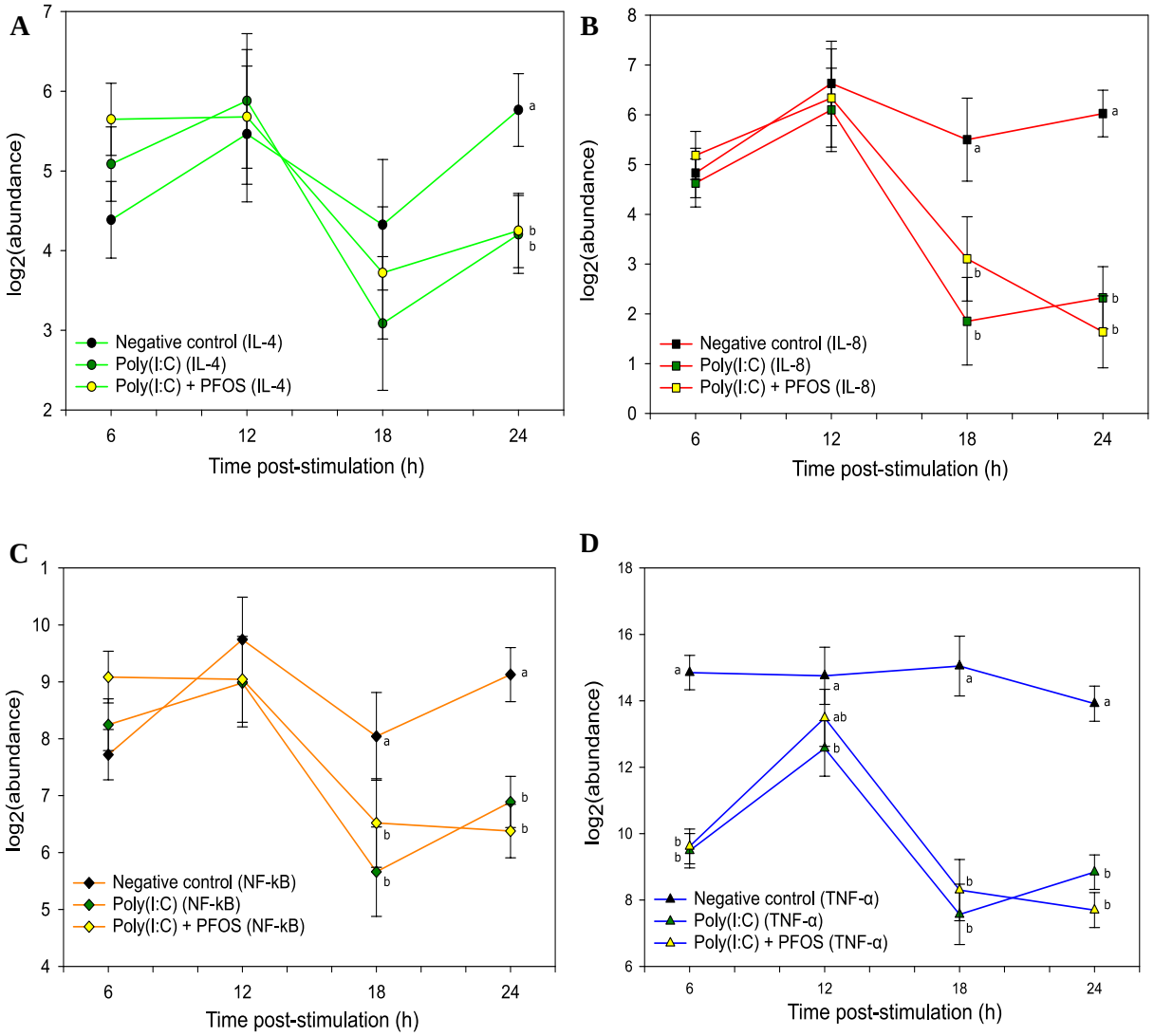

Figure E6. log_2(abundance) of gene transcripts (mRNA expression) in chicken embryo fibroblasts (CEFs) infected with polyinosinic:polycytidylic acid (poly(I:C)) (green symbol), treated with PFOS and stimulated with poly(I:C) (yellow symbol) versus the negative control (black symbol).The x-axis denotes duration of the post-stimulation period and the y-axis the model estimate for IL-4 (A), IL-8 (B), NF-κB (C) and TNF-α (D). Model estimates are presented along with the SD in whiskers. Different letters denote a significant pairwise difference between the illustrated treatments. Reactions were performed in two technical replicates.

Appendix F

Table F1. Limit of detection (LOD), limit of quantification (LOQ), samples (*n*) above the LOD and LOQ, quantification frequency (QF), mean and range of concentrations (ng/mL) in plasma of goshawk nestlings from Trøndelag, Troms and Murcia (*n*=38). LOQ was defined as three times the LOD. Mean concentrations are based on samples above the LOQ, and may slightly differ from those used in statistical analysis.

Compound	LOD	n>LOD	LOQ	n>LOQ	QF	Mean	Range
PFBA	0.05	0	0.15	0	0	-	<0.05
PFPA	0.10	0	0.30	0	0	-	<0.10
PFHxA	0.10	0	0.30	0	0	-	<0.10
PFHpA	0.05	3	0.15	0	0	-	<0.05
PFOA	0.05	38	0.15	34	89	0.60	<0.15 – 1.92
PFNA	0.075	38	0.225	38	100	1.28	0.33 – 6.49
PFDA	0.05	38	0.15	37	97	0.68	<0.15 – 2.17
PFUnDA	0.075	38	0.225	38	100	1.14	0.39 – 2.78
PFDoDA	0.075	38	0.225	32	84	0.81	<0.225 – 1.99
PFTrDA	0.10	37	0.30	32	84	0.87	<0.10 -1.39
PFTeDA	0.10	19	0.30	8	21	0.50	<0.10 – 1.43
PFHxDA	0.15	0	0.45	0	0	-	<0.15
PFODcA	0.15	0	0.45	0	0	-	<0.15
PFBS	0.05	0	0.15	0	0	-	<0.05
PFPS	0.05	0	0.15	0	0	-	<0.05
PFHxS	0.05	33	0.15	30	79	0.47	<0.10 – 2.13
PFHpS	0.075	6	0.225	2	5	0.32	<0.075 -0.41
linPFOS	0.10	38	0.30	38	100	5.30	0.45 – 21.65
brPFOS	-[a]	-[a]	-[a]	-[a]	-[a]	0.76	<0.10 - 3.14
PFOSA	0.10	0	0.30	0	0	-	<0.10
PFNS	0.10	0	0.30	0	0	-	<0.10
PFDS	0.10	0	0.30	0	0	-	<0.10
8:2 FTS	0.10	0	0.30	0	0	-	<0.10
6:2 FTS	0.10	0	0.30	0	0	-	<0.10
4:2 FTS	0.10	0	0.30	0	0	-	<0.10
6:2 Cl-PFAES	0.20	0	0.60	0	0	-	<0.10

[a]LOD and LOQ are not available because brPFOS concentrations were estimated from the difference between totalPFOS and linPFOS.

Table F2. Limit of detection (LOD), limit of quantification (LOQ), samples (*n*) above the LOD and LOQ, quantification frequency (QF), mean and range of concentrations (ng/g ww) in feathers of goshawk nestlings from Trøndelag, Troms and Murcia (pooled per nest) (*n*=39). LOQ was defined as three times the LOD. Mean concentrations are based on samples above the LOQ, and may slightly differ from those used in statistical analysis.

Compound	LOD	n>LOD	LOQ	n>LOQ	QF	Mean	Range
PFBA	0.27	0	0.58	0	0	-	<0.27
PFPA	0.27	0	0.58	0	0	-	<0.27
PFHxA	0.19	0	0.58	0	0	-	<0.19
PFHpA	0.27	0	0.80	0	0	-	<0.27
PFOA	0.21	12	0.63	2	5	0.74	<0.21 – 0.83
PFNA	0.26	29	0.78	9	23	1.11	<0.26 – 1.68
PFDA	0.26	16	0.79	3	8	0.99	<0.26 – 1.12
PFUnDA	0.18	33	0.54	27	69	1.11	<0.18 - 2.47
PFDoDA	0.15	25	0.53	19	49	1.07	<0.15 – 2.62
PFTrDA	0.19	38	0.56	33	85	1.92	<0.19 – 4.04
PFTeDA	0.20	32	0.60	17	44	1.31	<0.20 – 5.26
PFHxDA	0.20	2	0.60	2	5	1.28	<0.20 – 1.51
PFODcA	0.20	0	0.60	0	0	-	<0.20
PFBS	0.10	0	0.30	0	0	-	<0.10
PFPS	0.10	0	0.30	0	0	-	<0.10
PFHxS	0.39	17	1.18	17	44	2.53	<0.39 – 5.34
PFHpS	0.13	10	0.380	4	10	0.80	<0.13 – 1.05
linPFOS	0.05	31	0.15	31	79	2.81	<0.05 – 9.38
brPFOS	0.05	0	0.15	0	0	-	<0.05
PFOSA	0.20	7	0.60	2	5	0.67	<0.20 – 0.70
PFNS	0.05	0	0.15	0	0	-	<0.05
PFDS	0.10	0	0.30	0	0	-	<0.10
8:2 FTS	0.10	5	0.30	2	5	-	<0.10
6:2 FTS	6.04	0	18.12	0	0	-	<6.04
4:2 FTS	0.10	0	0.30	0	0	-	<0.10
6:2 Cl-PFAES	0.05	0	0.15	0	0	-	<0.05

Table F3. Individual concentrations of PFAS compounds in plasma (ng/mL) of goshawk nestlings from Troms (TOS), Trøndelag (TRD) and Murcia (MUR). The blood was taken from the oldest nestling of each nest.

ID	PFBA	PFPA	PFHxA	PFHpA	PFOA	PFNA	PFDA	PFUnDA	PFDoDA
NG.16.TOS-1	<0.05	<0.05	<0.10	<0.05	0.231	0.531	0.211	0.632	0.299
NG.16.TOS - 2	<0.05	<0.05	<0.10	<0.05	0.532	1.26	0.711	1.88	0.591
NG.16.TOS - 3	<0.05	<0.05	<0.10	<0.05	0.135	0.362	0.166	0.387	0.197
NG.16.TOS - 4	<0.05	<0.05	<0.10	<0.05	0.186	0.584	0.243	0.560	0.160
NG.16.TOS - 5	<0.05	<0.05	<0.10	<0.05	0.879	0.901	0.721	1.46	0.951
NG.16.TOS - 6	<0.05	<0.05	<0.10	<0.05	0.597	1.13	0.663	1.16	0.949
NG.16.TOS - 7	<0.05	<0.05	<0.10	<0.05	0.517	0.884	0.656	1.55	0.654
NG.16.TOS - 8	<0.05	<0.05	<0.10	<0.05	1.05	1.13	0.888	1.85	0.699
NG.16.TOS - 9	<0.05	<0.05	<0.10	<0.05	0.153	0.330	0.078	0.408	0.124
NG.16.TOS - 10	<0.05	<0.05	<0.10	<0.05	0.267	0.658	0.351	0.733	0.475
NG.16.TOS - 12	<0.05	<0.05	<0.10	<0.05	0.289	0.506	0.255	0.435	0.112
NG.16.TRD - 1	<0.05	<0.05	<0.10	<0.05	0.071	0.380	0.269	0.474	0.288
NG.16.TRD - 2	<0.05	0,080	<0.10	0.080	1.62	2.27	1.28	1.75	1.99
NG.16.TRD - 3	<0.05	0,059	<0.10	0.059	0.463	1.08	0.390	1.04	0.593
NG.16.TRD - 4	<0.05	0,076	<0.10	0.076	0.254	0.456	0.345	1.10	0.683
NG.16.TRD - 5	<0.05	<0.05	<0.10	<0.05	0.134	0.807	0.330	0.962	0.294
NG.16.TRD - 6	<0.05	<0.05	<0.10	<0.05	0.127	0.401	0.173	0.464	0.146
NG.16.TRD - 7	<0.05	<0.05	<0.10	<0.05	0.525	1.48	0.625	1.08	0.510
NG.16.TRD - 8	<0.05	<0.05	<0.10	<0.05	0.416	1.38	0.512	1.54	0.799
NG.16.TRD - 9	<0.05	<0.05	<0.10	<0.05	0.330	1.22	0.431	1.36	0.747
NG.16.TRD - 10	<0.05	<0.05	<0.10	<0.05	0.243	0.631	0.432	0.818	0.358
NG.16.TRD - 11	<0.05	<0.05	<0.10	<0.05	0.263	1.32	0.521	1.06	0.524
NG.16.TRD - 12	<0.05	<0.05	<0.10	<0.05	0.673	1.17	0.873	1.32	1.53
NG.16.TRD - 13	<0.05	<0.05	<0.10	<0.05	0.886	1.37	0.645	0.998	0.940
NG.16.TRD - 14	<0.05	<0.05	<0.10	<0.05	0.355	0.825	0.504	1.12	0.872
NG.16.TRD - 15	<0.05	<0.05	<0.10	<0.05	0.268	1.025	0.486	1.04	0.298
NG.16.TRD - 16	<0.05	<0.05	<0.10	<0.05	0.444	0.938	0.749	1.21	0.944
NG.16.TRD - 17	<0.05	<0.05	<0.10	<0.05	0.780	0.891	0.671	1.14	0.901
NG.16.TRD - 18	<0.05	<0.05	<0.10	<0.05	0.594	0.872	0.699	1.34	1.70
NG.16.TRD - 19	<0.05	<0.05	<0.10	<0.05	0.717	1.640	0.833	1.50	0.750
NG.16.TRD - 20	<0.05	<0.05	<0.10	<0.05	0.423	0.911	0.356	0.682	0.219
NG.16.MUR - 1	<0.05	<0.05	<0.10	<0.05	1.25	3.91	2.03	2.16	1.18
NG.16.MUR - 2	<0.05	<0.05	<0.10	<0.05	0.754	2.04	1.01	1.14	0.840
NG.16.MUR - 3	<0.05	<0.05	<0.10	<0.05	1.07	2.41	1.73	1.43	1.36
NG.16.MUR - 4	<0.05	<0.05	<0.10	<0.05	0.810	2.28	1.09	1.37	0.747
NG.16.MUR - 5	<0.05	<0.05	<0.10	<0.05	0.340	1.34	0.579	0.702	0.407
NG.16.MUR - 7	<0.05	<0.05	<0.10	<0.05	1.92	6.49	2.17	2.78	1.34
NG.16.MUR - 8	<0.05	<0.05	<0.10	<0.05	0.365	0.944	0.712	0.619	0.632

ID	PFTrDA	PFTeDA	PFHxDA	PFODcA	PFBS	PFPS	PFHxS	PFHpS
NG.16.TOS - 1	0.631	0.081	<0.15	<0.15	<0.05	0.448	0.448	3.11
NG.16.TOS - 2	1.24	0.194	<0.15	<0.15	<0.05	0.466	0.466	9.73
NG.16.TOS - 3	0.517	<0.10	<0.15	<0.15	<0.05	0.114	0.114	2.42
NG.16.TOS - 4	0.269	<0.10	<0.15	<0.15	<0.05	0.231	0.231	1.79
NG.16.TOS - 5	1.13	0.312	<0.15	<0.15	<0.05	0.540	0.540	8.58
NG.16.TOS - 6	1.22	0.321	<0.15	<0.15	<0.05	0.587	0.587	11.2
NG.16.TOS - 7	1.07	0.151	<0.15	<0.15	<0.05	0.440	0.440	11.9
NG.16.TOS - 8	0.956	0.169	<0.15	<0.15	<0.05	0.944	0.944	12.9
NG.16.TOS - 9	<0.10	<0.10	<0.15	<0.15	<0.05	0.165	0.165	1.57
NG.16.TOS - 10	0.148	<0.11	<0.15	<0.15	<0.05	0.214	0.214	4.14
NG.16.TOS - 12	0.220	<0.10	<0.15	<0.15	<0.05	0.687	0.687	2.67
NG.16.TRD - 1	0.554	<0.10	<0.15	<0.15	<0.05	0.167	0.167	1.17
NG.16.TRD - 2	0.957	1.43	<0.15	<0.15	<0.05	1.59	1.59	16.8
NG.16.TRD - 3	0.776	0.132	<0.15	<0.15	<0.05	0.208	0.208	1.90
NG.16.TRD - 4	0.497	<0.10	<0.15	<0.15	<0.05	0.321	0.321	2.46
NG.16.TRD - 5	0.799	<0.10	<0.15	<0.15	<0.05	0.240	0.240	3.27
NG.16.TRD - 6	0.264	<0.10	<0.15	<0.15	<0.05	0.190	0.190	0.64
NG.16.TRD - 7	1.186	0.393	<0.15	<0.15	<0.05	0.321	0.321	4.15
NG.16.TRD - 8	0.847	<0.10	<0.15	<0.15	<0.05	0.480	0.480	4.43
NG.16.TRD - 9	1.39	0.225	<0.15	<0.15	<0.05	0.190	0.190	6.81
NG.16.TRD - 10	0.662	<0.10	<0.15	<0.15	<0.05	0.245	0.245	3.76
NG.16.TRD - 11	0.544	<0.10	<0.15	<0.15	<0.05	0.251	0.251	5.54
NG.16.TRD - 12	1.32	0.339	<0.15	<0.15	<0.05	0.680	0.680	9.13
NG.16.TRD - 13	0.934	0.164	<0.15	<0.15	<0.05	0.545	0.545	8.73
NG.16.TRD - 14	0.766	0.174	<0.15	<0.15	<0.05	0.182	0.182	1.96
NG.16.TRD - 15	0.673	0.121	<0.15	<0.15	<0.05	0.166	0.166	3.69
NG.16.TRD - 16	0.862	0.214	<0.15	<0.15	<0.05	0.597	0.597	6.33
NG.16.TRD - 17	0.963	0.276	<0.15	<0.15	<0.05	2.13	2.13	21.6
NG.16.TRD - 18	1.01	0.335	<0.15	<0.15	<0.05	0.354	0.354	7.54
NG.16.TRD - 19	0.733	0.150	<0.15	<0.15	<0.05	0.246	0.246	7.42
NG.16.TRD - 20	0.507	<0.10	<0.15	<0.15	<0.05	0.210	0.210	1.95
NG.16.MUR - 1	0.978	0.375	<0.15	<0.15	<0.05	0.035	0.035	2.02
NG.16.MUR - 2	0.563	<0.10	<0.15	<0.15	<0.05	<0.05	<0.05	2.36
NG.16.MUR - 3	0.964	0.464	<0.15	<0.15	<0.05	<0.05	<0.05	2.22
NG.16.MUR - 4	0.870	<0.10	<0.15	<0.15	<0.05	<0.05	<0.05	1.03
NG.16.MUR - 5	0.287	<0.10	<0.15	<0.15	<0.05	0.116	0.116	0.45
NG.16.MUR - 7	1.31	<0.10	<0.15	<0.15	<0.05	0.056	0.056	3.02
NG.16.MUR - 8	0.352	<0.10	<0.15	<0.15	<0.05	<0.05	<0.05	0.871

ID	linPFOS	brPFOS	PFOSA	PFNS	PFDS	8:2 FTS	6:2 FTS	4:2 FTS	F-53B
NG.16.TOS - 1	3.11	0.14	<0.10	<0.10	<0.10	<0.10	<0.10	<0.10	<0.20
NG.16.TOS - 2	9.73	1.54	<0.10	<0.10	<0.10	<0.10	<0.10	<0.10	<0.20
NG.16.TOS - 3	2.42	0.30	<0.10	<0.10	<0.10	<0.10	<0.10	<0.10	<0.20
NG.16.TOS - 4	1.79	0.28	<0.10	<0.10	<0.10	<0.10	<0.10	<0.10	<0.20
NG.16.TOS - 5	8.58	1.59	<0.10	<0.10	<0.10	<0.10	<0.10	<0.10	<0.20
NG.16.TOS - 6	11.2	1.56	<0.10	<0.10	<0.10	<0.10	<0.10	<0.10	<0.20
NG.16.TOS - 7	11.9	1.55	<0.10	<0.10	<0.10	<0.10	<0.10	<0.10	<0.20
NG.16.TOS - 8	12.9	2.56	<0.10	<0.10	<0.10	<0.10	<0.10	<0.10	<0.20
NG.16.TOS - 9	1.57	0.14	<0.10	<0.10	<0.10	<0.10	<0.10	<0.10	<0.20
NG.16.TOS - 10	4.14	0.57	<0.10	<0.10	<0.10	<0.10	<0.10	<0.10	<0.20
NG.16.TOS - 12	2.67	0.29	<0.10	<0.10	<0.10	<0.10	<0.10	<0.10	<0.20
NG.16.TRD - 1	1.17	0.06	<0.10	<0.10	<0.10	<0.10	<0.10	<0.10	<0.20
NG.16.TRD - 2	16.8	3.14	<0.10	<0.10	<0.10	<0.10	<0.10	<0.10	<0.20
NG.16.TRD - 3	1.90	0.35	<0.10	<0.10	<0.10	<0.10	<0.10	<0.10	<0.20
NG.16.TRD - 4	2.46	0.31	<0.10	<0.10	<0.10	<0.10	<0.10	<0.10	<0.20
NG.16.TRD - 5	3.27	0.35	<0.10	<0.10	<0.10	<0.10	<0.10	<0.10	<0.20
NG.16.TRD - 6	0.64	0.09	<0.10	<0.10	<0.10	<0.10	<0.10	<0.10	<0.20
NG.16.TRD - 7	4.15	0.34	<0.10	<0.10	<0.10	<0.10	<0.10	<0.10	<0.20
NG.16.TRD - 8	4.43	0.51	<0.10	<0.10	<0.10	<0.10	<0.10	<0.10	<0.20
NG.16.TRD - 9	6.81	1.09	<0.10	<0.10	<0.10	<0.10	<0.10	<0.10	<0.20
NG.16.TRD - 10	3.76	0.47	<0.10	<0.10	<0.10	<0.10	<0.10	<0.10	<0.20
NG.16.TRD - 11	5.54	1.04	<0.10	<0.10	<0.10	<0.10	<0.10	<0.10	<0.20
NG.16.TRD - 12	9.13	1.34	<0.10	<0.10	<0.10	<0.10	<0.10	<0.10	<0.20
NG.16.TRD - 13	8.73	1.56	<0.10	<0.10	<0.10	<0.10	<0.10	<0.10	<0.20
NG.16.TRD - 14	1.96	0.43	<0.10	<0.10	<0.10	<0.10	<0.10	<0.10	<0.20
NG.16.TRD - 15	3.69	0.43	<0.10	<0.10	<0.10	<0.10	<0.10	<0.10	<0.20
NG.16.TRD - 16	6.33	0.47	<0.10	<0.10	<0.10	<0.10	<0.10	<0.10	<0.20
NG.16.TRD - 17	21.6	1.87	<0.10	<0.10	<0.10	<0.10	<0.10	<0.10	<0.20
NG.16.TRD - 18	7.54	0.60	<0.10	<0.10	<0.10	<0.10	<0.10	<0.10	<0.20
NG.16.TRD - 19	7.42	1.06	<0.10	<0.10	<0.10	<0.10	<0.10	<0.10	<0.20
NG.16.TRD - 20	1.95	0.41	<0.10	<0.10	<0.10	<0.10	<0.10	<0.10	<0.20
NG.16.MUR - 1	2.02	0.25	<0.10	<0.10	<0.10	<0.10	<0.10	<0.10	<0.20
NG.16.MUR - 2	2.36	0.25	<0.10	<0.10	<0.10	<0.10	<0.10	<0.10	<0.20
NG.16.MUR - 3	2.22	0.54	<0.10	<0.10	<0.10	<0.10	<0.10	<0.10	<0.20
NG.16.MUR - 4	1.03	0.15	<0.10	<0.10	<0.10	<0.10	<0.10	<0.10	<0.20
NG.16.MUR - 5	0.45	0.07	<0.10	<0.10	<0.10	<0.10	<0.10	<0.10	<0.20
NG.16.MUR - 7	3.02	0.81	<0.10	<0.10	<0.10	<0.10	<0.10	<0.10	<0.20
NG.16.MUR - 8	0.871	0.24	<0.10	<0.10	<0.10	<0.10	<0.10	<0.10	<0.20

Table F4. Concentrations of PFAS compounds in feathers (ng/g ww) of goshawk nestlings (pooled per nest) from Troms (TOS), Trøndelag (TRD) and Murcia (MUR).

ID	PFBA	PFPA	PFHxA	PFHpA	PFOA	PFNA	PFDA	PFUnDA	PFDoDA
NG.16.TOS-1	<0.27	<0.27	<0.19	<0.27	<0.21	<0.26	<0.26	0.49	<0.14
NG.16.TOS - 2	<0.27	<0.27	<0.19	<0.27	<0.21	<0.26	0.27	1.25	0.21
NG.16.TOS - 3	<0.27	<0.27	<0.19	<0.27	<0.21	<0.26	<0.26	<0.18	<0.14
NG.16.TOS - 4	<0.27	<0.27	<0.19	<0.27	<0.21	0.37	0.42	0.62	<0.14
NG.16.TOS - 5	<0.27	<0.27	<0.19	<0.27	<0.21	<0.26	<0.26	<0.18	<0.14
NG.16.TOS - 6	<0.27	<0.27	<0.19	<0.27	0.21	0.62	<0.26	1.37	1.08
NG.16.TOS - 7	<0.27	<0.27	<0.19	<0.27	<0.21	0.68	<0.26	1.65	0.73
NG.16.TOS - 8	<0.27	<0.27	<0.19	<0.27	<0.21	<0.26	<0.26	<0.18	<0.14
NG.16.TOS - 9	<0.27	<0.27	<0.19	<0.27	<0.21	<0.26	<0.26	<0.18	<0.14
NG.16.TOS - 10	<0.27	<0.27	<0.19	<0.27	<0.21	0.54	<0.26	1.82	<0.14
NG.16.TOS - 12	<0.27	<0.27	<0.19	<0.27	<0.21	<0.26	<0.26	<0.18	<0.14
NG.16.TRD - 1	<0.27	<0.27	<0.19	<0.27	0.43	1.13	<0.26	1.05	<0.14
NG.16.TRD - 2	<0.27	<0.27	<0.19	<0.27	<0.21	<0.26	<0.26	0.52	<0.14
NG.16.TRD - 3	<0.27	<0.27	<0.19	<0.27	<0.21	0.28	0.58	0.90	1.97
NG.16.TRD - 4	<0.27	<0.27	<0.19	<0.27	<0.21	0.34	<0.26	0.50	<0.14
NG.16.TRD - 5	<0.27	<0.27	<0.19	<0.27	<0.21	0.57	0.35	0.54	0.41
NG.16.TRD - 6	<0.27	<0.27	<0.19	<0.27	<0.21	0.41	<0.26	0.82	0.43
NG.16.TRD - 7	<0.27	<0.27	<0.19	<0.27	<0.21	<0.26	<0.26	0.54	<0.14
NG.16.TRD - 8	<0.27	<0.27	<0.19	<0.27	<0.21	1.19	<0.26	0.56	1.09
NG.16.TRD - 9	<0.27	<0.27	<0.19	<0.27	<0.21	0.30	<0.26	0.97	0.53
NG.16.TRD - 10	<0.27	<0.27	<0.19	<0.27	<0.21	0.79	<0.26	0.61	0.76
NG.16.TRD - 11	<0.27	<0.27	<0.19	<0.27	0.83	0.54	<0.26	0.72	0.56
NG.16.TRD - 12	<0.27	<0.27	<0.19	<0.27	0.24	0.53	<0.26	1.05	<0.14
NG.16.TRD - 13	<0.27	<0.27	<0.19	<0.27	<0.21	0.45	0.33	1.13	0.96
NG.16.TRD - 14	<0.27	<0.27	<0.19	<0.27	<0.21	0.47	0.29	0.86	0.61
NG.16.TRD - 15	<0.27	<0.27	<0.19	<0.27	0.64	0.36	<0.26	0.86	0.23
NG.16.TRD - 16	<0.27	<0.27	<0.19	<0.27	<0.21	0.84	0.38	0.76	0.59
NG.16.TRD - 17	<0.27	<0.27	<0.19	<0.27	<0.21	0.66	0.46	1.01	1.63
NG.16.TRD - 18	<0.27	<0.27	<0.19	<0.27	0.27	0.38	0.51	1.15	1.59
NG.16.TRD - 19	<0.27	<0.27	<0.19	<0.27	0.49	1.68	0.52	1.48	2.62
NG.16.TRD - 20	<0.27	<0.27	<0.19	<0.27	<0.21	0.58	0.26	0.91	0.61
NG.16.MUR - 1	<0.27	<0.27	<0.19	<0.27	<0.21	0.82	<0.26	<0.18	<0.14
NG.16.MUR - 2	<0.27	<0.27	<0.19	<0.27	0.46	1.18	1.04	2.04	1.15
NG.16.MUR - 3	<0.27	<0.27	<0.19	<0.27	0.28	0.62	0.73	1.08	0.70
NG.16.MUR - 4	<0.27	<0.27	<0.19	<0.27	0.38	<0.26	0.82	1.24	1.40
NG.16.MUR - 5	<0.27	<0.27	<0.19	<0.27	<0.21	1.00	<0.26	0.88	0.31
NG.16.MUR - 7	<0.27	<0.27	<0.19	<0.27	0.24	0.35	0.30	0.57	0.28
NG.16.MUR - 8	<0.27	<0.27	<0.19	<0.27	0.52	1.34	1.12	2.47	1.22

ID	PFTrDA	PFTeDA	PFHxDA	PFODcA	PFBS	PFPS	PFHxS	PFHpS
NG.16.TOS - 1	0.45	0.47	<0.20	<0.20	<0.10	<0.10	<0.39	<0.13
NG.16.TOS - 2	1.42	0.36	<0.20	<0.20	<0.10	<0.10	2.72	<0.13
NG.16.TOS - 3	0.33	<0.20	<0.20	<0.20	<0.10	<0.10	1.18	<0.13
NG.16.TOS - 4	0.27	<0.20	<0.20	<0.20	<0.10	<0.10	3.79	0.78
NG.16.TOS - 5	0.98	0.41	<0.20	<0.20	<0.10	<0.10	<0.39	<0.13
NG.16.TOS - 6	1.11	<0.20	<0.20	<0.20	<0.10	<0.10	<0.39	<0.13
NG.16.TOS - 7	1.26	0.79	<0.20	<0.20	<0.10	<0.10	1.77	<0.13
NG.16.TOS - 8	<0.19	<0.20	<0.20	<0.20	<0.10	<0.10	<0.39	<0.13
NG.16.TOS - 9	0.26	0.23	<0.20	<0.20	<0.10	<0.10	<0.39	<0.13
NG.16.TOS - 10	0.50	0.36	<0.20	<0.20	<0.10	<0.10	<0.39	<0.13
NG.16.TOS - 12	0.57	0.31	<0.20	<0.20	<0.10	<0.10	<0.39	<0.13
NG.16.TRD - 1	0.70	0.45	<0.20	<0.20	<0.10	<0.10	<0.39	1.05
NG.16.TRD - 2	1.90	0.81	<0.20	<0.20	<0.10	<0.10	1.70	0.21
NG.16.TRD - 3	4.04	5.26	1.06	1.06	<0.10	<0.10	3.97	<0.13
NG.16.TRD - 4	2.07	0.63	<0.20	<0.20	<0.10	<0.10	3.22	<0.13
NG.16.TRD - 5	3.00	0.84	<0.20	<0.20	<0.10	<0.10	1.76	<0.13
NG.16.TRD - 6	1.84	0.47	<0.20	<0.20	<0.10	<0.10	<0.39	<0.13
NG.16.TRD - 7	2.16	0.34	<0.20	<0.20	<0.10	<0.10	2.48	0.28
NG.16.TRD - 8	3.50	1.08	<0.20	<0.20	<0.10	<0.10	<0.39	0.20
NG.16.TRD - 9	3.21	0.81	<0.20	<0.20	<0.10	<0.10	5.34	0.25
NG.16.TRD - 10	3.41	0.78	<0.20	<0.20	<0.10	<0.10	2.01	<0.13
NG.16.TRD - 11	1.80	0.40	<0.20	<0.20	<0.10	<0.10	1.85	<0.13
NG.16.TRD - 12	2.42	0.69	<0.20	<0.20	<0.10	<0.10	2.52	0.52
NG.16.TRD - 13	2.59	1.23	<0.20	<0.20	<0.10	<0.10	2.33	0.24
NG.16.TRD - 14	2.85	1.39	<0.20	<0.20	<0.10	<0.10	2.97	<0.13
NG.16.TRD - 15	2.41	0.28	<0.20	<0.20	<0.10	<0.10	1.74	<0.13
NG.16.TRD - 16	2.00	0.66	<0.20	<0.20	<0.10	<0.10	<0.39	<0.13
NG.16.TRD - 17	2.32	1.70	<0.20	<0.20	<0.10	<0.10	<0.39	0.85
NG.16.TRD - 18	1.97	1.59	<0.20	<0.20	<0.10	<0.10	<0.39	0.26
NG.16.TRD - 19	2.61	2.09	1.51	1.51	<0.10	<0.10	<0.39	<0.13
NG.16.TRD - 20	1.74	0.55	<0.20	<0.20	<0.10	<0.10	<0.39	<0.13
NG.16.MUR - 1	1.71	<0.20	<0.20	<0.20	<0.10	<0.10	<0.39	<0.13
NG.16.MUR - 2	1.64	1.01	<0.20	<0.20	<0.10	<0.10	<0.39	<0.13
NG.16.MUR - 3	1.25	0.54	<0.20	<0.20	<0.10	<0.10	1.67	<0.13
NG.16.MUR - 4	1.32	0.97	<0.20	<0.20	<0.10	<0.10	<0.39	<0.13
NG.16.MUR - 5	1.21	<0.20	<0.20	<0.20	<0.10	<0.10	<0.39	<0.13
NG.16.MUR - 7	0.67	0.22	<0.20	<0.20	<0.10	<0.10	<0.39	<0.13
NG.16.MUR - 8	1.08	<0.20	<0.20	<0.20	<0.10	<0.10	<0.39	<0.13

ID	linPFOS	brPFOS	PFOSA	PFNS	PFDS	8:2 FTS	6:2 FTS	4:2 FTS	F-53B
NG.16.TOS - 1	<0.05	<0.05	<0.20	<0.05	<0.10	<0.10	<6.04	<0.10	<0.05
NG.16.TOS - 2	2.33	<0.05	<0.20	<0.05	<0.10	<0.10	<6.04	<0.10	<0.05
NG.16.TOS - 3	1.40	<0.05	<0.20	<0.05	<0.10	<0.10	<6.04	<0.10	<0.05
NG.16.TOS - 4	<0.05	<0.05	<0.20	<0.05	<0.10	<0.10	<6.04	<0.10	<0.05
NG.16.TOS - 5	1.67	<0.05	<0.20	<0.05	<0.10	<0.10	<6.04	<0.10	<0.05
NG.16.TOS - 6	2.23	<0.05	<0.20	<0.05	<0.10	<0.10	<6.04	<0.10	<0.05
NG.16.TOS - 7	6.69	<0.05	<0.20	<0.05	<0.10	<0.10	<6.04	<0.10	<0.05
NG.16.TOS - 8	<0.05	<0.05	<0.20	<0.05	<0.10	<0.10	<6.04	<0.10	<0.05
NG.16.TOS - 9	<0.05	<0.05	<0.20	<0.05	<0.10	<0.10	<6.04	<0.10	<0.05
NG.16.TOS - 10	0.84	<0.05	0.36	<0.05	<0.10	<0.10	<6.04	<0.10	<0.05
NG.16.TOS - 12	1.01	<0.05	<0.20	<0.05	<0.10	<0.10	<6.04	<0.10	<0.05
NG.16.TRD - 1	6.24	<0.05	<0.20	<0.05	<0.10	<0.10	<6.04	<0.10	<0.05
NG.16.TRD - 2	1.14	<0.05	<0.20	<0.05	<0.10	<0.10	<6.04	<0.10	<0.05
NG.16.TRD - 3	5.47	<0.05	0.43	<0.05	<0.10	0.63	<6.04	0.63	<0.05
NG.16.TRD - 4	1.48	<0.05	0.33	<0.05	<0.10	0.20	<6.04	0.20	<0.05
NG.16.TRD - 5	1.36	<0.05	<0.20	<0.05	<0.10	<0.10	<6.04	<0.10	<0.05
NG.16.TRD - 6	0.90	<0.05	<0.20	<0.05	<0.10	<0.10	<6.04	<0.10	<0.05
NG.16.TRD - 7	<0.05	<0.05	<0.20	<0.05	<0.10	0.24	<6.04	0.24	<0.05
NG.16.TRD - 8	2.46	<0.05	<0.20	<0.05	<0.10	<0.10	<6.04	<0.10	<0.05
NG.16.TRD - 9	1.27	<0.05	<0.20	<0.05	<0.10	<0.10	<6.04	<0.10	<0.05
NG.16.TRD - 10	2.17	<0.05	<0.20	<0.05	<0.10	<0.10	<6.04	<0.10	<0.05
NG.16.TRD - 11	2.12	<0.05	<0.20	<0.05	<0.10	<0.10	<6.04	<0.10	<0.05
NG.16.TRD - 12	3.14	<0.05	<0.20	<0.05	<0.10	<0.10	<6.04	<0.10	<0.05
NG.16.TRD - 13	5.13	<0.05	0.38	<0.05	<0.10	<0.10	<6.04	<0.10	<0.05
NG.16.TRD - 14	4.63	<0.05	<0.20	<0.05	<0.10	<0.10	<6.04	<0.10	<0.05
NG.16.TRD - 15	1.22	<0.05	0.47	<0.05	<0.10	<0.10	<6.04	<0.10	<0.05
NG.16.TRD - 16	1.63	<0.05	<0.20	<0.05	<0.10	0.17	<6.04	0.17	<0.05
NG.16.TRD - 17	3.57	<0.05	0.65	<0.05	<0.10	<0.10	<6.04	<0.10	<0.05
NG.16.TRD - 18	9.38	<0.05	0.70	<0.05	<0.10	<0.10	<6.04	<0.10	<0.05
NG.16.TRD - 19	6.31	<0.05	<0.20	<0.05	<0.10	0.59	<6.04	0.59	<0.05
NG.16.TRD - 20	4.14	<0.05	<0.20	<0.05	<0.10	<0.10	<6.04	<0.10	<0.05
NG.16.MUR - 1	<0.05	<0.05	<0.20	<0.05	<0.10	<0.10	<6.04	<0.10	<0.05
NG.16.MUR - 2	1.93	<0.05	<0.20	<0.05	<0.10	<0.10	<6.04	<0.10	<0.05
NG.16.MUR - 3	0.90	<0.05	<0.20	<0.05	<0.10	<0.10	<6.04	<0.10	<0.05
NG.16.MUR - 4	1.07	<0.05	<0.20	<0.05	<0.10	<0.10	<6.04	<0.10	<0.05
NG.16.MUR - 5	<0.05	<0.05	<0.20	<0.05	<0.10	<0.10	<6.04	<0.10	<0.05
NG.16.MUR - 7	<0.05	<0.05	<0.20	<0.05	<0.10	<0.10	<6.04	<0.10	<0.05
NG.16.MUR - 8	0.99	<0.05	<0.20	<0.05	<0.10	<0.10	<6.04	<0.10	<0.05

Appendix G

Table G1. Measures of sampling adequacy to examine factorability. The Kaiser-Meyer-Olkin (KMO) index should be > 0.6 and Bartlett's sphericity test should be significant.

KMO index and Bartlett's sphericity test		
Meyer-Olkin Measure of Sampling Adequacy		.696
Bartlett's sphericity test	Aprox. Chi-square	592.762
	df	120
	Sig.	.000

Table G2. Eigenvalues associated with the PCA. The matrix had 16 dimensions (only 10 shown here). The first two explained together 66% of the total variance and were used for interpretation.

	PC1	PC2	PC3	PC4	PC5	PC6	PC7	PC8	PC9	PC10
Variance	6.16	4.31	1.37	1.11	0.68	0.59	0.55	0.34	0.24	0.20
% of var	38.52	26.94	8.56	6.94	4.25	3.71	3.44	2.13	1.51	1.22
Cumul. %	38.52	65.46	74.02	80.96	85.21	88.91	92.35	94.48	95.99	97.22

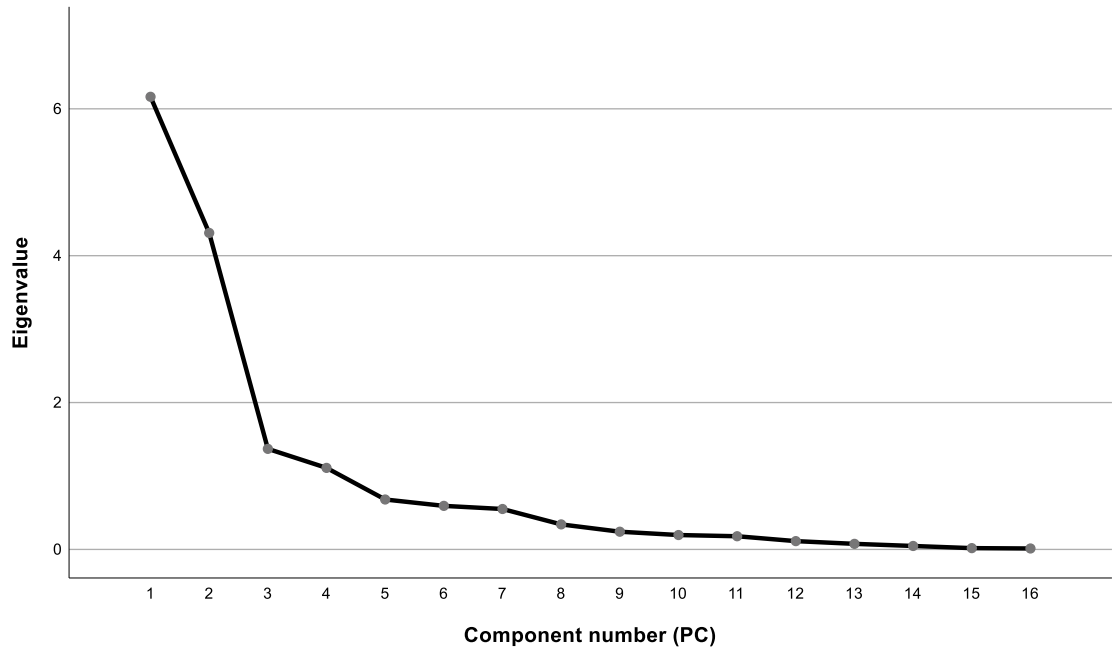

Figure G1. Scree plot showing the decreasing variance explained by each factor (principal component) in factor analysis. A big gap exists betwee the second and third eigenvalues. It was used to decide on the optimal number of factors to consider in the PCA.

Table G3. Rotated component matrix (loadings) containing estimates of the correlations between the selected quantitative variables and the extracted components. Moderate-to-strong correlations between PC1 and trophic level, PFHxS (p), linPFOS (p), brPFOS (p) and linPFOS (f). Moderate-to-strong correlations between PC1 and PFOA (p), PFNA (p), PFUnDA (p), PFDoDA (p), PFTrDA (p), PFUnDA (f) and $\delta^{13}C$.

	PC1	PC2
PFHxS (p)	.075	.852
linPFOS (p)	.241	.909
brPFOS (p)	.352	.804
PFOA (p)	.908	.215
PFNA (p)	.919	-.217
PFDA (p)	.963	-.075
PFUnDA (p)	.906	.190
PFDoDA (p)	.752	.431
PFTrDA (p)	.626	.453
linPFOS (f)	,126	,714
PFUnDA (f)	,764	-,017
PFTrDA (f)	,090	,517
Age	-.303	.502
Trophic level	-.142	.834
Body condition	.167	.123
$\delta^{13}C$	.634	-.546

Table G4. PCA individual scores (vector) corresponding to investigated nests (ID), according to their loadings in a two-dimensional space delimited by PC1 and PC2. NG.16.TOS – 7 and NG.16.TOS – 11 are left blank owing to missing stable isotope and pollutant data, respectively.

ID	Region	PC1	PC2
NG.16.TOS - 1	Troms	-0.85	-0.62
NG.16.TOS - 2	Troms	0.47	0.55
NG.16.TOS - 3	Troms	-1.19	-0.62
NG.16.TOS - 4	Troms	-1.03	-0.63
NG.16.TOS - 5	Troms	0.23	0.44
NG.16.TOS - 6	Troms	0.36	0.77
NG.16.TOS - 7	Troms	-	-
NG.16.TOS - 8	Troms	0.53	1.17
NG.16.TOS - 9	Troms	-1.30	-0.50
NG.16.TOS - 10	Troms	-0.55	-0.37
NG.16.TOS - 11	Troms	-	-
NG.16.TOS - 12	Troms	-0.88	-0.27
NG.16.TRD - 1	Trøndelag	-1.03	-0.59
NG.16.TRD - 2	Trøndelag	1.26	2.61
NG.16.TRD - 3	Trøndelag	-0.54	-0.08
NG.16.TRD - 4	Trøndelag	-0.51	-0.33
NG.16.TRD - 5	Trøndelag	-0.54	-0.45
NG.16.TRD - 6	Trøndelag	-1.19	-0.50
NG.16.TRD - 7	Trøndelag	-0.19	0.43
NG.16.TRD - 8	Trøndelag	0.09	0.20

ID	Region	PC1	PC2
NG.16.TRD - 9	Trøndelag	-0.09	0.67
NG.16.TRD - 10	Trøndelag	-0.63	-0.18
NG.16.TRD - 11	Trøndelag	-0.30	0.17
NG.16.TRD - 12	Trøndelag	0.53	1.23
NG.16.TRD - 13	Trøndelag	0.09	1.08
NG.16.TRD - 14	Trøndelag	-0.32	-0.04
NG.16.TRD - 15	Trøndelag	-0.50	-0.29
NG.16.TRD - 16	Trøndelag	-0.19	0.73
NG.16.TRD - 17	Trøndelag	0.02	2.85
NG.16.TRD - 18	Trøndelag	0.53	0.86
NG.16.TRD - 19	Trøndelag	0.27	0.39
NG.16.TRD - 20	Trøndelag	-1.00	0.01
NG.16.MUR - 1	Murcia	2.39	-1.25
NG.16.MUR - 2	Murcia	0.74	-1.26
NG.16.MUR - 3	Murcia	1.41	-0.83
NG.16.MUR - 4	Murcia	0.82	-1.20
NG.16.MUR - 5	Murcia	-0.13	-1.64
NG.16.MUR - 7	Murcia	3.58	-1.41
NG.16.MUR - 8	Murcia	-0.34	-1.08

Table G5. Alternative candidate models predicting variation in plasma levels of individual PFASs (ng/mL) in relation to nestling age, trophic level and dietary carbon source of Norwegian goshawk nestlings (*n*=30). Alternative models are shown if their ΔAIC<2 (relative to the most parsimonious).

log(PFOA)	β	SE	t	*p*-val
intercept	-2.58	0.54	-4.79	<0.001
TL	0.41	0.10	5.17	<0.001
Age	0.02	0.02	1.22	0.24
F(1,28)=15.50 (p<0.001) R^2=0.53 ΔAIC = 1.10				

log(brPFOS)	β	SE	t	*p*-val
intercept	-2.78	0.88	-3.16	0.04
TL	0.49	0.13	3.77	0.001
Age	0.02	0.03	0.83	0.41
F(1,28)=8.15 (p=0.002) R^2=0.38 ΔAIC = 1.92				

log(PFTrDA)	β	SE	t	*p*-val
intercept	-0.665	0.37	-1.80	0.083
TL	0.24	0.06	4.36	<0.001
Age	0.01	0.01	-1.09	0.29
F(1,28)=9.57 (p=0.001) R^2=0.42 ΔAIC = 1.10				

Appendix H

Relationships between PFASs in plasma and feathers

The linear relationships between individual PFAS compounds in the two target matrices were explored to assess the suitability of feathers in PFAS biomonitoring. linPFOS, PFUnDA and PFTrDA were included in this analysis, as they were detected above the LOQ in more than 50% of the samples in both plasma and feathers. Significant positive associations were reported between all individual PFAS in plasma and feathers, as well as for ∑PFASs (Figure 3.1.7): linPFOS (P) – linPFOS (F) (ρ=0.64, p<0.001), PFUnDA (P) – PFUnDA (F) (ρ=0.61, p<0.001), PFTrDA (P) – PFTrDA (F) (ρ=0.36, p=0.028) and ∑PFASs (P) - ∑PFASs (F) (ρ=0.62, p<0.001). Additionally, the two individuals with the highest burdens of PFASs in plasma (31.36 ng/mL and 30.99 ng/mL) belonged to the nests with highest feather burdens (10.41 ng/g ww and 12.50 ng/g ww).

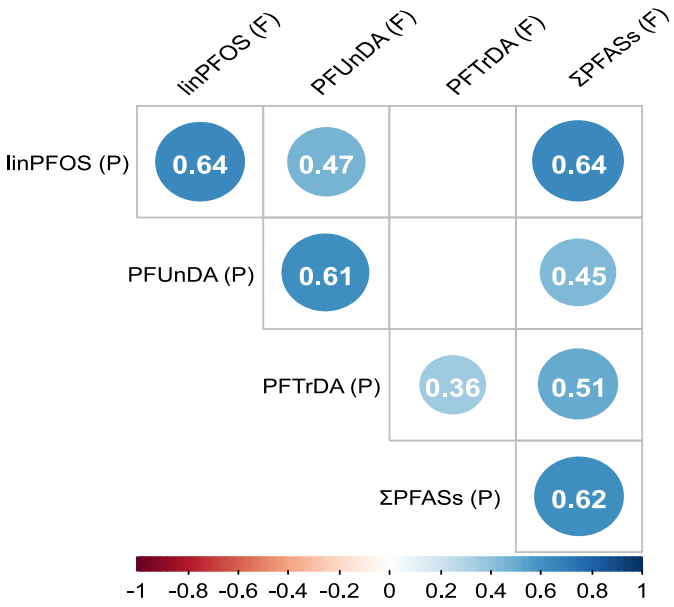

Figure H1. Non-parametric Spearman rank correlations between individual PFAS compounds in plasma (P) and feathers (F) (*n*=38). To facilitate interpretation, the correlation matrix was combined with the p-values from a significance test. Positive correlations are shown in blue circles, with colour intensity and circle size being proportional to the Spearman's rank correlation coefficients (rho). Correlations with p>0.05 are considered as insignificant and left blank in the plot.

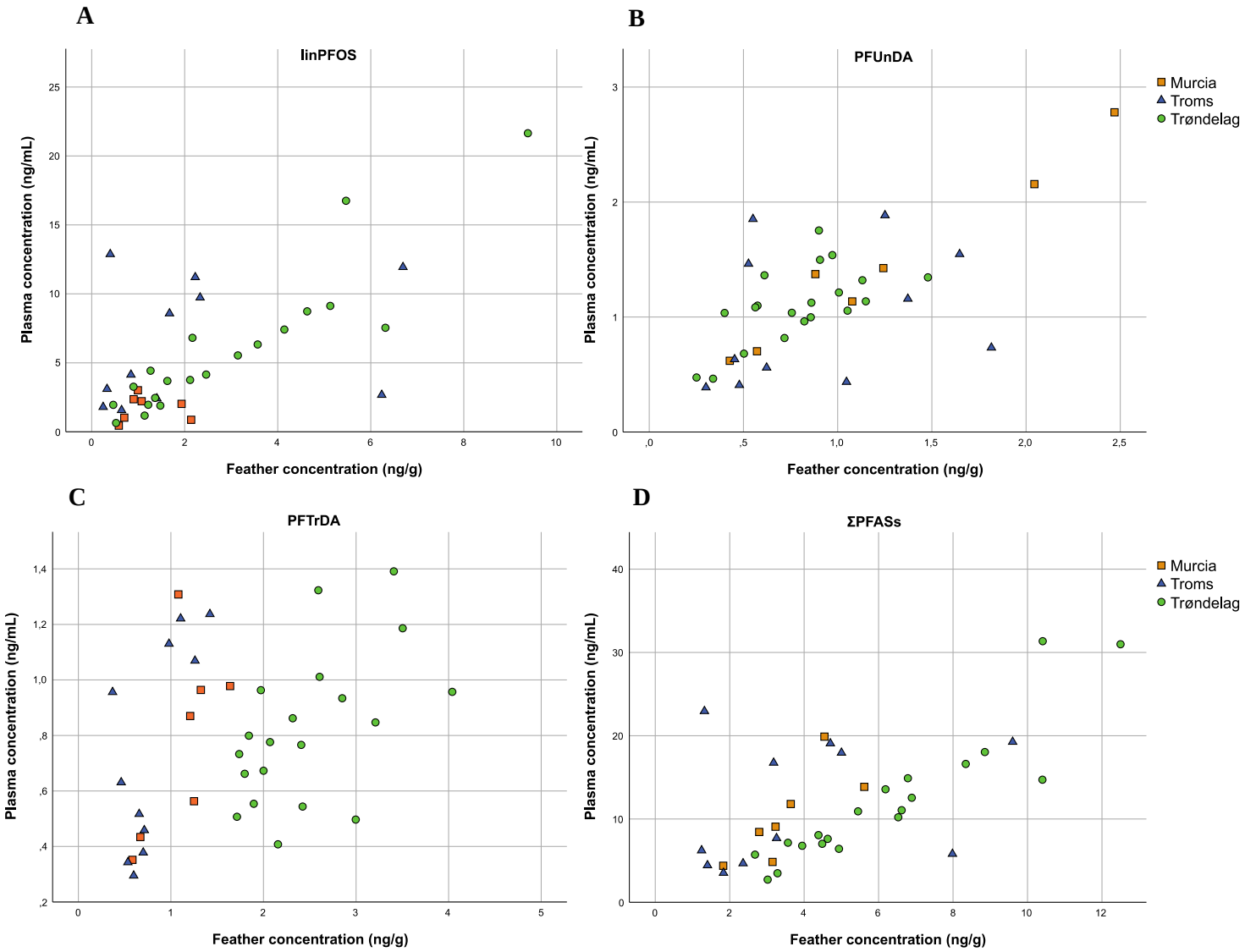

Figure H2. Correlation plots of concentrations in feathers (ng/g ww) and plasma (ng/mL) from goshawk nestlings from Murcia, Troms and Trøndelag. Plasma concentrations represent individual burdens whereas feathers were pooled per nest.

Appendix I

Table I1. Mean, median and ranges for stable isotope data from goshawk nestling feathers (pooled per nest), separated by breeding region. Trophic level (TL) was baseline-corrected using raw δ15N individual values. table isotope data

	Troms (*n*=11)			**Trøndelag** (*n*=20)			**Murcia** (*n*=7)		
	Mean	Median	Range	Mean	Median	Range	Mean	Median	Range
C:N	3.12	3.12	3.07 , 3.14	3.14	3.14	3.11 , 3.18	3.16	3.17	3.13 , 3.19
$\delta^{13}C$	-23.17[a]	-23.28	-23.92 , -21-50	-23.18[a]	-23.25	-23.94 , -22.12	-20.84[b]	-20.58	-21.67 , -20.11
$\delta^{15}N$	6.04	5.14	4.27 , 10.77	7.34	7.27	5.11 , 10.64	7.67	7.69	5.74 , 9.27
TL	3.49[a]	3.22	2.97 – 4.88	3.68[a]	3.85	3.21 , 4.84	2.63[b]	2.64	2.06 – 3.10

Table I2. Individual stable isotope data for goshawk (nestling feathers (pooled per nest). Trophic level (TL) was baseline-corrected using raw δ15N individual values.

ID	C:N	$\delta^{13}C$	$\delta^{15}N$	TL
NG.16.TOS - 1	3.11	-23.49	4.88	3.15
NG.16.TOS - 2	3.08	-23.19	6.83	3.72
NG.16.TOS - 3	3.07	-23.59	4.72	3.10
NG.16.TOS - 4	3.11	-23.55	4.28	2.97
NG.16.TOS - 5	3.12	-23.24	6.63	3.66
NG.16.TOS - 6	3.13	-22.83	8.15	4.11
NG.16.TOS - 8	3.13	-21.50	10.77	4.88
NG.16.TOS - 9	3.13	-23.92	5.14	3.22
NG.16.TOS - 10	3.12	-22.81	6.42	3.60
NG.16.TOS - 11	3.14	-23.28	4.27	2.97
NG.16.TOS - 12	3.14	-23.54	4.33	2.99
NG.16.TRD - 1	3.13	-22.46	6.39	3.59
NG.16.TRD - 2	3.15	-23.27	8.59	4.24
NG.16.TRD - 3	3.16	-22.84	6.10	3.51
NG.16.TRD - 4	3.11	-22.90	5.81	3.42
NG.16.TRD - 5	3.18	-22.70	5.11	3.21
NG.16.TRD - 6	3.17	-23.33	5.50	3.33
NG.16.TRD - 7	3.15	-23.44	8.70	4.27
NG.16.TRD - 8	3.15	-22.12	6.88	3.74
NG.16.TRD - 9	3.13	-23.60	7.47	3.91
NG.16.TRD - 10	3.12	-23.22	7.71	3.98
NG.16.TRD - 11	3.14	-23.26	6.24	3.55
NG.16.TRD - 12	3.12	-23.61	8.44	4.19
NG.16.TRD - 13	3.14	-23.54	7.61	3.95
NG.16.TRD - 14	3.13	-23.09	5.77	3.41
NG.16.TRD - 15	3.18	-23.25	7.07	3.79
NG.16.TRD - 16	3.12	-23.82	8.23	4.13
NG.16.TRD - 17	3.14	-23.76	9.07	4.38
NG.16.TRD - 18	3.17	-22.55	10.64	4.84
NG.16.TRD - 19	3.11	-22.92	6.97	3.76
NG.16.TRD - 20	3.14	-23.94	8.44	4.19
NG.16.MUR - 1	3.17	-20.11	7.25	2.51
NG.16.MUR - 2	3.17	-20.57	7.69	2.64
NG.16.MUR - 3	3.16	-21.66	9.27	3.10
NG.16.MUR - 4	3.13	-20.58	8.67	2.93
NG.16.MUR - 5	3.18	-20.56	5.74	2.06
NG.16.MUR - 7	3.15	-20.76	6.90	2.41
NG.16.MUR - 8	3.19	-21.67	8.18	2.78

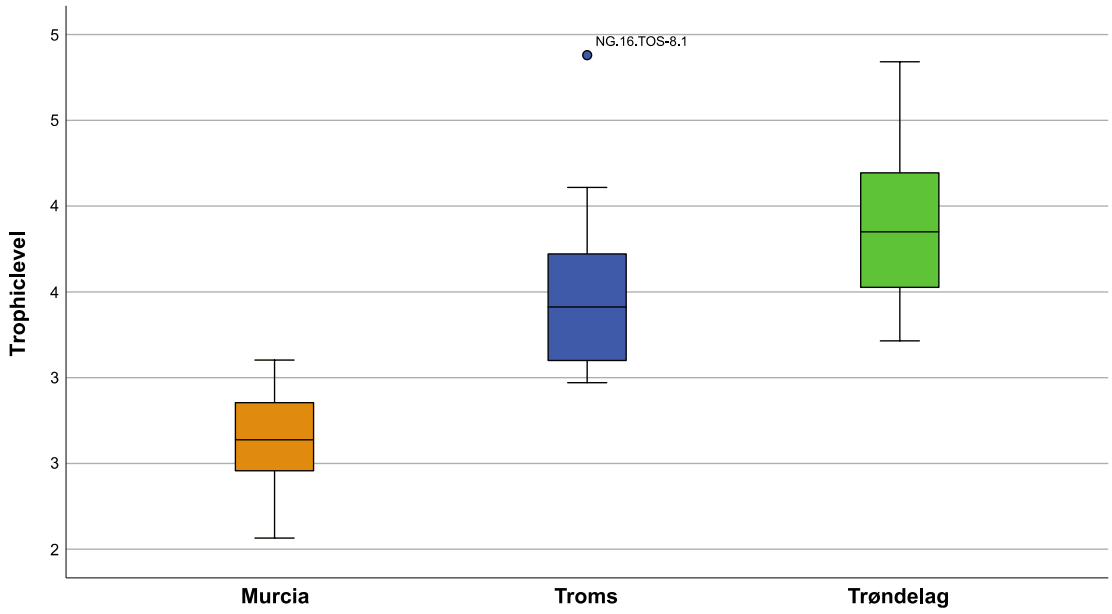

Figure I1. Box and whisker plot of estimated trophic level of goshawk nestlings from Murcia, Troms and Trøndelag. Horizontal lines represent median values. Boxes represent 25th – 75th percentiles, whiskers correspond to 95% confidence intervals and outliers are shown as dots.

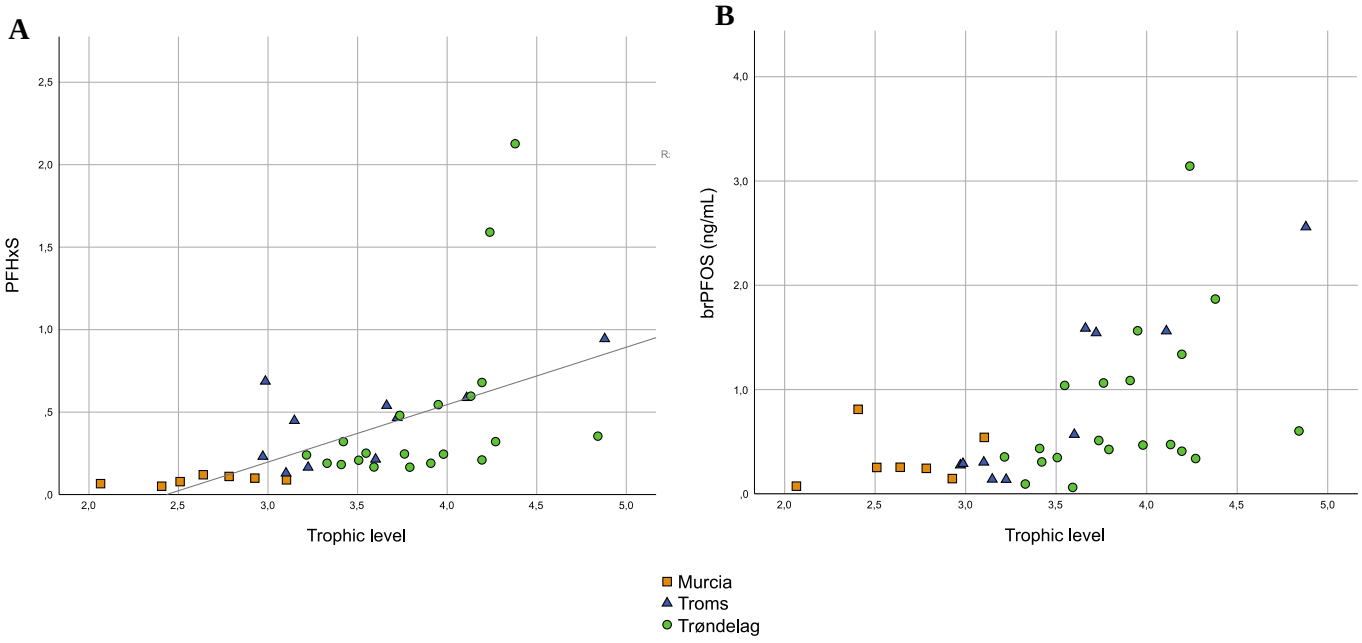

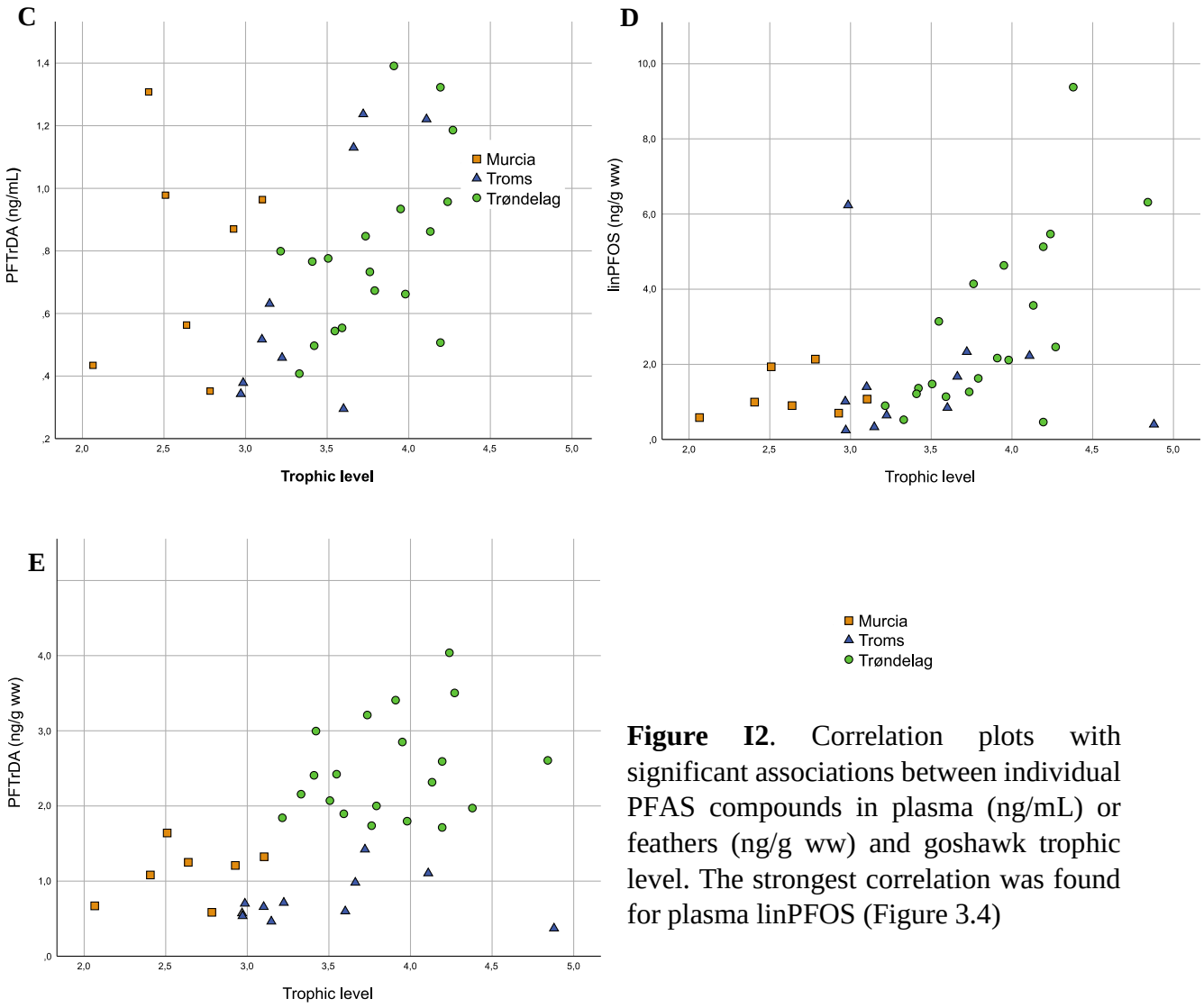

Figure I2. Correlation plots with significant associations between individual PFAS compounds in plasma (ng/mL) or feathers (ng/g ww) and goshawk trophic level. The strongest correlation was found for plasma linPFOS (Figure 3.4)